MDOT
Michigan Department of Transportation

PRCE

IDENTIFY CAUSES FOR UNDER PERFORMING RUBBLIZED CONCRETE PAVEMENT PROJECTS

PHASE II

FINAL REPORT
VOLUME I

AUGUST 2002

Michigan State University
Pavement Research Center of Excellence
Department of Civil and Environmental Engineering
East Lansing, Michigan 48824-1226

TESTING AND RESEARCH SECTION
CONSTRUCTION AND TECHNOLOGY DIVISION
RC - 1416 - VOLUME I

FINAL REPORT

DISCLAIMER

This document is disseminated under the sponsorship of the Michigan Department of Transportation (MDOT) in the interest of information exchange. The MDOT assumes no liability for its contents or use thereof.

The contents of this report reflect the views of the contracting organization, which is responsible for the accuracy of the information presented herein. The contents may not necessarily reflect the views of the MDOT and do not constitute standards, specifications, or regulations.

Technical Report Documentation Page

1. Report No. Research Report RC-1416	2. Government Accession No.	3. MDOT Project Manager Vernon Barnhart
4. Title and Subtitle Causes of underperformance of rubblized pavements		5. Report Date August 2002
7. Author(s) Gilbert Baladi & Tunwin Svasdisant		6. Performing Organization Code
9. Performing Organization Name and Address Michigan State University Dept. of Civil and Environmental Engineering E. Lansing, MI 48824-1226		8. Performing Org Report No.
12. Sponsoring Agency Name and Address Michigan Department of Transportation Construction and Technology Division P.O. Box 30049 Lansing, MI 48909		10. Work Unit No. (TRAIS) 11. Contract Number: 94-1699 11(a). Authorization Number: 00-3-1
15. Supplementary Notes		13. Type of Report & Period Covered Final – August 2002 14. Sponsoring Agency Code

16. Abstract

When an asphalt concrete is placed on top of an existing concrete pavement, within a relatively short time period (3 to 5 years depending on the thickness of the AC overlay and the pre-overlay repairs of the original concrete pavement), the resulting composite pavement would typically exhibit reflective cracking from the underlying concrete pavement. Since 1986, the Michigan Department of Transportation (MDOT) and other State Highway Agencies are rubblizing concrete pavements to prevent reflective cracking through the bituminous surfaces. Over time, special provisions for rubblizing concrete pavements have evolved (see Appendix A). However, some rubblized pavement projects are very successful and are expected to last their intended design life. Others are under performing and have shown a reduced service life. The under performing pavement sections have shown various types of distress including cracking, rutting and raveling. The overall objective of this study is to determine the causes of under performance of rubblized concrete pavements.

17. Key Words Rubblized pavements, Performance, Mechanistic analyses	18. Distribution Statement No restrictions. This document is available to the public through the Michigan Department of Transportation.		
19. Security Classification (report) Unclassified	20. Security Classification (Page) Unclassified	21. No of Pages 217	22. Price

TABLE OF CONTENTS

TABLE OF CONTENTS (continued)

TABLE OF CONTENTS (continued)

TABLE OF CONTENTS (continued)

TABLE OF CONTENTS (continued)

TABLE OF CONTENTS (continued)

ABBREVIATIONS

Abbreviations	Meanings
2-D	Two dimensional
3-D	Three dimensional
AASHTO	American Association of State Highway and Transportation Officials
AC	Asphalt concrete
AR	Aged residue
ASTM	American Society for Testing and Materials
BBR	Bending beam rheometer
BMP	Beginning mile post
CRCP	Continuous reinforced concrete pavement
CS	Control section
CV	Coefficient of variation
δ	Phase angle
D1	Deflection at sensor 1
D2	Deflection at sensor 2
D3	Deflection at sensor 3
D4	Deflection at sensor 4
D5	Deflection at sensor 5
D6	Deflection at sensor 6
D7	Deflection at sensor 7
DOT	Department of Transportation
DSR	Dynamic shear rheometer
DTT	Direct tension tester
E	Modulus
EMP	Ending mile post
FEM	Finite element
FWD	Falling weight deflectometer
G'	Storage modulus
G"	Loss modulus
G*	Complex shear modulus
GPR	Ground penetration radar
HMA	Hot mix asphalt
ITCLT	Indirect tensile cyclic load test
ITST	Indirect tensile strength test
ITT	Indirect tensile test
JN	Job number
JPCP	Jointed plane concrete pavement
JRCP	Jointed reinforced concrete pavement

ABBREVIATIONS (continued)

Abbreviations	Meanings
LTDC	Longitudinal top-down cracks
LVDT	Linear variable differential transducer
MC	Medium curing
MDOT	Michigan Department of Transportation
MDT	Mid-depth temperature
MSU	Michigan State University
MR	Resilient modulus
MTS	Mechanical testing & simulation
NDT	Nondestructive deflection test
PAV	Pressure aging vessel
PG	Performance grade
PMS	Pavement management system
PRCE	Pavement Research Center of Excellent
RB	Roadbed
RC	Rapid curing
RCS	Rubblized concrete slab
RMS	Root mean square error
RTFOT	Rolling thin-film oven test
RV	Rotational viscometer
SBR	Styrene-butadiene rubber
SBS	Styrene-butadiene-styrene
SC	Slow curing
SGC	Superpave gyratory compactor
SHA	State highway agency
SHRP	Strategic highway research program
SIS	Styrene-isoprene-styrene
SST	Superpave shear test
STDEV	Standard deviation
TCAC	Temperature corrected asphalt concrete (modulus)
TDC	Top-down cracks
TTDC	Transverse top-down cracks

EXECUTIVE SUMMARY

Rubblization is one of the rehabilitation options for distressed concrete pavements. The main objective of rubblization is to eliminate or to reduce reflective cracking potential. Two types of rubblizing equipment are being used the resonant frequency and the multi-head breakers. Since 1986, the Michigan Department of Transportation (MDOT) has rubblized more than 80 deteriorated concrete pavement projects and, in the main time, has developed and recalibrated special provisions for rubblizing pavements. Some rubblized projects are relatively successful and are expected to last their intended design life. Others are under performing and have shown a reduced service life. The under-performing rubblized pavement sections have shown various types of distress including Top-Down Cracks (TDC), joint reflective cracks, rutting and raveling. Note that TDC is not a unique problem in rubblized pavement. The occurrences of TDC in conventional flexible pavements have been reported by several highway agencies including MDOT.

The main objective of this two-phase study is to identify the causes for the under performing rubblized concrete pavements and to recommend implementable solutions. During the study, several rubblized pavements projects were thoroughly investigated during the rubblization and construction phases and after opening the pavements to traffic. The investigation consisted of:

- Excavating trenches in the rubblized pavements.
- Conducting nondestructive deflection testing and coring.
- Performing laboratory investigation.
- Conducting two manual distress surveys.
- Analyzing rubblized pavements using two and three dimensional finite element models.

Results of the analyses and the laboratory and field investigations indicated that:

1. TDC, joint reflective cracks and raveling are the major distresses contributing to the underperformance of rubblized pavements. The majority of TDC and raveling was found in segregated areas where the AC mix has low density and low tensile strength.

2. The underperformance of rubblized pavements is caused by:

   - Poor and non-uniform quality of the rubblization operation, which leads to joint and reflective cracks and TDC in the rubblized pavements. In this regard, the resonant frequency and the multi-head breakers did not deliver the best possible quality of rubblized concrete, although the resonant frequency breaker delivers, on average, better and more uniform rubblized products than the multi-head breaker. Further, the operation of both breakers and the resulting products often violate the MDOT special provisions for rubblizing pavements.
   - Lack of calibration of the rubblizing equipment.
   - Poor construction quality causing segregation in the AC mix which leads to TDC and raveling.

➢ Inadequate selection of deteriorated concrete pavement projects for rubblization.

Based on the results of the investigations and the analyses, it is strongly recommended that the following steps be adopted for immediate implementation:

1. Revise the acceptance criteria of the MDOT special provision for rubblizing concrete pavements to include:

   ➢ The scoring scheme of the quality of rubblization presented in chapter 4.
   ➢ The calibration procedure presented in chapter 4.
   ➢ Maximum variation of 20 percent in the peak pavement deflection measured at any 10 points spaced at 5-feet along the pavement and at any 5 points spaced at 2-feet across the pavement.

2. Strictly enforce the MDOT special provision for rubblizing concrete pavements.

3. Strictly enforce quality control measures to eliminate segregation in the asphalt courses. This could be achieved by officially adopting the implementation of the segregation program.

4. Provide the Regions and the Transportation Service Centers a list of deteriorated concrete pavements that should not be selected for rubblization (see chapter 4).

5. Implement the layer coefficients and/or modulus values of the rubblized materials presented in chapter 6.

As an alternative to method specifications, the following performance measures are highly recommended for inclusion in a 5-year warranty period.

1. No longitudinal and/or transverse top-down cracks.
2. No reflective or regular transverse or longitudinal cracks.
3. No faulting (differential elevation) between two adjacent lanes.
4. No shear failure.
5. No raveling
6. Less than 0.25-inch rut depth.

CHAPTER 1
INTRODUCTION AND BACKGROUND

1.0 INTRODUCTION

Substantial resources are required to preserve and rehabilitate the aging highway systems, which are subjected to increasing traffic demand. Over time, various alternatives have been developed and used for the rehabilitation of deteriorated concrete pavements. These include:

- Bonded and unbonded concrete overlays.
- Full depth repair with and without asphalt overlay.
- Crack and seat with asphalt overlay.
- Joint and crack repairs with and without asphalt overlay.
- Rubblization with asphalt surface overlay.

When an asphalt concrete is placed on top of an existing concrete pavement, within a relatively short time period (3 to 5 years depending on the thickness of the AC overlay and the pre-overlay repairs of the original concrete pavement), the resulting composite pavement would typically exhibit reflective cracking from the underlying concrete pavement. Since 1986, the Michigan Department of Transportation (MDOT) and other State Highway Agencies are rubblizing concrete pavements to prevent reflective cracking through the bituminous surfaces. Over time, special provisions for rubblizing concrete pavements have evolved (see Appendix A). However, some rubblized pavement projects are very successful and are expected to last their intended design life. Others are under performing and have shown a reduced service life. The under-performing pavement sections have shown various types of distress including cracking, rutting and raveling. The overall objective of this study is to determine the causes of under performance of rubblized concrete pavements (detailed research plan and objectives are presented in Chapter 2).

This study was originally divided into two phases. In the Phase I Study, rubblized concrete pavements were investigated by mainly excavating trenches through the rubblized materials before the asphalt concrete (AC) was placed. Some trenches were made at mid-slab while others were made at old transverse joints and cracks. In some trenches, drainability tests were conducted. The objectives of the trenches were to determine:

- The depth of rubblization
- The degree of debonding of the temperature steel
- The integrity of the concrete joints
- The size distribution of the rubblized material
- The permeability of the rubblized material

In addition, few rubblized projects that were constructed earlier and were showing signs of early distress were subjected to nondestructive deflection tests (NDT) and then cored. The NDT data were used to assess the variation in the structural capacity of the pavement along and across the traffic lane. The cores, which were taken over cracks, were examined to determine the status of the cracks (e.g., bottom-up or top-down cracks (TDC)). Results of the investigation were included in an interim report that was submitted to MDOT at the conclusion of the Phase I Study. The report presents and discusses the advantages and shortcomings of the rubblization procedure. It is shown that well-executed rubblization and construction practices (rubblization and asphalt placement) lead to good performing pavements. Further, for certain concrete pavements rubblization is not a viable option, as it may lead to inadequate pavement performance.

The investigation in the Phase II Study consisted of four activities as follows:

1. Field Investigation - Extensive NDT were conducted and cores over cracked and non-cracked areas were extracted. The deflection data were used to backcalculate the pavement layer moduli and to determine the variation in the deflection data along and across the pavements. The cores obtained from cracked areas were examined to confirm the existence of TDC.

2. Lab Investigation – The cores that were extracted from non-cracked areas were subjected to indirect cyclic tensile stress and indirect tensile strength tests. The data were used to calculate the laboratory resilient modulus and the indirect tensile strength of the asphalt concrete.

3. Mechanistic Analysis – The layer moduli obtained from the backcalculation and the layer thicknesses were used in two- and three-dimensional finite element programs to determine the load-induced stresses in the pavement structure. The analyses were designed to study the effects of the thickness of the rubblized material and the geometry of the interface between the rubblized and the fractured portions of the concrete on the magnitude of the load-induced stresses.

4. Pavement Performance – Available historical rubblized pavement distress data were obtained from MDOT and examined against those obtained from manual distress surveys. The data were used to determine the predominant type of distress in rubblized pavements and the possible causes of premature distress.

2.0 BACKGROUND

Three of the rehabilitation options that are used to preserve distressed concrete pavements are concrete repair and bituminous overlay, crack and seat and bituminous overlay and rubblization and bituminous surfacing. In general, the pavement design life for the first two options ranges from 8 to 12 years compared to 20 years for rubblized pavements. Since 1988, MDOT has constructed 86 rubblized projects. Each project was designed to perform for a 20-year period. The original rigid pavements that were selected for rubblization had a variety of distress conditions, traffic volumes and base/subbase and roadbed soil support.

Using the pavement management system, MDOT has analyzed the performance of rubblized pavements constructed to date. Based on a network type analysis, the data indicates that

some rubblized pavement projects are very successful and are expected to last their intended design life of 20 years. Others are under performing and have shown a reduced service life. The poor performance of some rubblized projects was investigated by MDOT. Cores obtained from under performing pavements were examined. The investigation did not yield consistent results relative to the causes of the poor performance. Subsequently, the problem was referred to the Pavement Research Center of Excellence (PRCE) at Michigan State University (MSU). Various projects that were rubblized over the last 14-year period as well as projects that were rubblized during the 1999, 2000, and 2001 construction seasons were investigated. This report presents and discusses the results of the investigation.
The report is organized in eight chapters and eleven appendices as follows:

Chapter 1 - Introduction and Background
Chapter 2 - Research Plan
Chapter 3 - Field and Laboratory Investigations
Chapter 4 - Rubblization
Chapter 5 - Backcalculation of Layer Moduli
Chapter 6 - Pavement Design Parameters
Chapter 7 - Mechanistic Analysis
Chapter 8 - Conclusions and Recommendations

Appendix A - Special Provision for Rubblizing Portland Cement Concrete Pavements
Appendix B - Field Investigation Conducted During the Rubblization Operation
Appendix C - Field Investigation of Rubblized Pavements after Opening the Pavements to Traffic
Appendix D - Deflection Data
Appendix E - Repeatability and Linearity Tests
Appendix F - Core and Specimen Measurements
Appendix G - Bulk Specific Gravity and Percent Air Voids
Appendix H - Indirect Tensile Cyclic Load Test Results
Appendix I - Indirect Tensile Strength Test Results
Appendix J - Backcalculated Layer Moduli
Appendix K - Literature Review

CHAPTER 2
STUDY OBJECTIVES AND RESEARCH PLAN

1.0 STUDY OBJECTIVES

The objectives of this study are divided into four categories and are presented below.

1.1 The Rubblization Procedures

Although the Phase I Study identified various equipment and rubblization procedure factors that affect the quality of rubblization, the relative impact of each factor on pavement performance and their interaction are not known. Hence, the objectives include:

1. Prioritize the various equipment and rubblization procedure factors that affect the quality of rubblization.

2. Develop detailed procedures to calibrate those factors before the commencement of rubblization.

3. Assess, if possible, the impact of each factor on the quality of rubblization and perhaps on pavement performance.

4. Identify when possible those factors that produce good and poor rubblization procedure, based on pavement performance and/or distress data.

1.2 Project Selection Process

The objective in this category is to develop an engineering investigation plan for the selection and construction of rubblized projects. The plan should address two areas as follows:

1. **Engineering Investigation** – Determine the types of distress data that need to be analyzed and the type of investigation, tests, and field sampling that need to be undertaken before a decision is made to consider rubblization as an alternative fix.

2. **Special Provision** - Based on the results of the engineering investigation, develop a plan detailing the steps that must be taken during rubblization and construction that lead to good pavement performance. The details of each step could be used by MDOT to develop performance-based specifications for rubblized pavements.

1.3 Factors Affecting Pavement Performance

During the Phase I Study, both successful and under-performing rubblized projects were investigated and nondestructive deflection data were collected. Although the data were used to compare various rubblized projects, due to time constraints (short duration of the Phase I

Study), complete analysis and assessment of the data were not undertaken. In this phase, the data were fully analyzed to accomplish the following objectives:

1. Determine rubblization and construction procedures, equipment and material factors that influence pavement performance.

2. Delineate and rank the above factors based on their impact on pavement performance.

3. Identify and rank the factors that have contributed to the under performance for each under performing rubblized project that was included in the Phase I Study.

4. Identify, when possible, the steps that must be taken to resolve the problem for each factor affecting pavement performance.

The results could be used by MDOT to develop performance-based specifications for rubblized pavements.

1.4 Pavement Design and Design Parameters

The design of rubblized pavement sections is typically constrained by the existing pavement cross-section. That is the pavement designer has no control over the thickness of the existing subbase material or the rubblized material. During the pavement design procedure, the pavement designer could determine the required thickness of fresh aggregate to be placed and compacted on top of the rubblized material prior to placing the AC and the required AC thickness if accurate input data are available. Hence, there is a need to determine the engineering properties of the existing and rubblized materials using deflection data. In lieu of this, the objectives of this part of the study are:

During the Phase II Study, the deflection data that were collected during the Phase I Study will be analyzed along with the pavement cross-section. The objectives of the analysis are:

1. Design and implement NDT test layout for the collection of representative deflection data.

2. Use the deflection data to determine the engineering characteristics (layer coefficient and resilient modulus) of the rubblized material to be used in the design process.

3. Conduct full engineering analysis of various rubblized pavement projects to determine the most likely design service life. The outcome of the analysis should indicate whether or not a rubblized pavement could be designed using a 20-year design life period.

4. Assess the impact of the as-designed pavement section on achieving the desired design service life.

5. Validate whether or not the AASHTO design procedure can be used to determine the thickness of the asphalt layer on rubblized pavement.

2.0 RESEARCH PLAN

To accomplish these objectives, a research plan was drawn and successfully executed. The plan consisted of the following tasks:

Task 1 – Quality of Rubblization – In this task, the term "quality of rubblization" will be defined. Several factors are proposed to be included in the definition are listed below.

After complete removal of the AC overlay, AC patches and filler material, and after only one pass of the rubblizing equipment, the quality of the rubblized concrete pavement should be determined based on several factors including:

- The maximum size of the rubblized material or the number of large concrete pieces that need to be broken using a grid roller or a jackhammer.
- The depth of the rubblized material and the thickness of the fractured concrete.
- The degree of debonding of the reinforced steel.
- The number of occasions where large concrete pieces rotate and/or penetrate the subbase material.
- The degree of segregation (coarse versus fine) that can be observed on the surface of the rubblized material.
- The variation in the density and perhaps the thickness of the rubblized material and/or fractured concrete.

This task can be accomplished based on:

1. Visual observations of the rubblization procedure using the considerable data that have been accumulated in the Phase I Study.

2. Examination and analysis of the nondestructive deflection data that have been collected during the Phase I Study. Based on this analysis, a nondestructive test procedure will be developed and implemented to verify the quality of rubblization and to assess the variation in the structural capacity along and across the rubblized pavement and before placing the AC layer. Although a Ground Penetrating Radar (GPR) could be used to detect the thickness and density of the rubblized material and the thickness of the fractured concrete, its costs are not included in the cost estimates of this proposal. If the GPR industry is willing to demonstrate the equipment potential, the findings will be included in the final report of the study.

This task will also explore the possibility of defining the quality of rubblization based on pavement performance.

Task 2 – The Rubblization Factors – In this task, the impact of the various rubblization factors such as speed, frequency, height of hammer drop, degree of overlapping, shoe width and compaction on the quality of rubblization will be prioritized. The activities in this task will also explore the possibility of prioritizing the rubblization factors based upon their impact on pavement performance.

Task 3 – Distress Data – In this task, available historical distress data will be examined against the deflection data that were collected during the Phase I Study. Given that the magnitudes and variations of the deflection data are indicators of the structural capacity of the pavement, the objective of the examination is to determine whether or not the deflection data can be used as a predictor or as an early warning of premature distress.

Task 4 – Compaction - Analysis of the deflection data collected during the Phase I Study indicates that the density and stiffness of the rubblized material are highly variable across the pavement. Such variations are likely the direct results of variation in the compaction of the rubblized material and the variation in the thickness of the fractured concrete. Hence, better compaction procedure, compaction specification, or quality control measures should be developed. The implementation of this recommendation would reduce the relatively high variation in the pavement deflection and it would likely results in enhanced pavement performance. In this regard, note that because of the presence of temperature steel, nuclear density gauges cannot be used to estimate the density of the compacted rubblized material. Hence, a new procedure must be developed. Such procedure could be based on the variation in the deflection data.

Task 5 – Factors Affecting Pavement Performance – The factors that affect pavement performance could be divided into four categories. Three of these categories are directly related to the three steps of rubblizing pavements stated in the introduction of this proposal. The fourth one is related to material and project selection.

The activities in this task will include:

1. Careful examination of all rubblization-related data (rubblizing procedure, deflection, distress, and material) that were collected during the Phase I Study.

2. Collecting other data elements such as the asphalt mix design and the type of binder used in the mix and the as-designed cross-section data.

3. Although various projects were visited during the Phase I Study, in all visits, only the rubblization procedure was observed and examined. During the Phase II Study, several projects will be visited and the construction of the asphalt layer will be carefully observed. The objective is to determine the differences, if any, between the constructions of the asphalt layer in conventional flexible pavement and in rubblized concrete pavement.

4. All projects that were visited during the Phase I Study will be revisited again. The purpose is to examine the pavement surface where trenches were excavated in the rubblized material. Since the locations of the trenches and the variation in the thickness of the fractured concrete were well documented during the Phase I Study, such examination would indicate the impact, if any, of the variation of the fractured concrete on pavement surface distress.

5. The detailed nondestructive deflection data that were collected during the Phase I Study on various rubblized projects will be examined against the pavement surface condition. The purpose of such examination is to determine the effects of the variation in the as-constructed deflection data on the pavement surface condition.

6. Some of the projects that were FWD tested during the Phase I Study will be FWD tested again. Differences in the deflection data would indicate differences in the structural capacity of the pavement and the effects of one or two years of traffic.

7. The historical distress data collected on projects that were rubblized prior to the 1999 construction season and were included in the Phase I Study will be analyzed against all other data, in general, and the FWD data, in particular.

The outcome of this task is to determine the true causes of the underperformance of some rubblized projects. Those causes will be classified in the four categories stated above. If possible, the differential impact of each cause on pavement performance will also be determined.

One other objective of conducting FWD tests (item 6 above) is that analysis of the historical FWD data would lead to 5-year performance based criteria, which can be used in future design and warranty projects. Such analysis must include the backcalculation of the layer moduli and the variation of the deflection data collected across and along the pavement structure.

Task 6 – Finite Element Analysis – Through the use of the measured deflection data and the three dimensional topography of the trenches that were excavated during the Phase I Study, three-dimensional finite element analysis will be conducted to obtain the pavement response due to single and multiple loads. The objective of the analysis is to determine the impact of the variation in the thickness of the fractured concrete on pavement response. It should be noted that during the Phase I Study, the potential of finite element analysis was explored using a single load (single tire) configuration. In the Phase II Study, multiple loads (dual tires) will be used in the analysis. The results of the analysis will be used to determine whether or not dual tires apply reverse bending action, which causes cracks to initiate at the pavement surface.

Task 7 – Implementation Plan – Based on the results of the study, an implementation plan will be developed. Some of the results could be implemented and verified during the study. Others could be implemented by MDOT after the proper approval.

3.0 HYPOTHESES

To this end, it was hypothesized that:

1. The average and the range of performance of rubblized concrete pavements are similar to conventional flexible pavements. This hypothesis is based on the assumption that the rubblized materials would have similar performance as that of conventional aggregate bases. When rubblized materials do not perform like conventional aggregate base, there exists a relationship between the rubblization procedure and the degree of under performance of the rubblized materials. Such relationship is affected by various factors including:

   - The operating parameters of the rubblizing equipment.
   - The type and the state of distress of the original concrete pavements being rubblized.
   - The degree of support provided by the existing subbase and roadbed soil.

2. There is a relationship between top-down cracks (TDC) potential and differential stiffness among the various asphalt concrete courses and among the asphalt concrete layer and the rubblized material. Said differential stiffness causes higher load-induced tensile stresses and higher TDC potential. Differential stiffness between the asphalt concrete courses and between the asphalt concrete and the rubblized material is affected by several factors including:

   - Construction, which may cause particle and temperature segregations in the asphalt mixes.
   - The types of the asphalt mixes.
   - Temperatures.
   - Differential aging.
   - The quality of the rubblization procedure.
   - Combination thereof.

   This hypothesis is based on field observation where the majority of cracks found in under performing rubblized concrete pavements were TDC that initiate at the top of the asphalt surface and over time propagate downward and outward.

3. There exists a relationship between the pavement's deflection response function and the degree of under performance of the rubblized concrete pavements in the form of the variability of the deflection along and across the pavements and the shape of the deflection basins. The characteristics of such variability and shape indicate the different manners by which the pavement attenuates energy induced by the passage of

a vehicle. Such relationship is affected by various variables including:

- The quality of the rubblization procedure and the type of the rubblized material produced.
- Differential stiffness between the various asphalt courses and between the asphalt concrete layer and the rubblized material.
- The as-designed pavement thickness.
- The type of the asphalt mixes.
- Construction variability such as segregation of the asphalt mix and high variability in the asphalt mat thickness
- Combination thereof

To accomplish the above stated objectives and to verify the hypotheses, a research plan was drawn and is presented in the next section.

4.0 ACTIVITIES

To accomplish the objectives and to verify the hypothesis of this study, various activities were designed to be undertaken. These include:

4.1 Literature Review

4.2 Field Investigation

The field investigation in this study consists of four activities as follows:

1. **Falling Weight Deflectometer (FWD) Tests** - For each selected 100-ft long test site, 30 to 40 FWD tests will be conducted along and across the pavement. The deflection data will be used to determine the engineering characteristics of the various layers and to assess the variability of the pavement support.

2. **Pavement Cores** – 6-in. diameter cores will be extracted from the pavement at each test site. The number of cores per site will be determined after visual examination of the pavement and review of the pavement management distress data. The average thickness of the cores will be used in the backcalculation and the cores will be tested in the laboratory to determine the resilient moduli of the asphalt mixes.

3. **Trenches** – Trenches will be excavated in the rubblized concrete slab prior to the placement of the AC layer and the variability of the rubblized material will be examined.

4. **Distress Survey and Distress Data** – Two distress surveys will be conducted to fill the time gap in the MDOT distress data. The data will be used to determine the degree of underperformance of rubblized pavements.

4.3 Laboratory Investigation

The lab investigation in this study consists of four major activities as follows:

1. Core Examination - All cores that were taken in distressed areas such as cracks will be thoroughly examined to determine the extent of distress and the dimensions of the crack. Special attention will be given to the depth and width of the crack. Crack depth would indicate the extent to which the bituminous courses have been cracked. Variation in crack width would indicate whether the crack was initiated at the top or bottom of the pavement. This information is very critical to determine the location of the highest tensile stress in the pavement and the boundary conditions.

2. Specific Gravity Tests - All pavement cores will be subjected to specific gravity tests. The results will be used to determine variations in the compacted AC mix along and across the pavement.

3. Indirect Tensile Cyclic Load Test (ITCLT) – ITCLT will be conducted to determine the resilient modulus of each asphalt mix.

4. Indirect Tensile Strength Test (ITST) - ITST will be conducted to determine the indirect tensile strength of each asphalt mix.

4.4 Analysis

The analysis in this study involves both empirical- and mechanistic-based investigations of the root causes and mechanisms of premature distress. The analyses address the high number of variables involved in rubblizing concrete pavements and surfacing with bituminous material. Said variables affect the pavement's performance and the type and mechanisms of premature distress. Such effects vary from one project to another. Therefore, the data analysis plan to be used in this study must be flexible in nature and it must be adjusted and calibrated to fit each project scenario.

In addition, the outcome of the analysis must address the engineering properties (modulus) and structural capacity (AASHTO layer coefficient) of the rubblized material. Such outcome is also affected by an unknown degree of variability along and across the pavement structure. Therefore, the following steps of the proposed data analysis plan are presented in generic terms.

1. Variability along the Project - The variability along a pavement section will be assessed using the FWD data, the distress data, the nuclear density data and the lab test data. The FWD data will yield information regarding the variability of the structural capacity of the pavement. The variability in the distress data indicates the over all variability that affects pavement performance. The nuclear density data would identify variability in the bituminous surface course only. The lab data would describe variability due to compaction, segregation and strength.

2. Cracks will be investigated through examination of those pavement cores that were taken over the cracks. The initiation of the crack is important in determining the cause of the distress. A thorough investigation of the cores will be done to determine:

   - The widths of the cracks at the pavement surface and at the bottom of the bituminous course (the crack end). This will help to determine the location of the highest tensile stress and the direction of bending.
   - The crack spacing in both the horizontal and vertical directions. Horizontal cracks indicate shear failure and/or lack of adhesion. Vertical cracks indicate either fatigue or bearing capacity types of failure.

3. The engineering properties of some pavement cores will be determined using cyclic load tests. The results will be compared to the modulus values obtained from MICHBACK. The results will be used to:

   - Conduct mechanistic analysis of the pavement sections to assess the magnitudes of the induced stresses and strains.
   - Characterize the properties of the various pavement layers and suggest design values (layer coefficients and modulus). These include the properties of the asphalt layer as well as the properties of the rubblized concrete slabs. It should be noted that the modulus values of the rubblized concrete slabs are currently not known and the validity of their correlation to the layer coefficient will be investigated.
   - Verify the findings of the study titled "The Engineering Characteristics of Michigan's Asphalt Mixtures."

   In addition, some cores will be subjected to indirect tensile strength to determine the field applied stress ratio due to traffic load. Results from the cyclic load and tensile strength tests will be used to calculate the modulus value of the asphalt layer. From the modulus values, the layer coefficients could be determined. The layer coefficient of the rubblized concrete slab is the desired value as little is known about its validity.

During the analysis, special efforts will be used to assess the mechanisms and the root causes of distress. Based on the results, remedial actions will be recommended to the rubblization and asphalt paving processes. Further, current MDOT specifications and regulations will be reviewed in lieu of the findings and possible modifications will be recommended.

4.5 Verification

All developed procedures will be verified using measured deflection data along and across a pavement section. The results of empirical and/or statistical equations will be verified using the measured deflection data. The performance of rubblized pavements will be analyzed using both the MDOT distress survey data and manual survey

CHAPTER 3
FIELD AND LABORATORY INVESTIGATIONS

1.0 GENERAL

During the Phase I and Phase II study, 88 rubblized and 3 flexible pavement projects were investigated to determine the causes of underperforming rubblized pavements. The investigations consisted of 2 categories; field and laboratory. The field investigation consisted of the following activities:

- Excavating trenches in the rubblized concrete slab prior to the placement and compaction of the AC layer.
- Conducting nondestructive deflection tests along and across the pavements in a predesigned pattern.
- Extracting cores from the pavements.
- Conducting manual distress surveys of rubblized pavements

The laboratory investigation consisted of the following tests:

- Measurements of the thickness of each AC course in the core and the total thickness of the cores.
- Specific gravity tests of the total cores and each of the AC courses.
- Indirect tensile cyclic load tests to determine the resilient modulus of the cores.
- Indirect tensile strength tests.

Details of the field and laboratory investigations are presented in this chapter.

2.0 FIELD INVESTIGATION

All pavement projects that were rubblized between the 1987 and 2001 construction seasons were investigated in this study. In addition, three conventional flexible pavement projects were also investigated. Two of these projects were constructed in 2000 and one in 1994. As stated above, the field investigation consisted of excavating trenches during the rubblization operation, conducting FWD tests and pavement coring after the completion of construction, and manual distress surveys. Details of the investigation are presented below.

2.1 Investigation during the Rubblization Operation

In this study, fifteen rubblized projects were investigated during the rubblization operation. The main objective of the investigation is to evaluate whether or not the rubblization operation satisfied the following four objectives of rubblizing pavements:

1. Breaking the concrete slabs into small pieces (less than 6-in. maximum dimension). This would eliminate independent movement of large pieces and would increase the degree of interlocking between the broken concrete pieces.

2. Debonding the temperature steel to decrease the amount of temperature expansion and contraction of the rubblized concrete slab and, hence, to eliminate the potential of reflective cracking.

3. Destroying the integrity of the concrete joints to prevent reflective cracking.

4. Eliminating or decreasing the potential of rubblizing the concrete slab into two distinctive layers; a rubblized layer and a fractured concrete layer. The two layers when capped with asphalt concrete would behave like a sandwich model (a soft layer between two hard layers). The differential stiffness between the three layers causes high load-induced tensile stress at the top of the AC causing top-down cracks (TDC).

During the rubblization operation, several trenches were excavated in the rubblized concrete slabs. Some trenches were located at mid-slab, others were located at joints and still others were located at a transverse crack. After excavation, the rubblized materials were piled to form the walls of a pool, the floor of the pool consisted of the fractured concrete. The pool was filled with water to test the permeability of the fractured concrete. Results of the investigation indicated that:

1. The rubblization operation produces two different layers in the rubblized concrete slabs, a rubblized material layer at the top and a fractured concrete layer at the bottom as shown in figures 3.1 and 3.2. The thickness of each layer varied from one location to another. In some areas, the fractured concrete extended to the original pavement surface while in other locations the rubblized material extended to the bottom of the original concrete slab. Further, the stiffnesses of the two layers were substantially different. It was estimated that the stiffness of the fractured concrete is an order of magnitude higher than that of the rubblized material layer. Such differential stiffness causes high load-induced tensile stress at the top of the AC surface, which increases the potential for TDC.

2. At a few locations, the temperature steel was debonded from the original concrete as shown in figure 3.3. However, at most locations, the integrity of the bond was not broken.

3. At some longitudinal and transverse joints, the integrity of the joints in the original slabs was not completely destroyed (see figure 3.4) and some dowel bars were found embedded in the concrete on both sides of the joint. These may cause the development of reflective cracks.

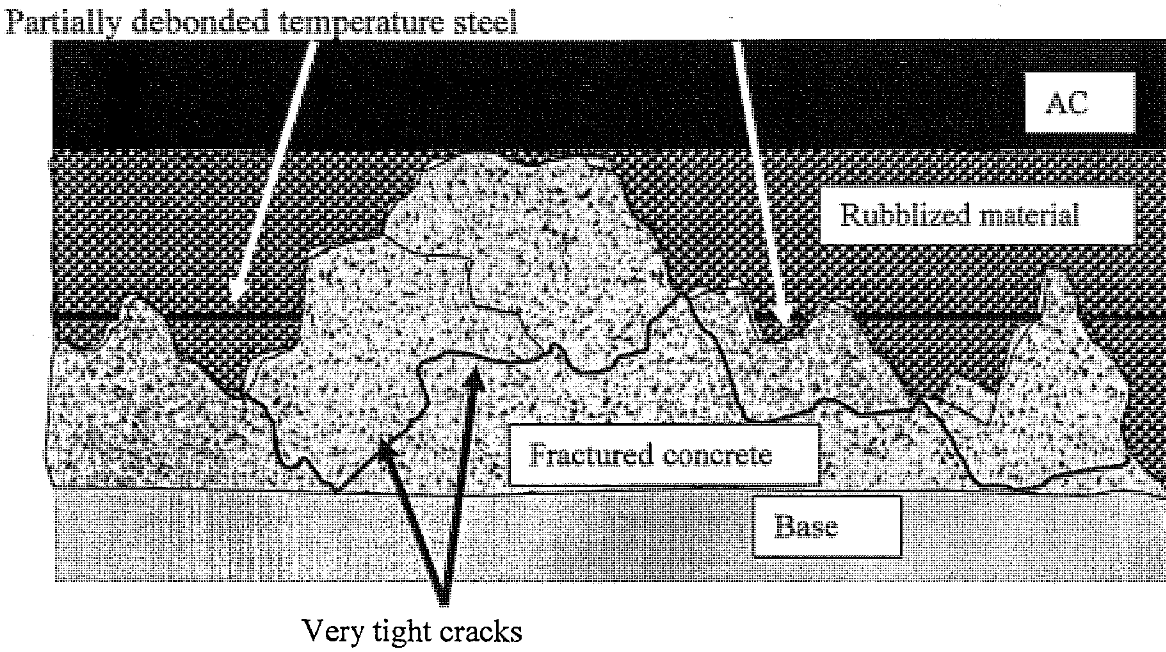

Figure 3.1 Schematic of rubblized concrete slab showing rubblized and fractured layers

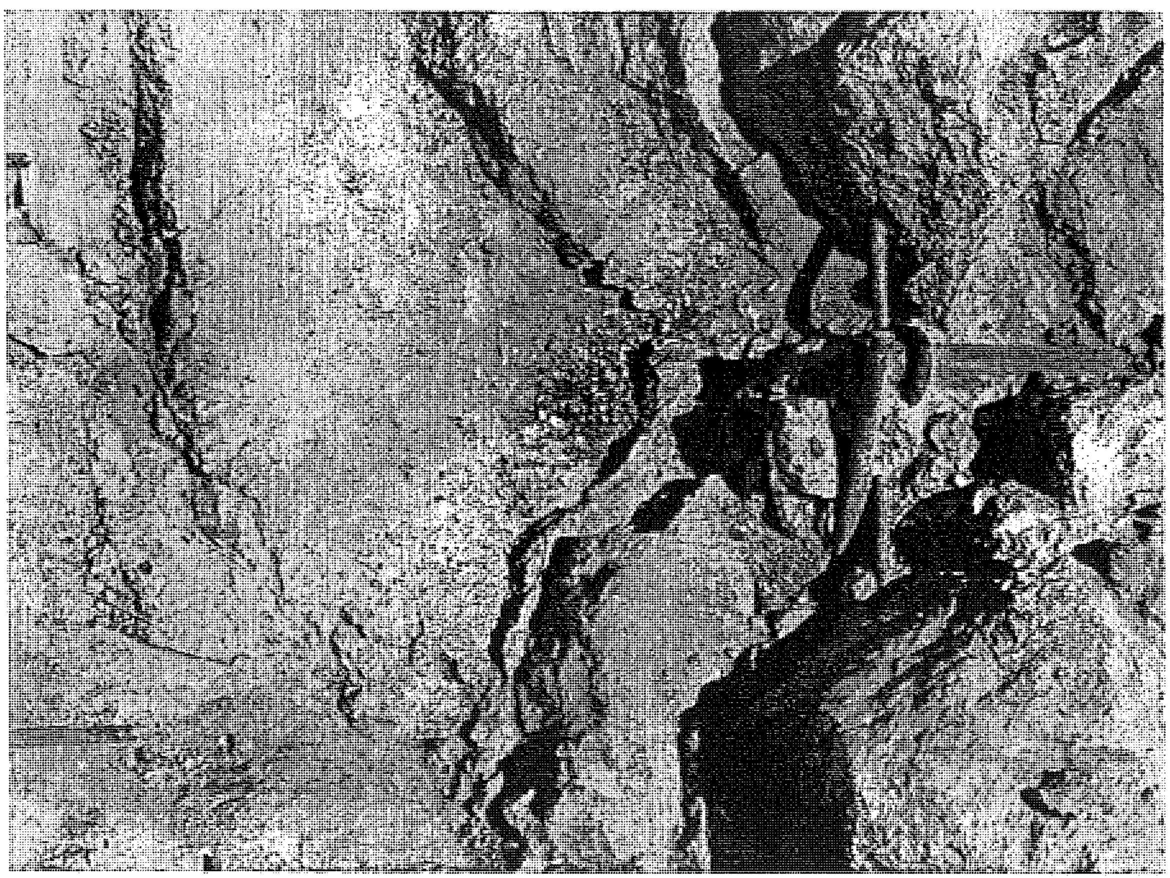

Figure 3.2 Close-up of the fractured concrete in a trench (M50)

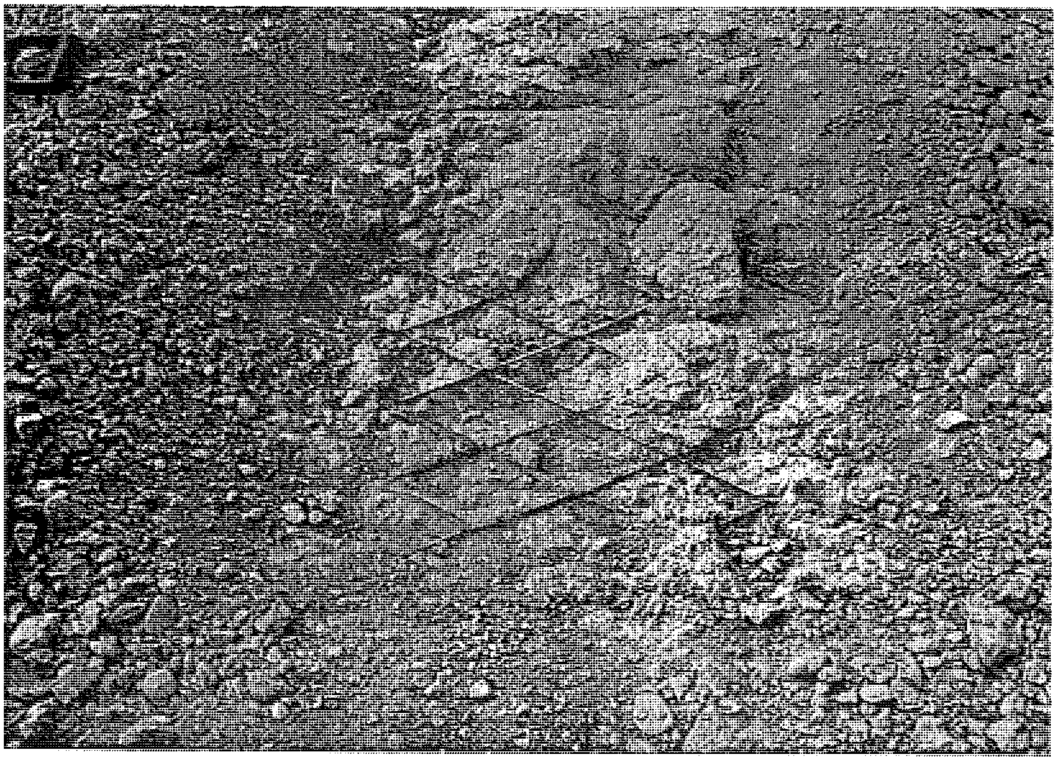

Figure 3.3 Partial debonding of the temperature steel (M21)

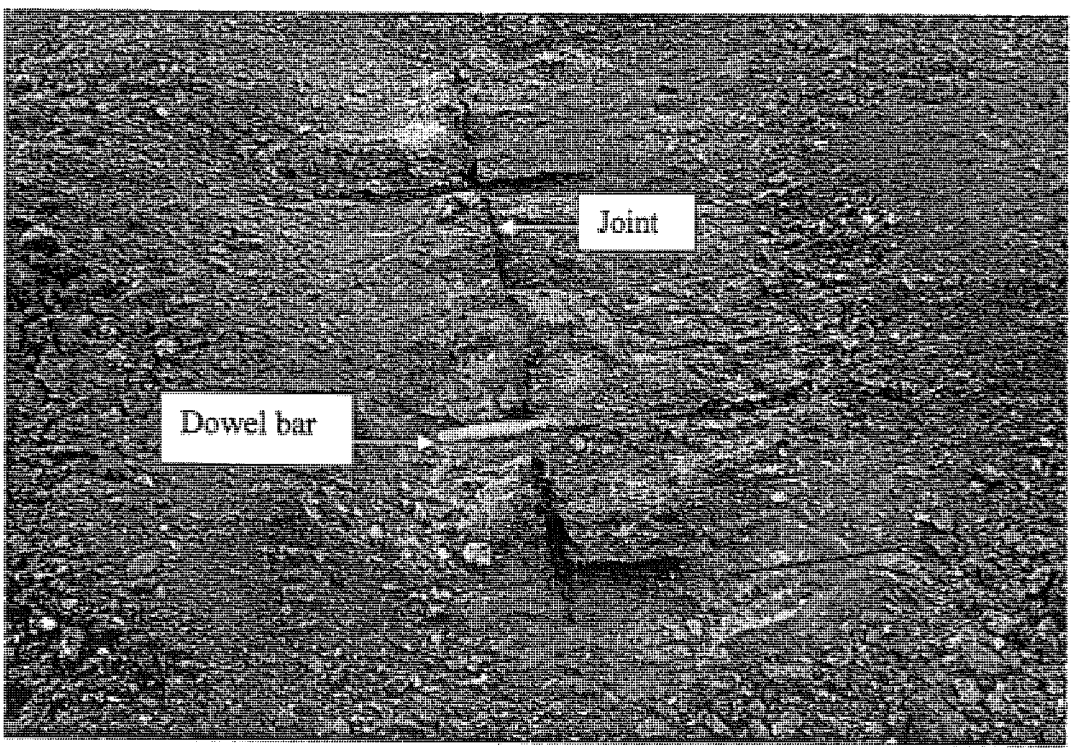

Figure 3.4 Partial destruction of the joint integrity (US 131)

4. On some projects, the drainability of the fractured concrete layer was poor (see figure 3.5). The layer would trap water that infiltrates through cracks in the asphalt layer. The trapped water under the asphalt layer would increase the stripping potential of the asphalt layer.

5. At some locations, the rubblization procedure caused some large concrete pieces (larger than 6 in.) to rotate and penetrate the underlying base or roadbed material. This implies that the base and/or the roadbed soil have failed in shear action (bearing capacity). This failure is mainly caused by soft base and/or roadbed soil.

6. For some projects, the frequency of the hammer drops and the speed of the equipment were set such that some large concrete pieces that were broken due to the impact of the first row of hammers were often struck again by the second row of hammers. At some locations, the second strike drove the broken concrete into the base/subbase layer causing shear failure. Such localized shear failure may cause depression in the AC. Calibration of the rubblizer speed and the drop frequency can overcome this problem.

7. On four projects (Old US-131, M-18, M-21 and M-53), after the water was placed on the fractured concrete surface, air bubbles were observed coming out of the cracks. When the cracks were saturated, the air bubbles stopped and the water did not drain. Another observation is that the water did not drain or permeate horizontally through the loose rubblized material, which made the pool walls. The implication of this observation is that if water infiltrates the asphalt layer through cracks, it could be trapped. This trapped water may cause softening of the loose rubblized material and stripping in the asphalt layer, which may lead to a lower pavement performance.

Tables 3.1 and 3.2 provide a summary of observations made during the Phase I Study of this investigation. The details were reported in an interim report that was submitted to MDOT at the conclusion of the Phase I study and are included in Appendix B of this report.

As can be seen from table 3.1, some of the pavement projects included in the investigation were rubblized using the multi-head breaker (for equipment details, see chapter 4) while others using the resonant frequency breaker. Examination of the rubblized materials and the fractured concrete and results of the permeability tests conducted in the trenches revealed two sets of information regarding concrete rubblization using the resonant frequency breaker and the multi-head breaker. The information is presented below along with the observations made during the drainability tests. The detailed observations are included in Appendix B.

2.1.1 The Resonant Frequency Breaker

The following observations are related to the operation of the resonant frequency breaker.

Table 3.1 Rubblizing equipment and the locations of trenches excavated at each project investigated during the Phase I Study

No	Project	Control section	Job number	Region	BMP	EMP	Rubblizing equipment	Trench locations
1	US-10 EB	67022	44986	North	9.657	12.087	Multi-head	19+867 - MS 20+144 - MS 20+389 - MS
2	US-23 SB	01052 04031 04031 04031 04031	32335 32335 32335 32335 44350	North	16.369 0.000 0.449 1.404 4.218	16.393 0.241 0.908 2.248 7.893	Resonant	465+21 -MS 465+85.5 - TJ
3	US-31 NB	10032	44113	North	11.430 13.905	13.874 14.340	Multi-head	26+130 - MS 26+652 - MS 26+680 - MS 27+324 - TJ 27+385 - TJ
4	US-31 SB	05011	44109	North	0.923	3.019	Multi-head	2+200 - MS 2+637 -MS
5	US-131 SB	41133 59012	33914	Grand	3.200 0.000	8.691 4.214	Resonant	37+558.5 - MS N/A - TJ N/A - MS
6	Old US-10 EB	56555 56041	48370	Bay	7.114	9.513	Resonant	25+064 - MS 25+594 - MS
7	Old US-131 NB	41401 41013	49321 45797	Grand	2.669 0.000	2.820 2.232	Resonant	9+858 - MS 10+690 - MS 11+641 - MS
8	M-18	26011	45410	North	4.860	12.000	Multi-head	3+180 - MS 3+194 - MS 4+034 - TJ
9	M-21	25081	38028	Bay	4.981	7.285	Multi-head	1+200 IL - MS 1+200 OL - MS 1+309 IL - TC 1+684 IL -MS
10	M-50	58042	43523	Univ.	0.143	4.521	Multi-head	10+441 -MS 10+803 - MS 11+151 -MS 12+000 - TJ
11	M-53	50012 44031	36021	Metro Bay	4.438 0.000 2.820 6.466	4.458 1.588 6.130 6.940	Multi-head	53+621 - MS 53+886 - TJ 53+900 - MS 54+210 - MS
12	Portage Road	39405	49551	SW	0.000	1.125	Resonant	3+609 - MS 3+901.5 - MS
13	Chicago Drive			Grand			Resonant	149+22 MS and 146+26 MS
14	US 27	37014	38205	Bay	0.00	1.53	Multi-head	1 trench MS and 1 at TJ
15	Beecher Road	STU25 402	50078 A	Bay			Multi-head	1+480 MS, 1+485 TJ, 1+322 MS and 1 + 140 MS

IL =Inner lane, OL =Outer lane, TJ =Transverse joint, MS =Mid-slab, TC =Transverse crack

Table 3.2 A summary of rubblization variables and observations made during the investigation of various projects

No.	Project	Rubblization process	Results of drainability tests
1	US-10 EB	• The quality of rubblization of the original concrete lane and widening strip varies from one location to another.	• Good drainage.
2	US-23 SB	• The quality of rubblization was poor along the concrete widening strip. • The original concrete lane was well rubblized to depths below the temperature steel., well-fractured concrete at the bottom • Poor rubblization at a transverse joint.	• No tests were conducted.
3	US-31 NB	• Most aggregates were broken, which indicates that the strength of the aggregate is less than that of the cement paste. • The quality of rubblization was good in all five trenches.	• Good drainage.
4	US-31 SB	• Shallow rubblization. • No steel was debonded in two trenches.	• Water drained laterally because of super-elevation.
5	US-131 SB	• Good rubblization in all three trenches. • Dowel bars were exposed.	• No tests were conducted.
6	Old US-10 EB	• Excellent rubblization through the entire concrete thickness in both trenches.	• Excellent drainage.
7	Old US-131 NB	• Good rubblization in two trenches. • Fair rubblization at the third trench.	• Poor drainage in 2 trenches
8	M-18 NB	• High amount of dust. • Poor quality of rubblization especially along the shoulder. • Few fractures were observed in the fractured concrete. • Dowel bars were exposed.	• Poor drainage in 2 trenches
9	M-21 WB	• Poor rubblization of the inner lane. • Fair rubblization of the outer lane. • A transverse crack had no apparent effect on the rubblization.	• Poor drainage in 2 trenches • Excellent drainage along the 4-ft concrete widening strip.
10	M-50 EB	• The quality of rubblization was excellent. • Dowel bars were exposed.	• No tests were conducted.
11	M-53 NB	• Poor rubblization at speed of 275-m/hr. • Good rubblization at speed of 245-m/hr. • The steel was poorly debonded.	• Poor drainage.
12	Portage Road	• Excellent rubblization through the entire concrete thickness in both trenches.	• No tests were conducted.
13	Chicago Drive	• Maximum of 4.5-in. rubblized material • Large pieces (1.5 to 2 ft)	• No tests were conducted
14	US 27	• Hammer bounces • Frequent large pieces (more than 6 in.) • No temperature steel debonding	• No tests were conducted
15	Beecher Road	• Poor rubblization at MS, TJ and cracks • Large pieces (more than 6 in.) throughout the project • Asphalt patches at cracks were not removed	• No tests were conducted

Figure 3.5 Trapped water above the fractured concrete in a trench (M-18)

1. On most projects, longitudinal strips of fine and coarse particles were found on the surface of the rubblized materials. The strips were evenly spaced at 175 mm (7 in.), which is almost the width of the resonant shoe. Further, on some projects, the rubblized material was about 1 in. higher than the adjacent unrubblized slab. This was expected because the rubblized material has a higher air void content than the original concrete slab.

2. In trenches made at transverse joints or cracks, large rubblized pieces of up to 250 mm (10 in.) were found above the temperature steel. The average coarse particle size was about 100 mm (4 in.). While in trenches made at mid-slab, the average rubblized particle size above the temperature steel was approximately 50 mm (2 in.).

3. In most trenches, steel debonding was achieved almost throughout the trench. However, in areas where the temperature steel overlaps, the two steel layers hindered the rubblization process by absorbing and/or deflecting part of its energy.

4. The rubblized concrete beneath the temperature steel appeared to be fractured concrete. The surface of the fractured concrete consists of peaks and valleys that extend in both longitudinal and transverse directions.

5. The cement mortar was stripped clean from a fair amount of aggregate.

6. In some trenches, the permeability of the rubblized concrete slabs was poor; water did not drain in more than 4 hours. This low permeability increases stripping potential.

2.1.2 The Multi-Head Breaker

The following observations were made in trenches excavated in pavement projects while being rubblized using the multi-head breaker:

1. In several areas along several projects, the strength of the subbase and/or subgrade material was exceeded. Hence, shear failure (bearing capacity failure) was evident upon the impact of the hammers (some large pieces of the concrete were broken off, rotated and penetrated the subbase material or the roadbed soil damaging both. Further, on some projects, the rubblized concrete was about 1 in. below the surface of the adjacent unrubblized concrete slab. This implies that on some projects, the rubblized concrete has penetrated the subbase or roadbed soils (shear failure).

2. In trenches that were made at mid-slab, the typical rubblized particle size above the temperature steel ranged from about 50 to 305 mm (2 to 12 in.). Some of the large pieces that were removed for more detailed inspection showed internal fractures.

3. Steel debonding was poor, in most trenches; about fifteen percent of the temperature steel was debonded. In areas where the temperature steel overlaps, no steel debonding was found. The two steel layers hindered the rubblization process by absorbing and/or deflecting part of its energy.

4. The rubblized concrete beneath the temperature steel appeared to be fractured concrete. The surface of the fractured concrete consists of peaks and valleys that extend in both longitudinal and transverse directions.

5. In some trenches, the permeability of the rubblized concrete was poor (water did not drain in more than 4 hours). This increases stripping potential.

2.2 FWD Testing and Coring

Nondestructive deflection tests were conducted on 18 rubblized projects. All tests were conducted using approximately 9,000-lb load. Each test consisted of four drops. The first drop was for instrument seating, which was not recorded while the last three drops were recorded. The layout of the FWS tests and core locations is shown in figure 3.6. The objectives of the tests were to:

1. Examine the structural capacity of the pavements.

2. Analyze the variation in the deflection data and hence in the structural capacity along and across the pavements.

3. Backcalculate the pavement layer and roadbed soil moduli.

4. Relate, if possible, variations in the deflection data to variation in the quality of rubblized pavements.

5. Compare the rubblized pavement responses to load to those of conventional flexible pavements.

At the conclusion of the FWD tests, several 6-in. diameter asphalt cores were extracted from the pavement. Some cores were located over a crack to verify whether or not the crack is a top-down crack. For these cores, the extent of the crack into the leveling and base course was also measured. The other cores were mostly located under the center of the load plate of the FWD. The cores were transported to the Pavement Research Center of Excellence where each core was examined and its thickness and the thickness of each asphalt course were measured and recorded. The average core thickness was then calculated and used in the backcalculation of the layer moduli. The cores were then tested to determine the physical and engineering properties (the specific gravity, resilient modulus and indirect tensile strength) of the asphalt concrete.

The breakdown of the FWD tests and coring between the Phase I and Phase II studies are listed in table 3.3. Seven rubblized pavement test sites were cored and nine

Table 3.3 List of rubblized and flexible pavement projects and the number of FWD tests conducted and cores obtained from each project.

Route	Control section	Job number	Test site*	Investigation date	Number of Cores			FWD test stations
					Total	Intact	With cracks /defects	
Investigated during Phase II								
I-69	76023	36020	10692-11	6/12/2001	12	10	0/2	40
I-69	76023	36020	10692-12	6/12/2001	12	9	0/3	40
I-75	16092	25559	10753-11	10/24/2001	14	11	3/0	42
I-75	16092	25559	10753-12	10/24/2001	15	12	3/0	43
I-194	13033	29670	11941-21	11/07/2001	15	10	5/0	43
I-194	13033	29670	11941-22	11/07/2001	15	8	5/2	43
US-10	53022	37974	20102-11	6/28/2001	12	12	-	40
US-10	53022	37974	20102-12	6/28/2001	12	12	-	40
US-23	04031	44350	20233-11	6/23/2001	11	10	0/1	52
US-23	04031	44350	20233-12	6/23/2001	10	7	0/3	30
US-27	37013	28116	20273-21	6/04/2001	15	11	4/0	45
US-27	37013	38205	20273-31	6/06/2001	12	12	-	40
US-27	37014	38205	20273-41	7/12/2001	12	12	-	40
US-31	70013	38179	20311-11	6/26/2001	12	12	-	40
M-15	25092	45534	30153-11	11/21/2001	16	12	4/0	43
M-37	41033	31068	30373-21	3/28/2001	10	7	0/3	24
M-37	41033	31068	30373-31	3/28/2001	9	3	4/2	-
M-37	41033	38190	30373-51	6/19/2001	12	12	-	40
M-37	41033	38190	30373-52	6/19/2001	12	12	-	40
M-37	41033	26691	30373-61	11/6/2001	18	15	2/1	42
US-27 [2]	37014	38205	20273-11	6/04/2001	12	-	-	39
M-37 [2]	61024		30373-41	6/08/2001	7	-	-	33
M-53	44031	36021	30531-11	11/02/1999	20	14	6/0	45
Investigated during Phase I								
I-96	23152	29581	10962-11	8/24/1999	-	-	-	28
I-96	33084	28213	10962-21	8/24/1999	5	-	5/0	29
I-96	33084	28213	10962-31	8/24/1999	7	2	5/0	37
I-96	33084	28213	10964-51	10/21/1999	2	-	2/0	36
I-194	13033	29670	11941-11	1999	10	0	10/0	-
US-131	41133	33914	21313-11	10/26/1999	-	-	-	30
US-131	03112	28143	21311-21	11/03/1999	-	-	-	34
US-131	03112	32373	21311-31	9/01/1999	-	-	-	51
M-37	41033	26691	30371-11	11/04/1999	5	0	5/0	-
M-37	41033	26691	30373-11	11/04/1999	4	0	4/0	83
I-96 [2]	23151	29581	10962-41	10/11/1999	-	-	-	34

1 A seven-digit designation number was assigned to each test site. The first digit represents the road type (1 = Interstate, 2 = U.S., 3 = Michigan). The second through the fourth digits represent the highway/route number. The fifth digit represents the traffic direction (1 = North, 2 = East, 3 = South, 4 = West). The sixth digit represents test section the number. The seventh digit represents test site number. For example, a designation number of 1194-12 implies I-194, northbound section 1 test site 2

2 Conventional flexible pavements

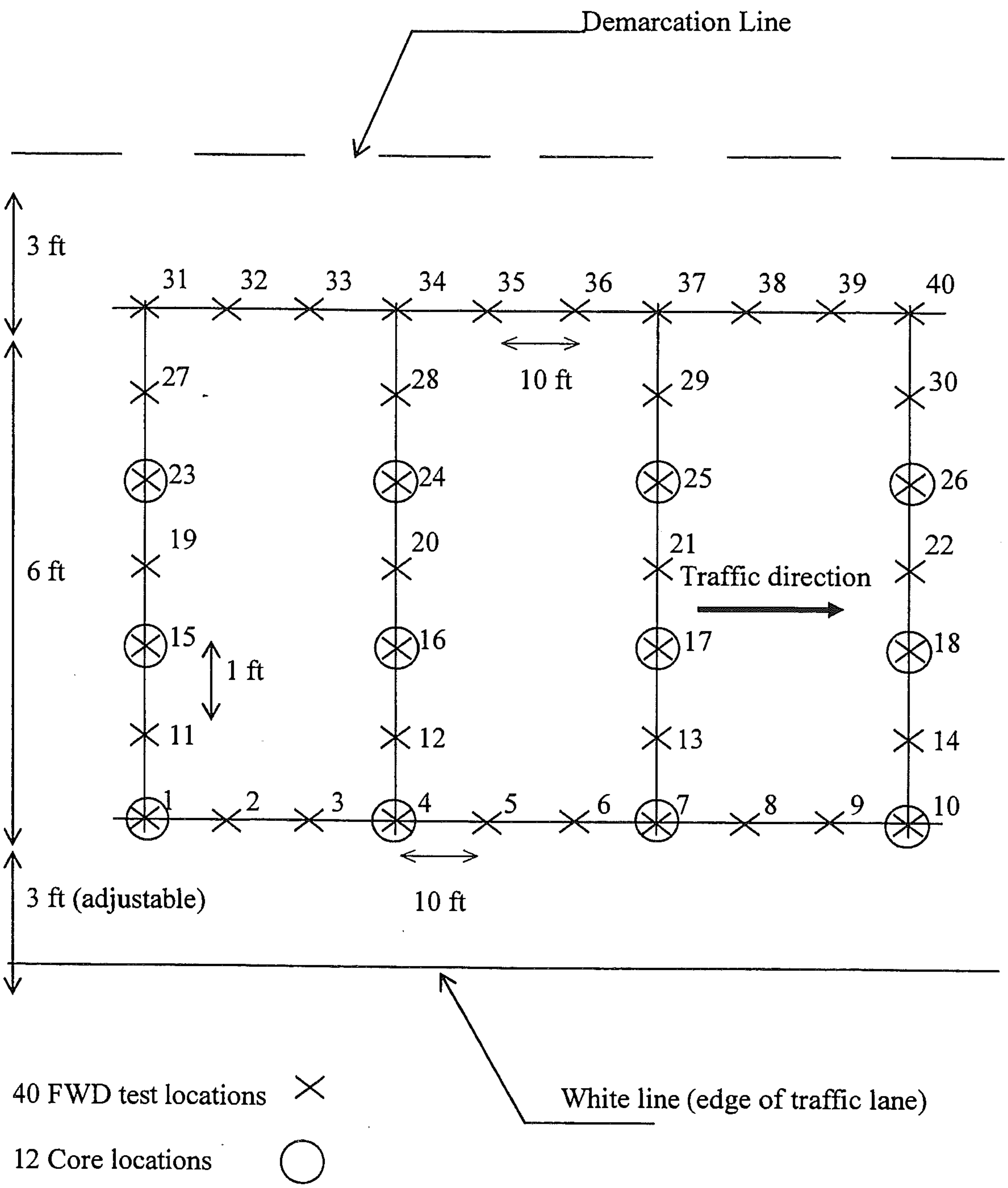

Figure 3.6 Standard layout of the FWD tests used in this study

rubblized and one flexible test sites were FWD tested during the Phase I study. In the Phase II study, twenty rubblized and two flexible test sites were cored and nineteen rubblized and two flexible test sites were FWD tested. Note that, in the Phase II study, the majority of the FWD tests were conducted according to the test location layout shown in figure 3.6. The letter "X" in the figure indicates an FWD test location while the letter "O" indicates a core location. At some test sites, the standard FWD tests and cores layout was slightly modified by adding few core locations (e.g., over a crack) and/or conducting additional FWD tests when required (e.g., repeatability and linearity). Detailed information regarding the test sites such as location, distresses observed within the test site area and others are presented in Appendix C. The measured deflection data at each test site are tabulated in Appendix D.

As stated above, during the Phase II study, special FWD tests were conducted on four test sites to check the accuracy of the FWD deflection data and the linearity of the pavement material response to load. In these tests, ten to twenty FWD tests were conducted at the same location at each of the following load levels: 5,500, 9,000, 16,000 and 21,000 lb. Table 3.4 provides a list of the number of the repeatability and linearity tests conducted at the four test sites. The measured linearity and repeatability deflection data are tabulated in Appendix E.

2.3 Distress Survey

Since MDOT collect distress data every other year and since rubblized projects are relatively new, only limited historical distress data were available in the PMS data files. Consequently, two manual distress surveys were undertaken by the research team to obtain two additional distress points in time. The first survey covered seventy five rubblized concrete pavement projects and was conducted between August 17 and September 2, 2001. The second survey was conducted in early May of 2002 and covered 79 rubblized projects. Note that only 70 rubblized projects were surveyed in both 2001 and 2002. Five rubblized projects that were surveyed in 2001 were not surveyed in 2002, on the other hand, nine rubblized projects that were surveyed in 2002, were not surveyed in 2001. By transferring the distress data from 2001 to 2002 and visa versa, manual distress data for 84 rubblized projects were obtained. Finally, in both surveys, the research team consisted of two persons and used the following procedure:

1. For each rubblized project, the inventory data (project location and boundaries, project age, asphalt mix types and rubblizing equipment) and the pavement historical distresses data were obtained from MDOT.

2. At each project location, the distress along the entire project was observed by driving on the right pavement shoulder at creep speed. During the drive notes were taken as to the consistency and uniformity of the pavement condition along the project.

3. After observing the general pavement condition, the survey crew walked along one to three 300-ft long segments located along the project. When the overall pavement condition was inconsistent, the research team walked or drove at creep speed along three 300-ft segment located at the beginning, middle and end of the project. On the

Table 3.4 A summary of the repeatability and linearity tests

Test sites	Load (lb)	Number of drops	Load (lb)	Number of drops	Load (lb)	Number of drops	Load (lb)	Number of drops
20273-21			9000	20	16000	10	21000	10
10692-12	5500	10	9000	20	16000	10	21000	10
30373-52	5500	10	9000	20	16000	10	21000	10
20102-11	5500	10	9000	20	16000	10	21000	10

other hand, when the pavement condition was uniform, the research team surveyed only one representative 300-ft long segment.

4. For each segment, detailed distress data were observed and recorded and digital images were obtained when needed for later verification. The distress data included the location, type, extent and severity of longitudinal and transverse cracks, raveling, segregation, patching, depression and other condition that adversely affect pavement performance. For transverse cracks, notes were made whether the cracks were reflective or regular (non-reflective). For longitudinal cracks, notes were made as to whether or not the cracks are likely TDC. Notes were also taken when longitudinal and/or transverse cracks have initiated in segregated areas.

5. For each surveyed segment, rut depth measurements were made at several locations using a 6 ft long beam.

6. For some projects, the research team drove along the project at the posted speed limit and observed and recorded the ride quality in terms of driving comfort.

The objectives of the distress survey were to:

1. Select pavement sections to be cored and FWD tested in late 2001 and early 2002.

2. Fill up the historical gaps in the MDOT PMS distress data and check its accuracy.

3. Determine the number of underperforming rubblized pavement projects exhibiting premature distresses.

4. Determine the number of rubblized project exhibiting TDC.

5. Determine the causes, if possible, of underperformance.

6. Estimate the rate of pavement deterioration.

7. Estimate the pavement structural and functional conditions in 2001 and 2002.

Summaries of the distress surveys conducted in August 2001 and 2002 are respectively provided in tables 3.5 and 3.6 in terms of the number of projects exhibiting certain types of distress. As can be seen from table 3.6, the distress data collected in May 2002 (all pictures were obtained in May 2002 unless indicated otherwise) indicate that:

1. Ten rubblized projects (about 11 percent of a total of 84 rubblized projects) showed no signs of distress.

2. Since 1988 when concrete pavement rubblization started, capital preventive maintenance and rehabilitation actions were taken on ten rubblized projects. These actions included mill and fill, AC overlay, chip seal and micro surfacing. Hence, for

Table 3.5 The number of projects exhibiting the indicated distress observed during the August 2001 distress survey

Distress type	No of projects	JTC	TTDC	RTC	LTDC	RLC	ALC	S	R	P	PH	RJ	Rut	B	BC	B-up	D
LTDC/TTDC/S/JTC/R/RTC/RLC/P/PH	1	1	1	1	1	1		1	1	1	1						
LTDC/TTDC/S/JTC/R/P/PH/Rut	1	1	1		1			1	1	1	1		1				
LTDC/TTDC/S/JTC/R/P/Rut/Break up	1	1	1		1			1	1	1			1			1	
LTDC/TTDC/S/JTC/Bleeding	1	1	1		1			1						1			
LTDC/TTDC/S/JTC/R/P	1	1	1		1			1	1	1							
LTDC/TTDC/S/JTC/R/RJ	1	1	1		1			1	1			1					
LTDC/TTDC/S/JTC/RLC/Rut	1	1	1		1	1		1					1				
LTDC/TTDC/S/JTC/Rut	2	2	2		2			2					2				
LTDC/TTDC/S/JTC/RTC	1	1	1	1	1			1									
LTDC/TTDC/S/JTC	3	3	3		3			3									
LTDC/TTDC/S/R/P/Rut	1		1		1			1	1	1			1				
LTDC/TTDC/S/Block crack	1		1		1			1							1		
LTDC/TTDC/S/R/RLC/Rut	1		1		1	1		1	1				1				
LTDC/TTDC/S/R	1		1		1			1	1				1				
LTDC/TTDC/S/R/Rut	1		1		1			1	1								
LTDC/TTDC/S/RJ/Rut	1		1		1			1				1	1				
LTDC/TTDC/S/RTC	1		1	1	1			1									
LTDC/TTDC/S/RLC	1		1		1	1		1									
LTDC/TTDC/S/Rut	1		1		1			1					1				
LTDC/TTDC/S	3		3		3			3									
LTDC/JTC/S/R/RTC	1	1		1	1			1	1								
LTDC/JTC/S/R/RLC/Rut	1	1			1	1		1	1				1				
LTDC/JTC/S/RTC/RLC/Rut	1	1		1	1	1		1					1				
LTDC/JTC/S	2	2			2			2									
LTDC/S/R/RTC/RLC	1			1	1	1		1	1								
LTDC/S/R/RLC/P/PH/RJ	1				1	1		1	1	1	1	1					
LTDC/S/RTC	1			1	1			1									
LTDC/S/RLC	1				1	1		1									
LTDC/S/RLC/RJ	1				1	1		1				1					
LTDC/S/RLC/P	1				1	1		1		1							
LTDC/S/Rut	1				1			1					1				
LTDC/S	5				5			5									
LTDC/RTC/P	1			1	1					1							

Table 3.5 The number of projects exhibiting the indicated distress observed during the August 2001distress survey (continued)

Distress type	No of projects	JTC	TTDC	RTC	LTDC	RLC	ALC	S	R	P	PH	RJ	Rut	B	BC	B-up	D
LTDC/RLC/RJ	1				1	1						1					
LTDC/Rut	1				1								1				
LTDC	2				2												
TTDC/JTC/S/RLC	1	1	1			1		1									
JTC/ALC/Rut	1	1					1						1				
JTC/RTC	1	1		1													
JTC/RLC/Rut	1	1				1							1				
JTC/RLC	1	1				1											
JTC	1	1															
S/Rut/Bleeding	1							1					1	1			
S/P	1							1		1							
S/PH	1							1			1						
S/RLC	2					2		2									
S/Depression	1							1									1
S	4							4									
RTC/RLC	1			1		1											
RLC	2					2											
RJ/Rut	1											1	1				
RJ	2											2					
Rut	2												1				
Bleeding	1													1			
No distress	12																
Total	**84**	**24**	**26**	**10**	**47**	**20**	**1**	**53**	**13**	**9**	**4**	**8**	**19**	**3**	**1**	**1**	**1**
Did not survey	2																
Not rubblized	2																

LTDC = Longitudinal top-down cracks, TTDC = Transverse top-down cracks, S = segregation, JTC Joint transverse crack, R = Raveling, RTC = Regular transverse crack, RLC = Regular longitudinal crack, P = Patch, PH = Pothole, RJ = Rough joint, D = Depression, B = Bleeding, ALC = Alligator cracks, BC = Block cracking, and B-up = Break up

Table 3.6 The number of projects exhibiting the indicated distress observed during the May 2002 distress survey

Distress type	No of projects	JTC	TTDC	RTC	LTDC	RLC	ALC	S	R	P	PH	RJ	Rut	B	BC	B-up	D
LTDC/TTDC/S/JTC/R/RTC/RLC/P/PH	1	1	1	1	1	1		1	1	1	1						
LTDC/TTDC/S/JTC/R/P/PH/Rut	1	1	1		1			1	1	1	1		1				
LTDC/TTDC/S/JTC/R/P/Rut/Break up	1	1	1		1			1	1	1			1			1	
LTDC/TTDC/S/JTC/R/P/Bleeding	1	1	1		1			1	1	1				1			
LTDC/TTDC/S/JTC/R/P	1	1	1		1			1	1	1							
LTDC/TTDC/S/JTC/R/RJ	1	1	1		1			1	1			1					
LTDC/TTDC/S/JTC/R/Rut	1	1	1		1			1	1				1				
LTDC/TTDC/S/JTC/RLC/Rut	1	1	1		1	1		1					1				
LTDC/TTDC/S/JTC/Rut/Bleeding	1	1	1		1			1					1	1			
LTDC/TTDC/S/JTC/Rut	2	2	2		2			2					2				
LTDC/TTDC/S/JTC	3	3	3		3			3									
LTDC/TTDC/S/R/P/Rut	1		1		1			1	1	1			1				
LTDC/TTDC/S/R/RLC/P/Block crack	1		1		1	1		1	1	1					1		
LTDC/TTDC/S/R/RLC/Rut	1		1		1	1		1	1				1				
LTDC/TTDC/S/R/Rut	1		1		1			1	1				1				
LTDC/TTDC/S/R	2		2		2			2	2								
LTDC/TTDC/S/RTC	1		1	1	1			1									
LTDC/TTDC/S/RLC	1		1		1	1		1									
LTDC/TTDC/S/Rut	1		1		1			1					1				
LTDC/TTDC/S	3		3		3			3									
LTDC/JTC/S/R/RTC	1	1		1	1			1	1								
LTDC/JTC/S/R/RLC/Rut	1	1			1	1		1	1				1				
LTDC/JTC/S/RTC/RLC/Rut	1	1		1	1	1		1					1				
LTDC/JTC/S/RTC	1	1		1	1			1									
LTDC/JTC/S	2	2			2			2									
LTDC/S/R/RTC/RLC	1			1	1	1		1	1								
LTDC/S/R/RLC/P/PH/RJ	1				1	1		1	1	1	1	1					
LTDC/S/R	1				1			1	1								
LTDC/S/RLC/RJ/Break up	1				1	1		1				1				1	
LTDC/S/RLC/RJ	1				1	1		1				1					
LTDC/S/RLC/P	1				1	1		1		1							
LTDC/S/Rut	1				1			1					1				

Table 3.6 The number of projects exhibiting the indicated distress observed during the May 2002 distress survey (continued)

Distress type	No of projects	JTC	TTDC	RTC	LTDC	RLC	ALC	S	R	P	PH	RJ	Rut	B	BC	B-up	D
LTDC/S	4				4			4									
LTDC/RTC/P	1			1	1					1							
LTDC/RLC/RJ	1				1	1						1					
LTDC/Rut	1				1								1				
LTDC	2				2												
TTDC/JTC/S/RLC/RJ	1	1	1			1		1				1					
TTDC/JTC/ALC/Rut	1	1	1				1						1				
JTC/RTC	1	1		1													
JTC/RLC/Rut	1	1				1							1				
JTC/RLC	1	1				1											
JTC	1	1															
S/R/RLC/P/PH	1					1		1	1	1	1						
S/P	1							1		1							
S/PH	1							1			1						
S/RJ	1							1				1					
S/RLC	1					1		1									
S/Depression	1							1									1
S	3							3									
RTC/RLC	2			2		2											
RTC	1			1													
RLC/RJ	1					1						1					
RLC	1					1											
RJ/Rut	2											2	2				
RJ	2											2					
Rut	1												1				
Bleeding	1													1			
No distress	10																
Total	**84**	**26**	**28**	**11**	**48**	**22**	**1**	**53**	**19**	**12**	**5**	**12**	**20**	**3**	**1**	**2**	**1**
Did not survey	2																
Not rubblized	2																

LTDC = Longitudinal top-down cracks, TTDC = Transverse top-down cracks, S = segregation, JTC Joint transverse crack, R = Raveling, RTC = Regular transverse crack, RLC = Regular longitudinal crack, P = Patch, PH = Pothole, RJ = Rough joint, D = Depression, B = Bleeding, ALC = Alligator cracks, BC = Block cracking, and B-up = Break up

those ten projects, the distress data listed in tables 3.5 and 3.6 were those observed on the new maintained or rehabilitated surface.

3. Fifty-three projects (58 percent) exhibited various degrees of segregation. On most of these projects, longitudinal and transverse TDC can be found in the segregated areas. Further, nineteen of these projects have developed various degrees of raveling in the segregated areas (see figures 3.7 and 3.8).

4. Longitudinal and transverse cracks are the dominant types of distress. Several types of longitudinal and transverse cracks were found as follows:

   a) Forty eight projects exhibited longitudinal TDC as shown in figure 3.9.
   b) Twenty eight projects exhibited transverse TDC as shown in figure 3.9.
   c) Twenty six projects exhibited joint reflective cracking as shown in figure 3.10.
   d) Eleven projects exhibited regular transverse cracks that are likely reflected from old cracks in the original concrete pavement as shown in figure 3.11.
   e) Twenty two projects exhibited regular longitudinal cracks (no TDC), seventeen of which are located near the longitudinal paving joints as shown in figure 3.12
   f) Only one project exhibited alligator type cracks in the wheel paths as shown in figure 3.13, which was taken in June 2001.

   Almost all the longitudinal and transverse TDC (items "a" and "b") are located in segregated areas. The reflective cracks in items "c" and "d" imply that the integrity of the joints in the concrete pavement was not destroyed and/or the temperature steel was not debonded.

5. Twelve projects exhibited roughness over transverse joints of the original concrete pavements of which eight projects did not develop transverse cracks as of August 2001. Further, on four projects, the reflective transverse cracks have already developed across some portions of the lanes while in the other portions the pavement exhibited rough joints only. A rough joint is a forerunner of reflective transverse cracks and is defined as a slight but measurable hump in the AC surface along the joint.

6. Twenty rubblized projects exhibited measurable rut. The rut depth varied from about 0.125 to slightly more than 0.5 in.

7. Potholes were found on five projects (see figure 3.14), patches on 12 projects (figure 3.15); three projects exhibited low severity bleeding; one project exhibited block cracking, pavement breakup was found on two projects, and one project exhibited depression along a limited area.

8. Shear failure (reported in the tables as patches) was found at three locations along I-196 south of Grand Rapids as shown in figure 3.16.

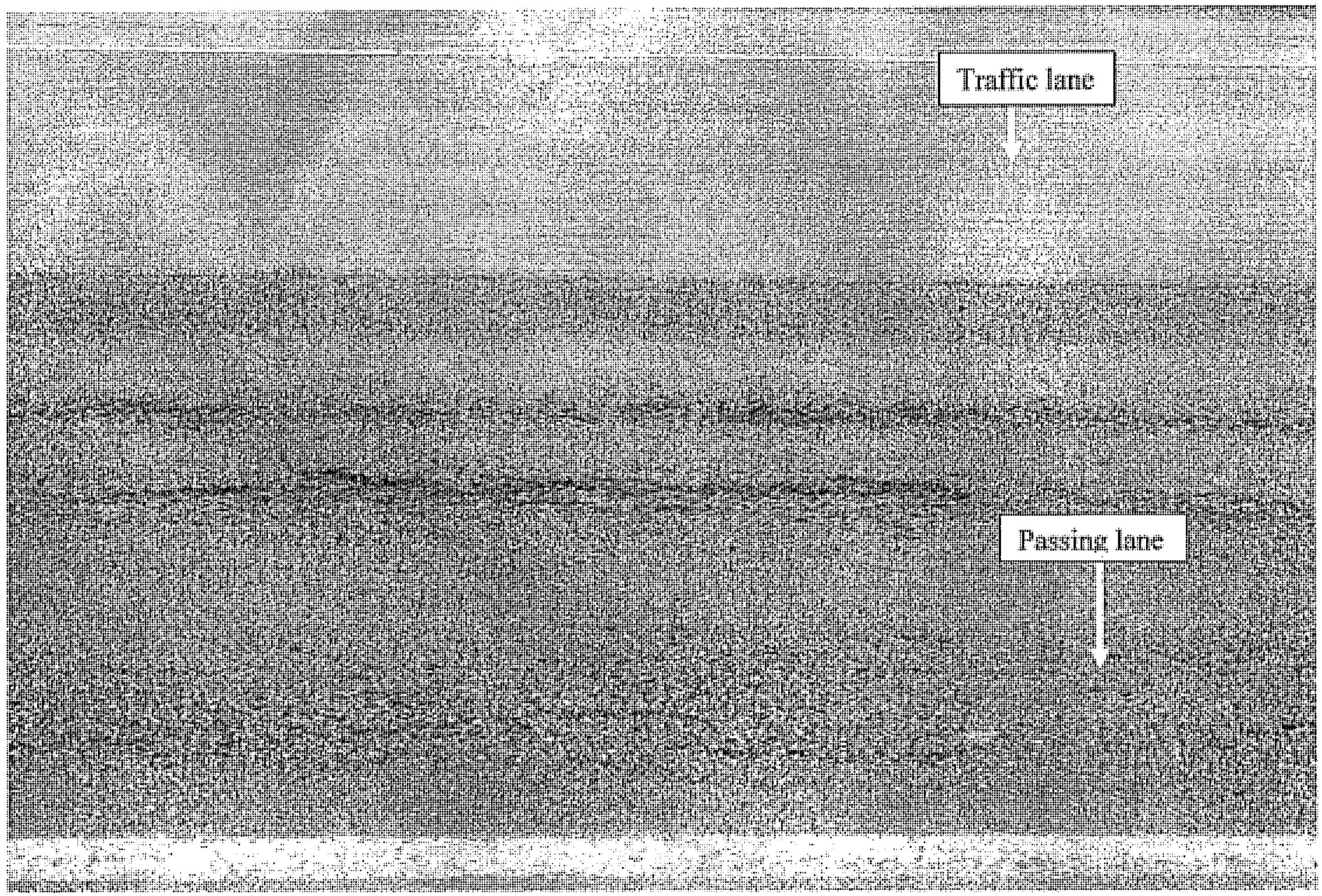

Figure 3.7 US-23 SB Control Section 47013, 47014 Job Number 29768 BMP 5.5, EMP 7.0; the relative pavement condition in segregated area (passing lane) and in a non-segregated area (traffic lane) 2-years after construction.

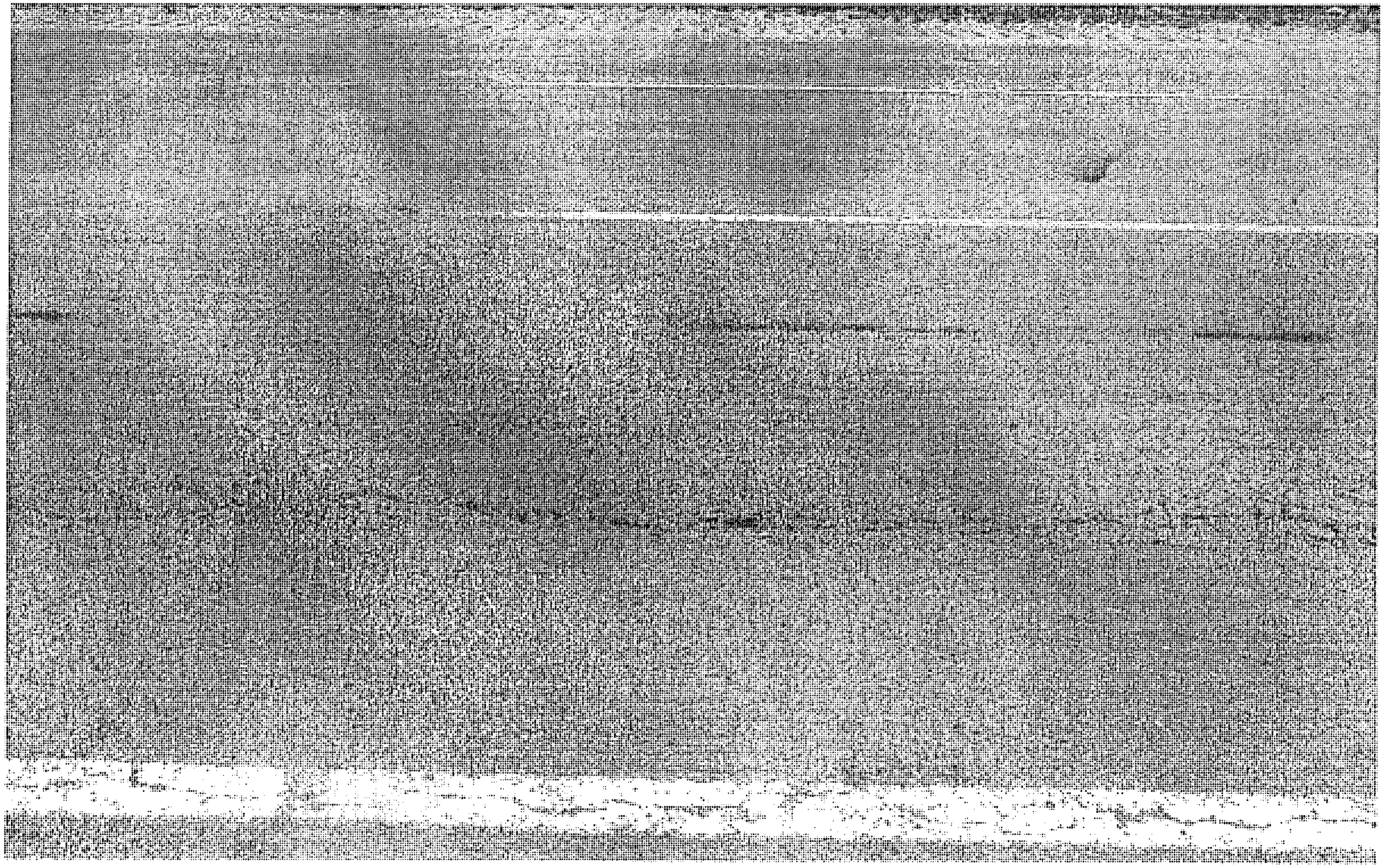

Figure 3.8 US 12 EB Control Section 81063 Job Number 26796 BMP 3.6, EMP 4.1; the pavement condition in segregated area

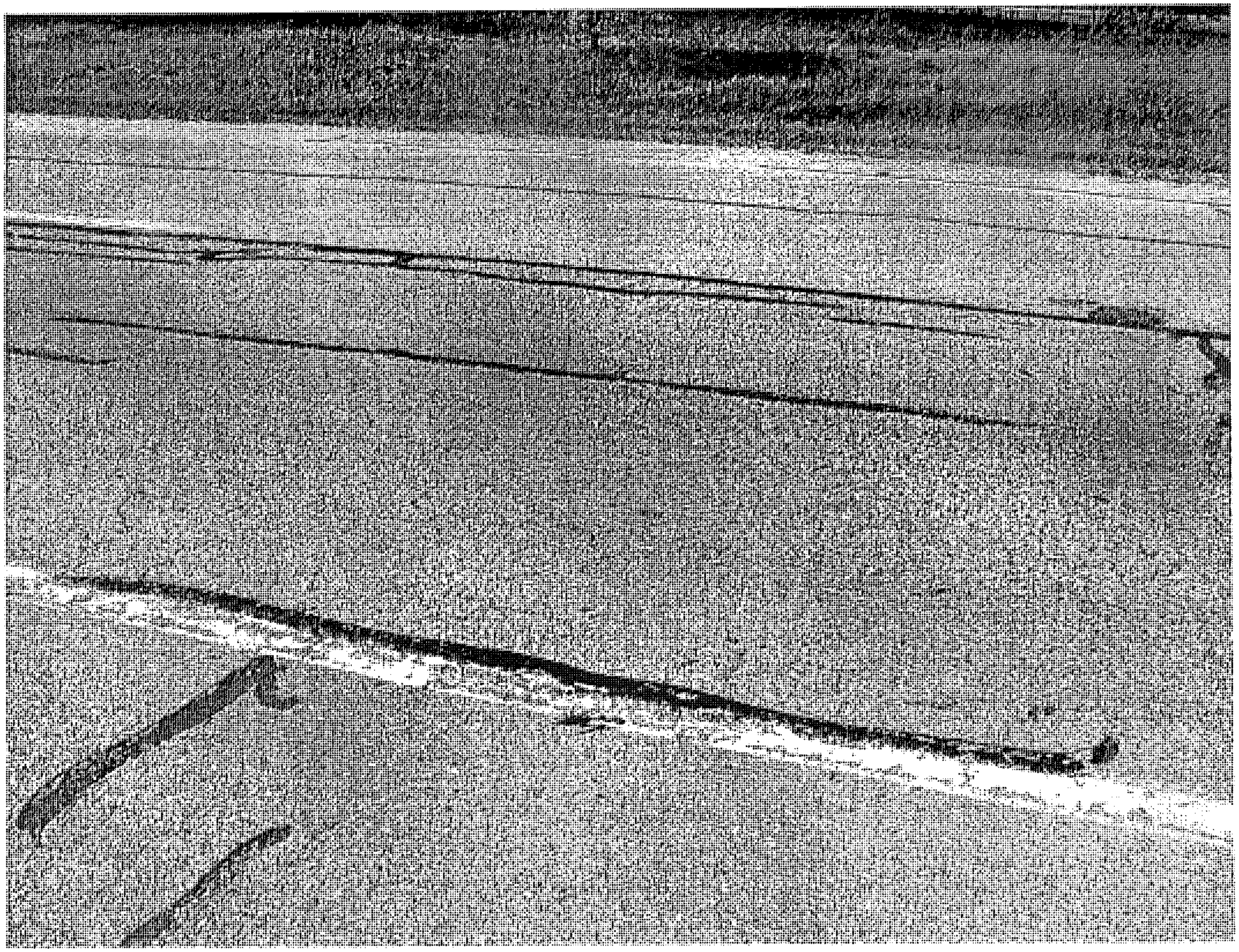

Figure 3.9 Longitudinal and transverse TDC on I-96 EB Control Section 33084 Job Number 28213 BMP 9.0, EMP 17.5

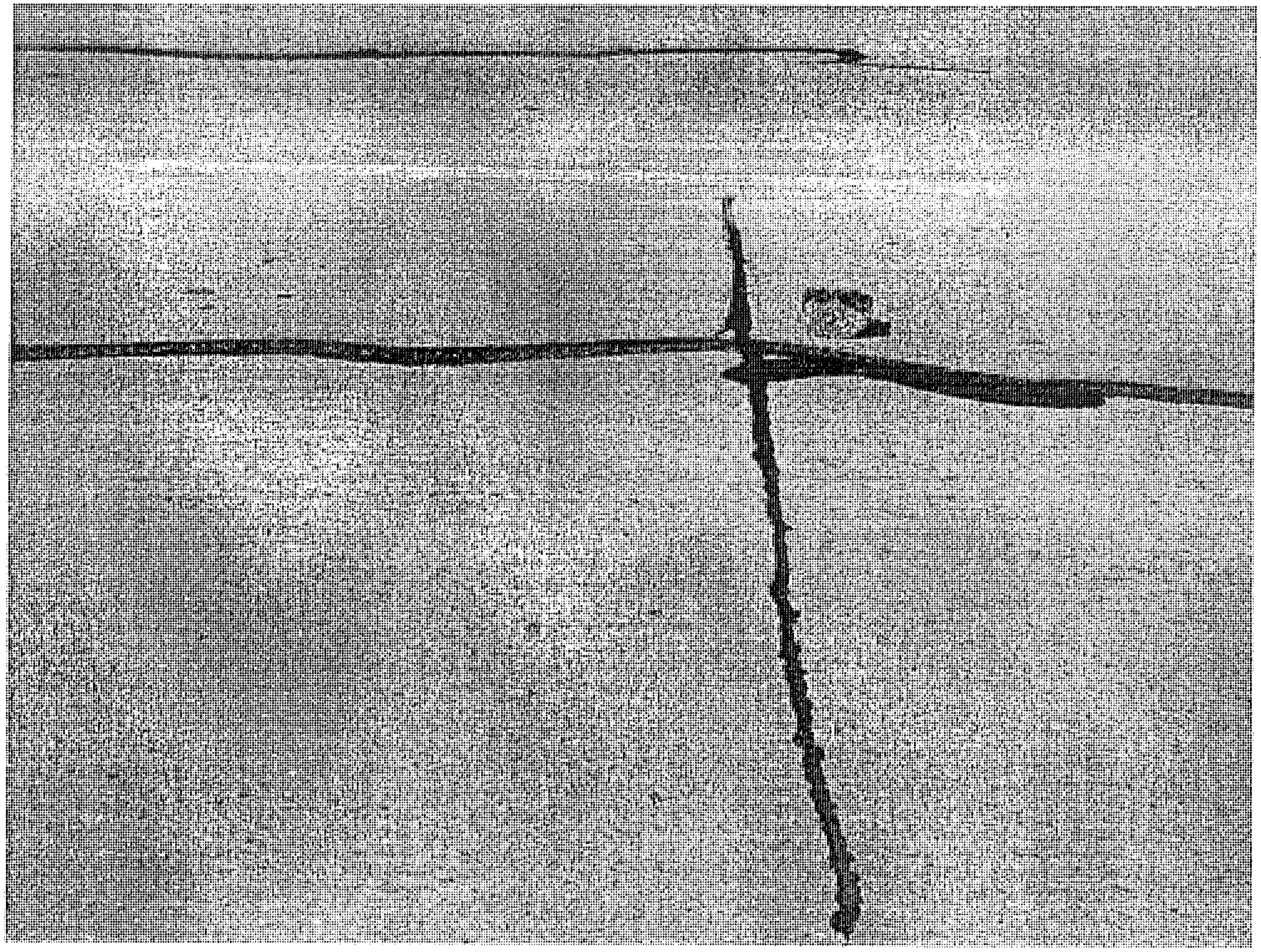

Figure 3.10 Reflective joint cracking on M-50, Control Section 46082 Job Number 30388 BMP 3.9 EMP 4.4

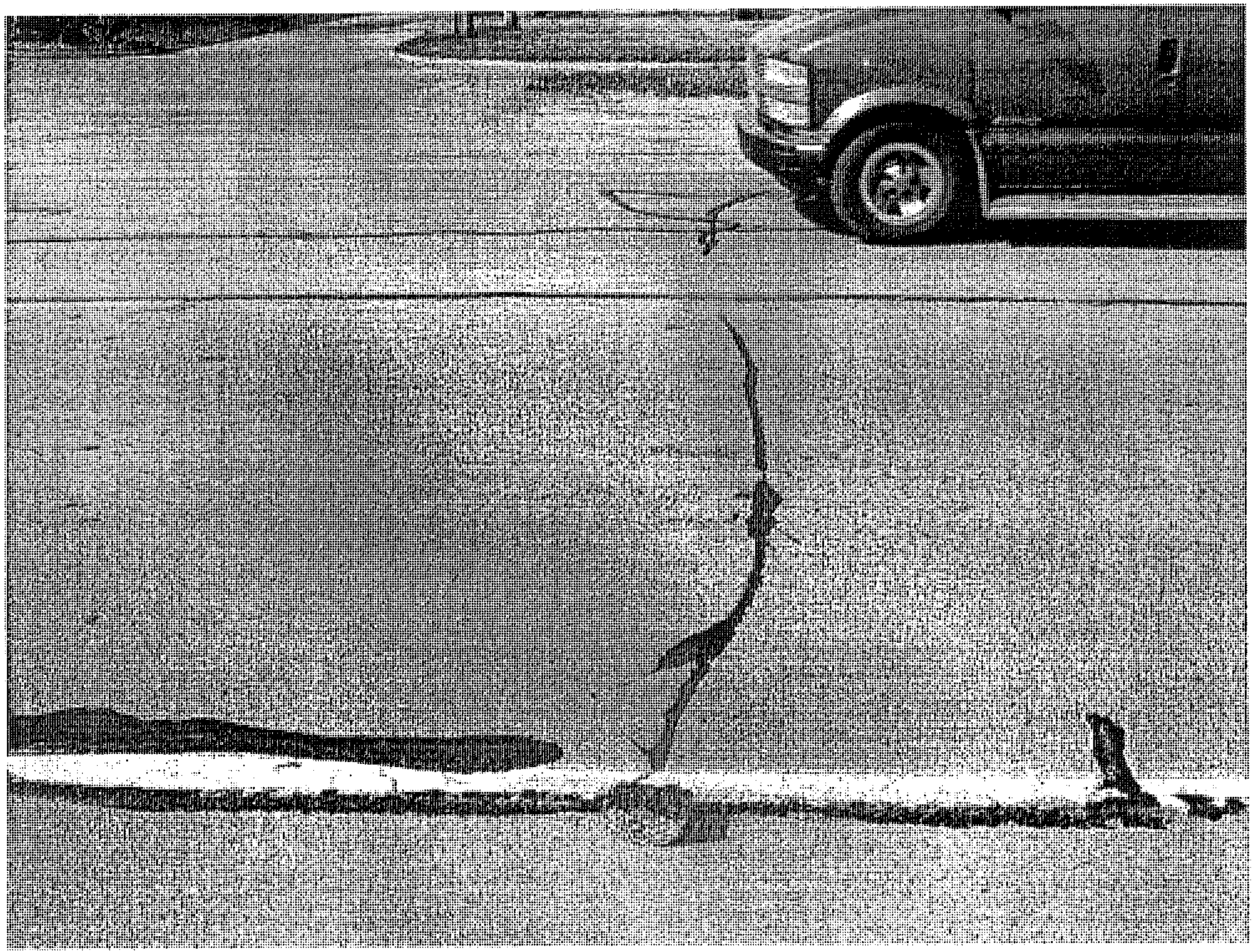

Figure 3.11 Reflective cracking on M-50, Control Section 46082 Job Number 32388 BMP 3.9, EMP 4.4

Figure 3.12 Longitudinal cracks by the paving joint on US-131, Control Section 83032 Job Number 34060 BMP 13.0, EMP 18.6

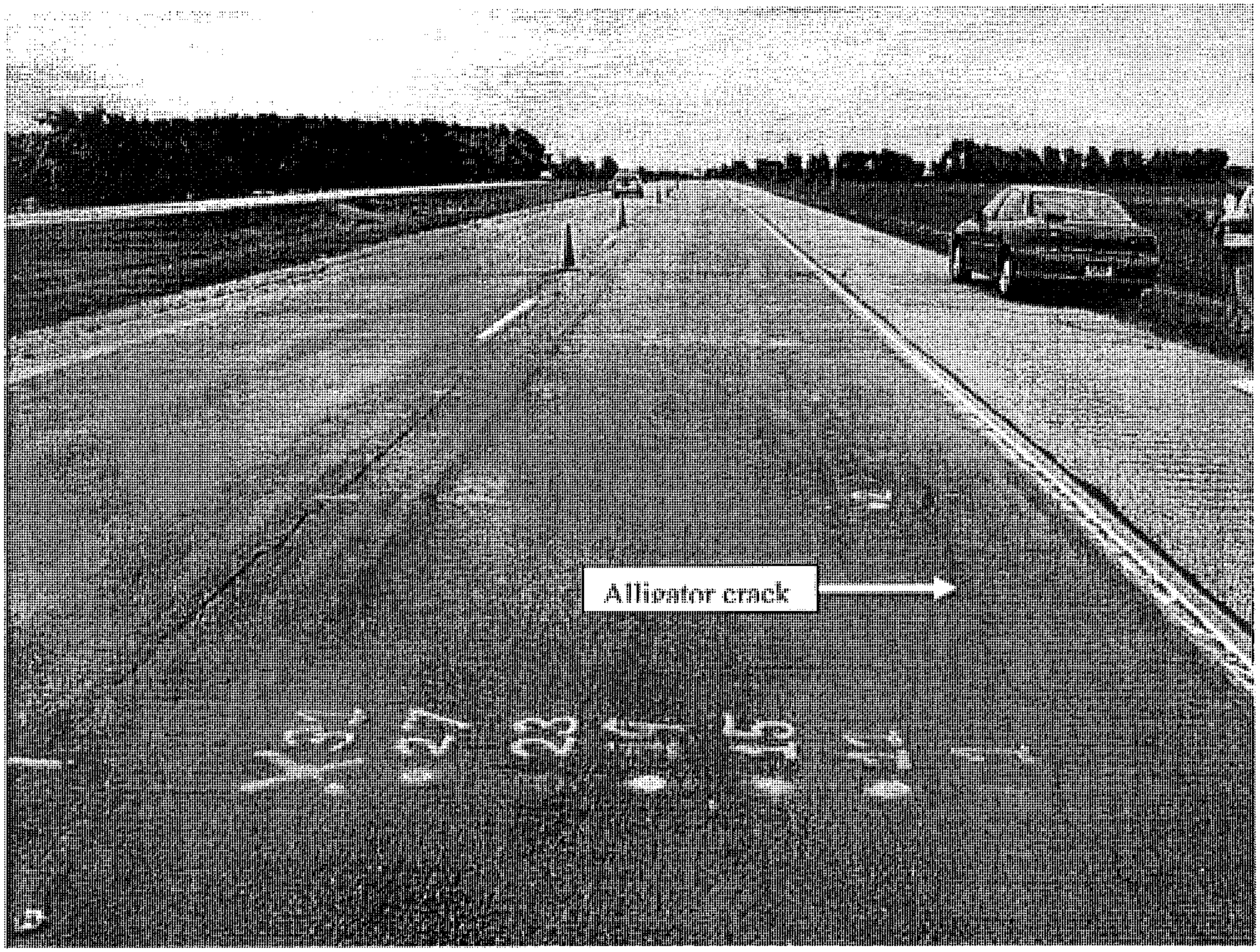

Figure 3.13 Alligator cracks in the wheel path, US-27, Control Section 37013 Job Number 28116 BMP 9.0, EMP 11.7, June 2001

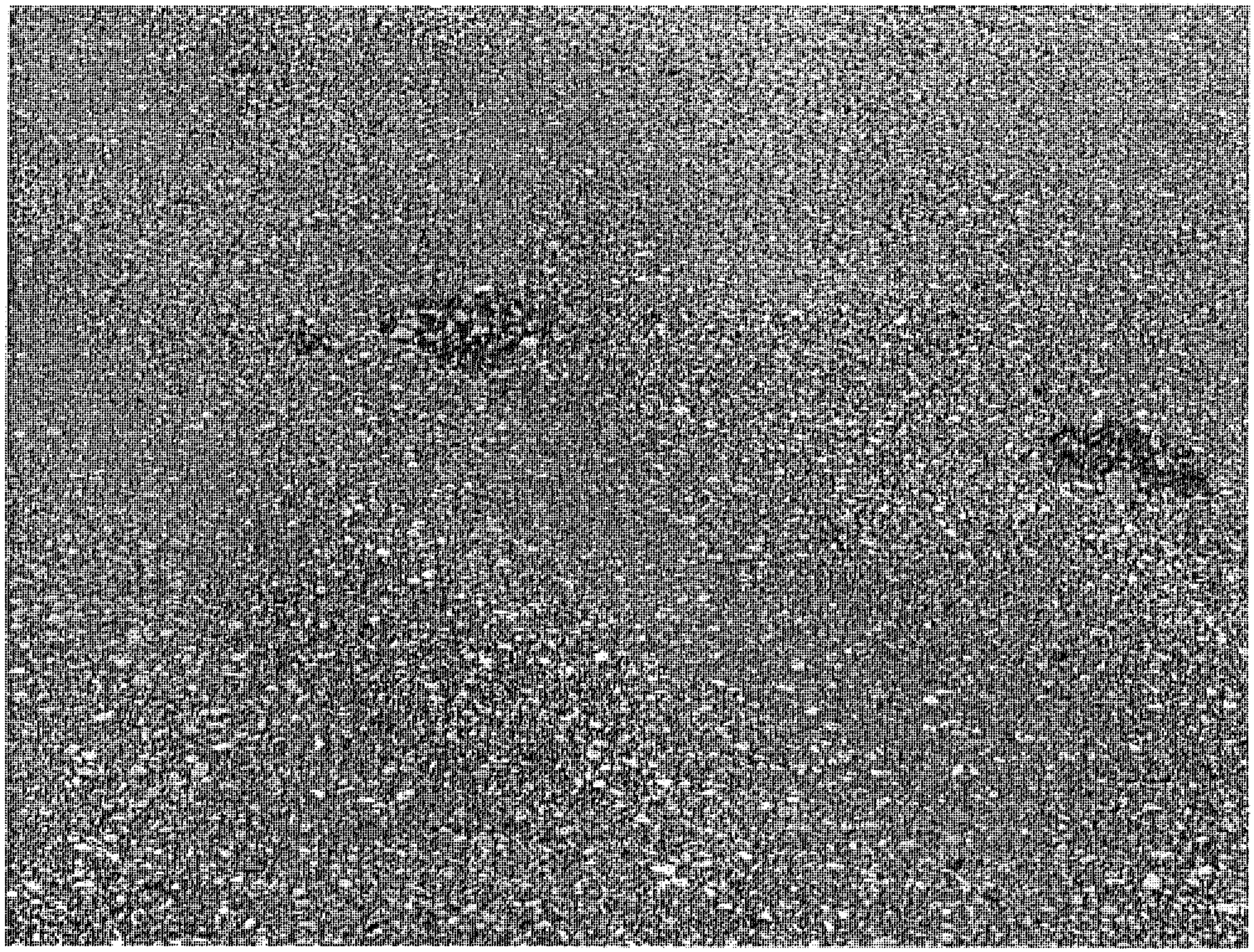

Figure 3.14 Pothole along US-131, Control Section 41133 Job Number 33914 BMP 3.2, EMP 8.7

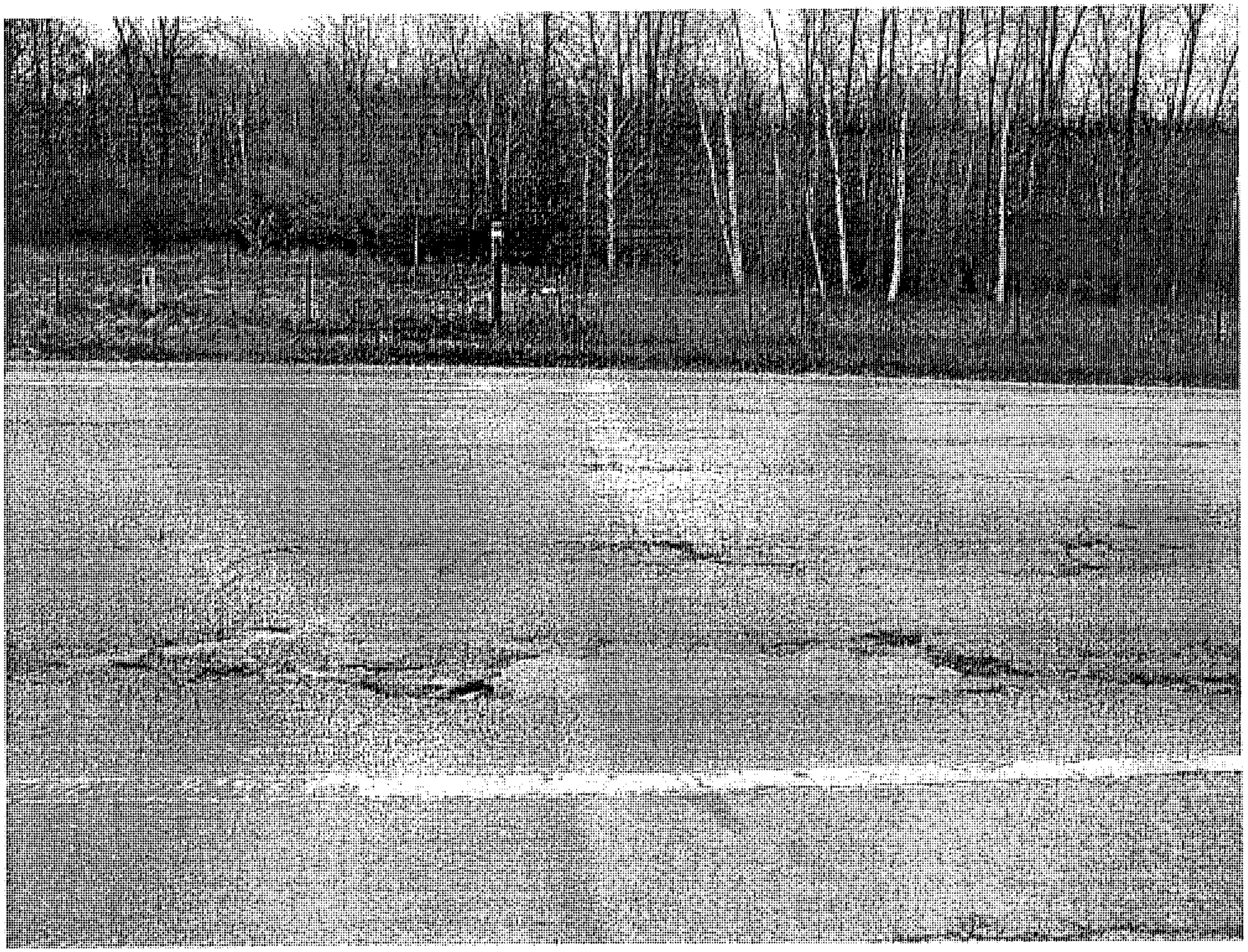

Figure 3.15 Patches along M-53, Control Section 74012 Job Number 29729 BMP 9.0, EMP 13.0

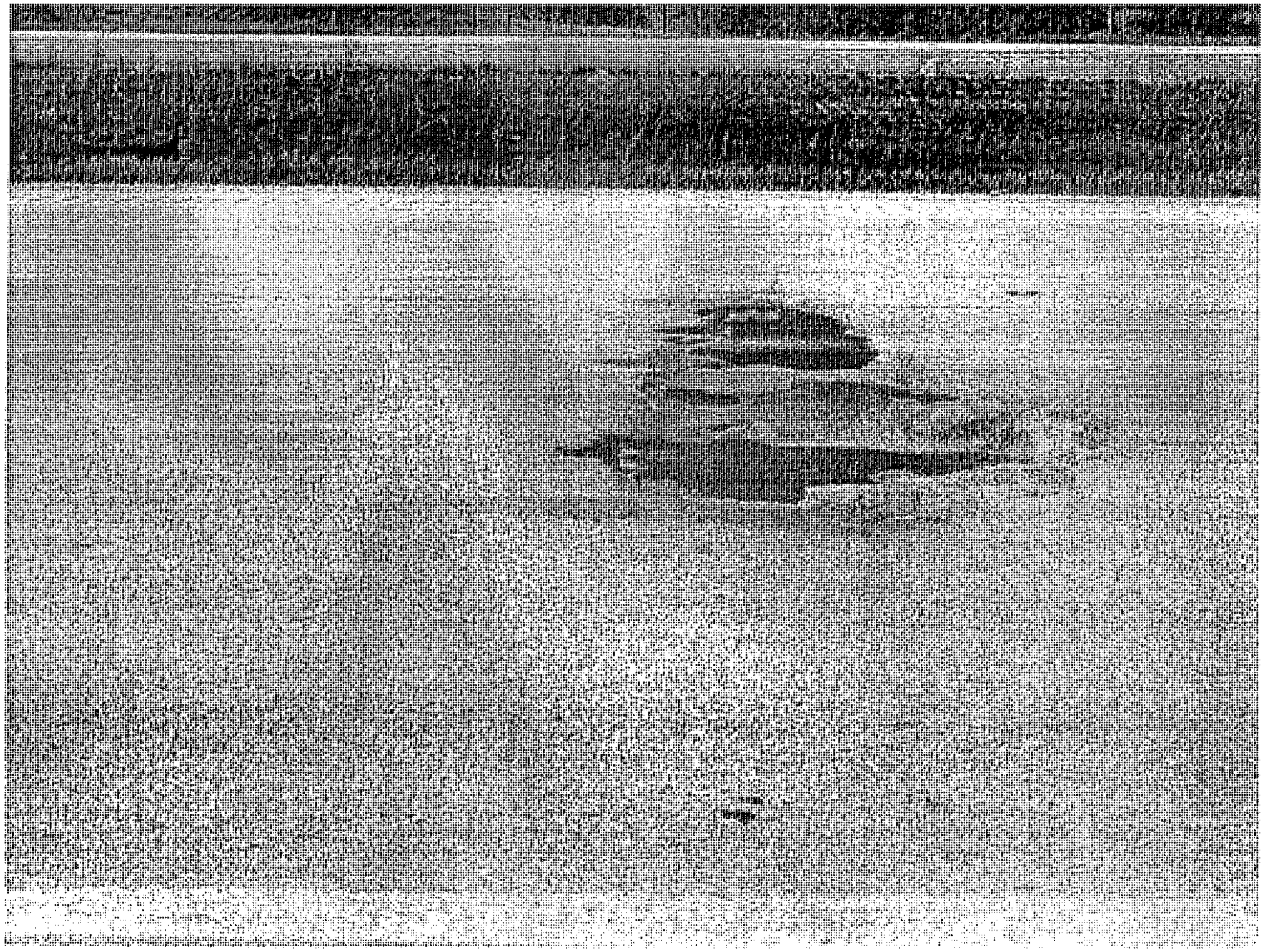

Figure 3.16 Shear failure along I-196 NB, Control Section 70024 Job Number 35987 BMP 12.6, EMP 15.6

Similar distress data were collected in 2001 and are summarized in table 3.5. The basic difference between the two tables is that, as expected, the total number of projects exhibiting certain type of distress has increased from 2001 to 2002 surveys.

Table 3.7 provides a list of the rubblizing equipment, the dominant types of distress, the type of asphalt mix, and the completion data of the 84 rubblized projects that were surveyed during this study.

3.0 LABORATORY INVESTIGATION

After the AC cores were extracted from the pavements during the field investigation, they were transported to the Pavement Research Center of Excellence (PRCE) to be tested in the laboratory. Each core was subjected to basically three tests in the following order:

1. Specific gravity test of the entire core and of each AC course. The data were used to estimate the percent air voids in the AC layer.

2. Indirect tensile cyclic load test (ITCLT) to determine the resilient modulus of each AC course and the weighted average modulus of the AC mat.

3. Indirect tensile strength test (ITST) to determine the tensile strength of the AC courses and the weighted average tensile strength of the AC mat.

The objectives of the tests were to:

1. Determine the weighted average physical and engineering characteristics of the AC mat.

2. Determine or calculate the physical and engineering properties of each AC course in the AC mat.

The steps that were taken during the sample preparation and details of each test are presented in the next sections.

3.1 Sample Preparation

In general, the AC cores that were extracted from the pavements could be divided into two categories; intact cores and cores with cracks and/or defects. Each core was carefully examined and cataloged. After cataloging all cores of one test site, the following steps were taken to prepare them for testing:

1. For each intact core, the diameter, the thickness of each AC course and the thickness of the core were measured. The latter was measured at the four ends of two orthogonal diameters and the average core thickness was calculated, recorded, and used in the backcalculation of the pavement layer moduli.

Table 3.7 List of rubblized pavement projects in Michigan

Control section	Job number	Route	Dir.[1]	Completion Date	POB	END	Rubblizer	Asphalt Mix			Distresses				
								Top	Level	Base	TTDC[2]	LTDC[3]	S[4]	Raveling	Rut depth (in)
10032	44113	US-31		9/30/1999	11.43	13.87	Multi -Head	4E3	4E3	3E3		Yes	Yes		
10032	44113	US-31		9/30/1999	13.91	14.34	Multi -Head	4E3	4E3	3E3		Yes	Yes		
21031	34050	M-35		7/23/1998	1.42	3.09	Multi -Head	4E3	3E3	3E3					
21031	34050	M-35		7/23/1998	8.70	10.43	Multi -Head	4E3	3E3	3E3					
38061	34106	M-60	EB	10/30/1998	12.65	16.41	Multi -Head	4E3	3E3	3E3		Yes	Yes		
38061	34106	M-60	WB	10/30/1998	12.65	16.42	Multi -Head	4E3	3E3	3E3		Yes	Yes		
58042	43523	M-50		6/15/1999	0.14	4.52	Multi -Head	4E3	3E3	3E3					1/8
58042	50711	M-50		7/6/2001	4.53	6.87	Multi -Head	4E3	3E3	3E3		Yes	Yes		
05011	44109	US-31		8/25/1999	0.92	3.02	Multi -Head	5E3	4E3	3E3			Yes		
25081	38028	M-21		10/30/1999	4.98	7.29	Multi -Head	5E3	4E3	3E3					
35032	35985	US-23		9/8/2000	19.12	22.01	Multi -Head	5E3	4E3	3E3			Yes		
41033	38190	M-37/M-46		5/12/2000	15.74	17.12	RMI	5E3	4E3	3E3	Yes	Yes	Yes		
53022	37974	US-10		9/28/2000	3.50	6.55	RMI	5E3	4E3	3E3					
53022	37974	US-10		9/28/2000	6.55	9.40	RMI	5E3	4E3	3E3					
61131	38190	M-37/M-46		5/12/2000	0.00	1.49	Multi -Head	5E3	4E3	3E3	Yes	Yes	Yes		
61171	38190	M-37/M-46		5/12/2000	0.00	0.57	RMI	5E3	4E3	3E3	Yes	Yes	Yes		
67022	44986	US-10		9/30/1999	9.66	12.09	Multi -Head	5E3	4E3	3E3					
41133	33914	US-131	NB	9/10/1999	3.20	8.69	RMI	4E10	3E10	3E10		Yes	Yes		
41133	33914	US-131	SB	9/10/1999	3.21	8.69	RMI	4E10	3E10	3E10		Yes	Yes		
41401	50230	Chicago Dr		10/31/2000	0.00	1.17	RMI	4E10	3E10	2E10			Yes		
59012	33914	US-131	NB	9/10/1999	0.00	4.21	RMI	4E10	3E10	3E10		Yes	Yes		
59012	33914	US-131	SB	9/10/1999	0.00	4.23	RMI	4E10	3E10	3E10		Yes	Yes		
37011	38205	US-27 BR		10/25/2000	0.00	0.46	Multi -Head	5E10	4E10	3E10			Yes		
37013	38205	US-27		6/1/2000	8.06	9.01	Multi -Head	5E10	4E10	3E10			Yes		

1, When no direction is specified, the pavement is rubblized in both directions; 2, TTDC = Transverse Top-Down Cracks; 3, LTDC = Longitudinal Top-Down Cracks; and 4, S = Segregation

Table 3.7 List of rubblized pavement projects in Michigan (continued)

Control section	Job number	Route	Dir.[1]	Completion Date	POB	END	Rubblizer	Asphalt Mix			Distresses				
								Top	Level	Base	TTDC[2]	LTDC[3]	SG[4]	Raveling	Rut depth (in)
37014	38205	US-27		6/1/2000	0.00	1.53	Multi -Head	5E10	4E10	3E10			Yes		
44031	36021	M-53		9/30/1999	0.00	1.59	Multi -Head	5E10	4E10	3E10		Yes	Yes		
44031	36021	M-53		9/30/1999	2.82	6.13	Multi -Head	5E10	4E10	3E10		Yes	Yes		
44031	36021	M-53		9/30/1999	6.47	6.94	Multi -Head	5E10	4E10	3E10		Yes	Yes		
50012	36021	M-53		9/3/1999	11.20	11.22	Multi -Head	5E10	4E10	3E10		Yes	Yes		
41026	35988	I-96	EB	10/30/1998	4.73	5.64	RMI	4E30	3E30	2E30					
41026	35988	I-96	EB	10/30/1998	5.87	6.10	RMI	4E30	3E30	2E30					
41026	35988	I-96	WB	10/30/1998	4.76	5.20	RMI	4E30	3E30	2E30					
41026	35988	I-96	WB	10/30/1998	5.51	6.07	RMI	4E30	3E30	2E30					
41131	35988	I-296	SB	10/30/1998	17.36	17.88	RMI	4E30	3E30	2E30					
41131	35988	I-296	NB	10/30/1998	17.59	17.76	RMI	4E30	3E30	2E30					
76023	36020	I-69		9/1/1998	0.04	5.93	Multi -Head	4E30	3E30	2E30		Yes	Yes		
16021	28111	M-68		11/14/1990	0.00	7.71	RMI	1100-20AA	1100-20AA	700 MOD-20C	Yes	Yes	Yes		1
20014	26755	I-75	SB	8/24/1990	0.00	3.73	RMI	1100-20AA	1100-20AA	700 MOD-20C					
34031	28115	M-66		10/24/1989	7.20	7.51	RMI	1100-20AA	1100-20AA	700 MOD-20C	Yes	Yes	Yes	Yes	3/8
34032	28115	M-66		10/24/1989	0.00	0.45	RMI	1100-20AA	1100-20AA	700 MOD-20C	Yes	Yes	Yes	Yes	3/8
34043	24662	I-96 Ramps		5/20/1987	11.63	12.03	RMI	1100-20AA	1100-20AA	700-20C					
56-52	33121	Saginaw Rd.		9/26/1992	13.27	13.74	RMI	1100-20AA	1100-20AA	700-20C	Yes	Yes	Yes		
17062	26637	M-28	EB	9/12/1989	18.69	22.29	RMI	1100-20AA	1100-20AA						
16032	26672	M-27		9/8/1990	1.00	2.57	RMI	1100-20AAA	1100-20AAA	700 MOD-20C	Yes	Yes	Yes	Yes	
16032	26672	M-27		9/8/1990	9.31	9.58	RMI	1100-20AAA	1100-20AAA	700 MOD-20C	Yes	Yes	Yes	Yes	
16032	26672	M-27		9/8/1990	9.66	11.38	RMI	1100-20AAA	1100-20AAA	700 MOD-20C	Yes	Yes	Yes	Yes	

Table 3.7 List of rubblized pavement projects in Michigan (continued)

Control section	Job number	Route	Dir.[1]	Completion Date	POB	END	Rubblizer	Asphalt Mix			Distresses				
								Top	Level	Base	TTDC[2]	LTDC[3]	SG[4]	Raveling	Rut depth (in)
16092	25559	I-75		12/6/1988	13.19	15.22	RMI	1300-20AAA	1300-20AAA	700-20C	Yes	Yes	Yes		
33403	33597	Jolly Road		6/1/1993	2.11	3.69	RMI	1300-20AAA	1300-20AAA	1300-20AAA					
61555	35396	Airline Rd.		6/25/1996	0.00	0.44	RMI	1300-20AAA	1300-20AAA	700-20C					3/8
61555	39233	Third Avenue		9/30/1996	0.40	0.84	RMI	1300T, 20AAA	1300L, 20AAA	700, 20C		Yes			3/4
25402	50078	Beecher Rd		10/15/2000	0.00	0.99	Multi -Head	13A	13A	700, 20C					
26011	45410	M-18		7/31/1999	4.86	12.00	Multi -Head	13A	13A	13A	Yes	Yes	Yes		
56200	35269	Saginaw Rd.		8/26/1994	9.52	12.11	RMI	13A	N/A	11A		Yes	Yes	Yes	
56555	35266	Saginaw Rd.		8/26/1994	0.00	3.57	RMI	13A	N/A	11A		Yes	Yes	Yes	
56555	48370	Saginaw Rd.		9/30/1999	7.11	9.51	RMI	13A	13A						
65555	39235	Old M-76		8/8/1996	5.24	6.60	RMI	13A	13A	11A	Yes	Yes	Yes		
65555	44467	Old M-76		8/20/1998	1.01	3.21	Multi -Head	13A	13A	11A	Yes	Yes	Yes		1/8
74073	33937	M-25		7/2/1998	0.48	4.94	RMI	13A	13A	13A	Yes	Yes	Yes		
64555	39385	Third Street		8/30/1998	0.13	0.44	RMI	13A-MOD	13A-MOD						
82400	44388	Larned St.		6/1/1998	0.00	1.49	Multi -Head	1500 T	31 A	1100 L	Yes	Yes	Yes		
09042	28163	M-25	EB	8/24/1990	0.06	1.27	RMI	1500-20AAA	1500-20AAA	700-MOD		Yes	Yes		
09101	28163	US-10	EB	11/1/1989	0.92	7.36	RMI	1500-20AAA	1500-20AAA	700-MOD		Yes	Yes		
09101	28163	US-10	EB	9/8/1990	9.12	11.36	RMI	1500-20AAA	1500-20AAA	700-MOD		Yes	Yes		

Table 3.7 List of rubblized pavement projects in Michigan (continued)

Control section	Job number	Route	Dir.[1]	Completion Date	POB	END	Rubblizer	Asphalt Mix			Distresses				
								Top	Level	Base	TTDC[2]	LTDC[3]	SG[4]	Raveling	Rut depth (in)
13081	24112	I-94	EB	6/8/1988	2.47	5.65	RMI	1500-20AAA	1500-20AAA	900 MOD-20C					
13081	24112	I-94	WB	6/8/1988	2.47	5.65	RMI	1500-20AAA	1500-20AAA	900 MOD-20C					
41131	21089	US-131	NB	6/12/1990	6.47	10.14	RMI	1500-20AAA	1500-20AAA	700 Mod-20C					1/2
41131	21089	US-131	SB	6/12/1990	6.47	10.32	RMI	1500-20AAA	1500-20AAA	700 Mod-20C					1/2
47555	29902	Old US-16		10/29/1990	0.00	1.41	RMI	1500-20AAA	1500-20AAA	700-20C		Yes	Yes		3/4
47013	29768	US-23	NB	10/15/1992	5.49	6.95	RMI	1500-20AAA	1500-20AAA		Yes	Yes	Yes	Yes	
47013	29768	US-23	SB	10/15/1992	5.49	6.95	RMI	1500-20AAA	1500-20AAA		Yes	Yes	Yes	Yes	
47014	29768	US-23	NB	10/15/1992	0.00	7.17	RMI	1500-20AAA	1500-20AAA		Yes	Yes	Yes	Yes	
47014	29768	US-23	SB	10/15/1992	0.00	7.17	RMI	1500-20AAA	1500-20AAA		Yes	Yes	Yes	Yes	
82400	44388	Lafayette St.		7/10/1998	0.00	1.03	RMI	1501 T	32	1101 L	Yes	Yes	Yes		
41013	31067	M-44	EB	8/13/1993	0.70	2.67	RMI	3B	3B	2B		Yes	Yes	Yes	1/4
41013	31067	M-44	WB	8/13/1993	0.70	2.67	RMI	3B	3B	2B		Yes	Yes	Yes	1/4
41033	31068	M-37	NB	9/13/1995	7.93	10.61	RMI	3B	3B	2B			Yes		
41033	31068	M-37	NB	9/13/1995	10.76	15.82	RMI	3B	3B	2B			Yes		
41033	31068	M-37	SB	9/13/1995	7.97	10.61	RMI	3B	3B	2B			Yes		
41033	31068	M-37	SB	9/13/1995	10.76	15.81	RMI	3B	3B	2B			Yes		
01052	31045	US-23		10/29/1996	0.49	2.47	RMI	4B	3B	3B		Yes	Yes		
03555	35605	Blue Star Hwy		5/30/1997	3.54	3.93	RMI	4B	3B	N/A		Yes			
03555	35605	Blue Star Hwy		5/30/1997	3.98	4.01	RMI	4B	3B	N/A		Yes			
13033	29670	I-194/M-66		6/4/1993	0.49	1.68	RMI	4B	3B	3B	Yes	Yes	Yes		1/8

Table 3.7 List of rubblized pavement projects in Michigan (continued)

Control section	Job number	Route	Dir.[1]	Completion Date	POB	END	Rubblizer	Asphalt Mix			Distresses				
								Top	Level	Base	TTDC[2]	LTDC[3]	SG[4]	Raveling	Rut depth (in)
13033	37138	M-66/I-194	NB	8/22/1997	0.06	0.49	RMI	4B	3B	3B		Yes			
13033	37138	M-66/I-194	SB	8/22/1997	0.02	0.49	RMI	4B	3B	3B		Yes			
25092	29727	M-15		9/22/1994	8.61	8.90	RMI	4B	3B	2B					
28091	34060	US-131		9/25/1997	0.00	0.13	Multi -Head	4B	3B	3B	Yes	Yes	Yes	Yes	1/2
33555	35233	Grand River		9/9/1998	0.10	1.06	RMI	4B	3B	3B		Yes	Yes	Few	
37013	28116	US-27	NB	10/14/1993	8.95	11.72	RMI	4B	3B	2B	Yes				1/5
37013	28116	US-27	SB	10/14/1993	8.95	11.36	RMI	4B	3B	2B	Yes				1/5
37013	28116	US-27	SB	10/14/1993	11.45	11.72	RMI	4B	3B	2B	Yes				1/5
37014	38206	US-27	NB	10/7/1997	7.15	14.43	RMI	4B	3B	2B	Yes	Yes	Yes		1/8
37014	38206	US-27	NB	7/31/1998	1.54	7.71	RMI	4B	3B	2B	Yes	Yes	Yes		1/8
37014	38206	US-27	SB	10/7/1997	7.21	14.51	RMI	4B	3B	3B	Yes	Yes	Yes		1/8
37014	38206	US-27	SB	7/31/1998	1.57	7.14	RMI	4B	3B	3B	Yes	Yes	Yes		1/8
41401	37494	Chicago Dr		10/16/1995	0.01	0.37	RMI	4B	3B	3B	Yes	Yes	Yes	Yes	1/8
46082	32388	M-50		9/29/1997	3.94	4.37	Multi -Head	4B	3B	3B	Yes	Yes	Yes	Yes	1/8
46082	32388	M-50		9/29/1997	0.11	1.82	Multi -Head	4B	3B	3B	Yes	Yes	Yes	Yes	1/8
46082	32388	M-50		9/29/1997	4.59	7.13	Multi -Head	4B	3B	3B	Yes	Yes	Yes	Yes	1/4
46082	32388	M-50		7/15/1998	9.58	12.38	Multi -Head	4B	3B	3B	Yes	Yes	Yes	Yes	1/8
56021	35139	M-20	WB	10/22/1994	6.05	10.59	RMI	4B	3B	2B	Yes	Yes	Yes		3/4
58041	32388	M-50		7/15/1998	0.00	5.02	Multi -Head	4B	3B	3B	Yes	Yes	Yes	Yes	1/8
58111	34596	M-50		6/15/1996	1.86	2.25	RMI	4B	3B	2B		Yes			
61407	56926	Airline Dr.		10/1/2000	0.00	0.64	RMI	4B	3B	3B					
70024	35989	I-196	EB	8/20/1997	6.58	10.58	RMI	4B	3B	3B	Yes	Yes	Yes	Yes	1/8
74012	29729	M-53		8/25/1995	9.00	13.00	RMI	4B	3B	3B	Yes	Yes	Yes	Yes	1/4
81063	26796	US-12	EB	11/9/1996	3.61	4.09	Whip Hammer	4B	3B	3B	Yes	Yes	Yes	Yes	

Table 3.7 List of rubblized pavement projects in Michigan (continued)

Control section	Job number	Route	Dir.[1]	Completion Date	POB	END	Rubblizer	Asphalt Mix			Distresses				
								Top	Level	Base	TTDC[2]	LTDC[3]	SG[4]	Raveling	Rut depth (in)
81063	26796	US-12	EB	11/9/1996	4.20	5.12	Whip Hammer	4B	3B	3B	Yes	Yes	Yes	Yes	
81063	26796	US-12	EB	11/9/1996	5.29	5.85	Whip Hammer	4B	3B	3B	Yes	Yes	Yes	Yes	
81063	26796	US-12	WB	11/9/1996	3.98	4.73	Whip Hammer	4B	3B	3B	Yes	Yes	Yes	Yes	
81063	26796	US-12	WB	11/9/1996	4.84	5.08	Whip Hammer	4B	3B	3B	Yes	Yes	Yes	Yes	
81063	26796	US-12	WB	11/9/1996	5.36	5.51	Whip Hammer	4B	3B	3B	Yes	Yes	Yes	Yes	
81063	26796	US-12	WB	11/9/1996	5.63	5.94	Whip Hammer	4B	3B	3B	Yes	Yes	Yes	Yes	
83032	34060	US-131		9/25/1997	12.97	18.66	Multi -Head	4B	3B	3B	Yes	Yes	Yes	Yes	1/2
1052	32335	US-23		11/1/1999	16.37	16.39	RMI	4C	3C	2C		Yes	Yes		
04031	32335	US-23		11/1/1999	0.00	0.24	RMI	4C	3C	2C		Yes	Yes		
04031	44350	US-23		11/1/1999	4.22	7.89	RMI	4C	3C	2C		Yes	Yes		
04032	32336	US-23		11/1/1999	0.45	0.91	RMI	4C	3C	2C		Yes	Yes		
04033	32337	US-23		11/1/1999	1.40	2.25	RMI	4C	3C	2C		Yes	Yes		
12555	39160	Broadway St.		10/25/1997	0.01	0.04	RMI	4C	3C	N/A					
12555	39160	Broadway St.		10/25/1997	0.07	0.22	RMI	4C	3C	N/A					
23012	32386	US-27 BR	NB	10/28/1998	10.69	13.01	RMI	4C	3C	3C	Yes	Yes	Yes	Yes	
23012	32386	US-27 BR	SB	10/28/1998	10.66	13.01	RMI	4C	3C	3C					
25092	45534	M-15		10/1/1998	9.50	10.41	Multi -Head	4C	3C	2C		Yes	Yes		
33083	29581	I-96	EB	7/30/1994	2.11	3.69	RMI	4C	3C	2C					
33084	28213	I-96	EB	10/27/1993	8.98	17.49	RMI	4C	2C	1C	Yes	Yes	Yes	Yes	
33084	29581	I-96	EB	11/8/1995	0.00	1.07	RMI	4C	3C	2C					
39052	48864	E. Michigan		6/11/1999	0.00	2.41	Multi -Head	4C	3C	2C					
39060	39503	E. Michigan		10/1/1998	0.99	3.61	RMI	4C	3C	2C			Yes		
39405	46994	Portage Rd.		11/29/1998	0.00	2.14	Multi -Head	4C	3C	2C		Yes	Yes	Yes	

Table 3.7 List of rubblized pavement projects in Michigan (continued)

Control section	Job number	Route	Dir.[1]	Completion Date	POB	END	Rubblizer	Asphalt Mix			Distresses				
								Top	Level	Base	TTDC[2]	LTDC[3]	SG[4]	Raveling	Rut depth (in)
39405	49551	Portage Rd.		9/15/1999	0.00	1.13	RMI	4C	3C	2C			Yes	Yes	
39405	50708	Shaver Rd		10/30/1999	1.28	1.93	Multi -Head	4C	3C	3C			Yes		
39555	39212	E. Michigan		9/4/1996	13.89	15.17	RMI	4C	3C	2C	Yes	Yes	Yes	Yes	
41013	45797	M-44		8/22/1999	2.67	2.82	RMI	4C	3C	2B, 2C	Yes	Yes	Yes	Yes	1/4
41033	26691	M-37	NB	8/14/1992	2.48	7.92	RMI	4C	2B	2B	Yes	Yes	Yes		
41033	26691	M-37	SB	8/14/1992	2.48	7.35	RMI	4C	2B	2B	Yes	Yes	Yes		
41033	26691	M-37	SB	8/14/1992	7.44	7.92	RMI	4C	2B	2B	Yes	Yes	Yes		
41401	49321	Wolverine Blvd		8/22/1999	0.00	1.39	RMI	4C	3C	2B, 2C	Yes	Yes	Yes	Yes	1/4
58171	34113	I-275	NB	Top in 98	0.47	1.96	Multi -Head	4C	3C	2C					1/4
58171	34113	I-275	SB	Top in 98	0.00	1.98	Multi -Head	4C	3C	2C					1/4
67021	45053	US-10		10/30/1998	1.94	2.63	Multi -Head	4C	3C	2C		Yes	Yes	Yes	
67022	45053	US-10		10/30/1998	0.00	1.52	Multi -Head	4C	3C	2C		Yes	Yes	Yes	
70013	38179	US-31	NB	9/12/1997	1.23	8.28	RMI	4C	3C	2C		Yes	Yes		1/2
70013	38179	US-31	NB	9/12/1997	8.93	13.01	RMI	4C	3C	2C		Yes	Yes		1/2
41029	35990	I-196	EB (NB)	7/31/1998	1.15	4.08	RMI	4C-MOD	3C-MOD	2C-MOD			Yes		
41029	35990	I-196	WB (SB)	7/31/1998	1.12	4.11	RMI	4C-MOD	3C-MOD	2C-MOD			Yes		
41029	45068	I-196	EB (NB)	7/31/1998	4.08	6.61	RMI	4C-MOD	3C-MOD	2C-MOD			Yes		
41029	45068	I-196	WB (SB)	7/31/1998	4.11	6.66	RMI	4C-MOD	3C-MOD	2C-MOD			Yes		
70024	35987	I-196	EB	9/30/1996	12.59	15.59	RMI	4C-SHRP	3C-SHRP	2C-SHRP		Yes			
65041	45865	I-75	NB	5/17/2001	6.54	9.54	Multi -Head								
65041	45865	I-75	SB	5/17/2001	6.62	9.34	Multi -Head								
65041	50649	I-75	NB	5/17/2001	9.54	11.37	Multi -Head								
65041	50649	I-75	SB	5/17/2001	9.34	11.27	Multi -Head								

Table 3.7 List of rubblized pavement projects in Michigan (continued)

Control section	Job number	Route	Dir.[1]	Completion Date	POB	END	Rubblizer	Asphalt Mix			Distresses				
								Top	Level	Base	TTDC[2]	LTDC[3]	SG[4]	Raveling	Rut depth (in)
83-81	33614	Mackinaw Trail		9/30/1992	0.0	0.0	RMI								
33084	28213	I-96	WB	10/27/1993	17.50	8.85	RMI	SMA-A or B	2C	1C	Yes	Yes	Yes	Yes	
03111	32373	US-131	NB	6/19/1997	6.73	7.96	RMI	SMA-C	3C	2C					
03111	32373	US-131	SB	6/19/1997	6.73	7.96	RMI	SMA-C	3C	2C					
03112	32373	US-131	NB	6/19/1997	0.02	1.94	RMI	SMA-C	3C	2C					
03112	32373	US-131	NB	6/19/1997	2.08	3.10	RMI	SMA-C	3C	2C					
03112	32373	US-131	NB	6/19/1997	0.00	0.00	RMI	SMA-C	3C	2C					
03112	32373	US-131	SB	6/19/1997	0.02	0.89	RMI	SMA-C	3C	2C					
03112	32373	US-131	SB	6/19/1997	1.18	1.94	RMI	SMA-C	3C	2C					
03112	32373	US-131	SB	6/19/1997	2.08	3.10	RMI	SMA-C	3C	2C					
81076	32390	US-23	NB	11/11/1997	0.54	6.62	Multi -Head	SMA-C	3C	2C					
81076	32390	US-23	SB	11/11/1997	0.54	6.43	Multi -Head	SMA-C	3C	2C					
03112	28143	US-131	NB	11/5/1993	3.07	8.56	RMI	SMA-C, SMA-P, 4C	3C	2C	Yes		Yes		
03112	28143	US-131	SB	11/5/1993	3.07	3.52	RMI	SMA-C, SMA-P, 4C	3C	2C	Yes		Yes		
03112	28143	US-131	SB	11/5/1993	3.76	8.56	RMI	SMA-C, SMA-P, 4C	3C	2C	Yes		Yes		
18555	55091	Clare Ave		5/15/2001	4.45	6.27	Multi -Head								
41402	50251	Chicago Dr		10/31/2000	1.17	1.77	RMI	4E10	3E10	2E10			Yes		

2. The bottoms of each core (attached to some rubblized material, see figure 3.17) was trimmed off by sawing (figure 3.17).

3. The specific gravity of the entire core was then determined according to ASTM standard test procedure D-2726.

4. The AC cores were then sawn to separate the various AC courses and to produce test specimens for the ITCLT and the ITST. The ideal theoretical test specimen thickness is 3.0 in. and the absolute minimum thickness is 2.2 in. (thinner than 2.2-in test specimens are not allowed because of edge effects), (see figure 3.18). Because of the 2.2-in. minimum thickness constraint, some test specimens contained more than one AC course. For example, the test specimen representing the AC surface course contained about 1.5-in. AC surface course and a minimum of 0.7-in. leveling course. Likewise, when an AC course was less than 2.2 in. thick, a part of the adjacent course was included in the test specimen.

5. The specific gravity of each test specimen was then determined according to ASTM standard test procedure D-2726.

6. Each test specimen was subjected to ITCLT (details of the test are presented in a later section).

7. Each test specimen was subjected to ITST (details of the test are presented in a later section).

Table 3.8 provides a summary of the total number of cores extracted from each test site for 19 rubblized pavement projects that were investigated during the Phase II Study. The table also provides information regarding the number of intact and defective cores, the average total thickness of all intact cores of each test site and the average thickness of each AC course. Table 3.9 provides detailed information of all cores that were extracted during the Phase I Study. All of these cores were taken over existing cracks to verify whether or not the crack is a top-down crack. Detailed data regarding the thickness of each core are presented in Appendix F.

3.2 Specific Gravity Test (SG test)

As stated earlier, specific gravity of each intact core was determined after bottom of each core was trimmed. In addition, the specific gravity of each test specimen was determined after each core was cut to test specimen size. Both tests were conducted according to the ASTM standard test procedure D 2726 (1) and the specific gravities were calculated using equation 3.1.

$$G_{mb} = A / (B-C) \tag{3.1}$$

Table 3.8 A summary of the average total thickness of the cores and the average thickness of each AC course for19 rubblized pavement test sites

Test sites	Number of Cores			Average thickness (in)				
	Total	Intact	With cracks /defects	Total core	Overlay	AC surface course	AC leveling course	AC base course
10692-11	12	10	0/2	8.2		1.5	2.2	4.5
10692-12	12	9	0/3	8.0		1.6	2.3	4.1
10753-11	14	11	3/0	4.5		1.6	1.0	1.8
10753-12	15	12	3/0	4.1		1.6	1.0	1.5
11941-21	15	10	5/0	7.8	1.5	1.6	2.3	2.6
11941-22	15	8	5/2	7.4	1.5	1.4	2.1	2.4
20102-11	12	12	-	6.5		1.4	2.1	2.9
20102-12	12	12	-	6.4		1.5	2.1	2.8
20233-11	11	10	0/1	5.5		1.5	1.8	2.2
20233-12	10	7	0/3	5.5		1.3	2.4	1.7
20273-21	15	11	4/0	4.6		1.3	1.5	2.0
20273-31	12	12	-	7.0		1.8	2.5	2.6
20273-41	12	12	-	6.5		1.7	2.0	2.8
20311-11	12	12	-	6.9		1.2	1.8	3.9
30153-11	16	12	4/0	5.3		1.4	1.8	1.8
30373-51	12	12	-	6.6		1.5	1.8	3.4
30373-52	12	12	-	6.4		1.4	1.8	3.3
30373-61	18	15	2/1	5.7		1.6	2.1	2.0
30531-11	20	14	6/0	5.5		1.2	2.2	2.1

Table 3.9 Detailed information of the cores extracted from each test site during the Phase I Study to verify the type of existing distresses

Test site	Crack type	Thickness (in)				Crack depth per AC course (%)		
		Total	Surface	Leveling	Base	Surface	Leveling	Base
11942-11	TJ	4.9	1.3	1.6	2.0	100	100	100
	LC	5.0	1.5	1.6	1.9	100	100	100
	LC	5.0	1.2	1.8	2.0	100	100	100
	D	6.3	1.5	2.2	2.6	100	100	0
	LC	5.9	1.6	1.6	2.8	100	100	25
	TJ	4.7	1.4	1.4	2.0	100	100	100
	LC/TC	5.8	1.7	2.4	1.8	100	100	100
	TC	6.1	1.7	2.2	2.2	100	100	100
	LC	5.9	1.3	2.6	2.1	100	100	0
	LC	6.5	1.3	2.4	2.7	100	100	0
30371-11	TC/LC	6.1	1.8	2.2	2.2	100	20	0
	LC	6.4	1.7	2.2	2.5	100	0	0
	LC	4.8	1.3	1.6	2.0	100	100	0
	LC	5.0	1.6	1.5	2.0	100	100	0
	LC	5.0	1.6	1.5	2.0	100	10	0
30373-11	LC	5.6	1.1	1.8	2.7	100	90	0
	LC	6.0	1.3	1.9	2.9	100	10	0
	LC	6.1	1.4	1.8	3.0	100	50	0
	TC	4.4	1.2	1.6	1.6	100	100	100
10962-21	LC	6.7	1.3	1.6	3.9	100	45	0
	LC	7.2	1.2	1.6	4.4	100	50	0
	LC	6.9	1.1	1.7	4.1	100	75	0
	LC	6.5	1.1	1.7	3.7	100	30	0
	LC	6.5	1.1	1.5	3.8	100	0	0
	C	6.9	1.1	1.8	3.9	0	0	0
	C	7.0	1.2	1.7	4.1	0	0	0
10962-31	LC	6.3	1.2	1.8	3.3	100	60	0
	LC	6.5	1.2	1.6	3.7	100	75	0
	TC	6.4	1.2	2.0	3.2	100	40	0
	TC	5.7	1.2	1.7	2.8	100	100	30
	TC	6.0	1.3	1.9	2.9	100	100	100
109642	LC	7.5	1.5	1.8	4.2	100	0	0
	TC	8.0	1.3	2.0	4.6	100	0	0

C = Control (No crack), D = Diagonal crack, LC = Longitudinal crack, TC = Transverse crack, TJ = Transverse joint

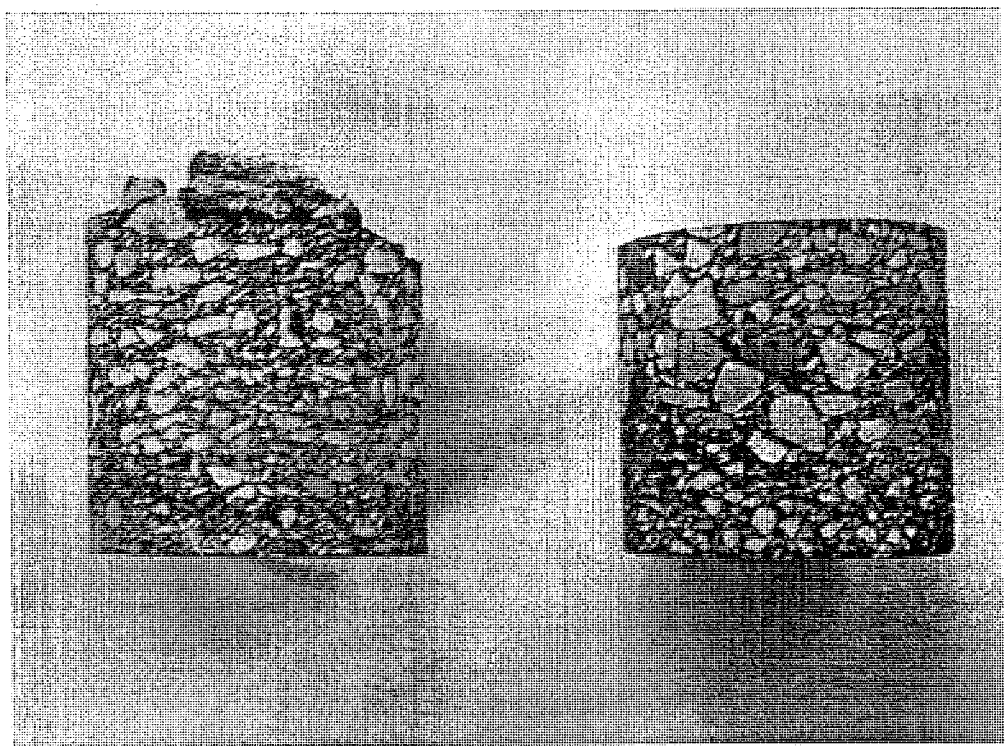

Figure 3.17 Untrimmed (left) and trimmed (right) AC cores

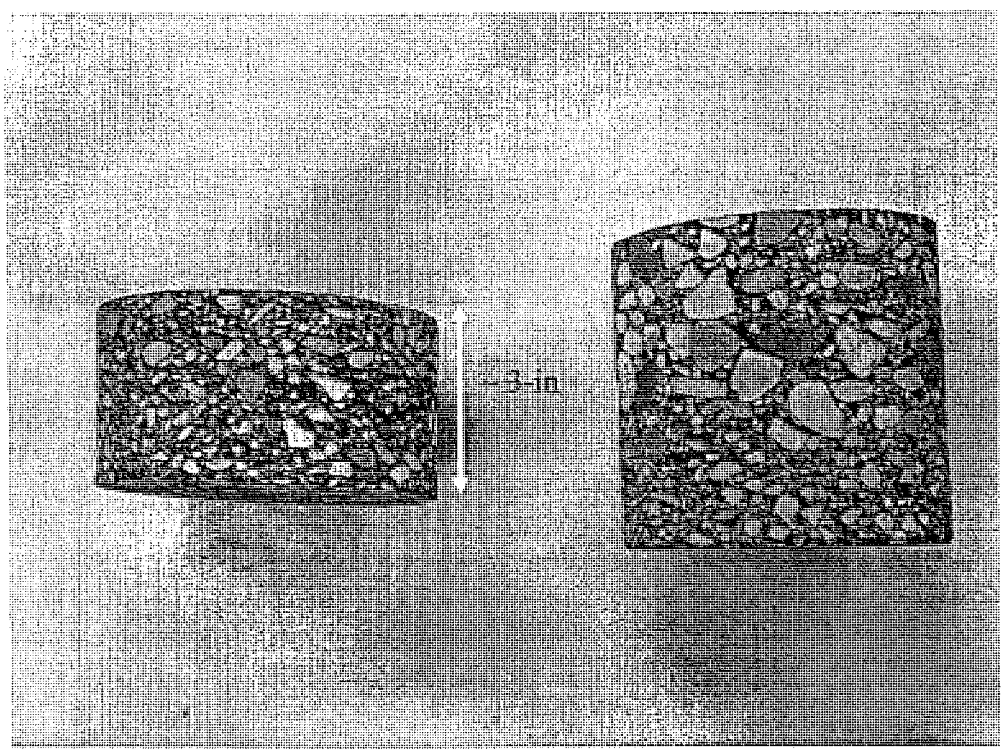

Figure 3.18 An AC test specimen (left) and a trimmed AC core (right)

where:

G_{mb} = bulk specific gravity,
A = mass of the dry test specimen in air, g,
B = mass of saturated surface-dry test specimen in air, g, and
C = mass of the test specimen in water, g.

Once the bulk specific gravities of the AC cores and the test specimens were obtained, their percent air voids were calculated using equation 3.2.

$$AV = 100*(1- G_{mb} / G_{mm}) \tag{3.2}$$

where:

AV = percent air voids,
G_{mb} = bulk specific gravity, and
G_{mm} = maximum theoretical specific gravity

The main objective of calculating the percent air voids of the core is to assess the degree of variation in the AC mix along the project. Given this objective and the destructive nature of the G_{mm} test (ATSM standard test procedure D 2041), the G_{mm} test was not conducted. Rather a G_{mm} value of 2.5 was assumed for all AC mixes. Table 3.10 provides a summary of the averages of the bulk specific gravity, percent air voids, resilient modulus, equivalent modulus and the indirect tensile strength of all asphalt cores obtained from each test site. The bulk specific gravities and percent air voids of the individual AC cores and test specimens of the 19 rubblized test sites are presented in Appendix G..

3.3 Indirect Tensile Cyclic Load Test (ITCLT)

The objective of the indirect tensile cyclic load test is to determine the resilient modulus of each course of the asphalt mat. The ITCLT was conducted using a computer-controlled closed-loop hydraulic system (MTS) and the ITCLT loading frame shown in figures 3.19 and 3.20. To accomplish the objective, the AC core was sawn to test specimen size between 2.2 and 3.3 in. When the thickness of an asphalt course exceeded 2.2 in., the test specimen consisted of that course only. On the other hand, when the AC course thickness was less than the minimum test specimen thickness of 2.2 in., the test specimen consisted of that entire AC course and a portion of the adjacent course. After sawing the test specimen and measuring its specific gravity, the ITCL was conducted using the following steps:

1. All moving parts and the two loading strips of the ITCLT loading device were cleaned and lubricated.

2. The ITCLT loading device was placed on the MTS loading frame such that the center of the device corresponded with the center of the MTS actuator and the center of the load cell.

Table 3.10 A summary of the average physical and engineering properties of the AC cores obtained from 19 rubblized test sites

Test sites	Bulk specific gravity	Air voids (%)	Resilient modulus (ksi)		Equivalent elastic modulus (ksi)	Indirect tensile strength (psi)
			One-dimension	Three-dimensions		
10692-11	2.32	7.3	177	171	52	97
10692-12	2.31	7.4	179	173	65	107
10753-11	2.38	4.7	209	202	62	146
10753-12	2.39	4.5	196	189	73	171
11941-21	2.40	4.0	203	196	85	211
11941-22	2.40	3.9	214	206	85	241
20102-11	2.33	6.9	188	181	61	126
20102-12	2.31	7.7	207	200	62	118
20233-11	2.39	4.3	202	195	73	138
20233-12	2.38	4.8	213	205	50	120
20273-21	2.45	2.1	291	281	108	213
20273-31	2.44	2.4	217	209	44	101
20273-41	2.45	1.9	258	249	41	100
20311-11	2.46	1.4	234	226	61	123
30153-11	2.35	6.0	220	212	84	172
30373-51	2.36	5.5	186	179	66	167
30373-52	2.35	5.8	196	189	70	154
30373-61	2.45	2.1	273	263	71	143
30531-11	2.33	6.7	170	164	84	172

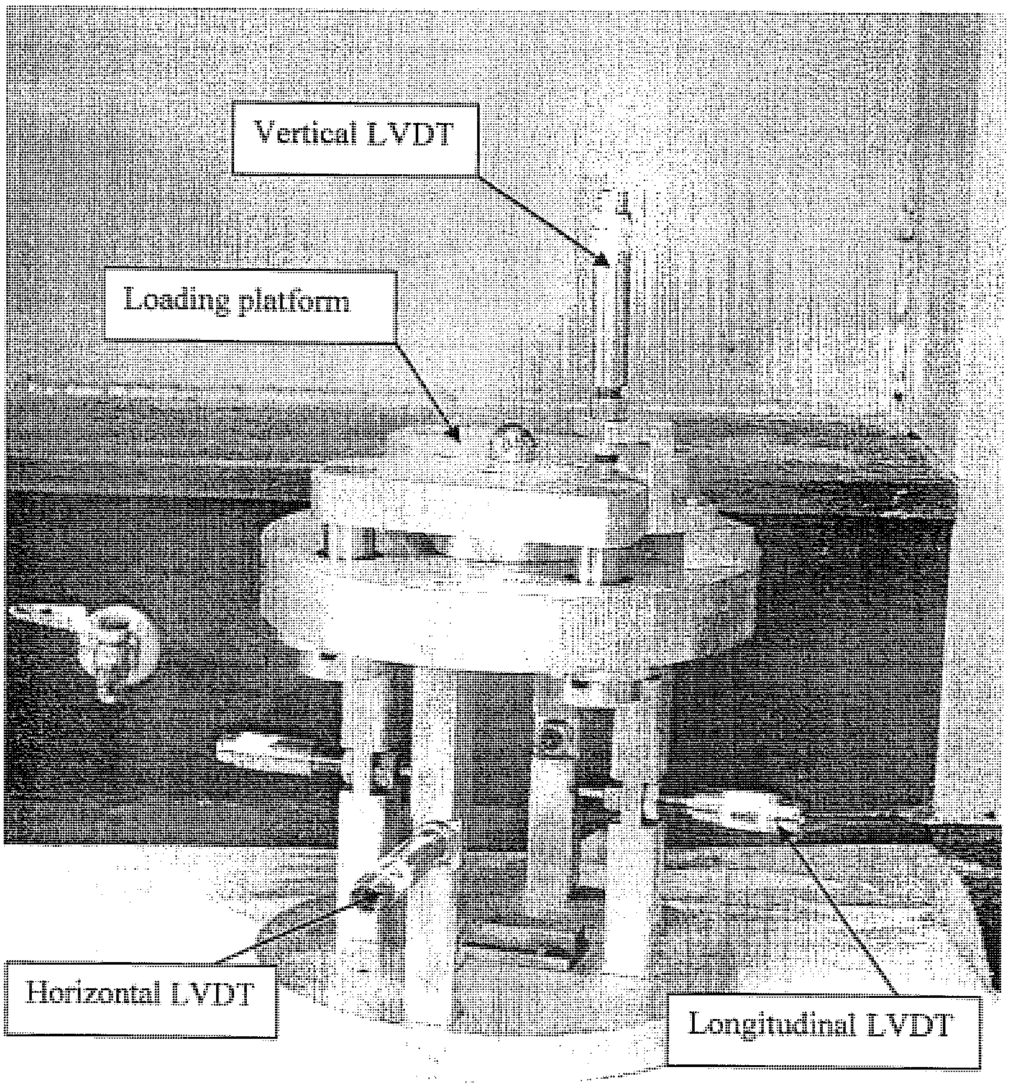

Figure 3.19 The ITCLT and ITST specimen holder device for a 6-in. diameter and 3-in. thick test specimen

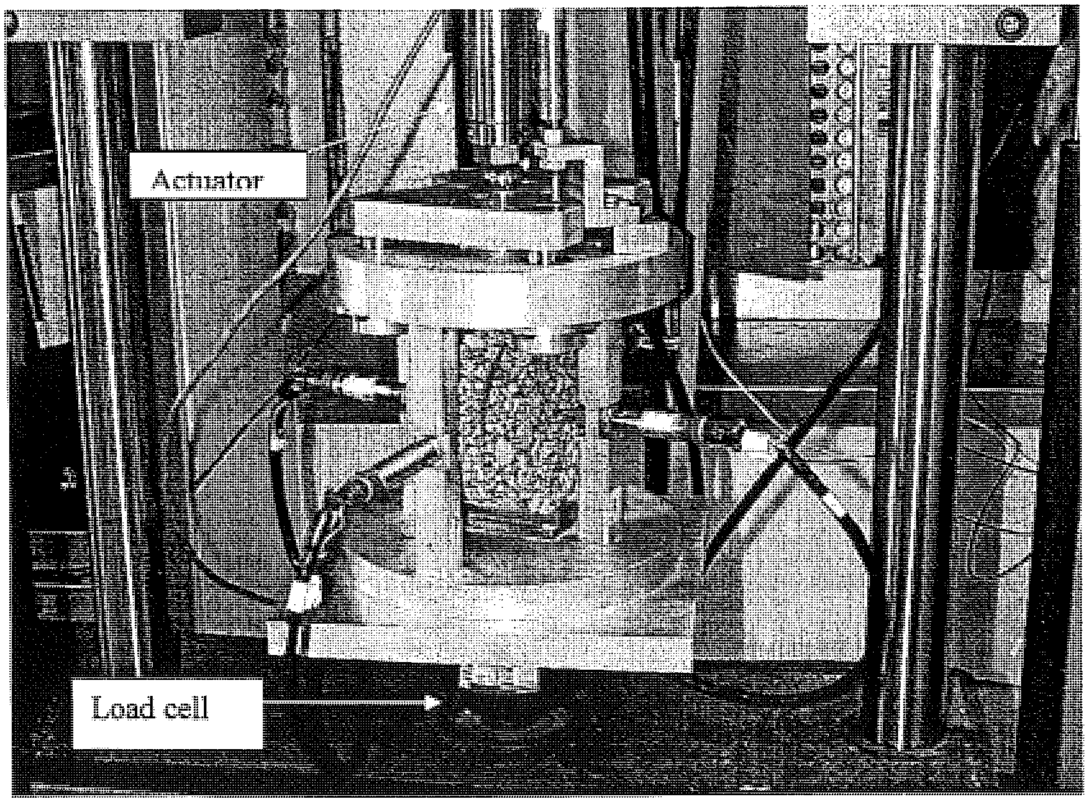

Figure 3.20 Test specimen in the specimen holding device during an ITCLT test

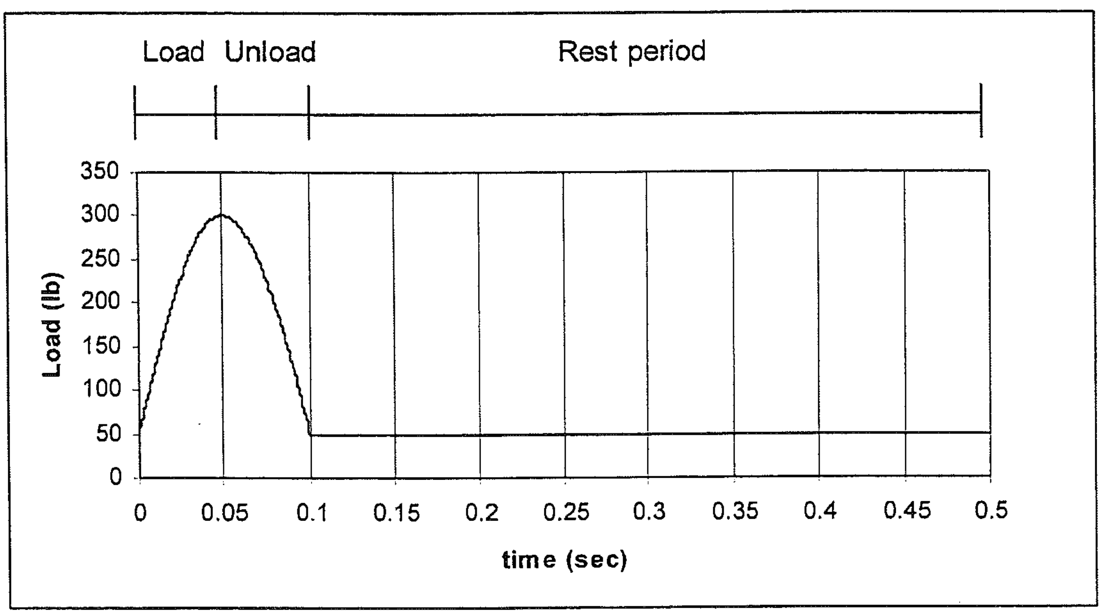

Figure 3.21 One load cycle consisting of 0.1-second load-unload period and 0.4-second relaxation period

3. The test specimen was placed on the loading frame and five linear variable differential transducers (LVDT) were placed in their respective positions as shown in figure 3.20. The accuracy and range of the LVDTs are tabulated below.

Number of LVDT	Position	Range (in)	Accuracy (in)
2	Horizontal diameter	$\pm$0.125	0.00005
2	Specimen Thickness	$\pm$0.100	0.00001
1	Vertical diameter	$\pm$0.250	0.00010

In addition, a sixth LVDT placed inside the actuator (a part of the MTS) was also used to measure the test specimen deformation along the vertical diameter.

4. The position of each LVDT on its holder was adjusted by moving the LVDT core toward or away from the test specimen using two position adjustment knots until the LVDT signal indicates that the core position would allow the use of a high percentage of the LVDT range.

5. A 50-lb sustained load was placed on the test specimen by lowering the actuator of the MTS and the resulting test specimen deformations were recorded.

6. When the rate of deformation due to the sustained load was small enough (not measurable), a 250-lb cyclic load was applied to the test specimen at a frequency of 2 Hz. Each cycle consisted of 0.1-second of load-unload period and 0.4-second relaxation period. The load-unload period simulates traffic movement at about 35 miles per hour while the rest period simulates the distance between two consequent loading (e.g., between the front and back tire and between two vehicles). Figure 3.21 illustrates a plot of one load cycle as a function of time.

7. Each test specimen was subjected to a minimum of 1000 load cycles. At certain specified cycles (e.g., the 200, 500 and 1000 cycles), the load magnitude and the test specimen deformations in three directions were recorded for three sequential cycles. The rate of data collection was set at one set of deformation readings every 0.0004-second. Hence, 250 deformation readings were collected by each LVDT during the load-unload cycle and 1,000 readings during the rest period. Note that the load data were collected using a 1000-lb capacity load cell located under the ITCLT loading frame.

8. The test was terminated and the data was downloaded for analysis.

9. The load and deformations data corresponding to load cycles 499, 500 and 501 were used to calculate the two resilient modulus of the test specimen using the deformations measured in one and three dimensions as follows: .

   a) **One-Dimensional Analysis** – The resilient modulus of the test specimen was calculated using the deformation measured along the vertical diameter of the test specimen (equation 3.3). In this calculation, since the impact of Poisson's ratio on the value of the resilient modulus is insignificant, a Poisson's ratio of 0.3 was assumed for all test specimens.

$$\mathrm{MR} = \frac{P * (4.085950 - 0.0417333 * \upsilon)}{L * D_v} \tag{3.3}$$

b) **Three-Dimensional Analysis** - The resilient modulus and Poisson's ratio of the test specimens were calculated using the deformations measured along the vertical and horizontal diameters and along the thickness of each test specimen using equations 3.4 and 3.5.

$$\mathrm{MR} = \frac{(0.1832585H + 4.2817159V - 0.0215089A)}{D} \tag{3.4}$$

$$D = 1.0468779(H^2 + V^2 + A^2) - (H - 0.0417333V + 0.212453A)^2 \tag{3.5}$$

Where

MR_v = Resilient modulus based on vertical deformation (psi),
P = peak load (lb),
υ = Poisson's ratio,
L = thickness of the test specimen (in.),
D_v = the deformation of the test specimen along the vertical diameter (in.),
D_h = the horizontal deformation = the sum of the displacements measured by the two LVDT along the horizontal diameter of the test specimen (in.),
DR = deformation ratio = D_v/D_h.,
H = $\frac{D_h * L}{P}$,
V = $\frac{D_v * L}{P}$,
A = $\frac{D_l}{P}$, and
D_l = the longitudinal deformation = the sum of the displacements measured by the two LVDT along the thickness of the test specimen (in.).

Note that the vertical deformation used in equations 3.3 through 3.5 was that obtained from the LVDT placed inside the MTS actuator. The reason is that the actuator and the LVDT were positioned at the center of the test specimen. The outside mounted LVDT was positioned at the corner of the top plate of the ITCLT device as shown in figure 3.20. Nevertheless, the resilient moduli obtained from equations 3.3 and 3.4 were compared. It was found that the differences between the two values are insignificant. Table 3.9 provides a summary of the average resilient moduli calculated using equations 3.3 and 3.4 of the AC cores obtained from 19 test sites. Detailed data (measured deformations in three dimensions, test specimen thickness, and the resilient moduli calculated using equations 3.3 and 3.4) for each core are tabulated in Appendix H.

3.4 Indirect Tensile Strength Test (ITST)

After all ITCLT tests were concluded, the ITST commenced. The objectives of the latter tests are to determine the indirect tensile strength and the equivalent modulus of the test specimens. The tests were conducted at 70°F using the ITCLT device and Marshall loading frame (see figure 3.22). The load was increased to failure by means of the constant rate of movement of the load jack of the Marshall apparatus of 2 in. per minute. The vertical deformation and the applied load were recorded and used in the calculation of the indirect tensile strength and the equivalent elastic modulus of the test specimen using equations 3.6 and 3.7.

$$\text{ITS} = \frac{2P}{\pi DL} \tag{3.6}$$

$$\text{EM} = \frac{\frac{P}{2} * (4.085950 - 0.0417333 * \nu)}{1000 * L * D_{HL}} \tag{3.7}$$

Where

ITS = indirect tensile strength (psi);
P = peak load at failure (lb);
D = test specimen diameter (in);
L = test specimen thickness (in);
EM = equivalent modulus (ksi); and
D_{HL} = vertical deformation at half the peak load (in).

The average values of the indirect tensile strength and the equivalent elastic modulus of the test specimens of each test site are reported in table 3.9. The indirect tensile strength and the equivalent elastic modulus of each test specimen obtained from 19 rubblized pavement test sites are tabulated in Appendix I.

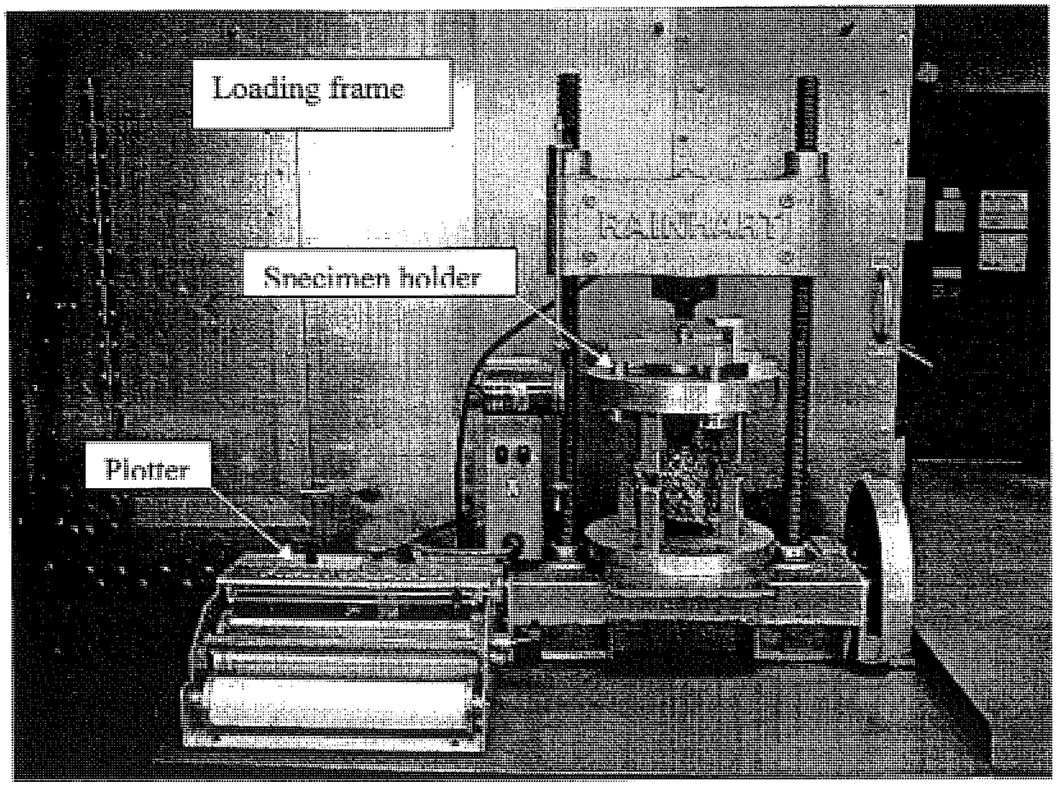

Figure 3.22 ITST loading frame and the specimen holder

REFERENCES

1. Annual Book of ASTM Standards - Section 4 - Construction, 1994, Vol. 04.03 Road and Paving Materials; Paving Management Technologies, The American Society for Testing and Materials, Philadelphia, Pennsylvania.

2. Federal Highway Administration, Integrated Material and Structural Design Method for Flexible Pavements, Vol. 1, Publication No. FHWA-RD-88-109, 1988.

CHAPTER 4
RUBBLIZATION

1.0 INTRODUCTION

With the aging of the pavement network, many techniques were developed for the rehabilitation of concrete, asphalt and composite pavements. For concrete pavements, these techniques include full and partial depth repairs with and without asphalt overlay, crack and seat with asphalt overlay and bonded and unbonded concrete overlays. Recently, the rubblization of concrete pavement with asphalt surfacing was introduced. Since the mid 1980s, considerable number of lane-miles of concrete pavements has been rubblized. Although a certain percent of the rubblized pavements have performed very well, few have under performed. The underperformance is mainly due to longitudinal and transverse cracks, segregation, raveling, block cracking and rutting. Some of these distresses were observed only few years after the completion of construction. The most dominant of these distresses are intermittent longitudinal cracks and partial- and full- width transverse cracks.

Fortunately, historical rubblized pavement performance data can be found in the pavement management databank of MDOT and other State Highway Agencies (SHAs). In Michigan, the data were and are being used to assess the performance of rubblized pavements, to develop performance prediction model; and to estimate the life cycle cost of the pavement. Analysis of the distress data and field investigation of under performing rubblized pavements indicated that the most predominant distress type is cracking, although few projects showed signs of raveling and rutting. The cracks can be divided into three categories:

1. Longitudinal cracks that initiate at the pavement surface and propagate downward and outward. Some cracks have extended through the asphalt surface and part of the asphalt leveling or the asphalt leveling and base courses. Others have propagated throughout the asphalt concrete layer. These types of cracks are referred to as "longitudinal top-down cracks (LTDC)."

2. Transverse cracks that also initiate at the pavement surface and propagate downward and outward. As is the case for LTDC, some cracks have extended through the asphalt surface course and part of the asphalt leveling or the asphalt leveling and base courses. Others have propagated throughout the asphalt concrete layer. These types of cracks are referred to as "transverse top-down cracks (TTDC)."

3. Transverse temperature cracks that extend throughout the depth of the various asphalt courses.

The underperformance of rubblized concrete pavements may be attributed to several variables including the rubblization procedure and equipment, construction procedure, the conditions of the existing concrete pavements before rubblization, the physical and engineering properties of the AC, base and subbase materials and the roadbed soils, and the aging (hardening) of the AC over time.

Unfortunately, the literature in this area is very poor to non-existent. During the course of this study, many efforts were spent searching for journal papers and other publications that address the performance of rubblized pavements; few were found, and are summarized in Appendix K of this report. This chapter addresses several topics related to the underperformance of rubblized and asphalt pavements including:

- The rubblized pavements
- The MDOT special provisions for rubblization
- The rubblization equipment and procedure
- The rubblization procedure
- The quality of rubblization
- The factors affecting the quality of rubblization
- Calibration of the rubblizing equipment
- Forensic investigation of candidate projects for rubblization

2.0 RUBBLIZED PAVEMENTS

Rubblization and AC surfacing is an alternative for the rehabilitation of distressed concrete pavements. There are three main objectives of rubblizing concrete pavements. These are:

1. Destroying the integrity of the concrete pavement joints and cracks such that reflective cracking will be eliminated.

2. Destroying the integrity of the concrete slab by debonding the temperature steel.

3. Changing the concrete slab into a particulate media whose maximum size is less than 8 in. Thus, the rubblized concrete slab would act like a base layer for the newly placed AC layer.

If the above three objectives are successfully achieved, the rubblizing alternative changes the pavement cross-section and its behavior from rigid to flexible pavements (see figure 4.1). Thus, rubblized pavement can be better explained, modeled and analyzed using the multi-layer elastic system rather than the Winkler's foundation, which is used in the analyses of rigid pavements.

If one or more of the above stated objectives are only partially achieved, then the rubblized pavement behavior will be somewhere between the behavior of flexible, composite and rigid pavements. This can be illustrated by the following examples:

Example 1 - If the integrity of the joints in the original concrete pavements is not completely destroyed, the newly surfaced pavement will behave like composite pavements and reflective joint cracking will not be eliminated as shown in figure 4.2.

Example 2 - If the temperature steel is only occasionally debonded, then the integrity of that portion of the concrete slab where the steel is not debonded remains intact and the slab will expand and contract due to temperature changes causing movements and perhaps reflective cracking in the AC layer as shown in figure 4.3.

Example 3 - If the pavement rubblization process produces fractured concrete that extends to the original pavement surface and/or large concrete pieces, the movements of these pieces will cause the asphalt layer to crack or to debond from the surface of the original concrete as shown in figure 4.4.

Note that all pictures shown in figures 4.2 through 4.4 were taken during the distress survey during May 2002.

3.0 MDOT SPECIAL PROVISION FOR RUBBLIZATION

The MDOT July 26, 2000 special provision for rubblizing concrete pavements is contained in Appendix A of this report. Note that the 2000 special provision evolved over time. Hence, many versions of the special provision affected those projects that were constructed prior to 2000 and were investigated during this study. The 2000 provision affected those projects that were constructed during the 2001 season and beyond. Hence, it might be too early to determine the impact of the new provision on pavement performance.

4.0 RUBBLIZING EQUIPMENT

As stated in the special provision (see Appendix A), MDOT allows two types of equipment for rubblizing concrete pavements; a resonant frequency pavement breaker and a multi-headed guillotine breaker, also known as a multi-head breaker. Some common characteristics and features of each machine and operational procedures are presented below.

4.1 Resonant Frequency Pavement Breaker

The resonant frequency pavement breaker was developed and became operational in 1986. From 1986 to about 1995, no other rubblizing equipment was available and therefore a large number of projects were rubblized using this type of equipment. As of 2001, more than thirty state highway agencies have used the equipment to rubblize more than 6,300 lane-miles of deteriorated concrete pavements.

The resonant breaker is a self-contained and propelled machine capable of delivering to the pavement surface low amplitude energy at high frequency of 43 to 46 cycles per second (Hz). The resonant rubblizer is composed of a shoe (hammer) located at the end of a pedestal, which is attached to 12.5-ft shaft (beam) whose thickness is 6.57 in. and

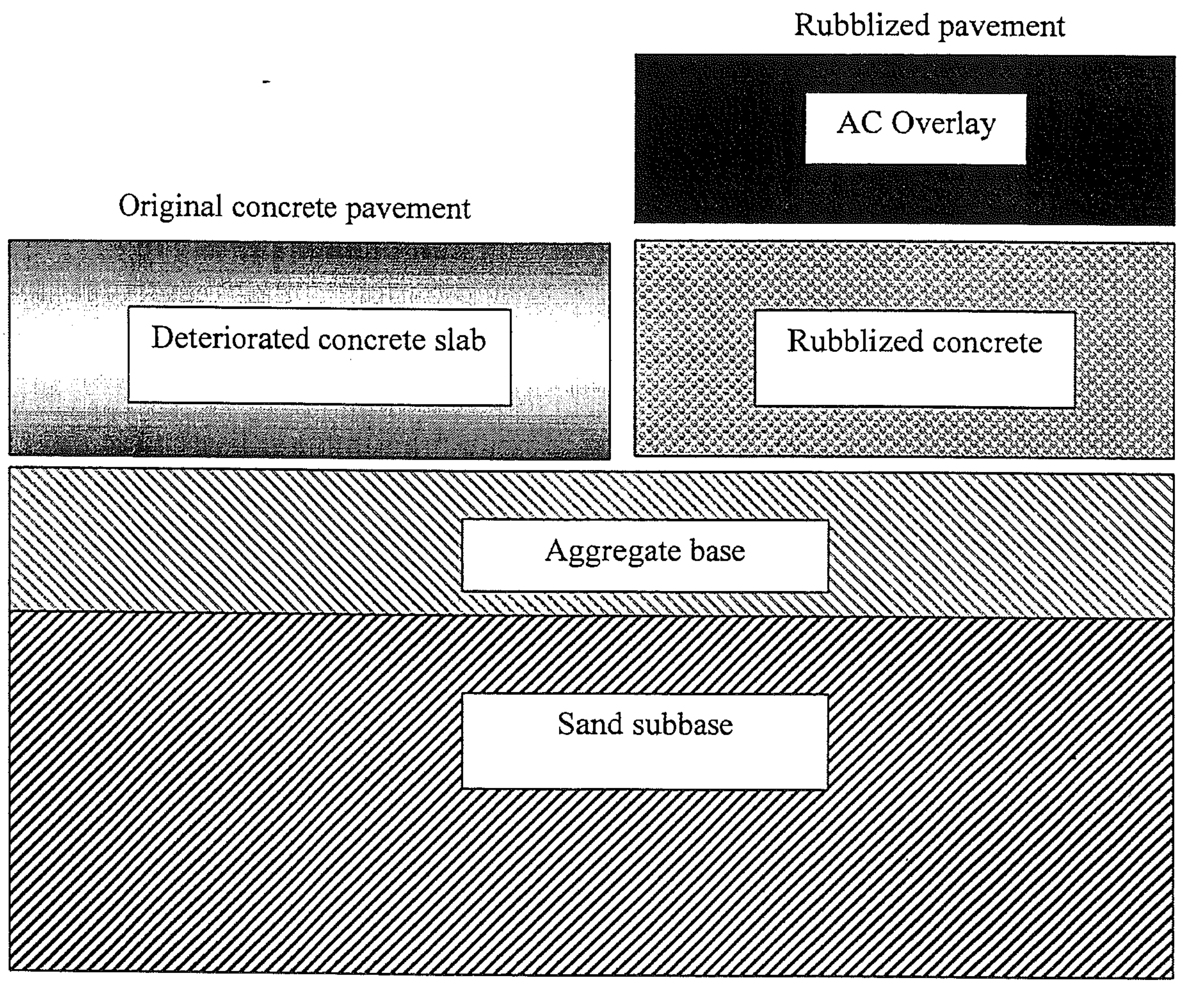

Figure 4.1 Concrete and rubblized pavement cross-sections

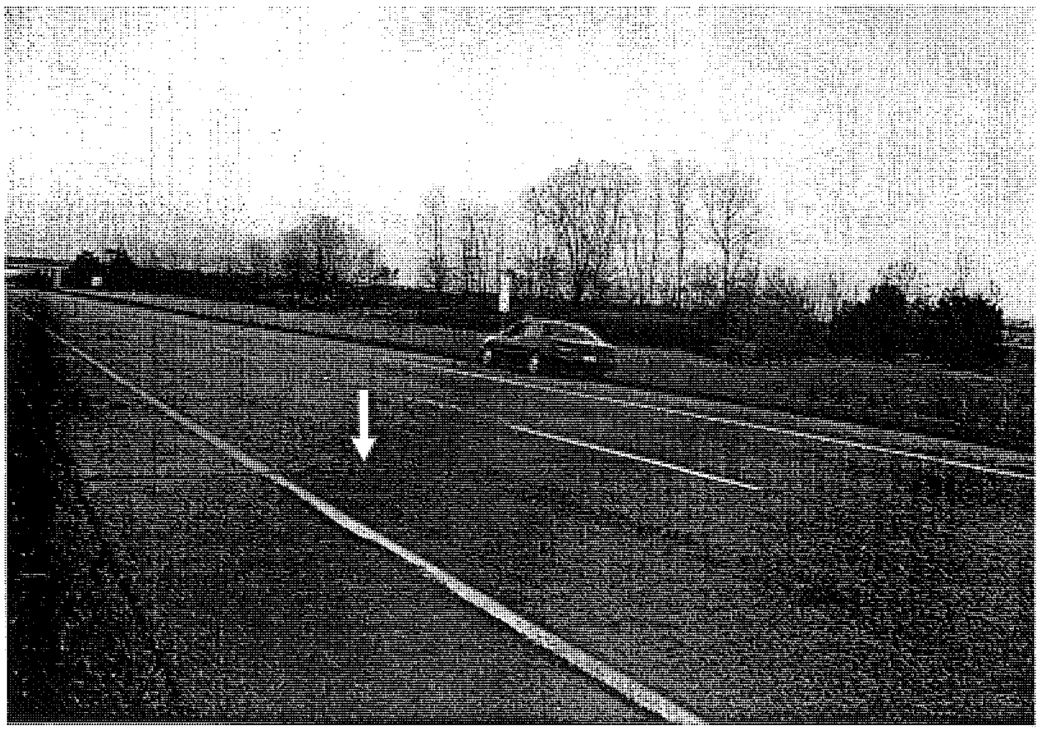

a) US 10

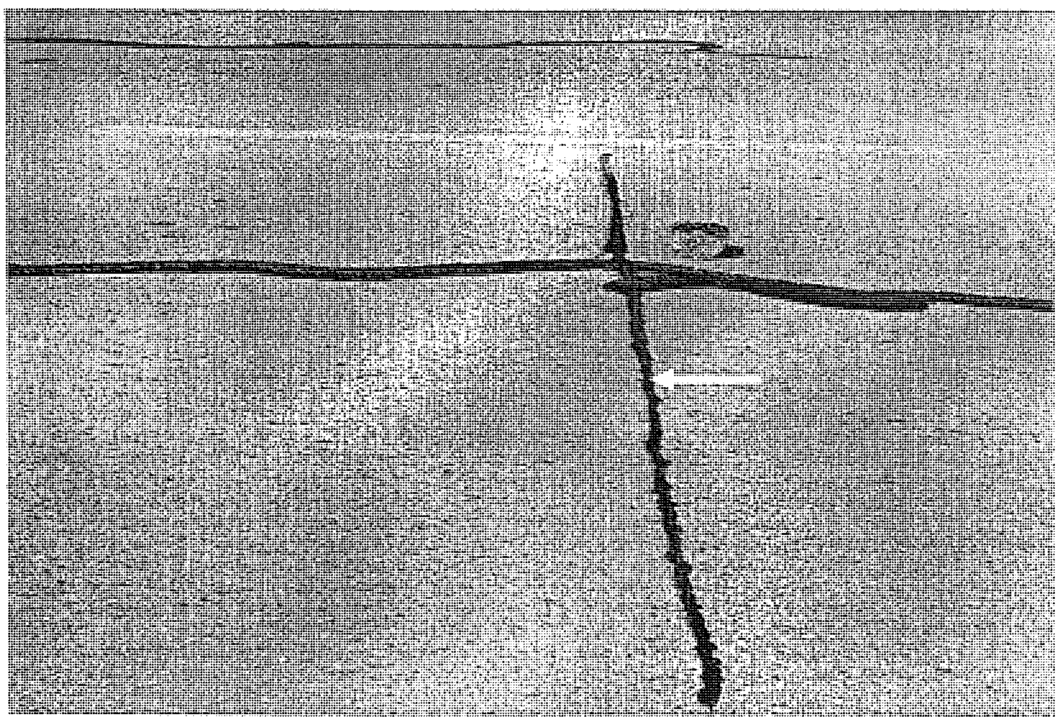

b) M-50

Figure 4.2 Reflective joint cracking in rubblized pavements

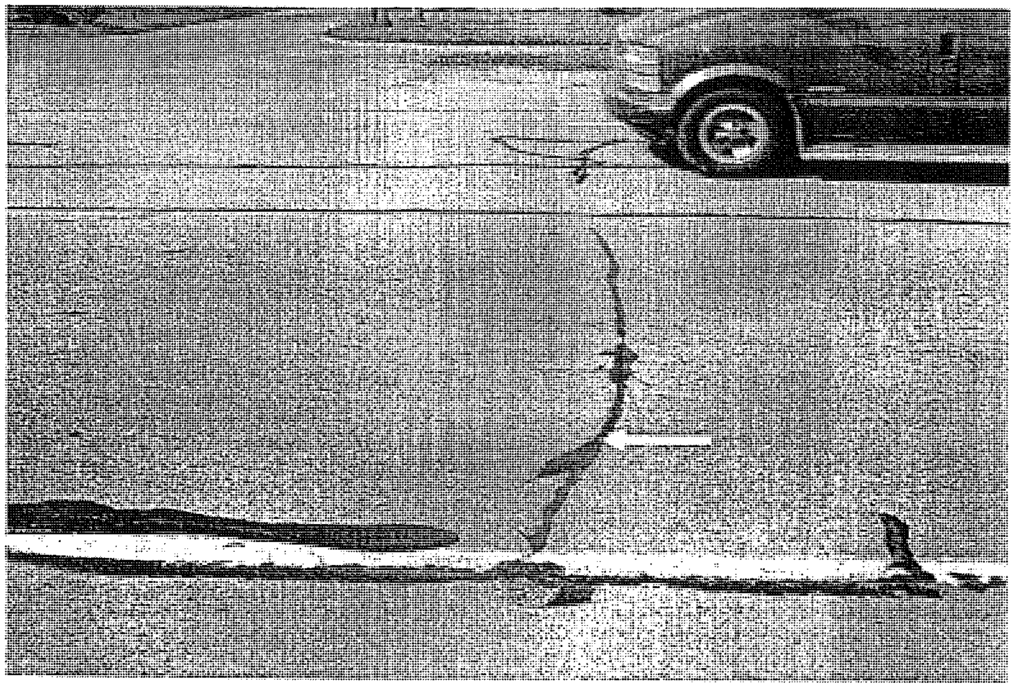

a) M-50

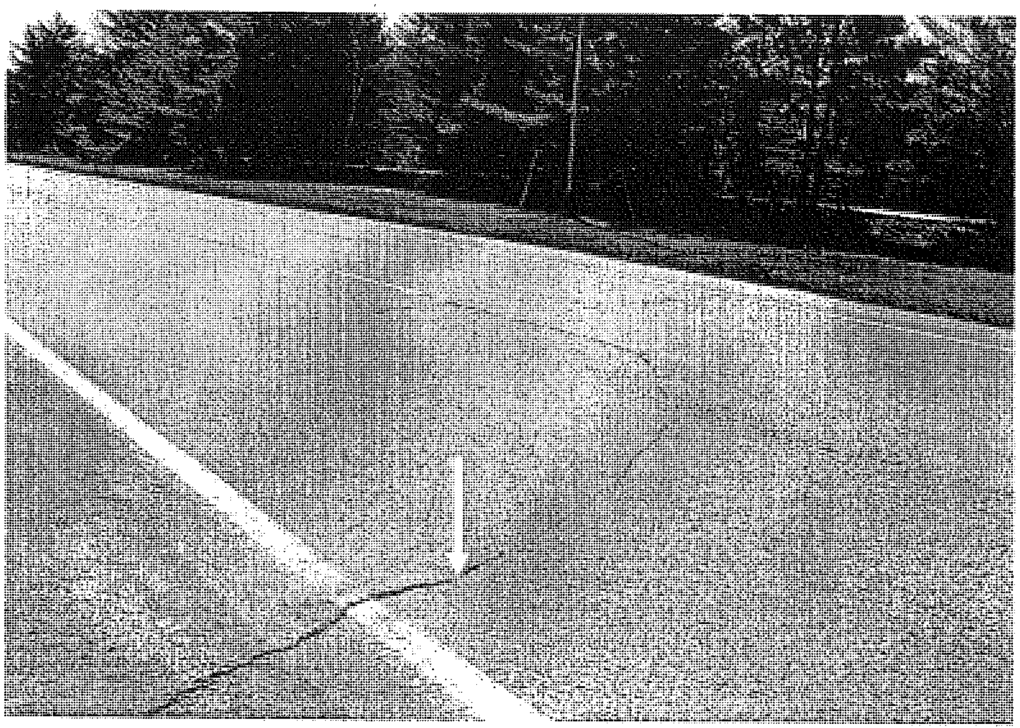

b) Saginaw Road

Figure 4.3 Reflective cracks in rubblized pavements

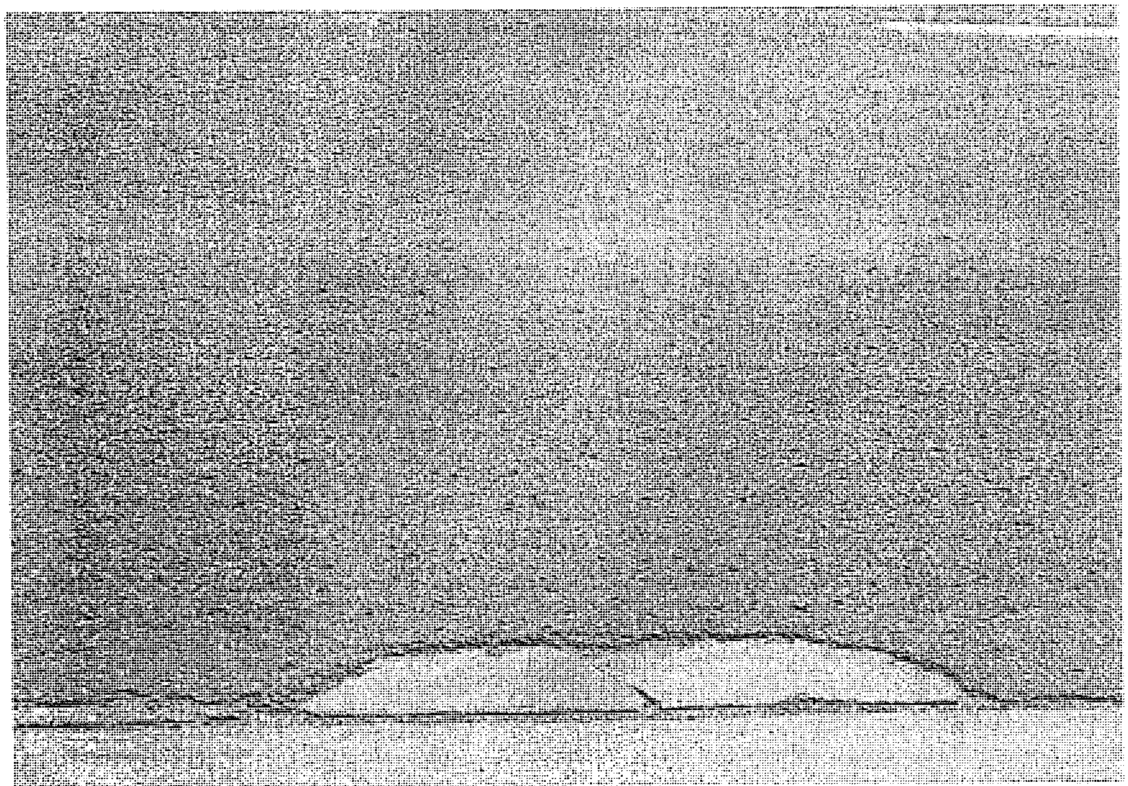

Figure 4.4 Debonding between the AC layer and the original concrete pavement where the fractured concrete extends to the original pavement surface and the integrity of the joint at that location is not destroyed – Portage Road.

loaded at the top by a 12,000-lb counter-weight. The principle on which the resonant breaker operates (figure 4.5) is that a low amplitude (0.5 in.) high frequency resonant energy is delivered to the concrete slab, which causes high tension at the top of the pavement. This causes the slab to fracture on a shear plane inclined at about 45-degrees from the pavement surface. Hence, the fractures are top-down cracking that start at the pavement surface and propagate downward. Figure 4.6 shows a schematic of the sonic shoe.

Several variables affect the rubblized products including shoe size, beam width, operating frequency, loading pressure, velocity of the rubblizer and the degree of overlapping of the various shoe passes. Typical ranges of values for the first five variables are listed below. The rate of production depends on the type of base/subbase material and is approximately 1.0 to 1.5 lane-miles per day.

During its operation, a resonant rubblizer may encounter difficulty in the vicinity of pavement discontinuities, such as joints or cracks. At a discontinuity, the microprocessor controller automatically increases the rubblizer speed causing a decrease in the energy delivered to the concrete or a shut down. Bituminous patches or un-milled asphalt overlays present another problem. The shoe penetrates the asphalt causing a large loss in the energy delivered to the concrete. When the applied pressure is low, the shoe bounces on the concrete surface and the shoe does not transfer the needed energy to breakup the concrete. Hence, the effective depth of rubblization decreases substantially and the temperature steel may not debond from the concrete. High pressures, on the other hand, cause the shoe to penetrate into the concrete.

Resonant rubblizer characteristics	Values
Resonant shoe width	7 to 12 in.
Contact strip width	Approximately 2 in.
Beam width	18, 20 and 22 in.
Loading force	5,000 to 25,000 lbs
Loading pressure	208 to 1,800 psi
Frequency	43 to 46 Hz
Velocity	3 to 6 mile/hr

4.2 Multi-head Breaker and Vibratory Grid Roller

A multi-head breaker operation includes multiple drop hammers arranged in two rows on a self-propelled unit (figure 4.7) and a vibratory grid roller (figure 4.8). The bottom of the hammer is shaped as to strike the pavement on a 1.5-in. wide and 8-in. long loading strip. The hammers in the first row strike the pavement at an angle of 30 degrees from the transverse direction. The hammers in the second row strike the pavement parallel to the transverse direction. The hammers strike the pavement approximately every 4.5 in. along the direction of travel. Figure 4.9 shows a typical hammer

a) General view

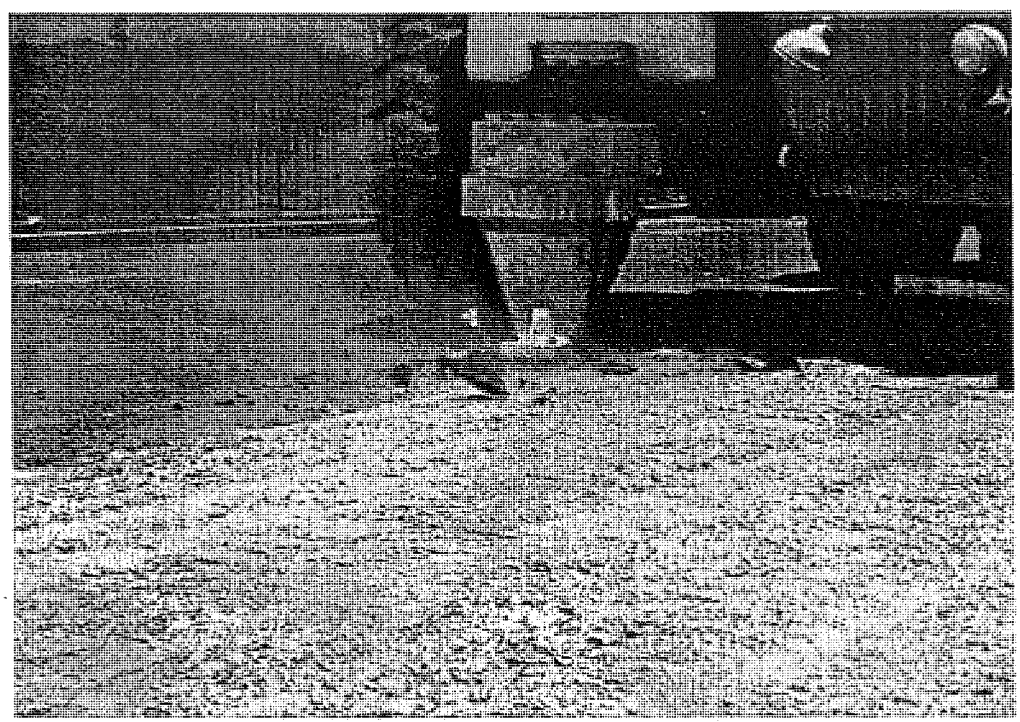

b) Close-up of the sonic shoe

Figure 4.5 Resonant frequency pavement breaker

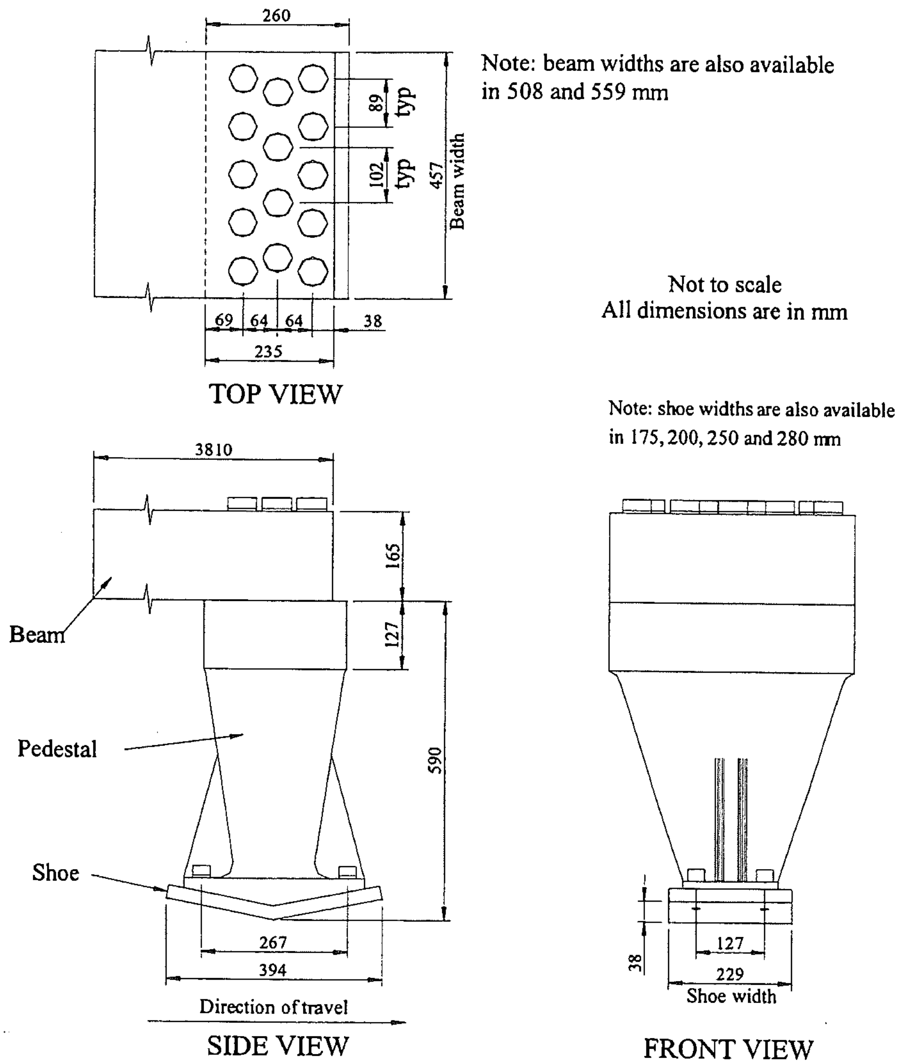

Figure 4.6 A schematic of the sonic shoe of the resonant frequency pavement breaker

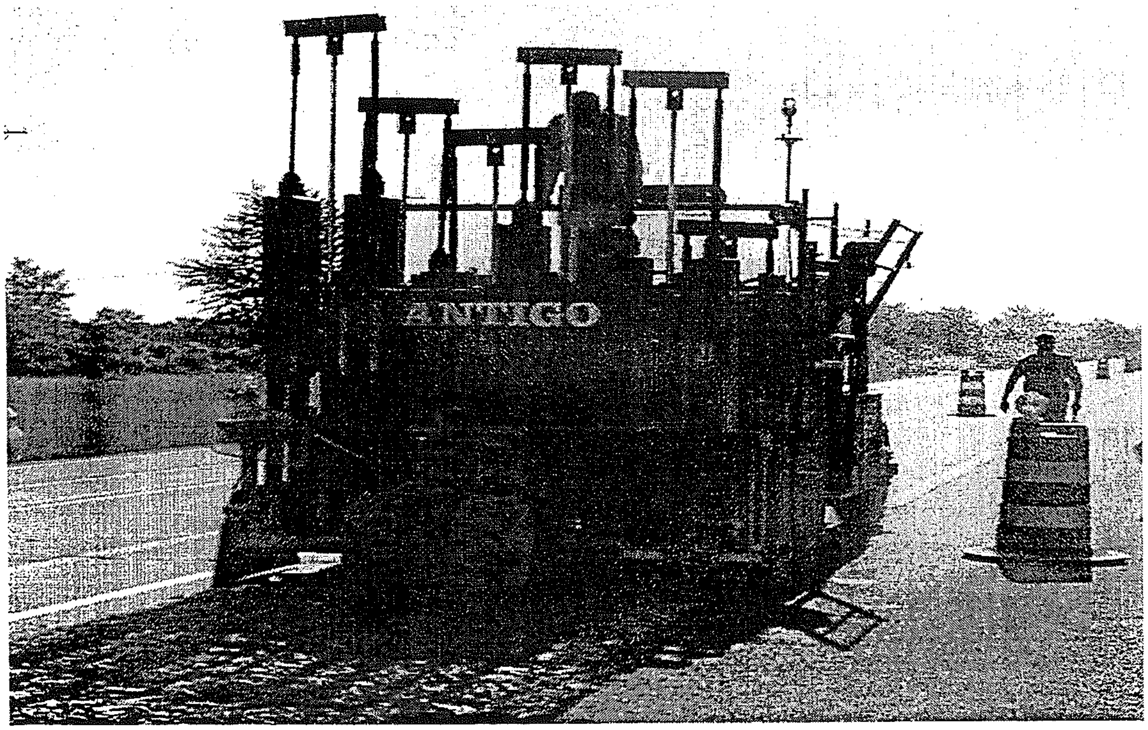

Figure 4.7 A multi-head breaker

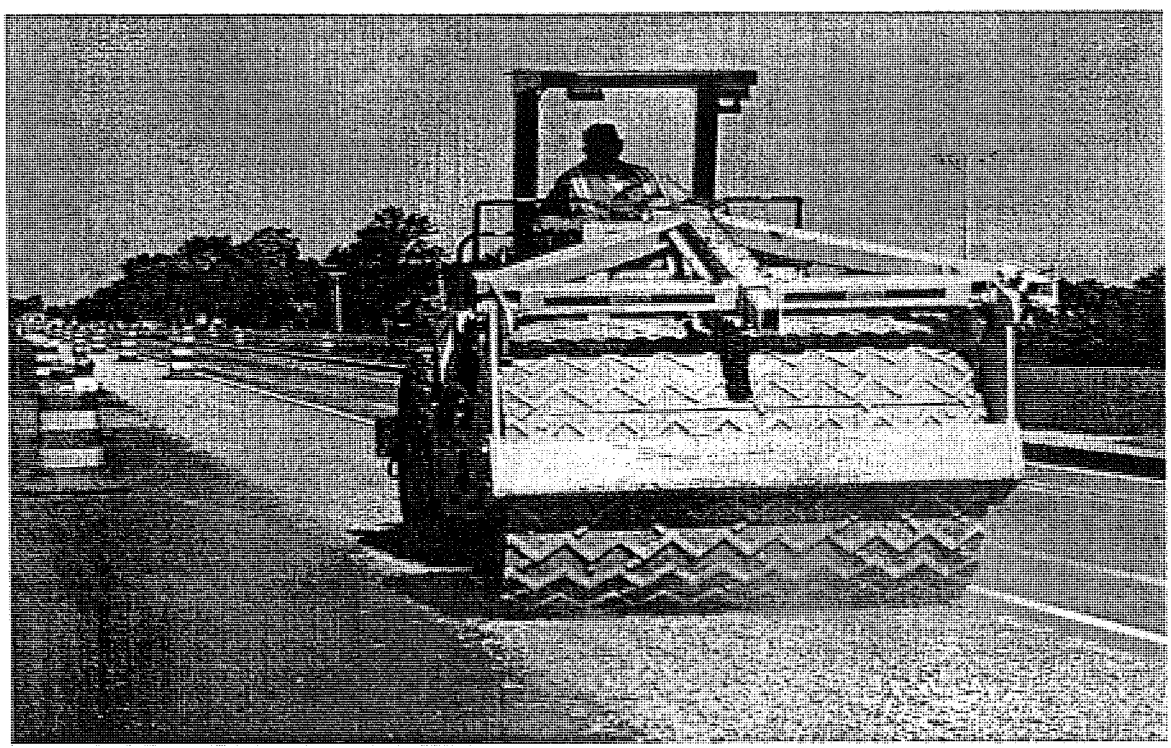

Figure 4.8 A vibratory grid roller

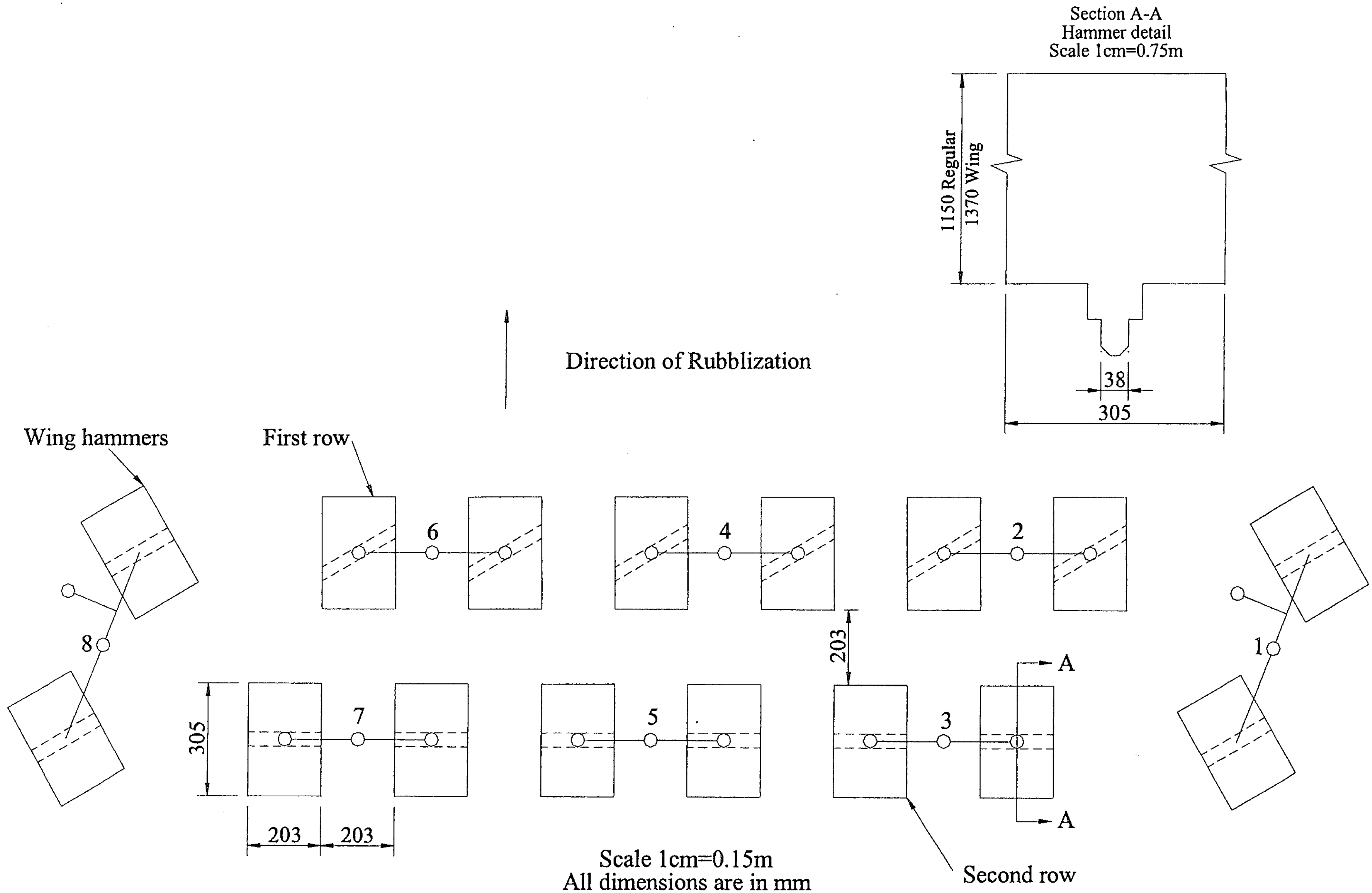

Figure 4.9 Typical hammer configuration of the multi-headed guillotine breaker (multi-head breaker)

configuration. The sequence of hammer drops is irregular because each cylinder is set on its own timer/frequency system. By disabling some cylinders, the width of the rubblized area can be varied from 2.5-ft to 12.67-ft. The 10-ton vibratory grid roller follows the multi-head breaker to reduce the size of the broken concrete. The rate of production of the multi-head breaker depends on the type of base/subbase material and is about 0.75 to 1 lane-mile/day. Some characteristics of the multi-head breaker are provided below.

Multi-head breaker characteristics	Values
Rubblization width	2.5 to 12.7 ft
Cylinders/row	4 or less
Number of rows	2
Distance between rows	20 in.
Number of hammers per cylinder	2
Hammer width	8 in.
Hammer length	12 in.
Pavement striking dimension	1.5 by 8 in.
Distance between hammers in one row	16 in.
Weight/hammer [wing hammer]	1200 to 1500 lbs
Maximum drop height [wing hammer]	48 to 60 in.
Rubblizer operating velocity	500 to 950 ft/hr

Several variables affect the quality of the rubblization operation including the speed of the rubblizer and height, weight and frequency of the drop hammers. The multi-head breaker encounters difficulties on saturated subbase and/or weak roadbed soil (less than 3000 psi modulus), which fail in shear causing large concrete pieces to rotate and/or penetrate the underlying material. Such failure would result in poor pavement performance.

5.0 RUBBLIZATION PROCEDURE STEPS

A typical rubblization procedure consists of several steps that affect the quality of the rubblization operation. Some steps are applicable to the resonant frequency breaker, others to the multi-head breaker and still others apply to both. These steps are:

1. Remove all asphalt overlays and/or asphalt materials from around deteriorated joints and in asphalt patches. Failure to do so would cause poor quality rubblization in these areas and, in the case of the resonant frequency equipment, may cause the automatic shut down of the equipment.

2. Calibrate the operational parameters (frequency, load and velocity) of the rubblizer at the start of every project as to:

   - Produce maximum size rubblized concrete of less than 8 in.

- Debond the temperature steel.
- Destroy the integrity of joints.

3. Slightly overlap the boundaries of the rubblized strips.

4. Add approved filler aggregate to areas where asphalt patches and/or concrete pieces have been removed.

5. Rubblize the same area only once.

6. Spray the rubblized materials with water to minimize dust and prevent the loss of fine materials.

7. Cut and remove all exposed temperature steel.

8. Compact the rubblized materials uniformly using vibratory roller.

6.0 QUALITY OF THE RUBBLIZATION AND PAVING OPERATIONS

There are four objectives (stated in chapter 3 and repeated here for convenience) that need to be achieved by the rubblization operation and one objective in placing the asphalt concrete. These are:

1. **Breaking the Concrete Slab** - Breaking the concrete slabs into small pieces (less than 8 in. maximum dimension). This would eliminate independent movement of large pieces and would increase the degree of interlocking between the broken concrete pieces.

2. **Steel Debonding** - Debonding the temperature steel to decrease the magnitudes of temperature expansion and contraction of the rubblized concrete slab and hence, to reduce the potential of reflective cracking.

3. **Joint Integrity** - Destroying the integrity of the concrete joints to prevent reflective joint cracking.

4. **Rubblized and Fractured Concrete Layers** - Eliminating or decreasing the potential of rubblizing the concrete slab into two distinctive layers; a rubblized material layer and a fractured concrete layer. The two layers when capped with asphalt concrete would behave like a sandwich model (a soft layer between two hard layers). Higher differential stiffness between the three layers causes increases in the load-induced tensile stress at the top of the AC layer, which may cause increases in top-down cracking potential.

5. **Segregation** - Eliminating particle and temperature segregations in the asphalt concrete. Physical or particle segregation substantially decreases the service life

of the segregated areas and decreases the tensile strength of the AC (2 and 3). Figure 4.10 shows two views of a rubblized pavement section along US 23. The construction was completed in 2000. Less than two years after the completion of construction, the segregated area along a part of the passing lane caused severe raveling. The traffic lane (outer lane) and the passing lane outside the segregated area were still in perfect condition in May 2002 (the surveying date). Likewise, figure 4.11 shows two views of an area along US 131where an end-of-load segregation was found.

Examination of rubblized concrete pavements where trenches were excavated at mid slab and transverse joints prior to the placement of the AC surface revealed that in general:

1. The rubblization procedure produced two different layers in the rubblized concrete slabs, a rubblized material layer at the top and a fractured concrete layer at the bottom as shown in figures 4.12 and 4.13. The thickness of each layer varied from one location to another. In some areas, the fractured concrete extended to the original pavement surface (see figures 4.14 and 4.15) while in other locations the rubblized material extended to the bottom of the original concrete slab. Further, the stiffnesses of the two layers were substantially different. It was estimated that the stiffness of the fractured concrete is in order of magnitude higher than that of the rubblized material layer. Such differential stiffness may cause high tensile stress at the top of the AC surface due to traffic load, which increases the potential for top-down cracking.

2. At few locations, the temperature steel was debonded from the original concrete as shown in figure 4.16. However, at most locations, the temperature steel was not debonded.

3. At some longitudinal and transverse joints, the integrity of the joints in the original slabs was not completely destroyed (see figure 4.17). Some dowel bars were found embedded in the concrete on both sides of the joint. This may cause the development of reflective joint cracking.

4. On some projects, the drainability of the fractured concrete layer was poor (see figure 4.18). The layer would trap water that infiltrates through cracks in the asphalt layer. The trapped water under the asphalt layer would increase the stripping potential of the asphalt layer.

5. At some locations, the rubblization procedure caused some large concrete pieces (more than 8 in.) to rotate and/or penetrate the underlying base or roadbed material. This implies that the base and/or the roadbed soil have failed in shear action (bearing capacity). This failure is mainly caused by saturated base and/or weak roadbed soil. If the shear failure in the base and/or subbase is not corrected, the finished pavement will experience shear failures in these locations as shown in figures 4.19 through 4.21.

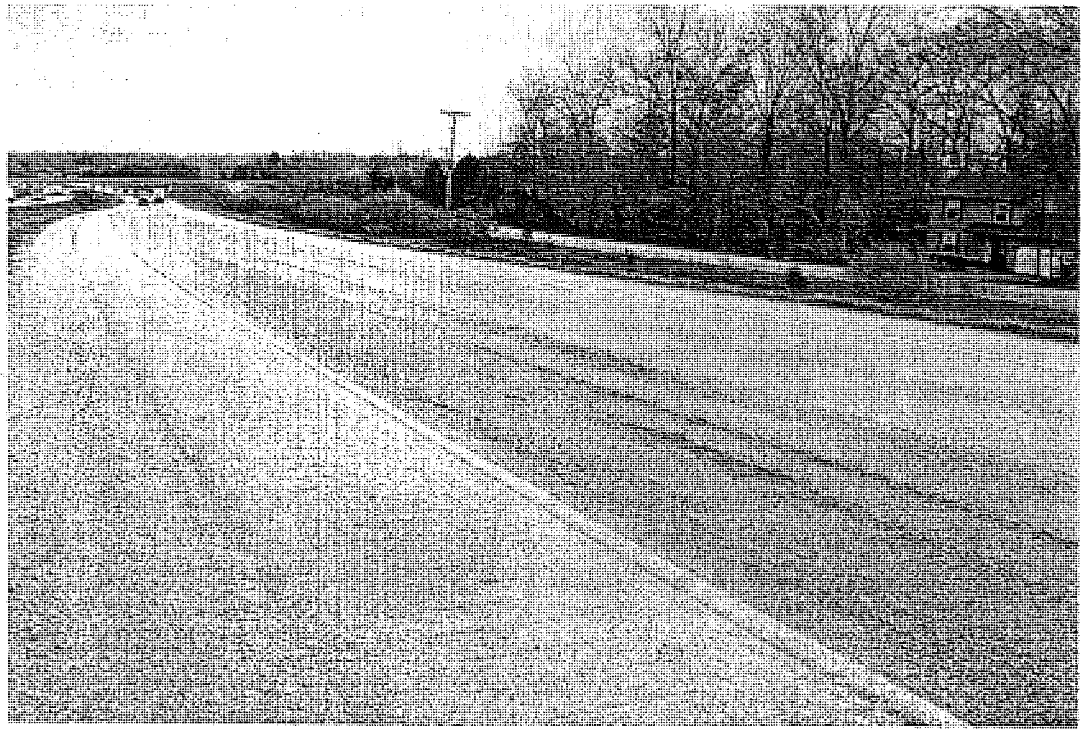

a) General view of a segregated area in the passing lane

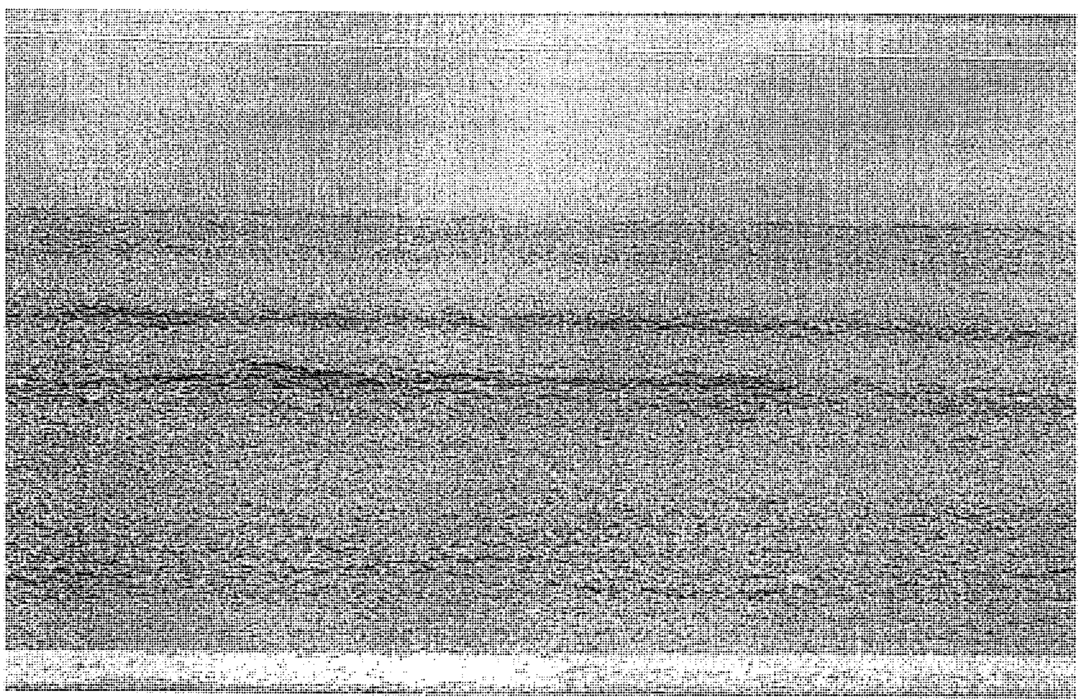

b) A close-up vies of the segregated area in the passing lane

Figure 4.10 Pavement condition in segregated and non-segregated areas along US 23 in May 2002, 2 years after construction,

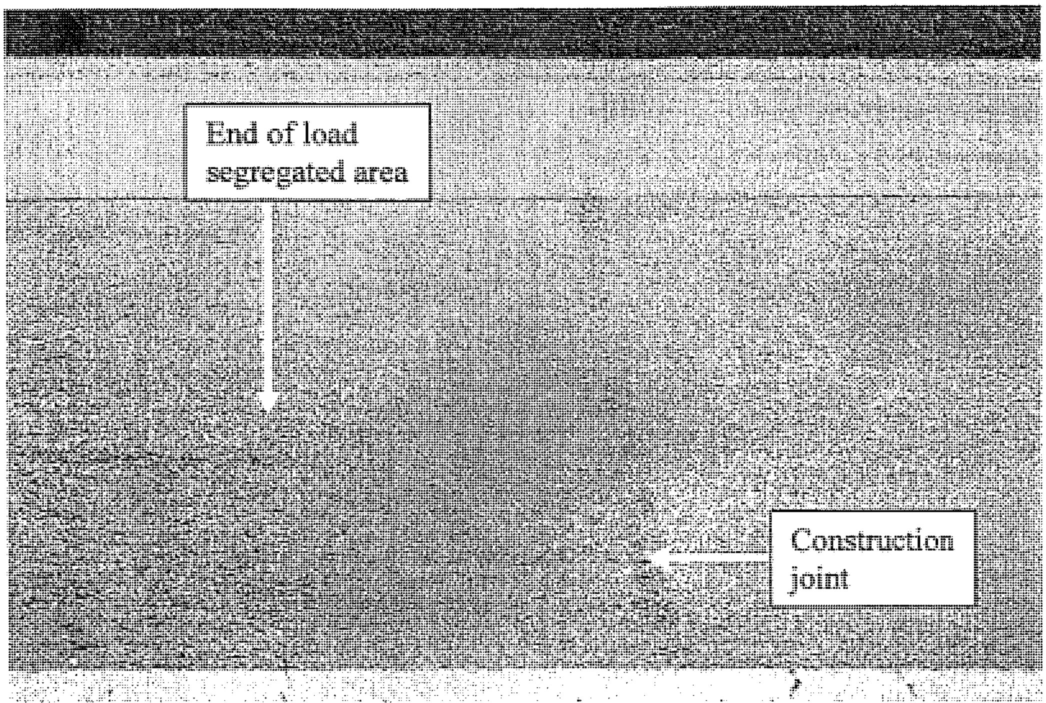

a) End of load segregated area

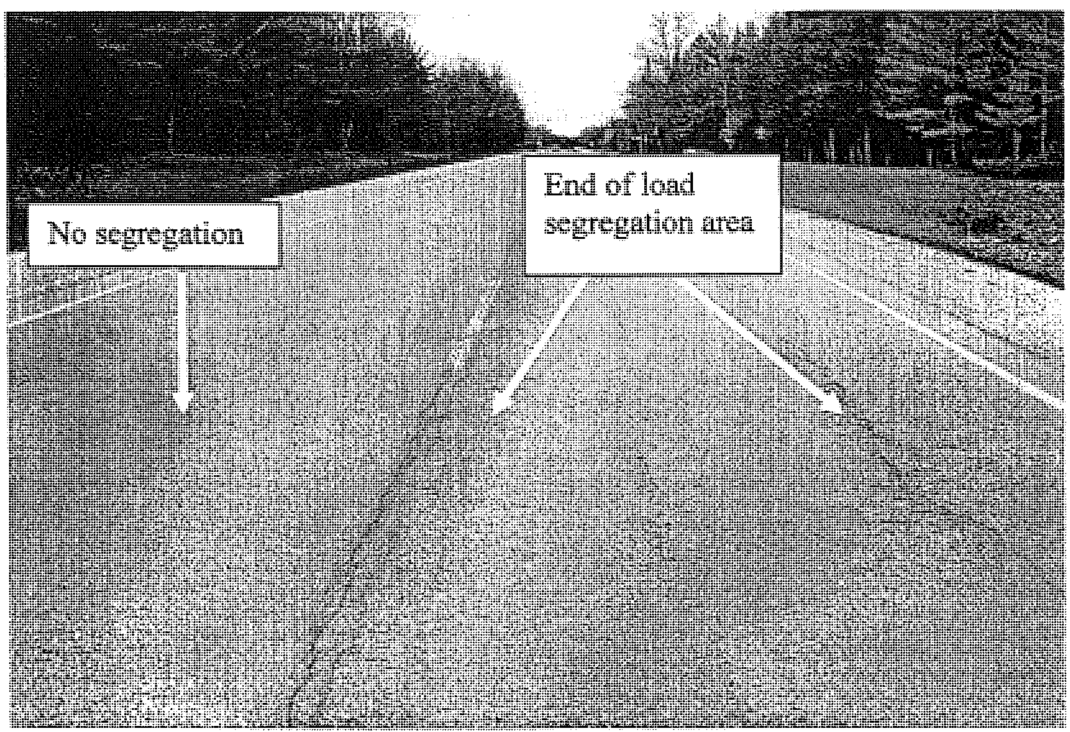

b) General pavement condition of segregated and not segregated areas

Figure 4.11 Pavement condition in segregated and not segregated areas along US-131 in May 2002, 5 years after construction

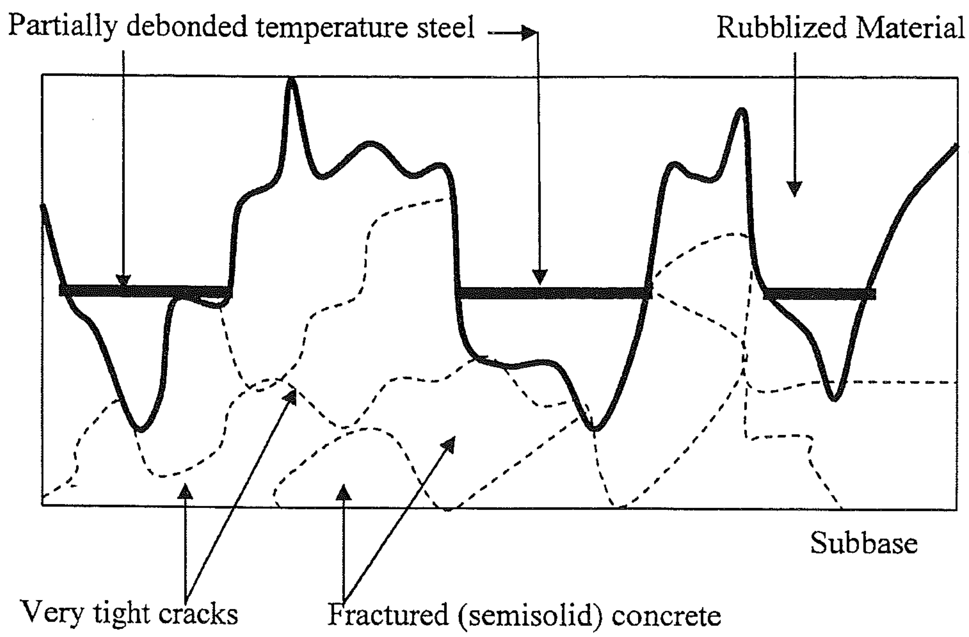

Figure 4.12 Schematic of rubblized concrete slab showing rubblized and fractured layers

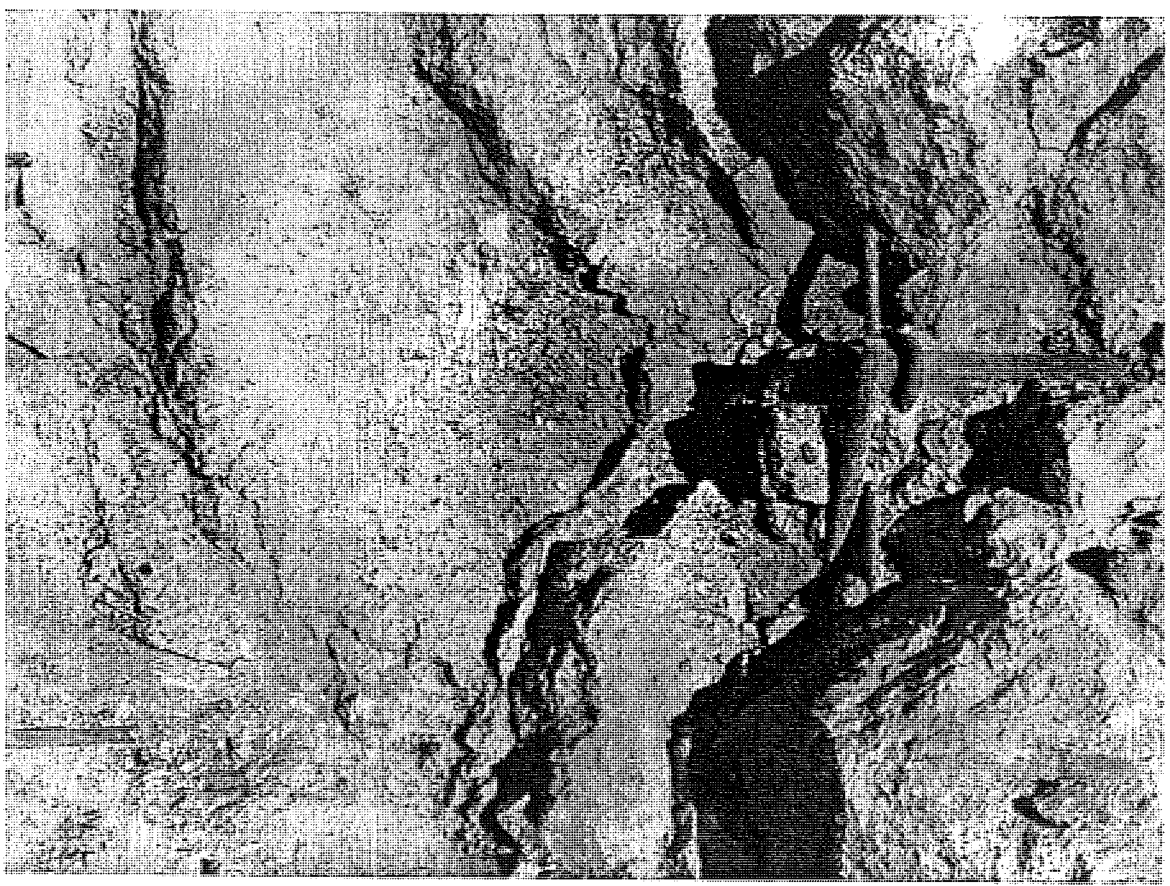

Figure 4.13 Close-up of the fractured concrete in a trench (M-50)

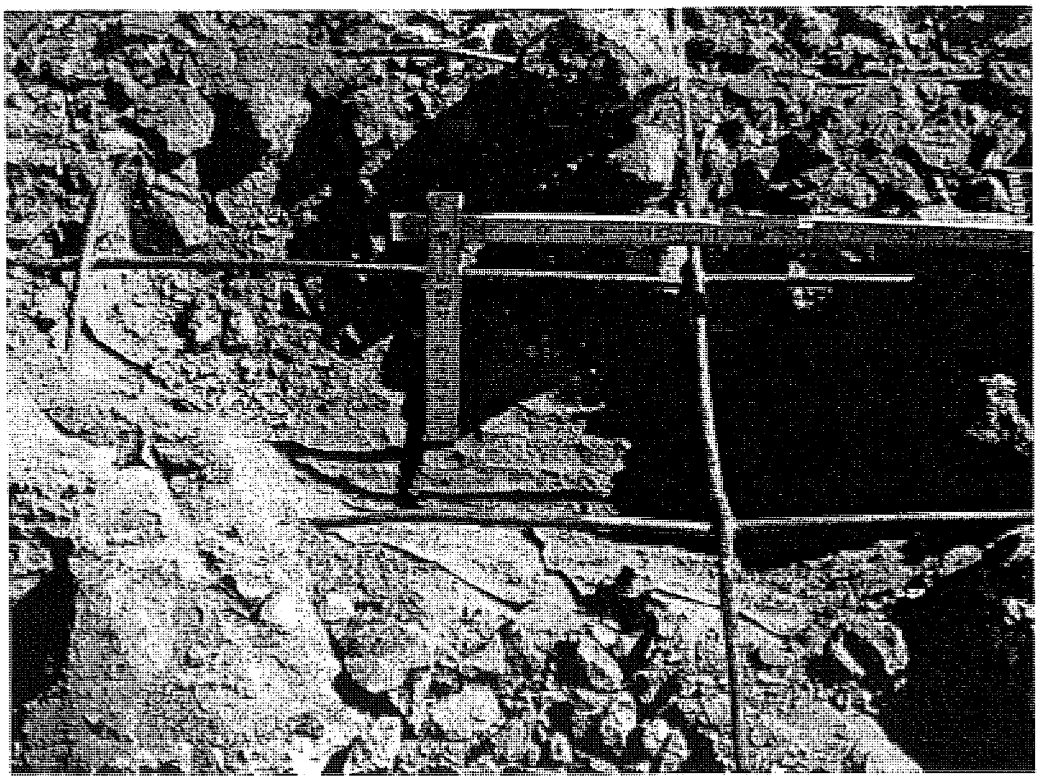

Figure 4.14 Excavated trench in a rubblized concrete slab showing the sand subbase and the fractured concrete

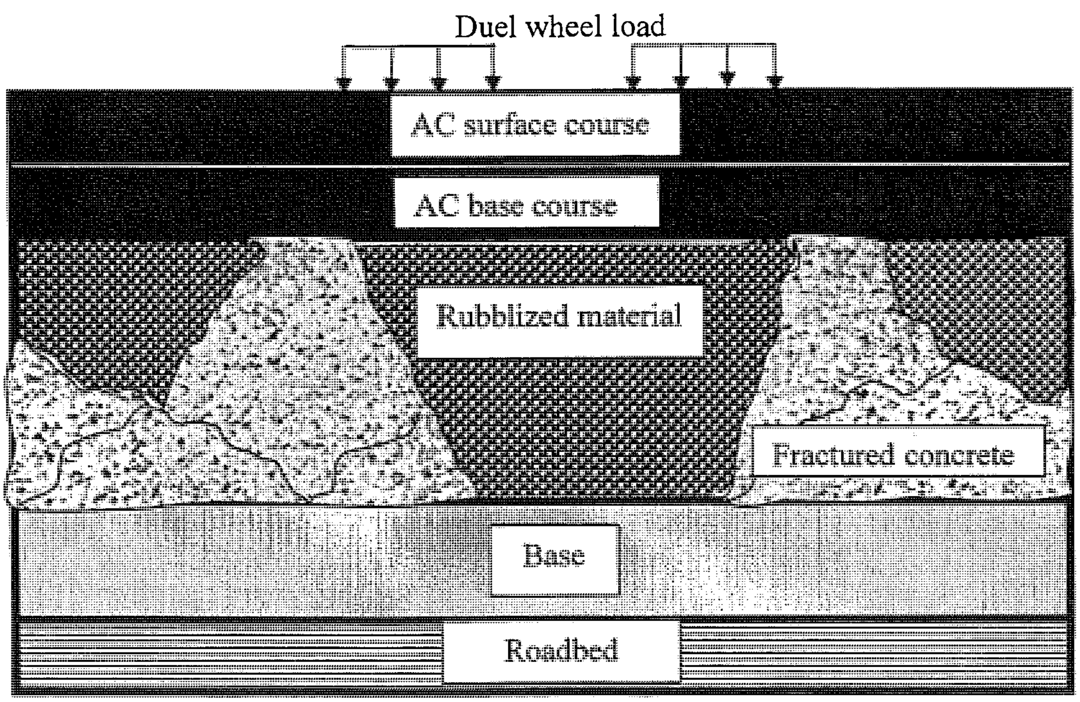

Figure 4.15 Schematic representation of the trench area of figure 4.13 after construction

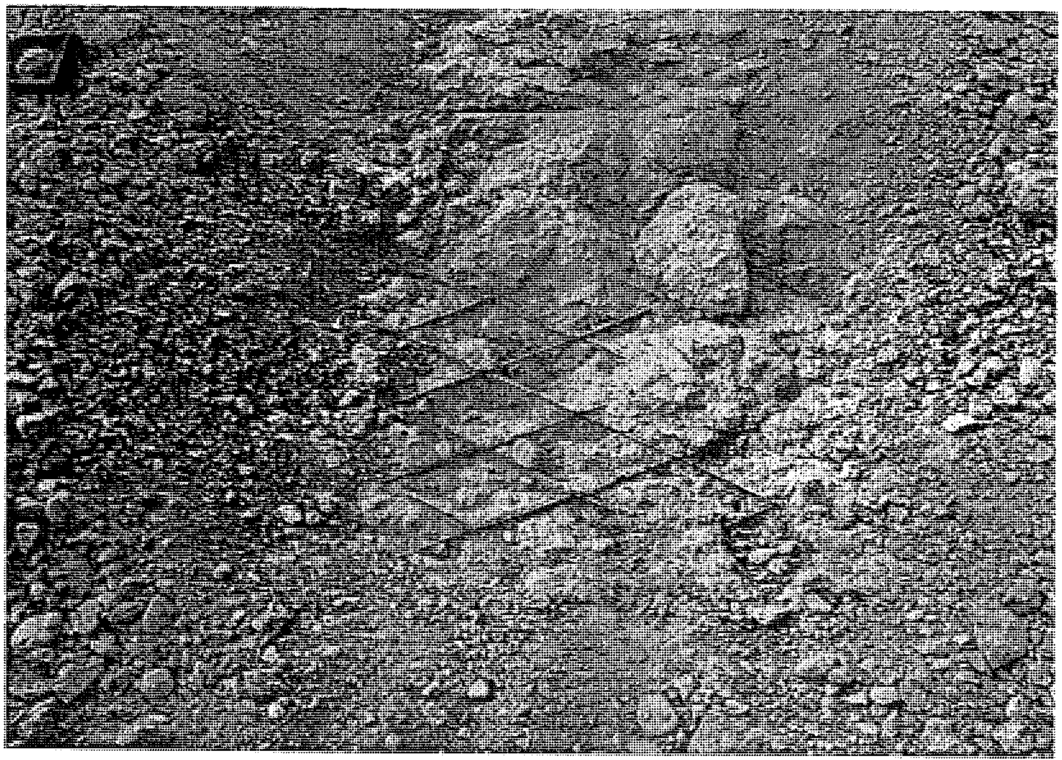

Figure 4.16 Partial debonding of the temperature steel (M-21)

Figure 4.17 Partial destruction of the joint integrity (US-131)

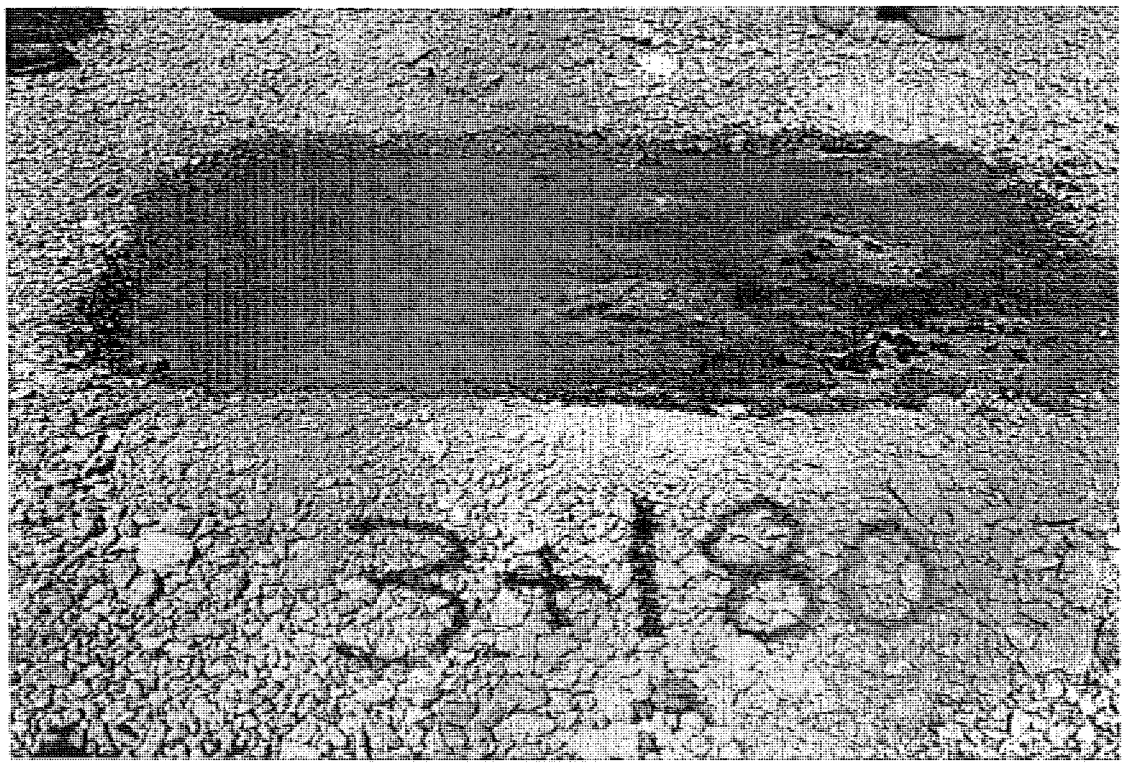

Figure 4.18 Trapped water above the fractured concrete in a trench along M-18

Figure 4.19 Shear failures in the rubblized pavement along NB I-196, August 2001

Figure 4.20 A shear failure along the rubblized pavement on NB I-196, May 2002

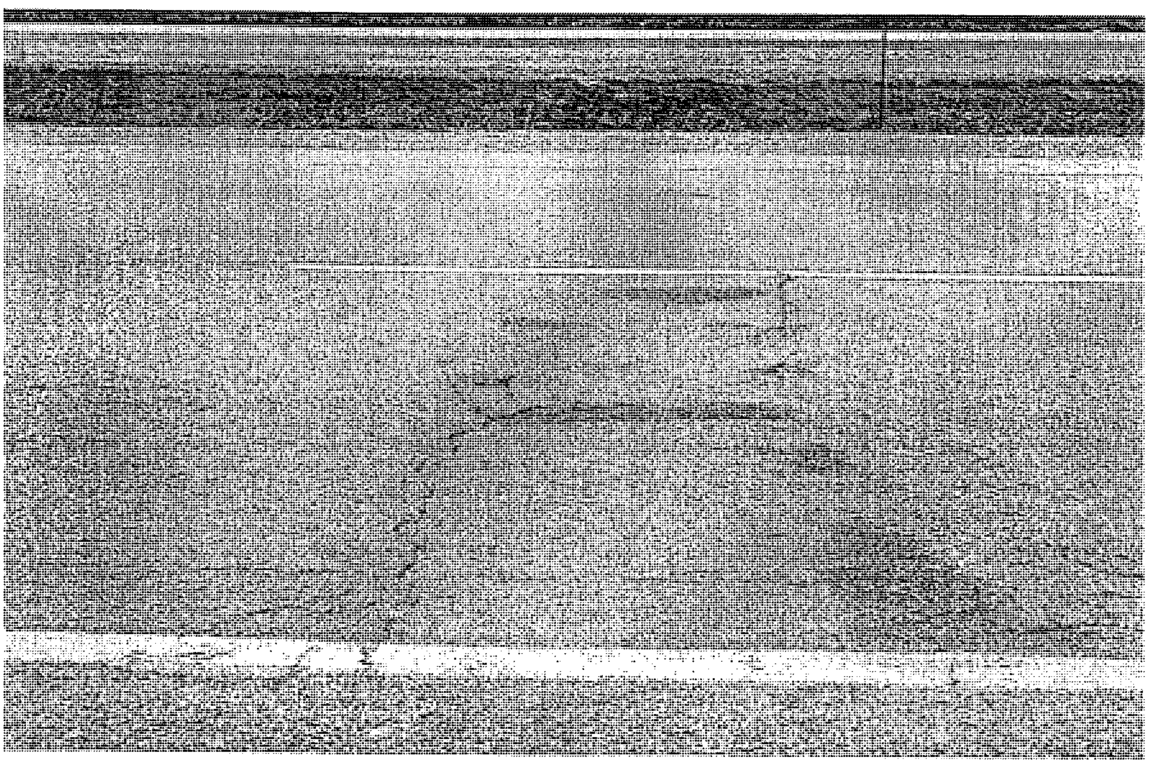

Figure 4.21 The initiation of a shear failure on rubblized project on NB I-196, May 2002

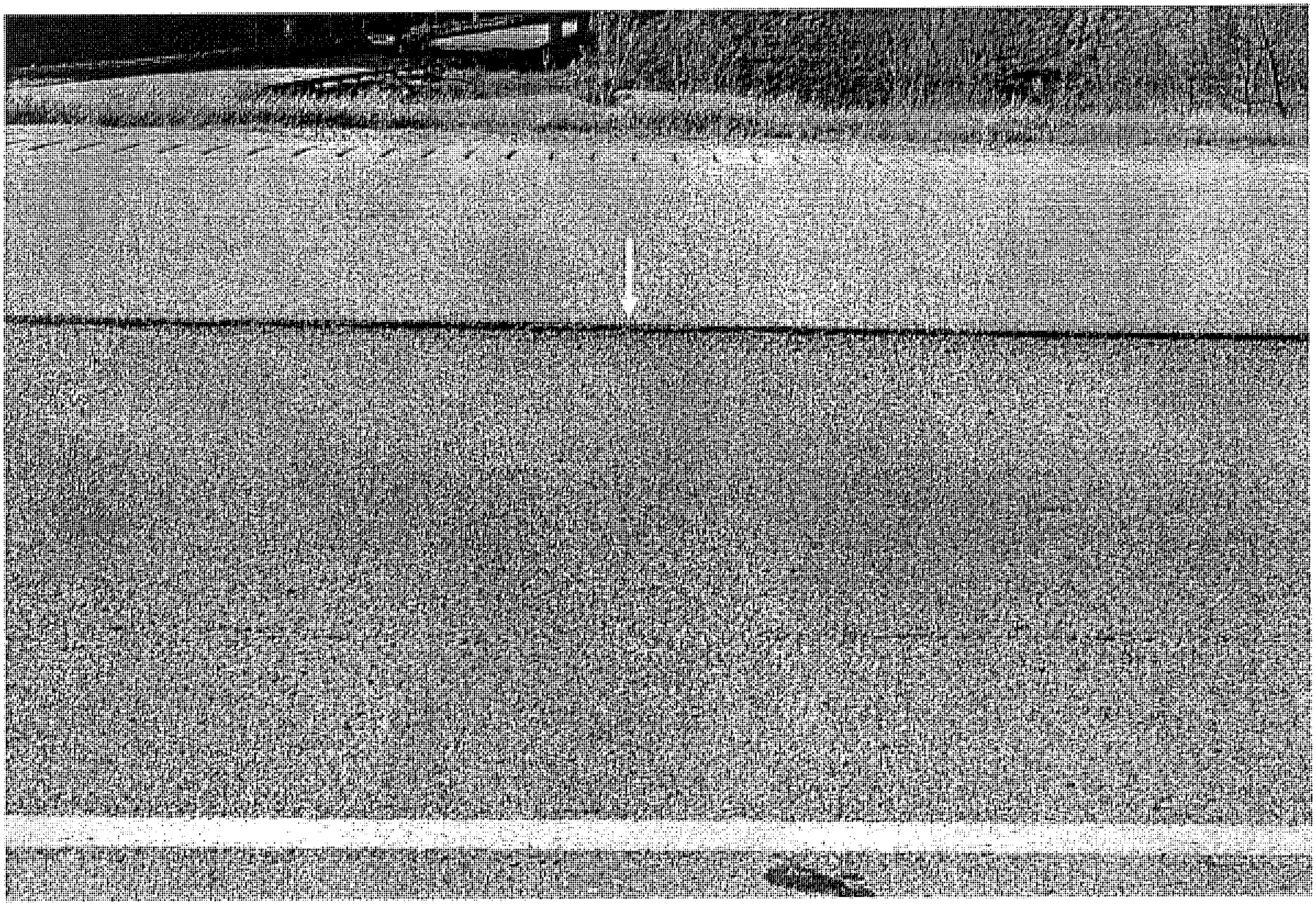

Figure 4.22 Differential settlements between the two lanes along NB I-196, May 2002

On some projects, the rubblization procedure produced rubblized material in one lane and mainly fractured concrete in the other lane along the longitudinal joint. This could mainly due to substantial difference in the concrete strength between the two lanes. The problem could be resolved by recalibration of the rubblizer parameters. If the situation is not corrected, it may cause differential settlement between the two lanes as shown in figure 4.22.

The significance of the above observations is that, in general, the objectives of rubblizing concrete pavements are not completely accomplished and that the rubblization procedure may adversely affect the pavement performance. Hence, the quality of rubblization could be defined in terms of the four objectives stated above and in terms of any variable that adversely affect the expected pavement service life of 20 years. Table 4.1 provides definition of the quality of rubblization along with a proposed method to assign a numerical value to the quality of rubblization:

The quality of the rubblization procedure could be substantially improved by implementing an equipment calibration procedure and by conducting adequate investigation during the project scoping process and prior to the selection of rubblization option. These issues are presented below.

6.1 Equipment Calibration

The quality of the rubblization procedure could be improved by calibrating the rubblizing equipment prior to the commencement of full-scale rubblization. Such calibration should be conducted at one end of the project using the following steps:

2. Divide the slab along one lane into twelve adjacent sections such that each section is 6-ft wide (across the slab) and 6-ft long (along the slab) as shown in figures 4.23 and 4.24 for the multi-hammer and the resonant frequency breakers, respectively.

3. Rubblize each section using different setting of the rubblizer parameters as follows:

Resonant Frequency Breaker		Multi-head breaker	
Frequency	43, and 45 Hz	Drop heights	48 and 60 in.
Velocity	2 and 3 mile per hour	Hammer weight	1200 and 1500 lb
Pressure	700, 800 and 1000 psi {pressure = force/(2*shoe width)}	Velocity	600, 700 and 800 ft/hr

4. Excavate two trenches along the slab as shown in figures 4.13 and 4.14 and examine the quality of rubblization as stated in the earlier section. That is,

Table 4.1 Definition, objectives and score of the quality of the rubblization operation

Definition, objectives and rating of rubblization			
Rubblization Definition and Objectives The quality of rubblization is a measure of the degree of success to which the rubblization procedure satisfies the following objectives. 1. Breaking the concrete slabs to pieces smaller than 6 in. (152 mm) 2. Completely debonding the temperature Steel 3. Destroying joint integrity 4. Producing full-depth rubblization The rating of the quality of rubblization can be calculated using the following equation: $$\mathbf{QR = Max\ (S_i)}$$ Where QR = quality of rubblization and S_i is a score relative to the i^{th} objective. Lower QR values imply better rubblization quality. A QR value of 50 is the threshold value above which the quality of rubblization is not acceptable. The proposed values of S_i are listed below.			
Score of each objective of the rubblization operation			
Objective	Measurements within a 3-ft wide and 6-ft long trench	Best score	Maximum acceptable score
1	50*the number of loose pieces larger than 6 in.	0	50
2	100* the area of the trench where steel is not debonded/the total area of the trench (%)	0	50
3	25* the number of dowel bars that cannot be easily extracted from the trench.	0	50
4	100* the thickness of the fractured concrete in the trench/the total slab thickness (%)	0	50

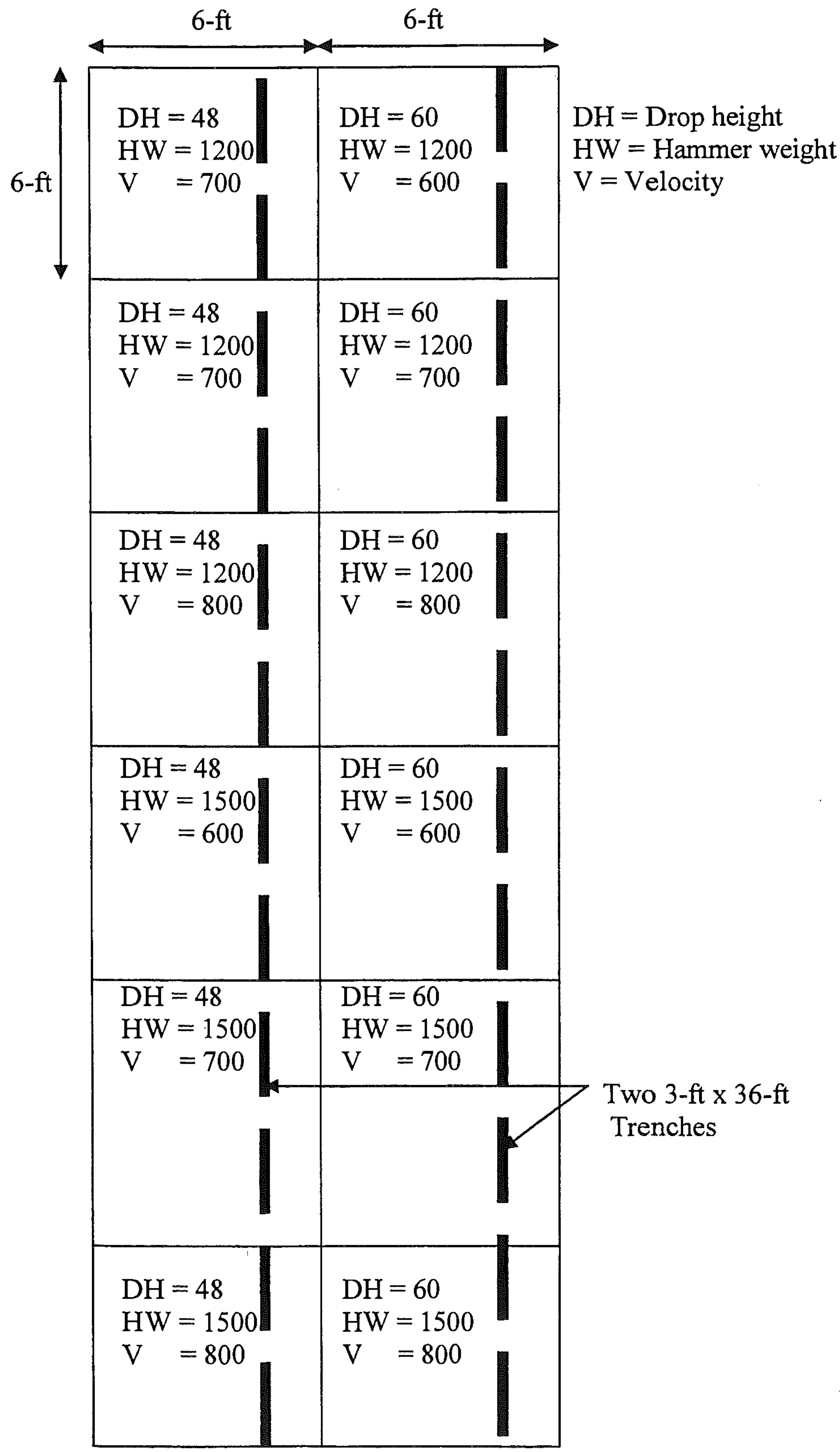

Figure 4.23 Calibration layouts for the multi hammer rubblizer

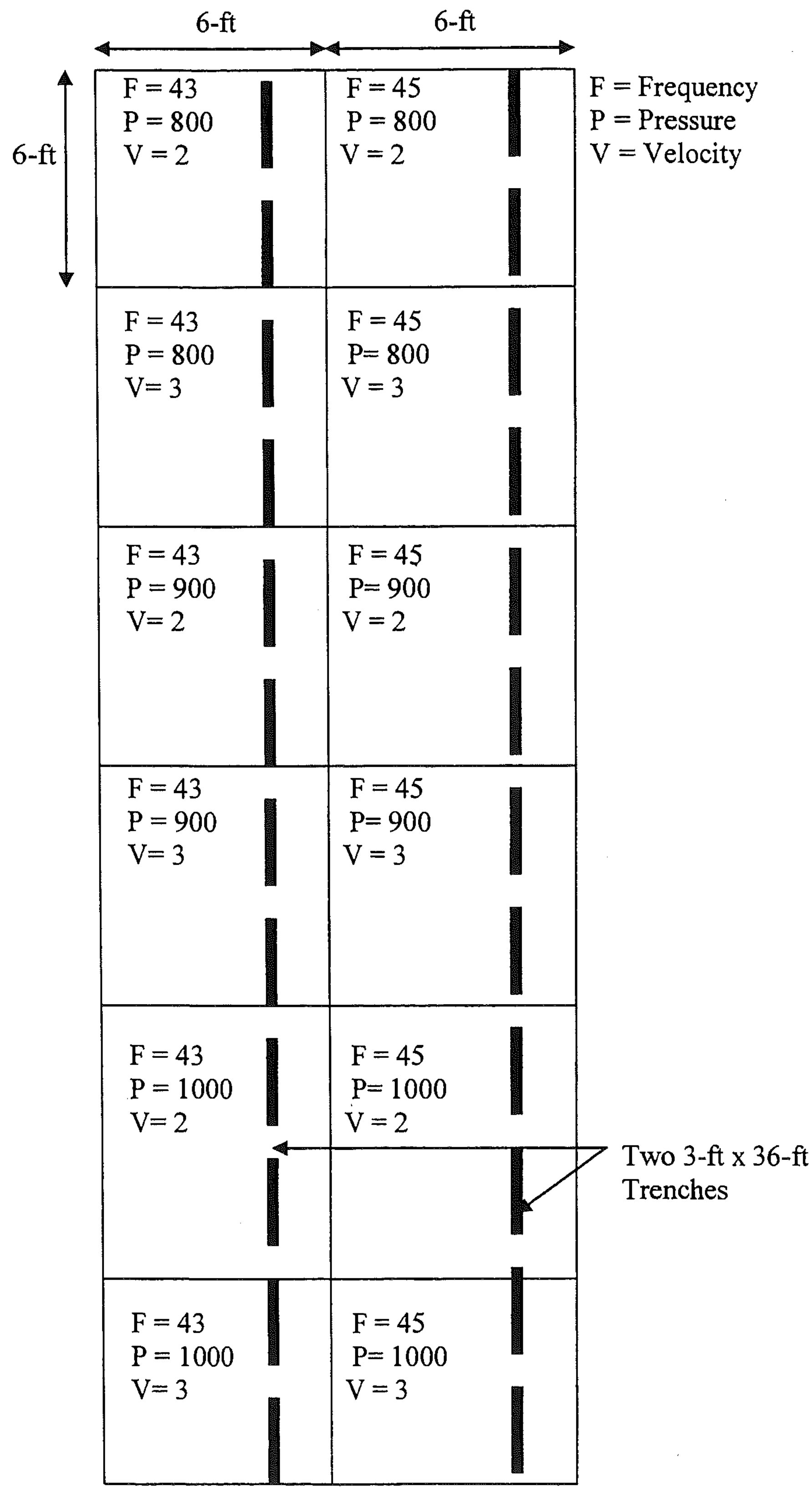

Figure 4.22 Calibration layouts for the resonant frequency breaker

investigate the degree of steel debonding, the depth of the rubblized material, and the thickness of the fractured concrete. The settings that yield the best results should be used to rubblize the rest of the concrete slabs.

4. Repeat the calibration when the unconfined compressive strength of the concrete along or across the pavement changes by more than 50 percent (the contractor can obtain the compressive strength data from MDOT, the data should be obtained by MDOT during the forensic investigation of the pavement). For example when a widening concrete strip exists, it is likely that the strength of the newer concrete is different than that of the original concrete. In such a scenario, the calibration should be conducted along the old concrete and the widening strip.

5. Excavate the rest of the rubblized material and fractured concrete and replace with approved filler aggregate. This section of the project will be later used by MDOT as a control section. Historical distress data collected along this section will be compared to those collected along the rubblized section, which would help MDOT to compare the performance of both sections.

6.2 Project scoping

Although the AASHTO 1993 Pavement Design Guide (1) states that rubblization can be used as a rehabilitation option for any distressed concrete pavement condition, field data do not support such statement. On the contrary, based on field observations that were conducted during the Phase I Study of this research project, rubblization is not an appropriate rehabilitation option for some distressed concrete pavements. Hence, prior to the selection of concrete pavement projects for rubblization, engineering forensic investigation should be conducted. The investigation should consist of the following items:

1. **History** – Obtain all available information regarding the original construction of the candidate pavement and its rehabilitation history. These include: temperature steel, dowel and tie bars, thickness, pavement type (JRCP, JPCP or CRCP), joint spacing, widening strip, full or partial depth patches, overlays and so forth.

2. **Distress** - Obtain the PMS distress data and conduct distress survey to determine the extent of longitudinal and transverse cracks and other discontinuities such as asphalt patches in the concrete pavement.

3. **Nondestructive Deflection Test (NDT)** – Conduct FWD test at 500-ft interval along the project. Use the deflection data to backcalculate the stiffness or modulus of subgrade reaction of the roadbed soil.

4. **Coring** – Obtain one concrete core for each 500-ft interval along the project. Examine the cores for delamination type cracks and record the width of the cracks. Determine the compressive strength of each core. If asphalt overlay is

present; determine the thickness of the overlay (for backcalculation and for milling purposes). If widening strips exist, obtain cores from the widening strip to determine the compressive strength of the concrete.

5. **Soil boring** - At two to three core locations, drill through the base, subbase and at least 2 ft through the roadbed soil. The objectives of the drilling are to document the type of base, subbase and roadbed materials and to determine whether or not the roadbed soil is saturated.

Based on the analysis of the above data, the following pavements should not be selected for rubblization:

1. Composite or concrete pavements that have extensive discontinuities. The rubblization energy will dissipate in the gaps at discontinuities instead of breaking the concrete slab. Such discontinuities include:

   a) Extensive longitudinal and transverse cracks as defined in MDOT distress manual.
   b) Concrete pavements that were previously rehabilitated using crack and seat method.
   c) Concrete pavements with frequent delamination type cracks.

2. Concrete pavements that are supported on soft or saturated subbase and/or roadbed soil. The term "soft subbase" refers to any subbase material having resilient modulus of less than 7000 psi. The term "soft roadbed soil" refers to any roadbed soil having a resilient modulus of less than 3000 psi.

3. Concrete pavements supported on a considerable soft subbase relative to the stiffness of the roadbed soil. The rubblization energy causes shear failure and lateral displacement of the subbase. For example, if a concrete pavement is supported on a base material with 10,000-psi modulus and a roadbed soil with 20,000-psi modulus, the rubblization energy may cause the softer subbase to fail in shear or be displaced laterally. This scenario is analogous to a sandwich model where a soft material is housed between two harder layers; the concrete and the roadbed soil.

In addition, the timing of the rubblization operation is very crucial to its success. For example, the operation should not commence immediately after a period of sustained rain (few days). The deteriorated and cracked concrete pavements would allow considerable water infiltration causing softening of the subbase material and roadbed soil. Likewise, commencing the rubblization operation shortly after the end of the thaw period is not desirable because of the high probability of roadbed saturation.

REFRENCES

1. The American Association of State Highway and Transportation Officials, "AASHTO Guide for Design of Pavement Structures", pp. 106-112, Washington D.C., 1993

2. Chang, Chieh-Min, Baladi, GY and Wolff, TF, "Using Pavement Distress Data to Assess the Impact of Construction on Pavement Performance", Journal of the Transportation Research Board no. 1761, 2001.

3. Chang, Chieh-Min, Baladi, GY and Wolff, TF, "Detecting Segregation in Bituminous Pavements", accepted for publication by the Transportation Research Board, paper no. 02-2634, January 2002.

CHAPTER 5
BACKCALCULATION OF LAYER MODULI

1.0 GENERAL

During the Phase I and Phase II studies, nondestructive deflection tests (NDT) were conducted on several rubblized pavement projects. The objectives of the tests include:

- Analyze the variations in the pavement deflections along and across the pavements.
- Backcalculate the moduli of the rubblized pavement layers.
- Assess the linearity of the pavement layers relative to load.

At each rubblized pavement project included in the NDT, a test section was selected and the section was divided into one or two 100-ft long test sites separated by 100-ft of pavement. At each test site, about forty FWD test locations were marked on the pavement surface as shown in figure 5. 1. The circles and the letter "X" in the figure indicate core and FWD test locations, respectively. The deflection data are discussed in later sections.

All NDT were conducted using the MDOT KUAB Falling Weight Deflectometer (FWD). The configuration and spacing of the 9 FWD deflection sensors are shown in figure 5. 2. All deflection data were recorded by an on-board computer to within 0.01 mils (0.00001 in.). Also at each FWD test location, the pavement and air temperatures were measured and the data were recorded. After the FWD tests were completed, between 5 and 12 pavement cores were extracted and the thickness of each core was measured. The thickness data were used as input to the backcalculation program. The deflections from sensors D1 through D7 (see figure 5. 2) were used to backcalculate the layer moduli using the MICHBACK computer software.

All FWD tests consisted of 4 drops, the deflection data from the first drop was not recorded while the data from the other three drops were recorded. Further, most tests were conducted using targeted 9000-lb load. On some projects, few FWD tests were conducted at different load levels in order to assess the linearity of the pavement response to load. Also on some projects, about ten FWD tests were conducted at the same test location in order to analyze the repeatability of the measured deflection data. Both linearity and repeatability are discusses in the next section.

2.0 REPEATABILITY AND LINEARITY OF THE DEFLECTION DATA

On seven pavement projects, several FWD tests were conducted at the same location for each of the following loads: 5,500, 9,000, 16,000 and 21,000 lb. The purposes of the test are to examine the repeatability and linearity of the deflection data at all seven sensor locations. Table 5.1 depicts the projects along which the repeatability and linearity tests were conducted along with the number of FWD tests (number of drops) for each load level. Typical results of the repeatability tests for I-69 EB, test section 1, site 1 are listed in table 5.2. The table provides a list of the average measured deflection at each sensor locations, the standard

Table 5.1 Pavement projects where repeatability and linearity tests were conducted

Test sites*	Load (lb)	Number of drops	Load (lb)	Number of drops	Load (lb)	Number of drops	Load (lb)	Number of drops
20273-21			9000	20	16000	10	21000	10
10692-12	5500	10	9000	20	16000	10	21000	10
30373-52	5500	10	9000	20	16000	10	21000	10
20102-11	5500	10	9000	20	16000	10	21000	10

* refer to the test sites reported in the investigations of rubblized pavements (Chapter 3)

Table 5.2 Averages and standard deviations of deflections D1 through D7 at different load levels, I-69 EB section 1 test site 1

Load (pound)	Number of drops	Statistics	Deflection (mils)						
			D1	D2	D3	D4	D5	D6	D7
5500	10	Average	4.93	3.40	2.85	2.42	2.09	1.56	0.84
		STDEV (mils)	0.07	0.04	0.04	0.04	0.03	0.03	0.04
		CV (%)	1.4	1.1	1.3	1.5	1.5	1.9	4.4
9000	20	Average	8.00	5.63	4.87	4.17	3.58	2.62	1.37
		STDEV (mils)	0.06	0.05	0.04	0.04	0.03	0.02	0.02
		CV (%)	0.8	0.9	0.9	0.9	0.8	0.9	1.6
16000	10	Average	14.35	10.24	8.93	7.59	6.58	4.77	2.55
		STDEV (mils)	0.04	0.04	0.10	0.04	0.03	0.03	0.03
		CV (%)	0.3	0.4	1.2	0.5	0.4	0.7	1.3
21000	10	Average	18.60	13.37	11.58	9.83	8.55	6.22	3.36
		STDEV (mils)	0.05	0.04	0.10	0.03	0.02	0.02	0.03
		CV (%)	0.3	0.3	0.9	0.3	0.3	0.3	0.8

STDEV = Standard deviation
CV = Coefficient of variation = standard deviation as a percent of the average

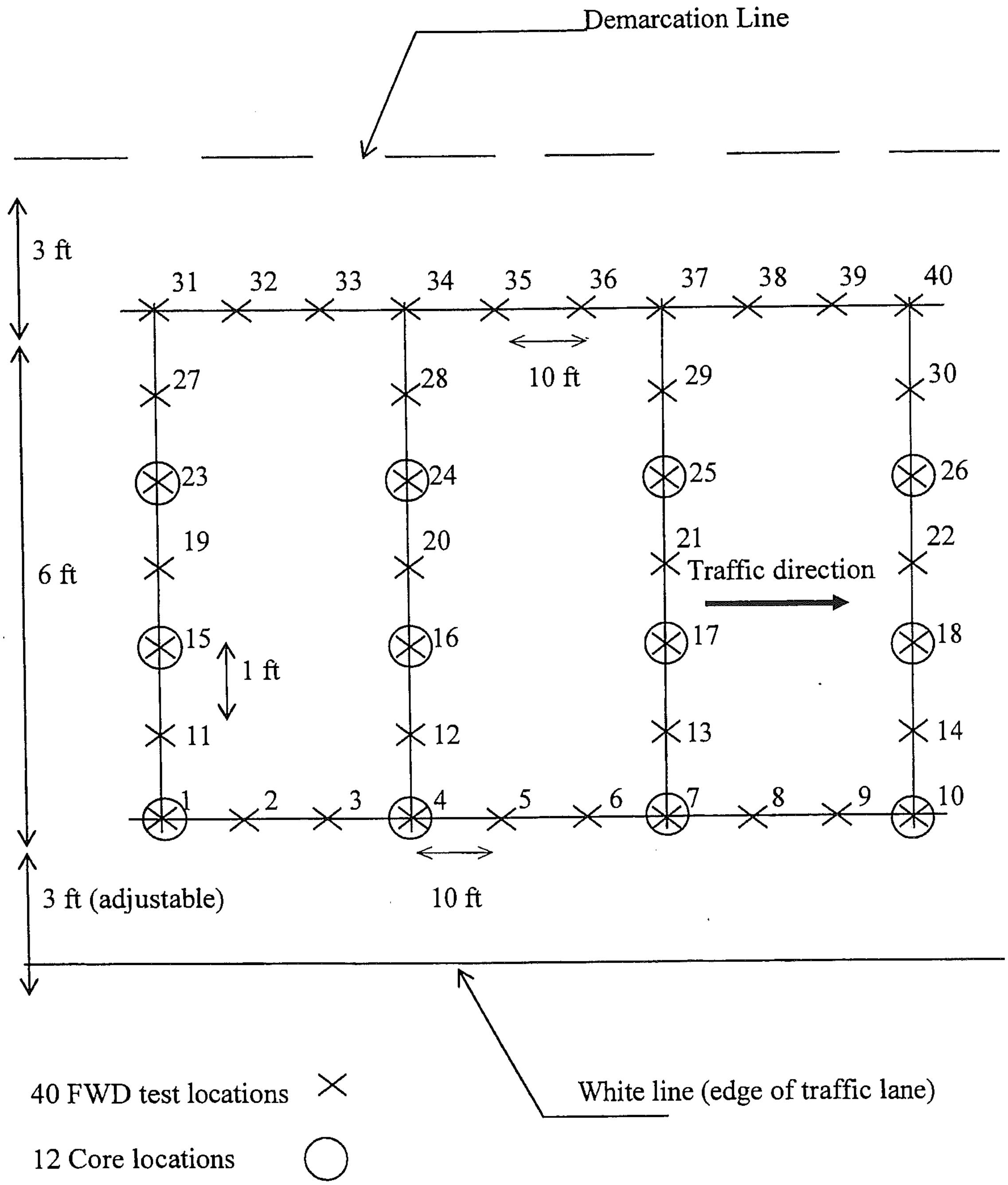

Figure 5.1 Typical FWD tests and cores layout

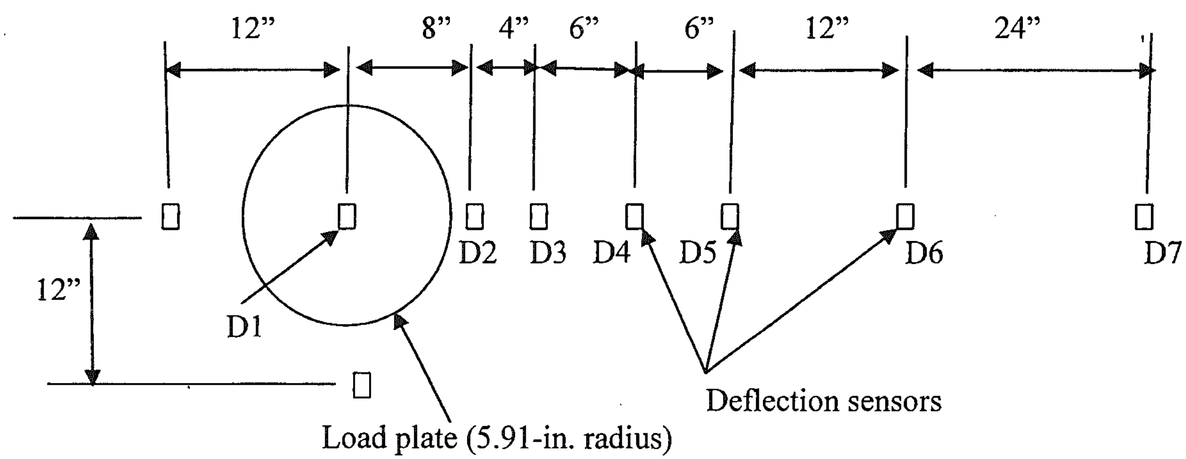

Figure 5.2 Schematic of FWD load plate and the deflection sensors

deviation and the coefficient of variation (standard deviation as percent of the average) of the deflection data at each load level. As can be seen, except for deflection sensor 3 (D3), the maximum standard deviation is 0.07 mils, which is well below the performance specifications for the FWD (1). Deflection sensor D3 shows good repeatability for the 5500- and 9000-lb load levels (standard deviation of less than 0.05 mils) and slightly higher standard deviation (0.1 mils) for the 16,000- and 21,000-lb loads, which is equal to the specified performance of FWD. Note that the impact of the repeatability (accuracy) of the measured deflection on the backcalculated layer moduli should not be measured in terms of absolute mils. It should be measured in terms of percent of the measured deflection. To illustrate, the impact of 0.07 mils error on 1.5 mils measured deflection is much higher than its impact on 9 mils measured deflection. Therefore, the coefficient of variation of each deflection sensor was calculated and is included in the table.

As stated above, linearity tests were also conducted together with the repeatability tests on seven pavement sections. As stated earlier, the purpose of the linearity tests is to assess whether or not the pavement response to load is linear. At each of the four load levels stated above, ten or twenty FWD tests were conducted. The average of the measured deflection data for each load level was calculated and then normalized relative to the average deflection at a 9,000-lb load. Typical results from I-69 EB, section 1, site 1 are provided in table 5.3. Figure 5.3 depicts the average measured deflections versus the applied load. The data in the table 5.3 and figure 5.3 indicate that, for all practical purposes, the pavement response to load is linear. Based on the linearity of the pavement response to load, the deflection data were used in the backcalculation of layer moduli using a linear elastic layered system.

3.0 DEFLECTION DATA

Pavement deflection represents its direct response to the applied load. Deflection can be thought of as an index expressing the structural capacity of the pavement. Hence, variations in the measured deflection reflect parallel variations in the structural capacity of the pavement. Tables 5.4 and 5.5 list the measured pavement deflections along and across the pavement of I-75 SB, section 1, test sites 1 and 2, respectively. Table 5.6 provides similar information for the flexible pavement along US 27 SB section 1test site 1.

The average and the coefficient of variation for D1 through D7 deflections are also listed in the three tables. Figures 5.4 and 5.5 depict plots of D1 through D7 deflections at the various test locations on test sites 1 and 2, respectively. The data in tables 5.4 and 5.5 and in figures 5.4 and 5.5 indicate that:

1. The variations in the deflections of the rubblized concrete pavement on I-75 SB, section 1, test sites 1 and 2 are much higher than the variation on flexible pavement (see table 5.6).

2. As it was expected, for both test sites, the peak pavement deflection (D1) shows the highest variation. The reason is that, the D1 deflection is a measure of the cumulative deflections of all pavement layers and of the roadbed soil. Hence, variations in these

Table 5.3 Average deflections D1 through D7 1 at different load levels normalized to the average deflection at 9,000 pound load, I-69 EB section 1 test site 2

Load (pound)	Deflection (mils)						
	D1	D2	D3	D4	D5	D6	D7
5500	4.93	3.40	2.85	2.42	2.09	1.56	0.84
9000	8.00	5.63	4.87	4.17	3.58	2.62	1.37
16000	14.35	10.24	8.93	7.59	6.58	4.77	2.55
21000	18.60	13.37	11.58	9.83	8.55	6.22	3.36
Normalized load	Normalized deflection						
	D1	D2	D3	D4	D5	D6	D7
0.6	0.62	0.60	0.59	0.58	0.58	0.60	0.61
1.0	1.00	1.00	1.00	1.00	1.00	1.00	1.00
1.8	1.79	1.82	1.84	1.82	1.84	1.82	1.87
2.3	2.33	2.37	2.38	2.36	2.39	2.38	2.46

Table 5.4 Deflections D1 through D7, I-75 SB section 1 test site 1

FWD Station	Deflection (mils)						
	D1	D2	D3	D4	D5	D6	D7
1	9.46	8.29	7.45	6.22	5.30	3.67	2.03
2	10.02	8.59	7.69	6.47	5.48	3.82	2.12
3	9.62	8.48	7.78	6.47	5.17	3.64	2.03
4	9.52	8.17	7.22	5.93	4.96	3.51	1.92
5	9.73	8.44	7.53	6.25	5.22	3.59	1.85
6	9.56	8.07	7.13	5.92	4.98	3.50	1.90
7	9.88	8.25	7.35	6.14	5.17	3.67	1.97
8	9.32	8.18	7.36	6.18	5.31	3.82	2.02
9	9.01	7.81	7.09	6.03	5.11	3.70	2.02
10	9.07	7.78	6.94	5.86	4.78	3.31	1.79
11	9.67	8.39	7.50	6.24	5.20	3.50	1.92
12	9.24	7.73	6.89	5.80	4.93	3.58	1.92
13	9.00	7.76	6.95	5.82	4.89	3.17	1.72
14	10.30	8.47	7.26	5.96	5.02	3.52	1.90
15	10.06	8.69	7.41	5.79	4.91	3.61	2.04
16	8.12	7.22	6.44	5.42	4.58	3.27	1.85
17	8.22	6.97	6.27	5.34	4.60	3.38	1.87
18	8.90	7.78	6.98	5.84	4.90	3.15	1.73
19	7.77	6.70	6.04	5.16	4.50	3.40	1.81
20	7.68	6.63	6.03	5.16	4.44	3.34	1.95
21	7.22	6.21	5.60	4.87	4.26	3.29	1.87
22	7.76	6.30	5.68	4.88	4.27	3.28	1.89
23	8.57	7.55	6.81	5.67	4.74	3.21	1.73
24	7.43	6.47	5.89	5.12	4.48	3.46	1.84
25	7.49	6.53	5.90	5.11	4.45	3.39	1.99
26	6.87	5.93	5.40	4.78	4.21	3.32	1.91
27	8.50	7.46	6.69	5.57	4.62	3.20	1.74
28	6.92	6.10	5.64	4.98	4.45	3.51	1.89
29	6.65	5.96	5.53	4.91	4.33	3.35	2.01
30	6.49	5.69	5.25	4.72	4.19	3.33	1.94
31	8.30	7.30	6.58	5.52	4.62	3.26	1.75
32	7.07	6.20	5.65	4.92	4.34	3.40	1.94
33	6.05	5.48	5.14	4.68	4.22	3.50	2.12
34	9.70	8.16	7.24	6.18	5.26	3.87	1.99
35	7.26	6.29	5.66	4.89	4.25	3.31	1.98
36	7.89	7.09	6.42	5.70	4.53	3.27	1.90
37	8.29	6.89	6.21	5.24	4.45	3.26	1.82
38	7.06	6.11	5.57	4.90	4.28	3.30	1.94
39	6.36	5.66	5.28	4.80	4.32	3.44	1.99
40	6.76	5.96	5.55	5.02	4.49	3.62	2.12
41	8.47	7.33	6.55	5.54	4.67	3.27	1.77
42	8.76	7.85	6.77	5.62	4.73	3.34	1.86
Average	8.33	7.21	6.48	5.51	4.70	3.44	1.91
CV (%)	14	13	12	10	8	5	6

CV = Coefficient of variation = standard deviation as a percent of the average

Table 5.5 Deflections D1 through D7, I-75 SB section 1 test site 2

FWD Station	Deflection (mils)						
	D1	D2	D3	D4	D5	D6	D7
1	10.45	8.53	7.37	5.95	4.87	3.45	1.89
2	9.30	7.84	6.92	5.74	4.80	3.46	1.83
3	9.98	8.42	7.38	6.08	5.07	3.51	1.78
4	8.38	7.15	6.41	5.45	4.68	3.34	1.66
5	10.55	8.38	7.07	5.61	4.60	3.26	1.68
6	9.12	7.68	6.74	5.53	4.56	3.14	1.60
7	8.98	7.39	6.44	5.24	4.31	2.90	1.46
8	10.01	8.00	6.85	5.43	4.33	2.85	1.32
9	10.83	8.70	7.35	5.82	4.61	2.93	1.25
10	9.33	7.49	6.49	4.89	4.07	2.81	1.41
11	7.85	6.66	5.85	4.82	3.95	2.72	1.42
12	10.30	8.34	7.11	5.58	4.45	2.82	1.29
13	9.31	7.62	6.68	5.51	4.63	3.40	1.83
14	8.37	7.50	6.54	5.39	4.57	3.23	1.70
15	9.40	7.23	6.22	4.91	4.03	2.74	1.36
16	6.86	6.05	5.37	4.50	3.80	2.70	1.45
17	8.09	6.57	5.81	4.97	4.25	3.22	1.84
18	8.17	7.05	6.29	5.34	4.55	3.24	1.72
19	9.03	6.76	5.78	4.66	3.88	2.68	1.35
20	6.16	5.40	4.90	4.24	3.64	2.69	1.42
21	7.68	5.99	5.27	4.52	3.93	3.09	1.81
22	8.03	6.93	6.29	5.50	4.85	3.26	1.76
23	8.63	6.41	5.51	4.48	3.72	2.60	1.36
24	6.79	5.80	5.12	4.37	3.77	2.80	1.50
25	6.79	5.96	5.25	4.32	3.63	2.62	1.41
26	7.22	5.82	5.19	4.50	3.95	3.14	1.87
27	7.89	6.82	6.23	5.51	4.89	3.35	1.79
28	7.52	6.08	5.20	4.26	3.59	2.58	1.40
29	7.16	6.22	5.48	4.49	3.74	2.18	1.34
30	6.47	5.72	5.18	4.58	4.08	3.24	1.92
31	8.08	7.05	6.37	5.60	4.96	3.37	1.80
32	7.53	6.22	5.32	4.41	3.76	2.79	1.54
33	7.52	6.46	5.70	4.67	3.88	2.68	1.37
34	6.57	5.69	5.14	4.47	3.91	3.13	1.89
35	6.53	5.77	5.34	4.72	4.11	3.18	1.82
36	7.26	6.38	5.78	4.94	4.24	3.20	1.80
37	8.73	7.58	6.82	5.88	5.11	3.42	1.74
38	5.93	5.27	4.84	4.28	3.77	2.97	1.67
39	6.65	5.84	5.28	4.53	3.92	2.97	1.65
40	7.65	6.31	5.51	4.58	3.90	2.89	1.57
41	7.20	6.21	5.63	4.89	4.30	3.17	1.69
42	10.54	7.66	6.54	5.28	4.47	3.26	1.80
43	8.40	6.82	5.99	4.92	4.05	2.81	1.42
Average	8.21	6.83	6.01	5.01	4.24	3.02	1.61
CV (%)	16	14	12	11	10	10	13

CV = Coefficient of variation = standard deviation as a percent of the average

Table 5.6 Deflections D1 through D7 on an asphalt pavement, US 27 SB section 1test site 1

FWD Station	Deflection (mils)						
	D1	D2	D3	D4	D5	D6	D7
1	7.50	6.48	5.81	4.91	4.18	2.93	1.43
2	7.39	6.36	5.68	4.79	4.07	2.86	1.44
3	7.33	6.34	5.69	4.80	4.07	2.85	1.37
4	7.58	6.48	5.80	4.85	4.11	2.86	1.36
5	7.32	6.27	5.64	4.75	4.03	2.84	1.40
6	7.52	6.40	5.74	4.85	4.12	2.91	1.40
7	7.68	6.60	5.90	4.97	4.24	2.99	1.47
8	7.51	6.45	5.78	4.91	4.15	2.95	1.44
9	7.58	6.41	5.80	4.93	4.18	2.94	1.46
10	7.43	6.34	5.71	4.84	4.12	2.90	1.46
11	7.44	6.36	5.75	4.89	4.14	2.90	1.43
12	7.44	6.34	5.66	4.75	3.99	2.80	1.36
13	7.49	6.37	5.73	4.87	4.15	2.90	1.44
14	7.24	6.22	5.59	4.75	4.03	2.87	1.44
15	7.23	6.23	5.60	4.71	4.03	2.82	1.43
16	7.32	6.20	5.55	4.64	3.93	2.75	1.35
17	7.28	6.30	5.65	4.79	4.10	2.91	1.42
18	7.12	6.12	5.51	4.69	3.98	2.78	1.44
19	7.05	6.14	5.53	4.68	3.97	2.85	1.41
20	7.16	6.13	5.48	4.60	3.93	2.74	1.34
21	7.09	6.11	5.50	4.71	3.98	2.86	1.45
22	7.13	6.09	5.50	4.66	3.97	2.81	1.44
23	7.03	6.08	5.46	4.64	3.96	2.86	1.45
24	7.17	6.12	5.47	4.62	3.93	2.79	1.39
25	7.06	6.07	5.48	4.67	4.01	2.86	1.46
26	7.22	6.20	5.60	4.72	4.04	2.86	1.48
27	7.14	6.20	5.57	4.69	4.01	2.80	1.38
28	7.15	6.19	5.58	4.75	4.05	2.93	1.45
29	7.27	6.25	5.65	4.80	4.07	2.94	1.49
30	7.17	6.22	5.60	4.75	4.06	2.89	1.45
31	7.32	6.31	5.71	4.80	4.08	2.88	1.45
32	7.43	6.41	5.80	4.93	4.15	2.93	1.45
33	7.23	6.26	5.66	4.81	4.10	2.88	1.43
34	7.06	6.10	5.47	4.67	3.97	2.79	1.39
35	7.10	6.13	5.53	4.73	4.04	2.88	1.42
36	7.31	6.29	5.69	4.83	4.13	2.91	1.44
37	7.22	6.21	5.58	4.72	4.02	2.85	1.45
38	7.15	6.18	5.56	4.75	4.02	2.88	1.49
39	7.51	6.43	5.76	4.89	4.15	2.92	1.45
40	7.27	6.19	5.55	4.62	3.92	2.74	1.39
Average	7.29	6.26	5.63	4.77	4.05	2.87	1.43
CV (%)	2	2	2	2	2	2	3

CV = Coefficient of variation = standard deviation as a percent of the average

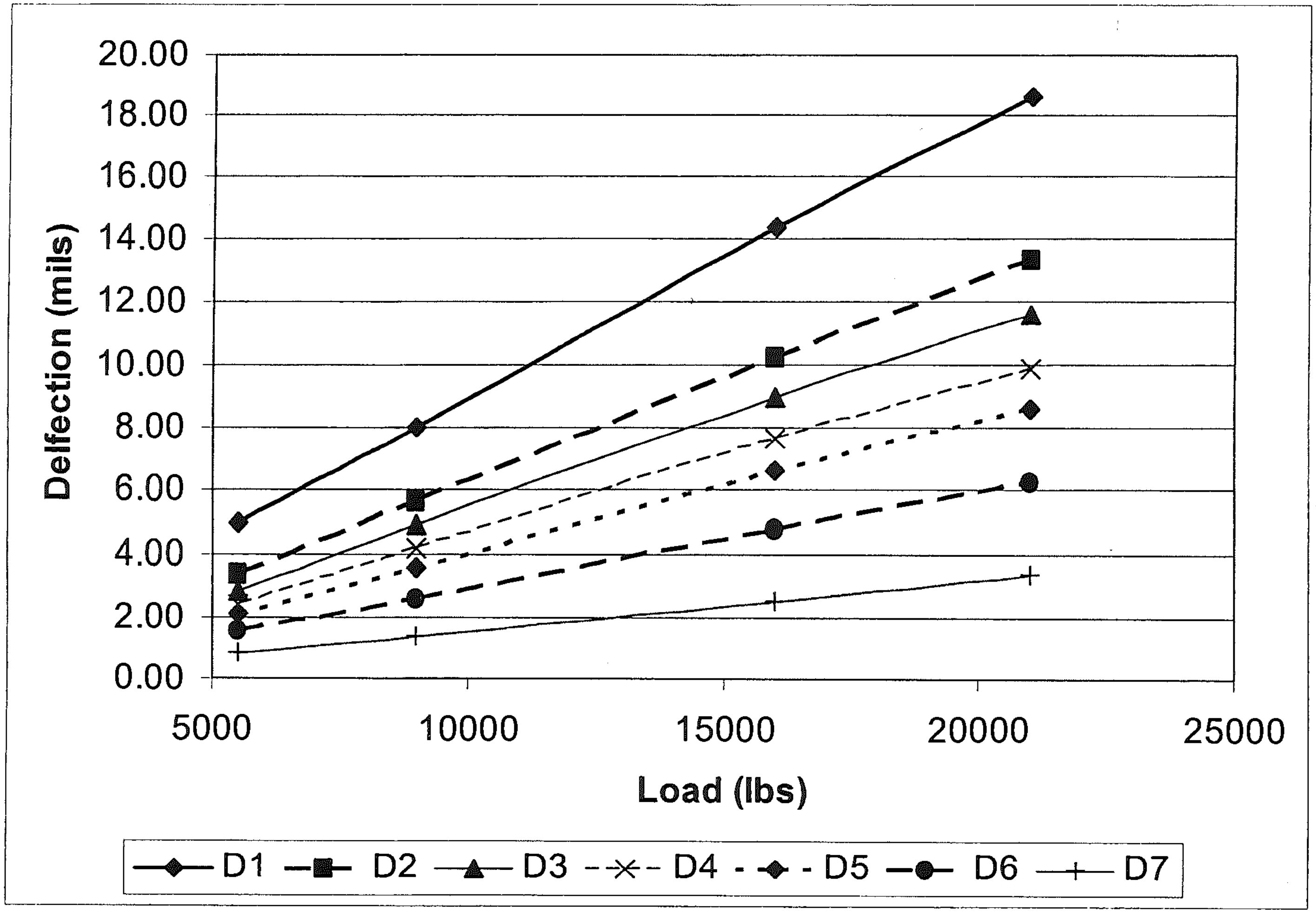

Figure 5.3 Average deflections D1 through D7 on I-69 section 1 site 1 at different load levels

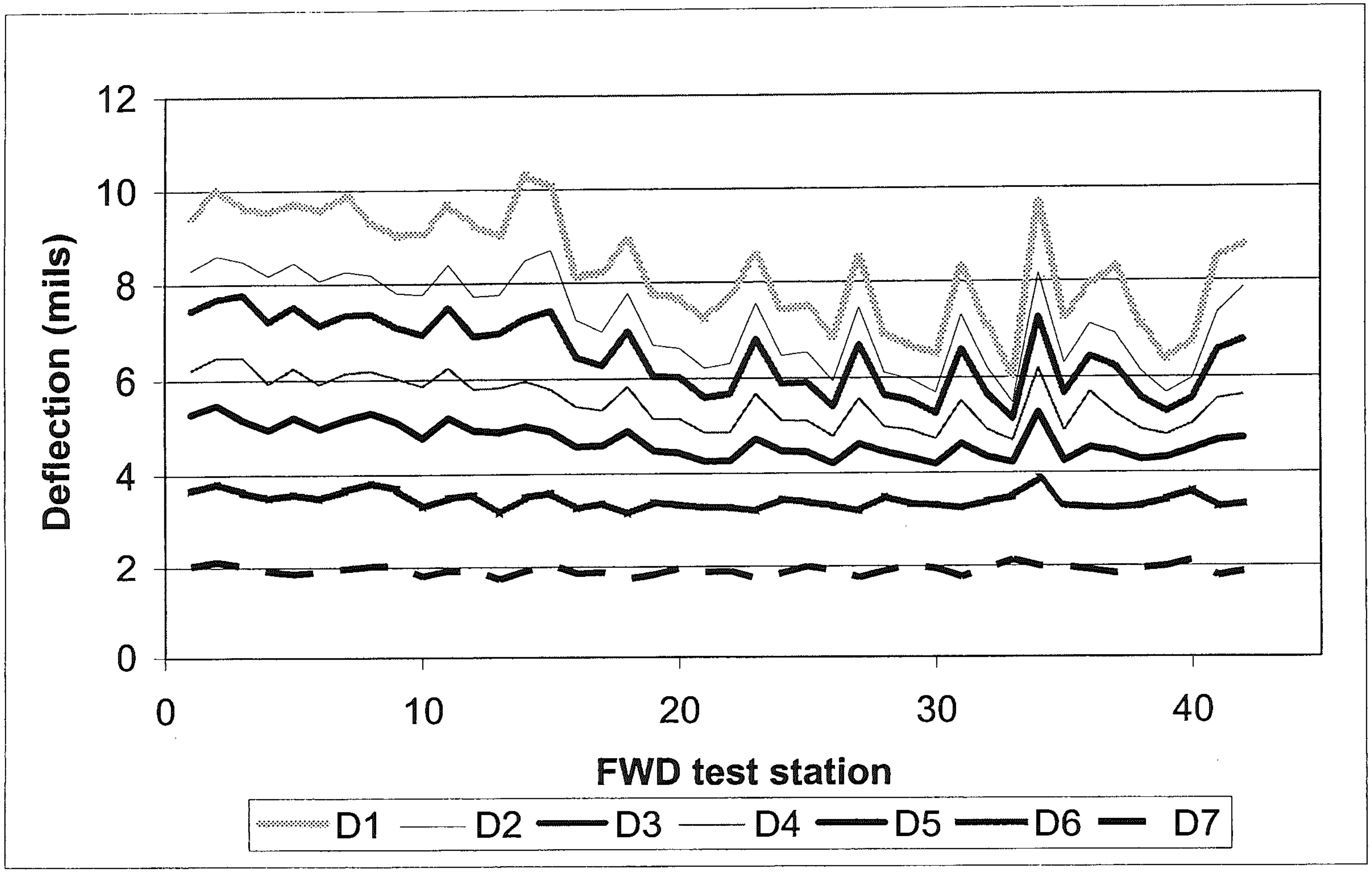

Figure 5.4 Variations of D1 through D7 deflections, I-75 SB, test section 1, site 1

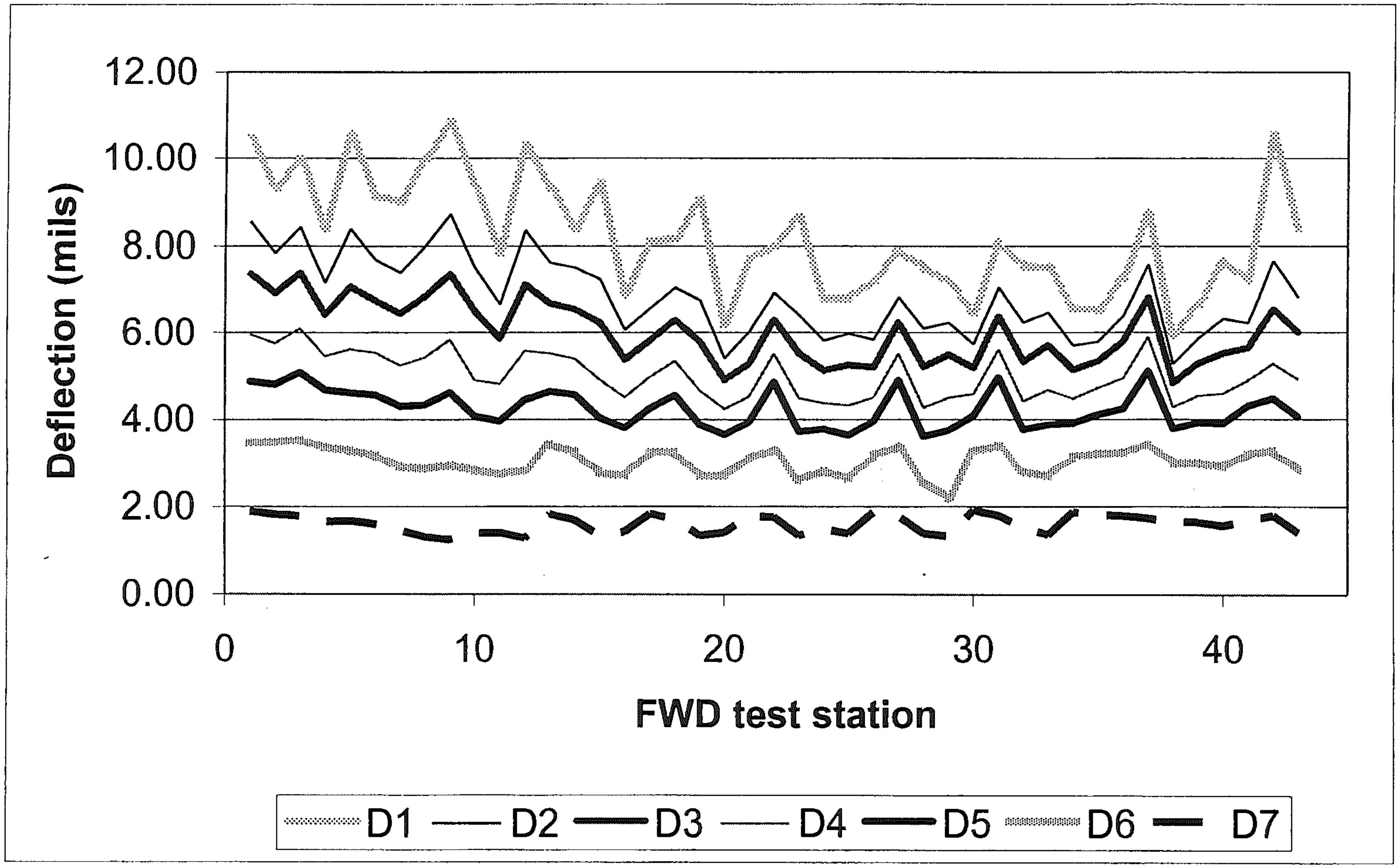

Figure 5.5 Variations of D1 through D7 deflections, I-75 SB, test section 1, site 2

layers and in the roadbed soil are reflected in the measured deflection. Further, the peak pavement deflection (D1) varies from about 6 to more than 10 mils.

3. The variations of D1 through D7 deflections for test site 1 are lower than those for test site 2.

4. The variation in the measured D7 deflection along test site 1 is much lower than that at test site 2.

The above observations are illustrated in figure 5.6. The figure shows the normalized D1 and D7 deflections for test sites 1 and 2. Examination of the figures indicates that relative to the normalized deflection value of 1:

1. The peak D1 deflections at test sites 1 and 2 vary by about $\pm$ 27 and $\pm$ 30 percent, respectively.

2. The D7 deflections at test sites 1 vary from about +10.3 to about – 8 percent whereas the variation at test site 2 is from about 10.3 to about – 27 percent.

For comparison purposes, the coefficients of variation of the measured D1 through D7 deflections for 18 test sites are listed in table 5.7. As can be seen, the coefficients of variation for I-75 SB section 1 test site 2 are relatively high compared to the other test sites.

Relative to table 5.7, it should be noted that the measured D1 through D7 deflections along all rubblized pavements included in this study show higher variation than the variation in the deflections of conventional flexible pavement. Given that the main difference between conventional flexible and rubblized pavement sections is the rubblized concrete slab, one can conclude that the high variations in deflections could be directly related to variations and/or non-uniformity of the rubblized concrete slab. Such non-uniformity was investigated while the pavement was being rubblized. Trenches were excavated in the rubblized concrete slab and the uniformity and thickness of the rubblized material were examined. It was observed that:

1. The rubblized concrete slab could be divided into two sublayers as follows:

   a) An upper rubblized material layer where the concrete has been broken to aggregate size material ranging in size from dust to more than 6-in.
   b) A lower fractured concrete layer where the rubblized concrete is semi-solid containing a network of micro cracks having random spacing.

2. The thickness of the rubblized material and the fractured concrete layers vary from zero to nine in. (the thickness of the concrete slab). Such variation yields geometry of the fractured concrete layer that consists of sharp peaks and valleys as shown in figure 5.7.

3. The temperature steel was occasionally debonded.

Table 5.7 Coefficients of variation in the measured D1 through D7 deflections for 18 test sites on rubblized pavements

	Coefficient of variation of the measured D1 through D7 deflections (%)						
Test site	D1	D2	D3	D4	D5	D6	D7
10692-11	9	10	11	10	10	10	15
10692-12	9	10	11	10	10	10	15
10753-11	14	13	12	10	8	5	6
10753-12	16	14	12	11	10	10	13
11941-21	8	7	7	7	7	7	4
11941-22	11	8	7	7	6	6	5
20102-11	7	7	7	7	7	7	6
20102-12	8	8	8	8	7	6	3
20233-11	12	12	11	10	8	7	15
20233-12	8	9	9	9	9	10	10
20273-21	15	13	11	8	6	4	4
20273-31	6	6	5	5	5	5	6
20273-41	8	12	11	9	7	6	4
20311-11	10	10	9	7	7	8	10
30373-21	19	14	10	17	14	12	10
30373-51	7	8	7	6	6	5	5
30373-52	15	16	15	14	14	13	11
30373-61	10	9	9	8	6	6	8

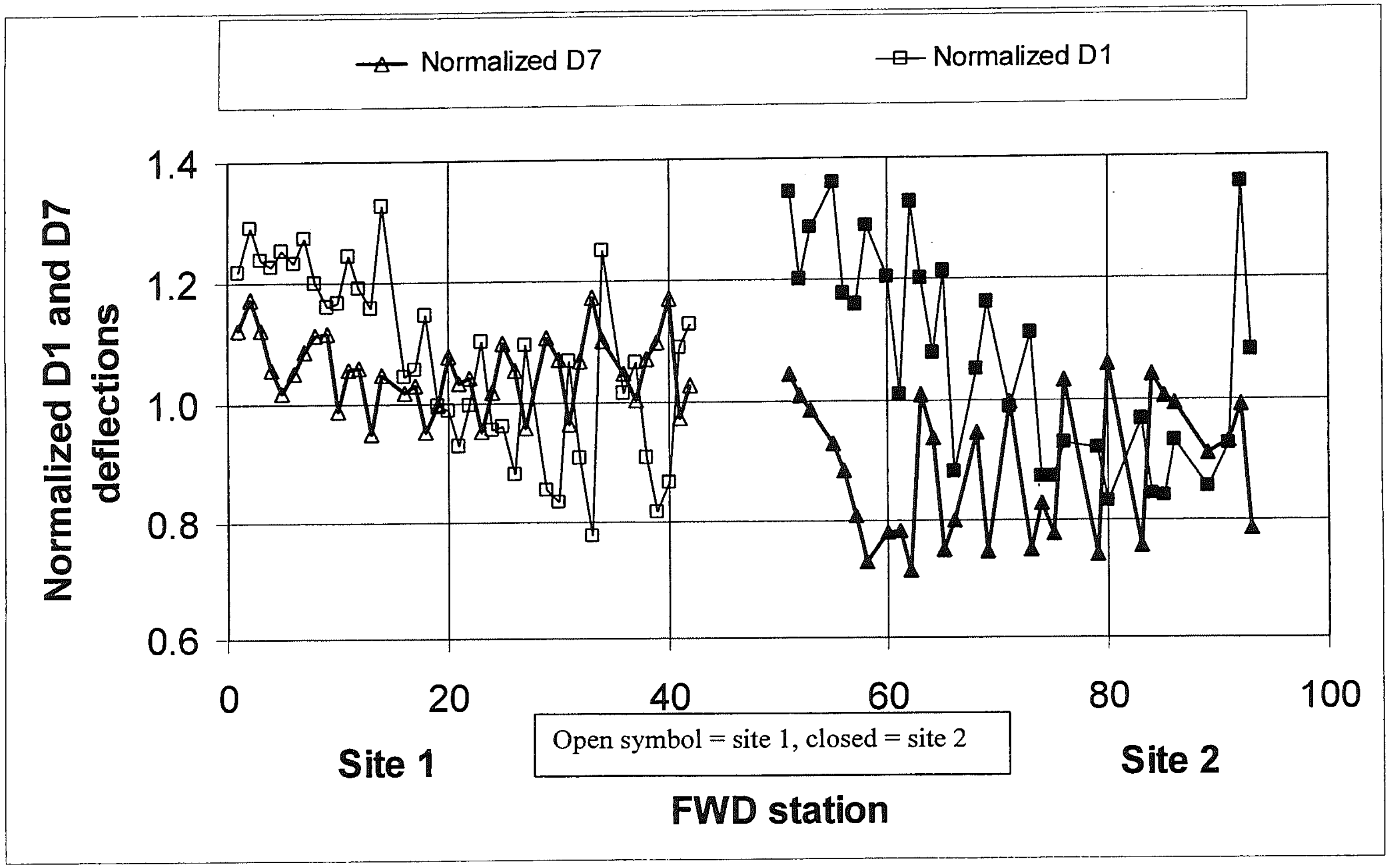

Figure 5.6 Normalized D1 and D7 deflection for I-75 SB, section 1, test sites 1 and 2

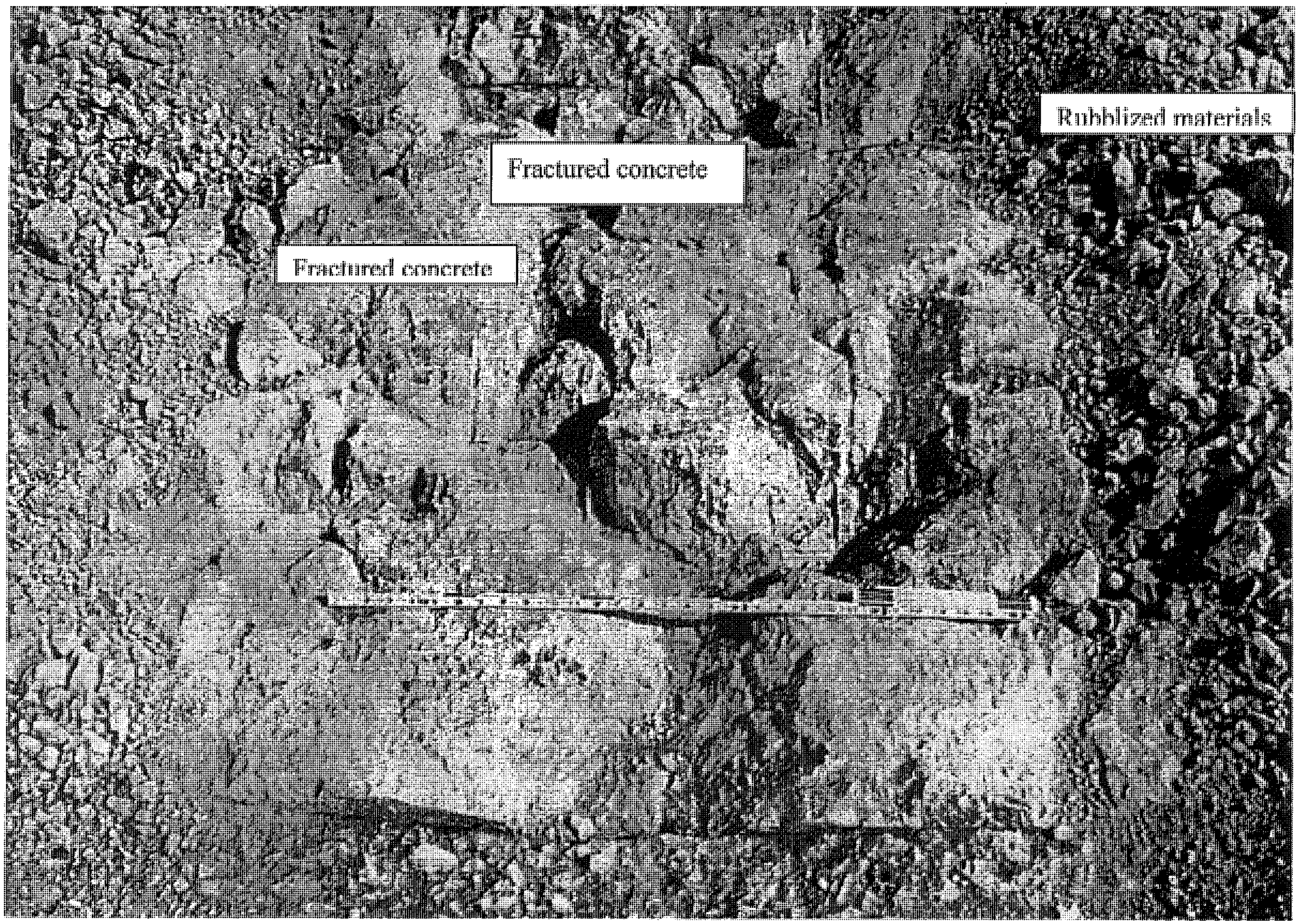

Figure 5.7 A typical trench in rubblized concrete pavement along US-10

Since variations in the thickness of the rubblized and fractured materials reflect the quality of the rubblization process and since said variations directly impact the variation in the measured deflection, the variation in the measured deflection could be used to express the quality of the rubblization process.

Finally variation in the outer deflection (sensor D7) is mainly related to the roadbed response to load. Said variation can be related to:

1. Variation in the roadbed soil in terms of moisture content, density, and material type.

2. Variations in the way the pavement layers distribute the load to the roadbed soil. For example, higher layer thickness causes decreases in the stress delivered to the roadbed soil due to the applied load and hence lower D7 deflection. Further, increases in the layer stiffness cause the applied load to be distributed to a wider area, which may cause higher D7 deflection. The reason is that the D7 deflection (located at 60-in. from the center of the load) may include some deflection from the subbase material.

The above scenario implies that, for some pavements or for some test locations, the D7 deflection may not correlate on one to one basis to the backcalculated roadbed soil modulus.

4.0 BACKCALCULATION PROCEDURE

Various computer software are available for the backcalculation of layer moduli. The differences between them are the forward software used to calculate pavement deflection and the convergence routine. The MICHBACK software uses the chevron-5 elastic layer system and a modified Newtonian algorithm (2 and 3) as a convergence routine to increment the modulus values of the various pavement layers. Hence, the use of MICHBACK is limited to 5-layer system including the stiff layer. In this study, pavements consisting of more than 5-layers were handled by combining two or more layers into one. Such combination was based on the proximity of the layer moduli of the combined layers and engineering judgment.

The accuracy of the backcalculation moduli is typically tested by conducting forward analyses of assumed pavement sections using a multilayer elastic computer program, backcalculating the layer moduli using the generated deflection basins and comparing the backcalculated moduli with the actual moduli used in the forward analysis. In general, the accuracy of the backcalculated moduli depends on several variables including:

1. The input seed modulus values
2. The accuracy of the measured deflection data
3. The number of deflection sensors
4. The accuracy and variability of the layer thicknesses
5. The number of pavement layers
6. The estimated depth to stiff layer

Unlike other backcalculation software, the results obtained from the MICHBACK computer software are independent of the assumed values of the seed modulus. For example, if the assumed seed modulus values are changed by ten folds, the backcalculated modulus values will change by less than 1 percent. The second item listed above (the accuracy of the measured deflection data) poses no problem as it was stated in the previous section regarding the repeatability of the MDOT FWD measured deflection data. Finally, the MDOT FWD is equipped with 9 deflection sensors spaced at 7 radial distances from the center of the loaded area. Hence, the deflection readings from three deflection sensors are similar and the deflection readings from only seven sensors can be used in the backcalculation of layer moduli. This limited number of deflection sensors causes no problem since, as stated earlier; the maximum number of pavement layers that can be handled by the Chevron-5 software (the forward engine in MICHBACK) is five. Indeed, the excess in the number of deflection sensors relative to the number of layers was advantageous in that it minimized the errors between the measured and the calculated deflection basins.

To minimize the errors due to the last three variables listed above; a backcalculation procedure was established and tested using forward and backward analyses. The procedure was used to backcalculate the layer moduli of all rubblized pavement sections included in this study after every step of it was verified. The procedure is detailed below relative to each of the three variables.

4.1 The Accuracy and Variability of the Layer Thicknesses

A typical rubblized pavement section consists of 4 or 5-layers situated on top of the roadbed soil as shown in figure 5.8. Relative to the two sections, the thickness of the pavement layers vary from one project to another. For example, the thickness of the:

- AC layer varies from about 4 to about 7 in. depending on the pavement section.
- Rubblized and fractured concrete layers is about 9 in. (the original thickness of the concrete pavement).
- Aggregate base varies from about zero (no aggregate base) to about 9 in.
- Sand subbase varies from about 9 to about 18 in.

Two unique features of the two typical sections shown in figure 5.8 are:

- For the same pavement section, the thickness of each of the rubblized and fractured concrete layers vary significantly from one point to another. For example, the thickness of the fractured concrete may vary along and across the pavement from zero to 9-in. Since the rubblized and fractured concrete layers are close to the pavement surface, such variation in their thicknesses significantly affects the accuracy of the backcalculated modulus values.
- The uneven surface between the rubblized material and the fractured concrete layer.

Further, note that for a given rubblized pavement section, the thicknesses of the AC, rubblized material, fractured concrete, aggregate base and sand subbase layers vary along and across the pavement. For example, a typical variation in the AC thickness along

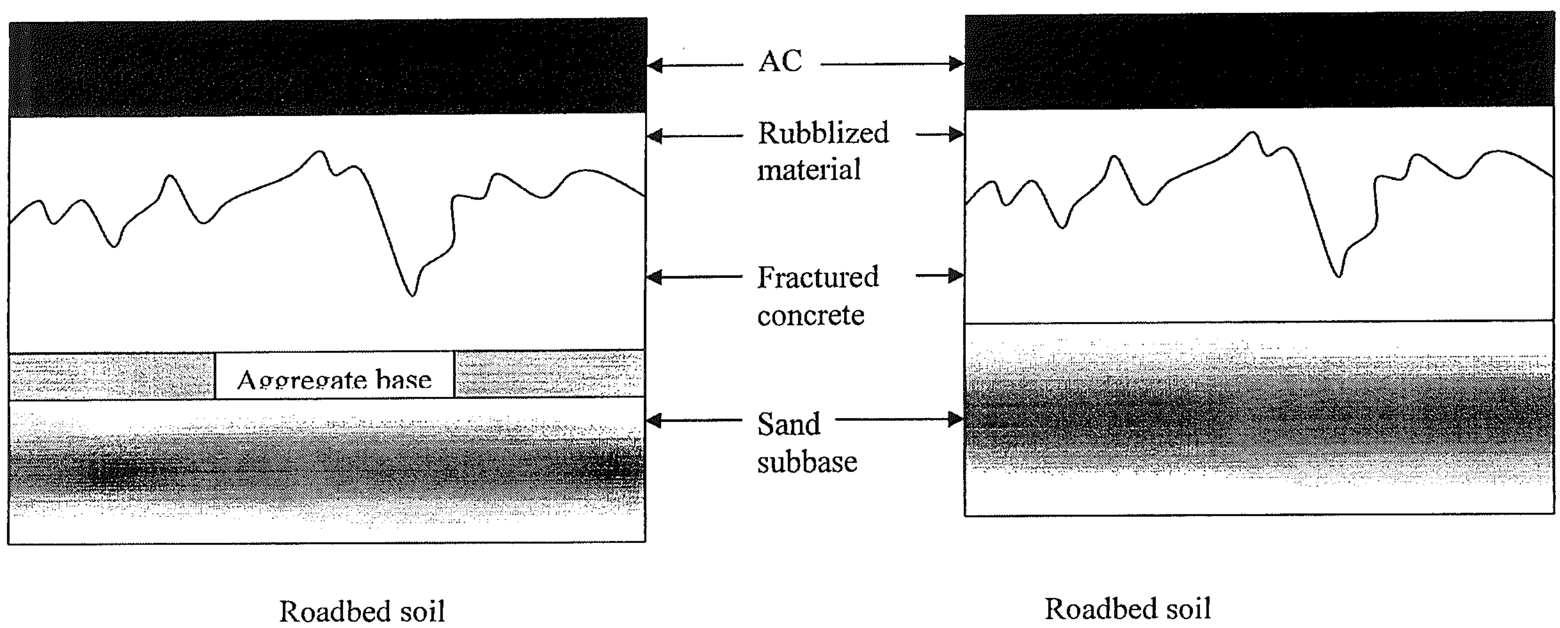

Figure 5.8 Typical rubblized pavement cross-sections

and across the pavement is about $\pm$ 1-in. Although variations in the thicknesses of the aggregate base and sand subbase have little impact on the backcalculated layer moduli, variation in the AC thickness has a substantial impact. Further, variation in the thickness of the rubblized material and fractured concrete impact their respective backcalculated moduli. To decrease the error in the backcalculated layer moduli due to variations in the AC thickness and the thicknesses of the rubblized and fractured concrete layers, the following procedure was adopted and used throughout the study.

4.1.1 The AC Thickness

At each test site, about 10 to 15 AC cores were extracted from the pavement and, for each core; four measurements of the AC thickness were made at the end of two orthogonal diameters. Hence, for each test site, a total of 40 to 60 AC thickness measurements were made. The average of all measurements was then calculated and used as input to the backcalculation routine. Examples of the variation in the AC thickness within 100 ft of pavement along I-75 SB, section 1, test sites 1 and 2 are shown in tables 5.8 and 5.9. As can be seen the AC thickness along test site 1 varies from 4.1 to 4.8 in. with an average of 4.5 in. and from 3.5 to 4.6 in. with an average of 4.1 in. for test site 2. Note that the MDOT inventory data for I-75 SB section 1 indicates that the AC thickness is 4.5 in. If this data is used in the backcalculation, one should expect larger errors in the backcalculated layer moduli for test site 2 than those for test site 1. Hence, efforts should be made to obtain the actual AC thickness from pavement coring. Nevertheless, the effect of using the average AC thickness on the backcalculated layer moduli was analyzed using forward and backward analysis. The forward analysis was based on an AC thickness of 4.5 in. The calculated pavement response (deflection) was then used to backcalculate the layer moduli. Ten trials were conducted where, in the backcalculation, the AC thickness was varied from 3.5 to 5.5 in. The results showed that, for a given error in the AC thickness, the backcalculated AC modulus varies relative to the true value. However, the average value of the ten backcalculated AC moduli has an insignificant error relative to the true modulus value.

To analyze the effect of using the average AC thickness on the backcalculated layer moduli, two backcalculation schemes were conducted as follows:

1. For each test site and at each core location, the measured deflection data and the measured core thickness were used to backcalculate the layer moduli at that location.

2. The layer moduli were backcalculated using the average measured AC thickness and the entire deflection data for the test site in question.

Table 5.8 Thickness, diameters and conditions of cores obtained from I-75 SB - section 1 test site 1

Core Designation	Total core thickness (in.)					Courses thickness (in.)			Core diameter (in.)	Crack/ defect
	1	2	3	4	Average	Surface	Leveling	Base		
10753-1101	4.2	4.4	4.5	4.2	4.3	1.5	1.1	1.7	5.7	None
10753-1104	4.1	4.1	4.3	4.1	4.2	1.5	1.0	1.7	5.7	None
10753-1107	4.8	4.5	4.4	4.8	4.6	1.6	1.0	2.0	5.7	None
10753-1110	4.0	4.1	4.1	4.0	4.1	1.4	1.0	1.7	5.7	None
10753-1115	4.6	4.6	4.8	4.6	4.7	1.8	1.4	1.5	5.7	Crack
10753-1116	4.8	4.6	4.6	4.7	4.7	1.6	1.1	2.0	5.7	None
10753-1117	4.8	4.7	4.8	4.8	4.7	1.8	1.1	1.8	5.7	None
10753-1118	4.3	4.4	4.5	4.3	4.3	1.6	1.0	1.7	5.7	None
10753-1123	4.8	4.8	4.8	5.0	4.8	1.8	1.0	2.0	5.6	None
10753-1124	4.5	4.5	4.6	4.5	4.5	1.7	1.0	1.8	5.7	None
10753-1125	4.8	4.5	4.8	4.6	4.7	1.8	1.0	1.9	5.7	None
10753-1126	4.5	4.5	4.5	4.5	4.5	1.7	0.9	1.9	5.6	None
10753-1150	4.8	4.8	4.5	4.6	4.7	1.8	1.0	1.9	N.A.	Broken
10753-1151	4.6	4.5	4.4	4.5	4.5	1.8	1.0	1.8	5.7	Crack
Average					4.5	1.7	1.0	1.8	5.7	
CV (%)					5	8	11	8	0	

Table 5.9 Thickness, diameters and conditions of cores obtained from I-75 SB - section 1 test site 2

Core Designation	Total core thickness (in.)					Courses thickness (in.)			Core diameter (in.)	Crack/ defect
	1	2	3	4	Average	Surface	Leveling	Base		
10753-1201	3.8	3.8	3.8	3.9	3.8	1.4	1.0	1.4	5.7	None
10753-1204	4.0	4.0	4.1	4.3	4.1	1.6	1.0	1.5	5.7	None
10753-1207	3.5	3.6	3.5	3.5	3.5	1.0	1.5	1.0	5.7	Crack
10753-1210	3.6	3.8	3.8	4.0	3.8	1.6	1.1	1.1	5.7	None
10753-1215	4.3	4.3	4.4	4.3	4.3	1.6	1.1	1.6	5.7	None
10753-1216	4.5	4.3	4.4	4.5	4.4	1.0	1.7	1.7	5.7	None
10753-1217	4.0	3.8	3.9	4.0	3.9	1.5	1.0	1.4	N.A.	Broken
10753-1218	4.2	4.2	4.2	4.2	4.2	1.6	1.0	1.6	5.7	None
10753-1223	4.4	4.4	4.4	4.5	4.4	1.7	1.1	1.6	5.6	None
10753-1224	4.5	4.8	4.6	4.5	4.6	1.9	1.0	1.7	5.7	None
10753-1225	4.3	4.3	4.4	4.3	4.3	1.7	1.0	1.6	5.7	None
10753-1226	4.3	3.9	3.9	4.0	4.0	1.6	1.1	1.3	5.7	None
10753-1250	3.6	3.5	3.5	3.5	3.5	1.5	0.9	1.1	5.7	None
10753-1251	4.4	4.3	4.3	4.4	4.3	1.7	1.0	1.6	5.7	None
10753-1252	3.5	3.5	3.5	3.5	3.5	1.0	1.4	1.1	N.A.	Broken
Average					4.1	1.6	1.1	1.4	5.7	
CV (%)					8	13	13	16	0	

Table 5.10 provides a list of the backcalculated moduli of the 2 schemes stated above. Examination of the results indicates that:

1. The backcalculated roadbed modulus based on the average AC thickness is almost the same as that based on the measured AC thickness (zero percent difference). This implies that errors in the AC thickness have no impact on the backcalculated layer moduli.

2. When the measured core thickness is lower than the average thickness of 4.5 in., the backcalculated AC and rubblized moduli based on the average thickness is lower than that based on the measured thickness (negative percent difference).

3. When the measured core thickness is equal to the average thickness of 4.5 in., the backcalculated AC and rubblized moduli based on the average thickness is almost the same as that based on the measured thickness (zero percent difference).

4. When the measured core thickness is higher than the average thickness of 4.5 in., the backcalculated AC and rubblized moduli based on the average thickness is higher than that based on the measured thickness (positive percent difference).

5. The average values of the moduli of the AC, rubblized and roadbed soil (that were backcalculated based on the average AC thickness of 4.5 in.) have insignificant differences (less than 3 percent) relative to those based on the measured core thickness.

6. The coefficients of variations of all the backcalculated moduli using the average AC thickness of 4.5 in. are similar to those backcalculated using the AC thickness at each core location.

The significance of the above observations is that, for each 100-ft long test site, when the thicknesses of the extracted cores are representative of the distribution of the thickness of the asphalt layer, the average core thickness could be used to backcalculate the layer moduli. In this study, the number of extracted cores within each 100-ft long test site is equal to or grater than 25 percent of the number of the FWD test locations. That is the ratio of the number of the FWD test locations to the number of extracted core is equal to or greater than 0.25. Further, for most test sites, the average core thickness is almost equal to the AC thickness found in the MDOT inventory file. The preliminary conclusion based on 18 test sites is that, when resources are not available, there is no absolute need (although it is highly recommended) to core the pavement section. The only requirement is to distribute about 40 FWD test locations along and across the asphalt mat within a short test site (e.g., 100-ft). In this regard, the FWD test layout shown in figure 5.1 is highly recommended.

Table 5.10 Backcalculated moduli at 14 core locations on I-75 SB section 1 test site 1 using the average AC thickness of 4.5-in. and the measured core thicknesses

Core no.	Measured AC thickness (in.)	Backcalculated modulus (psi)								
		Using the average AC thickness of 4.5-in.			Using the measured AC thickness at the core location			Error (%)		
		AC	Rubblized	Roadbed	AC	Rubblized	Roadbed	AC	Rubblized	Roadbed
10	4.1	1,917,561	102,669	17,752	2,371,494	110,442	17,752	-19	-7	0
4	4.2	1,317,448	125,546	16,779	1,526,898	131,539	16,784	-14	-5	0
1	4.3	2,041,531	106,098	15,865	2,262,151	110,175	15,866	-10	-4	0
18	4.3	2,728,687	68,577	18,406	3,060,106	71,237	18,402	-11	-4	0
26	4.5	2,346,427	101,879	18,372	2,352,325	101,679	18,373	0	0	0
51	4.5	536,489	452,420	18,055	536,530	452,393	18,055	0	0	0
24	4.5	1,365,183	302,454	16,820	1,364,897	302,484	16,820	0	0	0
7	4.6	1,115,255	133,978	16,190	1,077,134	131,401	16,188	4	2	0
25	4.7	960,796	467,837	17,498	954,398	442,757	17,458	1	6	0
15	4.7	677,201	142,011	16,919	649,673	136,186	16,907	4	4	0
16	4.7	2,144,219	147,111	17,682	1,958,521	141,734	17,679	9	4	0
17	4.7	1,196,843	215,286	17,415	1,140,703	206,343	17,403	5	4	0
23	4.8	2,454,067	211,126	17,330	2,235,075	196,141	17,326	10	8	0
Average	4.5	1,600,131	198,230	17,314	1,653,070	194,962	17,309	-3	2	0
CV (%)	5	44	66	4	47	65	4			

CV (%) = Coefficient of variation = standard deviation divided by average

Note that similar observations were also made on other test sites. Based on the above observations, the backcalculation of layer moduli was accomplished by using the average core thickness. The results are listed in Appendix B along with the average values and the coefficient of variation.

4.1.2 The Rubblized Material and the Fractured Concrete Thicknesses

Since the thicknesses of the rubblized and fractured concrete layers vary literally from one point to another, in the backcalculation, the two layers were treated as one combined layer. The thickness of the combined layer was assumed to be the same as the thickness of the original concrete slab. The impact of such an assumption on the backcalculated modulus values of the AC, base and subbase layers and on the roadbed soil was analyzed using forward and backward analyses of 111 pavement sections having the various layer thicknesses and modulus values that are listed below. Note that the variations in the layer properties were designed to simulate the spectrum of actual rubblized pavement sections in Michigan.

Layer	Modulus (ksi)	Thickness (in)	Poisson ratio
AC	500, 1000 and 2,000	6.0	0.3
Rubblized material	30, 100, 200, 300 and 400	3.0, 4.5, 5.0 and 7.0	0.4
Fractured concrete	300, 500, 1000 and 2,000	6.0, 4.5, 4.0 and 2.0	0.2
Base	20, 30, 40 and 60	4.0, 12.0, 15.0 and 18.0	0.4
Roadbed soil	10, 15, 20 and 40	infinite	0.45

As stated above, the forward analyses resulted in 111 deflection basins, which were used to backcalculate the layer moduli. In all backcalculation, the rubblized material and the fractured concrete layers were combined as one 9-in. thick layer. Figures 5.9 through 5.11 depict the backcalculated and the actual modulus values of the AC layer, roadbed soil and base layer, respectively. The straight line in the figures is the line of equality between the backcalculated and the actual layer moduli. Examination of the three figures indicates that combining the rubblized material and the fractured concrete layers into one layer produces:

1. Insignificant errors in the backcalculated moduli of the AC layer (figure 5.9) and roadbed soil (figure 5.10) relative to the actual modulus values.

2. Significant error in the backcalculated base modulus when the base thickness is 4 in. and insignificant error when the base thickness is between 12 and 18 in. as shown in figure 5.11.

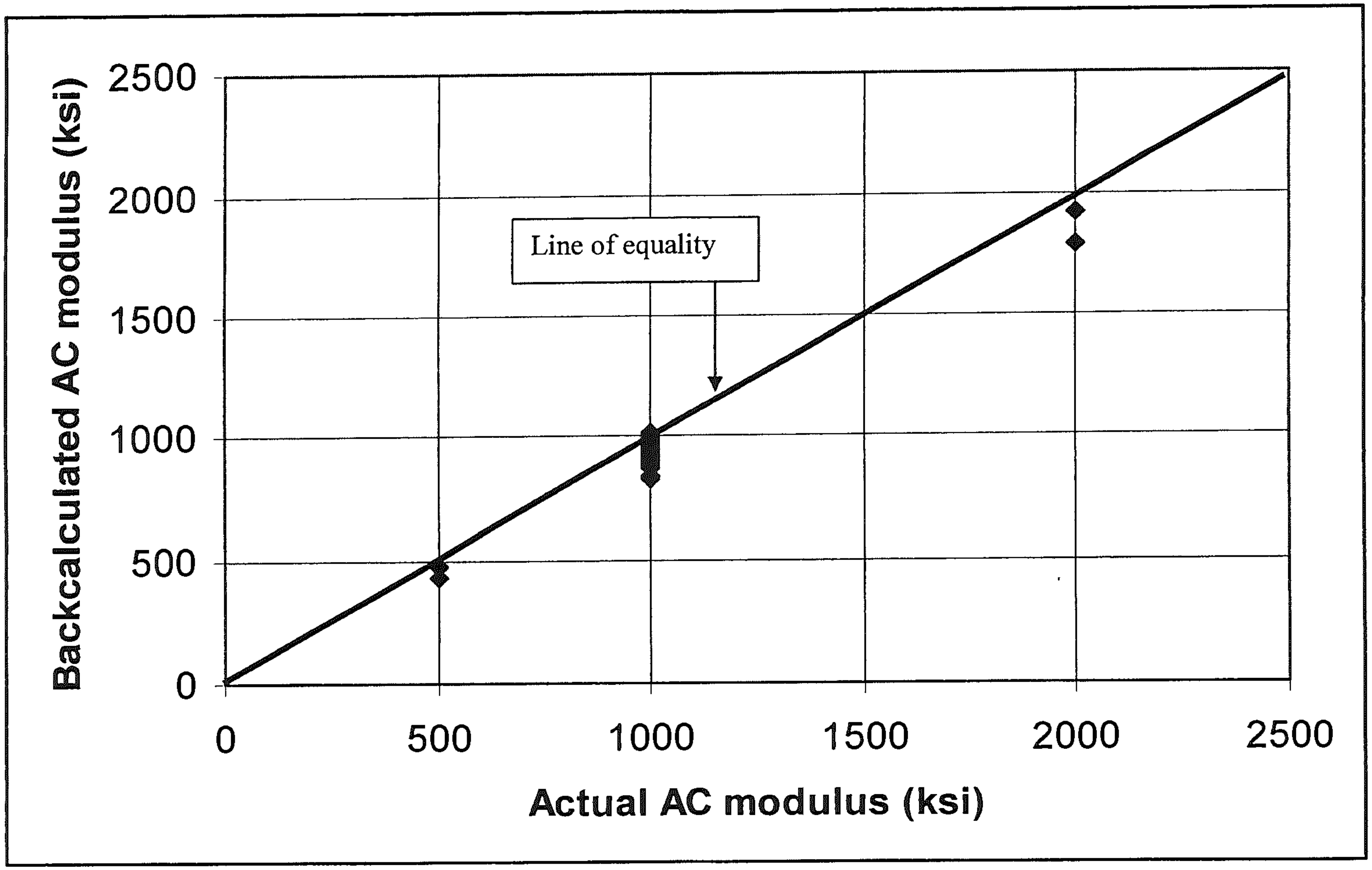

Figure 5.9 Backcalculated AC moduli when the rubblized and fractured concrete layers are combined as one layer

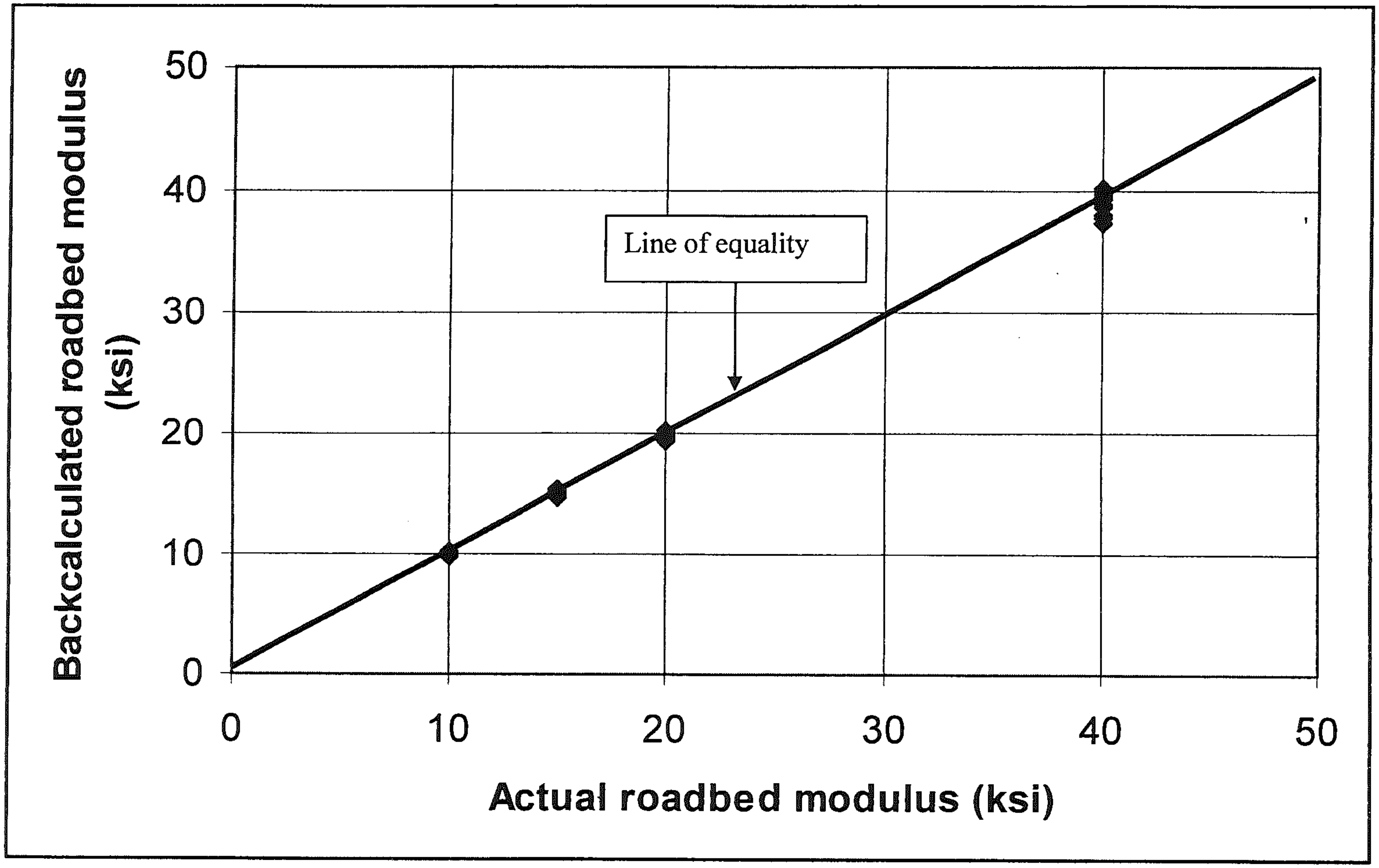

Figure 5.10 Backcalculated roadbed soil moduli when the rubblized and fractured concrete layers are combined as one layer

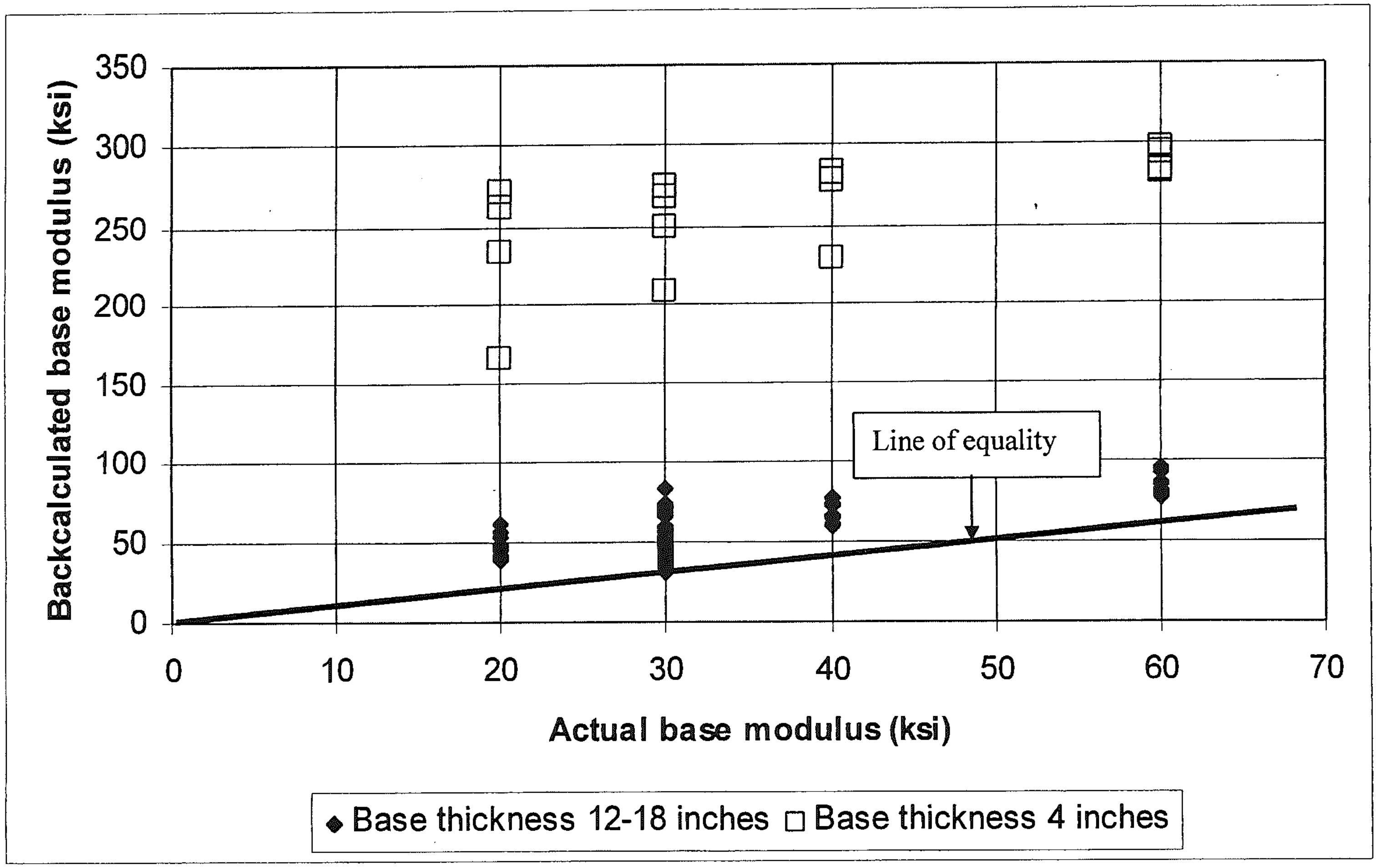

Figure 5.11 Backcalculated base moduli when the rubblized and fractured concrete layers are combined as one layer

A second backcalculation was also conducted using the 111 deflection basins where the rubblized material and the fractured concrete layers were handled separately and the thickness of each was assigned value of 4.5 in. The results of this backcalculation showed similar trends to those shown in figures 5.9 through 5.11. However, backcalculation of layer moduli based on the separation of the rubblized material and the fractured concrete layers cannot be extended to the measured deflection data for two reasons:

1. The high variability in the thickness of both layers.

2. For some pavement sections, the separation of the two layers makes the total number of layers more than five (AC, rubblized, fractured, base, roadbed and stiff layer). The reason is that the Chevronx computer program (which is the forward engine in MICHBACK) is limited to 5-layer systems.

For these two reasons, and for consistency, the backcalculation of layer moduli of all rubblized pavements were accomplished by combining the rubblized material and the fractured concrete layers into one layer.

Finally, the impact of variation in the thicknesses of the AC, rubblized material and fractured concrete layers on the backcalculated moduli of the AC and base layers and on the roadbed soil were also examined using forward and backward analyses. A total of twenty pavement sections having the material properties listed below were analyzed and the resulting deflection basins due to a 9000 lb load were calculated.

Properties	AC	Rubblized material	Fractured concrete	Base layer	Roadbed soil
Thickness (in.)	5.0 5.5 6.0 6.5 7.0	2.0 4.0 6.0 8.0	7.0 5.0 3.0 1.0	15.0	Infinite
Modulus (psi)	1,000,000	100,000	1,000,000	15,000	15,000
Poisson's ratio	0.3	0.4	0.2	0.45	0.45

The calculated deflection basins of the twenty pavement sections were then used to backcalculate the known layer moduli. In the backcalculation, the rubblized material and the fractured concrete layers were combined into one 9-in. thick layer. Further, an average AC thickness of 6 in., a base thickness of 15 in. and an infinite depth of the roadbed soil were used in the backcalculation. These and other layer properties (Poisson's ratio) and the average backcalculated layer moduli of the twenty pavement sections are listed below. For each layer used in the backcalculation, the percent error of each backcalculated layer modulus relative to the true modulus is also listed below.

Layer properties for backcalculation				
Properties	AC	Rubblized concrete slab	Granular base layer	Roadbed soil
Thickness (in.) Poisson' ratio	6.0 0.3	9.0 0.3	15.0 0.4	- 0.45
Backcalculated layer moduli (psi)				
Average backcalculated moduli (psi)	902,265	203,470	16,180	14,697
Error (%)	9.77		7.86	2.02

Examination of the layer moduli used in the forward analyses, the average backcalculated layer moduli, and the percent errors listed above indicates that:

- The backcalculated moduli of the AC and base layers and the roadbed soil are not significantly affected by combining the rubblized material and the fractured concrete layers into one rubblized concrete slab layer. The percent error for the AC and base layers are less than 10 percent and for the roadbed soil is less than 2.5 percent.

- The average backcalculated AC modulus is not significantly affected by the variation in the AC thickness used in the forward analyses. Note that, for those locations where the true AC thickness was $\pm$ 1 in. from that used in the backcalculation, the backcalculated AC modulus values were significantly different than the actual values. However, the average backcalculated AC modulus value (the average of the twenty tests) was not significantly affected. The implication of this is that, in the field, the impact of variation in the AC thickness on the backcalculated results could be significantly decreased by increasing the number of FWD tests along a project and by using the average AC core thickness in the backcalculation.

- The backcalculated modulus of the rubblized concrete slab does not resemble the moduli of the rubblized material nor the fractured concrete layers. It represents the weighted average modulus of the two layers based on their space location and thickness.

The above observations are more or less similar to those reported earlier using the 111 forward analyses. Based on the analyses of the 131 pavement sections (111 + 20) presented above and the MDOT pavement design and construction practice (the thickness of the combined base and subbase layers for rigid pavement is 12 in. or more), the procedure of combining the rubblized material and the fractured concrete layers into one layer was adopted and used throughout the study. The results (the backcalculated moduli of the AC and base layers and of the roadbed soil) were found, for most cases, to be acceptable. On the other hand, given the high variations in the thicknesses of the rubblized material and fractured concrete layers; the moduli of these two layers cannot be accurately backcalculated. Consequently, statistical procedures were developed in this study to estimate these moduli. The procedures are presented in section 5 of this chapter.

In the remaining parts of this report the combination of the rubblized material and the fractured concrete layers is termed "the rubblized concrete slab". The applicability of combining the rubblized material and the fractured concrete layers into one layer procedure to real deflection data is illustrated in section 6.0 of this chapter using the measured deflection data on I-75 SB, section 1, test sites 1 and 2.

4.1.3 The Granular Base Thickness

The impact of errors in the thickness of the aggregate base and sand subbase on the backcalculated layer moduli was also analyzed using forward and backward analyses. Since, for rubblized pavements the influence of the surface load on the base and subbase layers is small (they are separated from the load by the AC and the rubblized concrete slab), the impact of errors in their thicknesses was found to be insignificant. For example, variations in the aggregate base and sand subbase thicknesses of $\pm$ 2 in. yield less than ten percent error in the backcalculated layer moduli. Based on the results of the analyses, it was concluded that the thickness of the sand subbase and the aggregate base can be obtained from available cross-section records (pavement coring is not required). Note that the above scenario is not valid for conventional asphalt pavements because only the AC layer separates the aggregate base from the surface load.

4.1.4 The Roadbed Soil

In some locations in the State of Michigan, the roadbed soil consists of a thick sand deposit. At these locations, the original concrete slab was constructed either on top of the roadbed soils or on top of an aggregate base (minimum thickness of 4 in.) that was placed on top of the roadbed soil. Therefore, the pavement section was treated either as a 3-layer (AC and rubblized concrete slab layers situated on a roadbed soil) or as a 4-layer (AC, rubblized concrete slab, and base layers situated on a roadbed soil) system.

4.2 Backcalculation Parameters

In this section, the parameters used in the backcalculation of the layer moduli for the 18 rubblized projects are summarized.

Table 5.11 Typical pavement layer properties used in the backcalculation

Layers	Thickness/ (Source of data)	Poison's ratio	Seed moduli (ksi)	
			minimum	maximum
AC	Coring (inventory data)	0.3	30	4,000
Rubblized	4.5-in.	0.4	30	4000
Fractured	4.5-in.	0.2	30	10,000
Combination of rubblized and fractured	9.0-in.	0.3	30	4000
Conventional aggregate base	Drilling (inventory data)	0.4	10	200
Roadbed	Infinite or finite depth	0.40 (sand) 0.45 (clay)	1	100
Stiff layer depth	Infinite or finite depth	0.2	2,000	2,000

Table 5.12 Lab test moduli of various types of sand and clay (4)

Soil types	Modulus of elasticity (psi) min.-max.
Loose sand	1,500-3,500
Medium dense sand	2,500-4,000
Dense sand	5,000-8,000
Silty sand	1,500-2,500
Sand and gravel	10,000-25,000
Soft clay	600-3000
Medium clay	3,000-6,000
Stiff clay	6,000-14,000

4.2.1. Seed Moduli and Poisson's Ratio

Table 5.11 provides a list of Poisson's ratios and seed moduli used in the backcalculation of the layer moduli of all rubblized pavements. The table also provides some information regarding the layer thicknesses and the source from which the data can be obtained. It is strongly recommended that the AC thickness be verified through coring and the other layer thicknesses be obtained from the inventory data or from drilling. Finally table 5.12 provides a list of typical lab modulus values of various roadbed soils. The data in the table can be used as guidelines keeping in mind that the backcalculated modulus values are about three times higher than those reported in the table.

4.2.2. Convergence Control

The MICHBACK program allows the users to specify the parameters of the convergence control criteria. The values of the parameters used in this study for the backcalculation of layer moduli using 3- and 4-layer systems are listed below.

1. Calculate the gradient matrix after each two iterations
2. Maximum number of iterations is sixty
3. Modulus tolerance was set at 0.1 percent
4. The desired RMS tolerance was set at 0.1%
5. Precision of deflection entries 3 decimal places

Note that lower percent modulus an RMS tolerances yields more accurate solution but requires more iterations. Detailed information regarding the effect of each parameter on the results of the backcalculation can be found in MICHBACK user's manual (7).

4.3 The Number of Pavement Layers

The two typical rubblized pavement sections shown in figure 5.8 indicate that a rubblized pavement consists of either 4- or 5-layers situated on a roadbed soil. In addition, the density and modulus of the roadbed soil typically change with depth. In a multilayer elastic system, an infinite depth is assigned to the last layer (the roadbed soil). Hence, the modulus of the roadbed soil is explicitly assumed as constant throughout its depth. This creates errors in the backcalculated layer moduli. To overcome the problem, a stiff layer is typically placed at certain depth below the pavement surface and the layer moduli are backcalculated (for more detail see the next section). Such placement is problematic in that the depth to stiff layer and its properties (modulus and Poisson's ratio) are not known. In addition, for MICHBACK, the inclusion of stiff layer increases the total number of layers beyond the capability of the chevron-5 program. Consequently, some layers must be combined to reduce the total number of layers to 5 or less.

The first layer combination (addressed in section 4.1.2) is that of the rubblized material and the fractured concrete layers. The two layers cannot be separated mainly because the thickness of each layer is unknown and may vary from zero to 9 in. within the deflection basin. Typically the original base (if it exists) and subbase of the old concrete pavement are also combined as one layer in the backcalculation to reduce the number of the pavement layers. The combination of the base and subbase into one layer, on one hand, and that of the rubblized material and fracture concrete layers, on the other hand, reduce the total number of layers including the roadbed soil to 4 or 5 as follows:

1. AC layer
2. Rubblized concrete slab (a combined layer of the rubblized material and fractured concrete layers)
3. Base (a combined layer of base and subbase layers)
4. Roadbed soil
5. A stiff layer (optional)

The backcalculation was then performed using 4-layer system (AC, rubblized concrete slab, and combined base and subbase layers, and roadbed soil) with an option to incorporate a stiff layer at certain depth. Further, as stated in the previous section, in certain scenarios, based on available information in the inventory data, the base and subbase layers and the roadbed soil were combined into one layer. Hence, for such scenario, a 3-layer system was used with the option of incorporating a stiff layer at certain depth.

Note that in the MICHBACK computer program, the stiff layer is not counted as a layer while it is counted in the chevron-5 program. For example, if a 4-layer system is specified in MICHBACK and if a stiff layer is incorporated, the total number of layers to be analyzed by the chevron-5 program is 5.

From this point forward, the number of layers used in the backcalculation will be counted in accordance with the MICHBACK computer program.

To summarize, the backcalculation of layer moduli must be based on the measured deflection data and on accurate information regarding the pavement cross-section specifically the top pavement layers. Given the lack of such information relative to the rubblized material and fractured concrete layers, the two layers must be combined to backcalculate the moduli of the roadbed soil and the AC layer. When accurate information are available regarding the base, subbase and the roadbed soil, two or more of these materials could be combined into one layer and the backcalculation could be accomplished based on 3 or 4-layer systems. The exact number of layers to be used in the backcalculation depends not only on accurate information but also on the possible incorporation of a stiff layer. These and other issues are addressed in detail in the next section along with some examples.

4.4 Depth to Stiff Layer

As stated earlier, most backcalculation software typically use mechanistic-based layer analysis routines to calculate stresses, strains and deflections induced in a given pavement section with known properties due to an applied load. For example, the MICHBACK software uses the Chevronx computer program (5-layer linear elastic program) as the forward engine to calculate pavement deflections. Like other two dimensional mechanistic programs, the chevronx algorithm is based on the assumption that the last layer (the roadbed soil) is semi-infinite. Therefore the calculated strain in that layer is integrated over an infinite depth while in reality, the load induced-stresses and strains in most pavement sections dissipate to insignificant values within few feet from the pavement surface. For this reason, most backcalculation software including the MICHBACK were designed to allow the users to place a stiff layer at a certain depth below the pavement surface. Such placement is problematic in that, if the estimated depth to stiff layer is incorrect, it produces errors in the backcalculated layer moduli. For example, for a 4-layer system, if the depth to stiff layer is erroneously estimated at 400 in. rather than the true 200 in. then the backcalculated roadbed and base moduli could be as high as70 percent and the error in the AC modulus could be of the order of 10 percent. The error in the backcalculated AC modulus could be more significant for a 3-layer system.

In most cases, the actual depth to stiff layer (the depth at which the load-induced stresses and strains are zero) is not known. Therefore, a depth to stiff layer is typically assumed. The problem with such an assumption is that there is a wide range of depths to stiff layer that existing backcalculation software including the MICHBACK could successfully produce layer moduli to closely match the measured deflection basin. The question becomes which set of modulus values are correct. For certain pavement sections where concrete culvert and/or cross-drains can be found, the depth to stiff layer must be specified to match the vertical distance between the pavement surface and the top of the culvert. In some others, where deep deposit of soft layer is encountered, no stiff layer needs to be included. The important point is that relatively accurate information regarding the original soil strata and the under pavement structures would assist a great deal in estimating the depth to stiff layer. Such information could be obtained from soil maps published by the Soil Conservation Service of the U.S. Department of Agriculture. When such information is lacking, a trial and error method must be used where the layer moduli are backcalculated using various depths to stiff layer and the resulting modulus values are selected based on engineering criteria and judgment.

So the first step needs to be taken is to answer the question "is there a need to incorporate a stiff layer?" The answer to this question can be easily obtained with the help of Boussinesq equivalent modulus procedure (8). In this procedure, the pavement is treated as a one layer system and the modulus of that layer is calculated using equation 5.1:

$$E = \frac{P\left(1-\upsilon^2\right)}{\pi(r)\left(d_r\right)} \tag{5.1}$$

Where E = modulus
P = applied load = 9000 lb for the normalized deflection file
υ = Poisson's ratio (assume 0.4)
R = radial distance from the center of the load (in.)
d_r = deflection at distance r from the center of the load (in.)

To determine whether or not a stiff layer should be incorporated, do the following steps"

1. Calculate E for each deflection sensor location excluding the center sensor.

2. Plot the calculated E versus the distance from the loaded area (the distance between the center of the load plate and the deflection sensor in question).

3. The E versus distance curves will have three possible shapes as follows:

   a) If the modulus "E" decreases with distance and then it increases (see figure 5.12), a stiff layer should be incorporated. Higher rates of increasing modulus imply shallower depths to stiff layer.
   b) If the modulus decreases with distance until it reaches almost a constant value, the stiff layer is about 400 in. deep.
   c) If the modulus continuously decreases with distance; the stiff layer is more than 500-in. deep or there may not be any stiff layer.

The above three scenarios are illustrated in figure 5.12. It can be seen that the shape of the curve changes with depth to stiff layer.

Next, one needs to determine the depth to stiff layer using a trial and error procedure. To illustrate such a procedure, three pavement sections were established. Each section consists of a 3-layer system; AC, rubblized and base, supported on roadbed soil and a stiff layer located 300 in. below the pavement surface. In each section, the base and roadbed soil were assigned equal modulus values of 30,000, 20,000 and 10,000 psi. The three sections were analyzed and the pavement deflections due to a 9,000-lb load were calculated. The calculated deflection and the pavement layer thicknesses were then used to backcalculate the layer moduli using variable depths to stiff layer and 3- and 4-layer systems. The 3-layer system consisted of AC and rubblized concrete slab layers situated on roadbed soil while the 4-layer system consisted of AC, rubblized slab and base layers situated on roadbed soil. A stiff layer was incorporated in both systems. The results of the backcalculation for the 20,000 psi base and roadbed modulus are shown in figures 5.13a, 5.13b and 5.13c. The figures depict each backcalculated modulus obtained by using 3 (closed symbols) and 4 (open symbols) layer systems and for different depths to stiff layer. Examination of the figures indicates that:

1. The backcalculated layer moduli vary significantly with the assumed depth to stiff layer except the modulus of the AC, which is the least sensitive to the depth to stiff layer.

2. Backcalculation of layer moduli using 3 and 4 layer systems produce different results for all depths to stiff layer except for the true depth of 300 in.

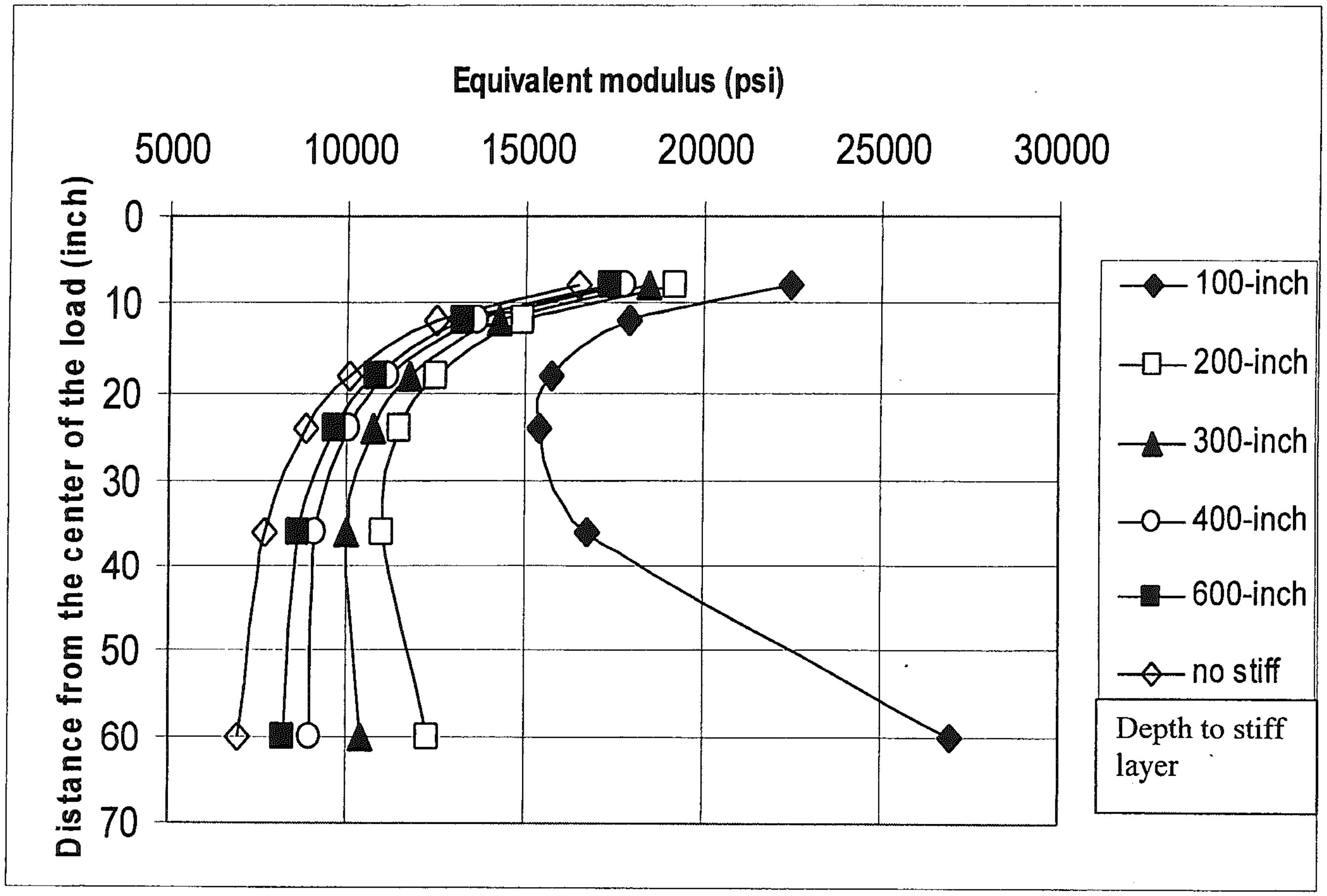

Figure 5.12 Equivalent moduli as function to the deflection sensor locations (Boussinesq procedure) for various depths to stiff layer

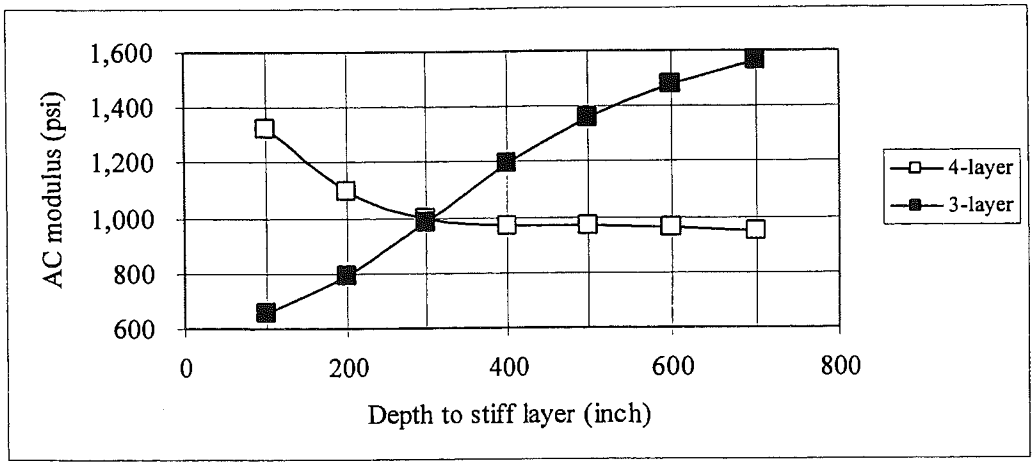

a) AC modulus (psi)

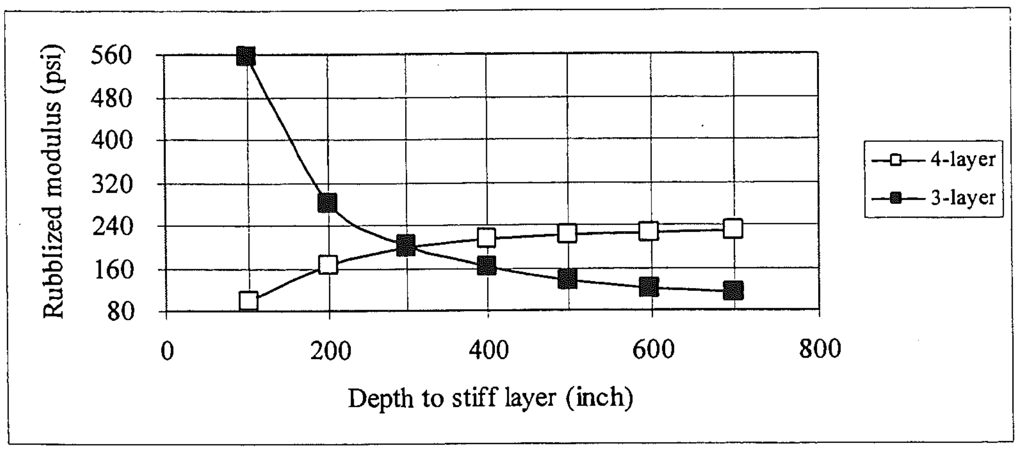

b) Rubblized modulus

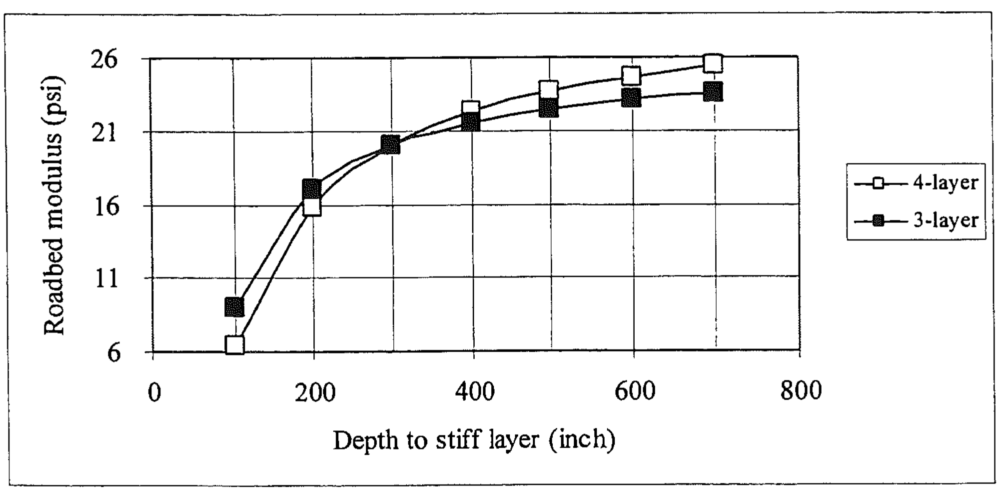

c) Roadbed modulus

Figure 5.13 Backcalculated layer moduli using 4 and 3 layer systems versus depth to stiff layer

3. At the true depth to stiff layer of 300 in., the backcalculated layer moduli (AC, rubblized concrete slab and roadbed) obtained from 3- and 4-layer systems are equal (the two curves intersect).

4. At a stiff layer depth of 300 in., all the backcalculated modulus values are within a fraction of one percent of their true values.

Recall that the forward analyses were conducted using equal modulus for the base and roadbed soil. For this case, the above findings can also be made by examination of figure 5.13. The figure shows the backcalculated base and roadbed modulus using a 4-layer system as a function of the depth to stiff layer. It can be seen that the two moduli are equal only at the true depth to stiff layer of 300 in.

The significance of figure 5.14 is that the figure can also be used to estimate the depth to stiff layer when the modulus of the roadbed soil is not equal to the modulus of the base layer. For such pavement layers, the curves representing the moduli of the base and roadbed soil as functions of the stiff layer depth will also intersect. On one side of the intersection, the base modulus will be lower than that for the roadbed soil. Since for most pavements the opposite is true (the base modulus is higher than that of the roadbed soil), then the true depth to stiff layer is within the region defined by the two curves where the modulus of the base is higher than that of the roadbed soil.

The above example illustrates that although the backcalculated modulus values were obtained based on trial and error (different depths to stiff layer), the true values can be obtained by a careful examination of the results. The application of the above and other procedures (the effects of the accuracy of layer thicknesses and the number of pavement layers) to measured pavement deflections are presented in the next section.

Figure 5.15 shows the results of the 30,000 and 10,000 psi base and roadbed moduli. It can be seen that the figure shows similar trends to those shown in figure 5.13. Finally, regardless of the procedure used to estimate the depth to stiff layer, the values of the backcalculated moduli must be scrutinized using engineering judgment. In this endeavor, three steps can be used as follows:

1. The variation in the backcalculated moduli should be the mirror image of the variation in the measured deflection. Such variations reflect the variability of the structural capacity of the pavement. For some pavement sections, the backcalculated layer moduli could vary as much as 100 percent along and across the pavement. For some others, this variation could be as low as 10 percent. In general, variations in the measured pavement deflections could be the direct results of:

    a) Variations in the layer thicknesses especially the AC, the rubblized material and the fractured concrete layers.
    b) Variations in the density/air voids of the compacted asphalt mat that may be caused by temperature and/or particle segregation.

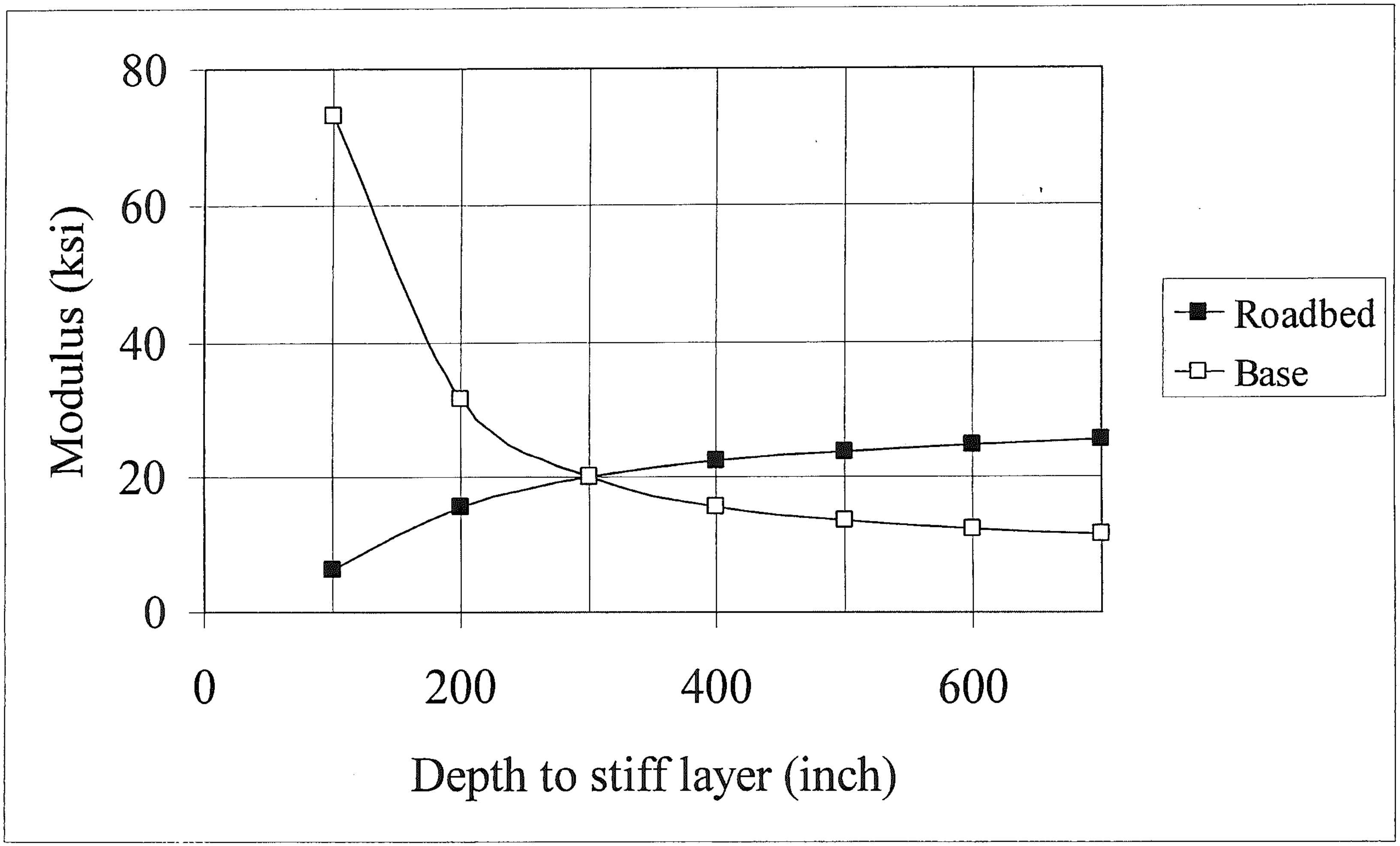

Figure 5.14 Backcalculated roadbed and base modulus using 4-layer system

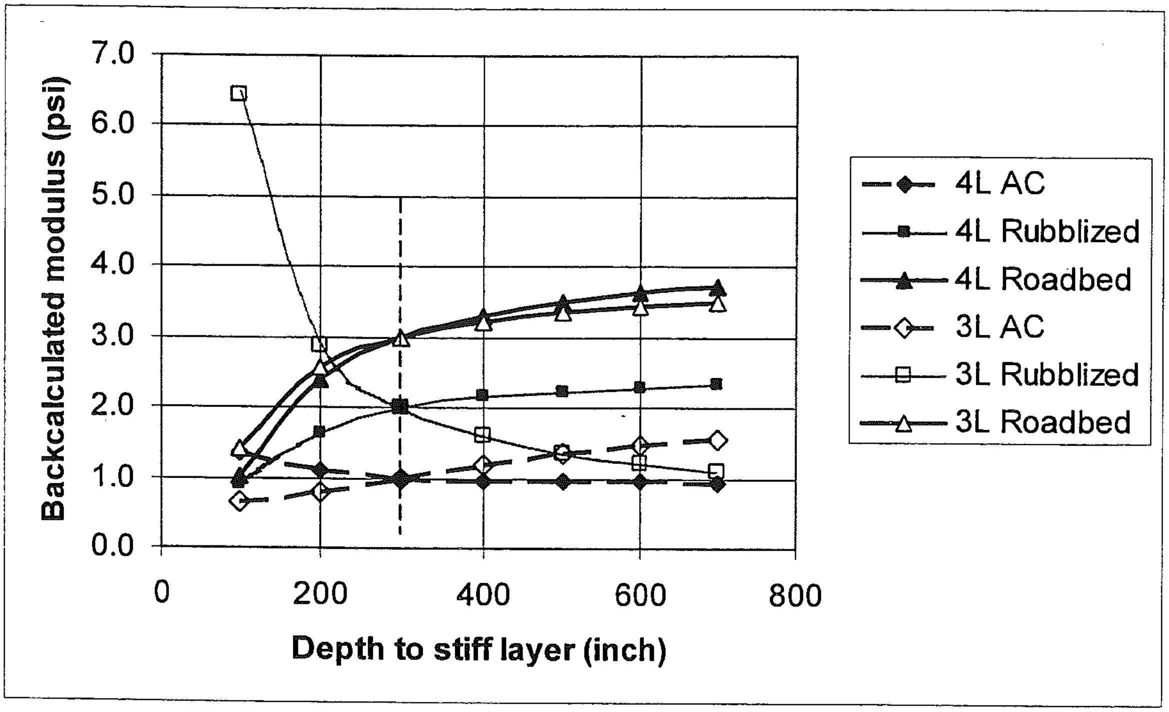

a) Base and roadbed moduli of 30,000 psi

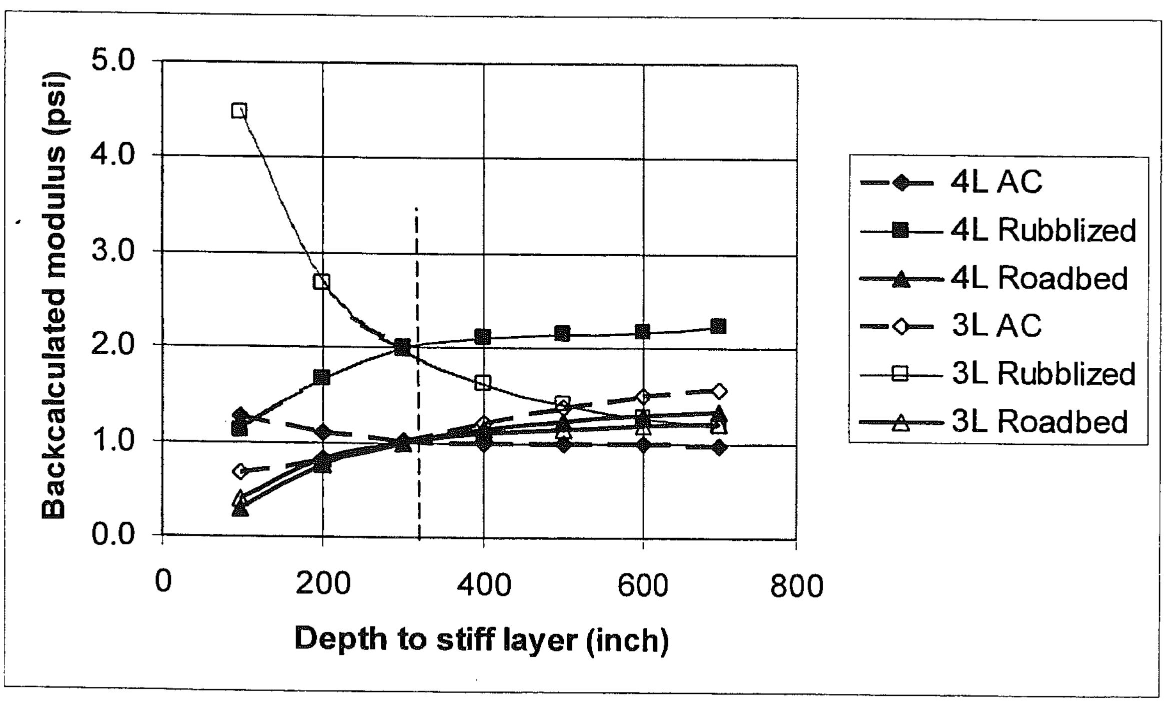

b) Base and roadbed moduli of 10,000 psi

Figure 5.15 Backcalculated modulus (AC $*10^6$, rubblized concrete slab$*10^5$, and roadbed $*10^4$) of 3 pavement sections with actual depth to stiff layer of 300 in.

2. The values of the backcalculated roadbed soil moduli should be reasonable. The data listed below could be used as guidelines for acceptance. Note that these values are based on laboratory tests, backcalculated moduli are typically much higher than those listed below.

Material	Modulus (psi)	
	Low	High
Clay	1,800	42,000
Sand	4,500	24,000

Further, the AASHTO Design Guide provides the following equation, which was derived from the Boussinesq equation by assuming a value of Poisson's ratio of 0.5, for estimating the modulus of the roadbed soil.

$$MR = \frac{0.24 * P}{D_r * r} \tag{5.2}$$

Where

- MR = estimated roadbed soil modulus (psi)
- P = applied load (lb)
- r = radial distance from center of load (in)
- D_r = deflection at the radial distance "r" (in)

It is highly recommended that measured deflection at distances of 50 in. or more from the center of the FWD load plate be used in the above equation. Further, the ASHTO Design Guide recommends that the roadbed modulus to be used in design be one third the backcalculate value.

3. Plots of the backcalculated roadbed modulus and the inverse of the measured outer sensor deflection along a project (see figure 5.16) should overlap.

5.0 THE MODULI OF THE RUBBLIZED MATERIAL AND FRACTURED CONCRETE LAYERS

As previously noted, a rubblized concrete slab can be divided into two distinctive layers; rubblized and fractured concrete layers. The insitu modulus of the rubblized and fractured concrete layers are very difficult or almost impossible to backcalculate from the measured deflection data. The reasons include:

1. The extreme variations in the thicknesses of the rubblized material and the fractured concrete layers.

2. The uneven interface between the rubblized material and the fractured concrete layers.

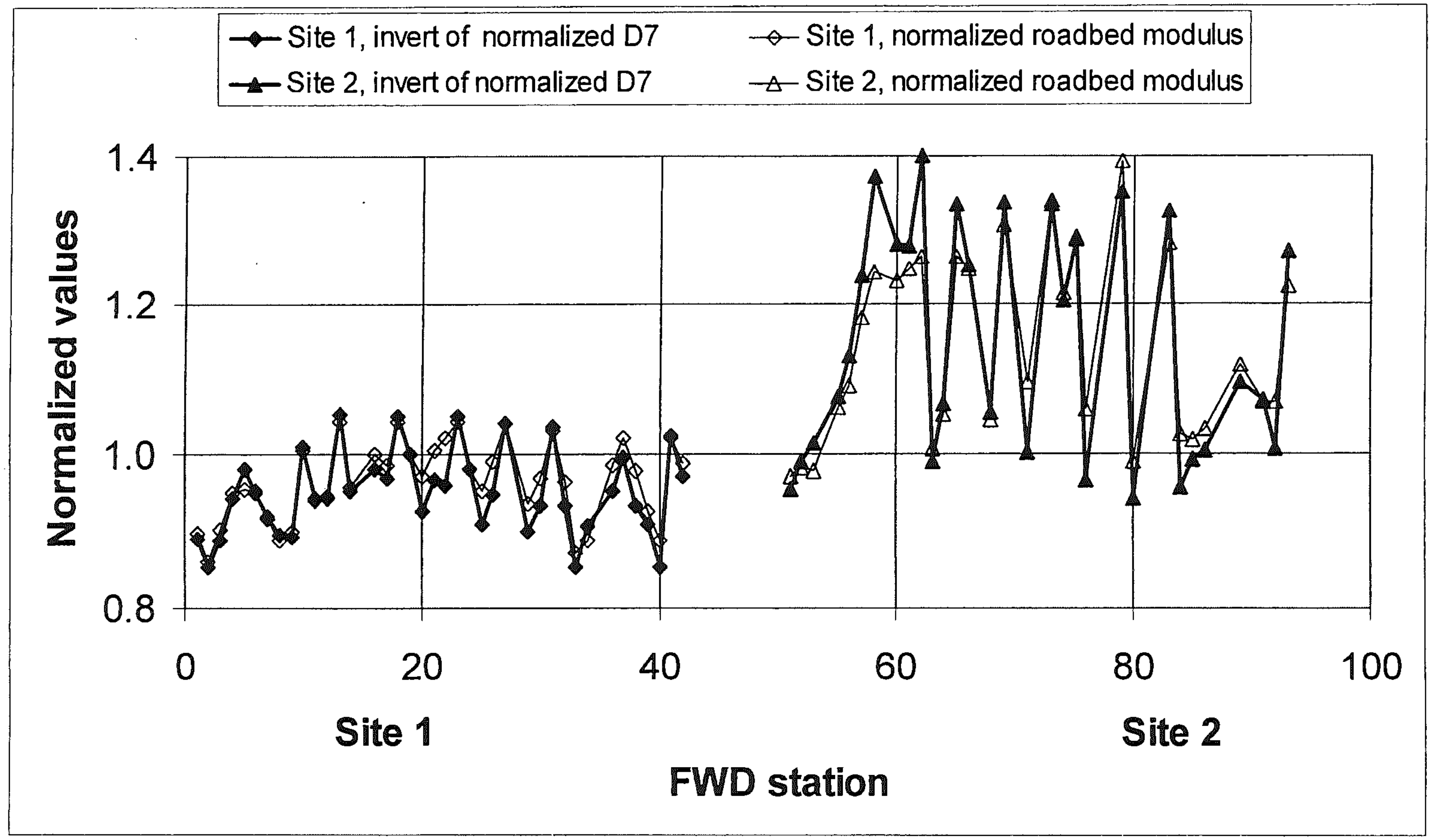

Figure 5.16 Normalized roadbed moduli and the invert of normalized D7 deflection at various test stations along I-75 SB, section 1, test sites 1 and 2

3. The random distribution of the crack network in the fractured concrete layer.

4. The number of rubblized material pieces larger than 6 in.

Because of these, the rubblized material and the fractured concrete layers were combined into one 9-in. thick layer (the rubblized concrete slab) and its modulus was backcalculated using the measured deflection data. It was shown in subsection 4.1.2 of this chapter that the combination of the rubblized material and the fractured concrete layers had no impact on the accuracy of the AC, base and roadbed soil moduli when the base is thicker than 12-in. Unfortunately, no procedure was found to verify the accuracy of the backcalculated modulus of the rubblized concrete slab.

Also as stated in section 4.1.2, a statistical equation (equation 5.3) was developed to estimate the modulus of the rubblized material layer. The equation is based on the backcalculated AC and roadbed soil moduli and on the measured deflection data. After estimating the modulus of the rubblized material, the modulus of the fractured concrete layer was estimated using equation 5.4. The latter equation is based on the mechanics of stress dissipation through the pavement structure and the relative geometry of the rubblized material and the fractured concrete layers.

$$E_{rubb} = (0.001*F_1/F_2) / (F_4* (1.055*F_3^{-1.5262}) * F_2^{2.22}/F_3^{0.15}) \tag{5.3}$$

$$E_{fract} = (E_{RCS}*9-4.5* E_{rubb}) / (4.5*((T_1+0.25*9)/(T_1+0.75*9))) \tag{5.4}$$

where

E_{rubb} = Estimated rubblized material modulus (ksi)
E_{fract} = Estimated fractured concrete modulus (ksi)
E_{RCS} = Backcalculated modulus of the rubblized concrete slab (ksi)
F_1 = Stress in rubblized concrete slab (psi)
$= 82*((5.91/(5.91+0.95*T_1))^2)*2.4*F_3^{0.1}$
F_2 = Compression in rubblized concrete slab (in.)
$= (0.8*\delta_1-(T_1*0.082*(5.9/(5.9+1.7*T_1/2))^2)/E_{AC})/(-0.002289*T_2+0.823492+\delta_2/10)$
F_3 = Compression in AC (in.)
$= T_1* (5.91/(5.91+T_1*0.7))^2*82/(E_{AC}*1000)$
F_4 $= (0.0632*T_1+0.7628)*(0.0128*T_2+0.7505)$
T_1 = AC thickness (in.)
T_2 = Base thickness (in.)
δ_1 = D1-D2 (in.)
δ_2 = D6-D7 (in.)
E_{AC} = Backcalculated AC modulus (ksi)

Note that both equations 3 and 4 were developed based on the assumption that the thickness of the rubblized material and the fracture concrete layers are 4.5 in. When the actual thickness of the rubblized material is more than 4.5 in., equation 3 will yield lower estimates of the modulus relative to the actual modulus. The inverse is also true, that is, when the actual thickness of the rubblized material is less than 4.5 in., equation 3 will yield higher estimates. Since the actual thicknesses of the rubblized material and the fractured concrete layers vary along and across the pavement from 0 to 9 in., their estimated moduli using equations 3 and 4 will also vary substantially from one point to another. To overcome this problem, the thicknesses of the two layers were measured in more than thirty trenches that were excavated during the rubblization operation. It was found that the average thickness of each layer is about 4.5 in. and that the average thickness varies only slightly from one project to another. Consequently, the modulus of the rubblized material and the fractured concrete layers were estimated using two averaging methods as follows:

> **Individual-Average** – In the first step of this method, the moduli of the rubblized material and the fractured concrete layers were estimated for each accepted individual FWD test location using equations 3 and 4. In the second step, the average of the estimated moduli and their coefficients of variation were calculated.
>
> **Average-Average** - In the first step of this method, for each test site, the average deflection and the average backcalculated AC and roadbed soil moduli for all accepted FWD test locations were calculated. In the second step, the average moduli of the rubblized material and the fractured concrete layers were estimated using equations 3 and 4 and the above averages.

Examination of the estimated moduli of the rubblized material and the fractured concrete layers using the two methods indicate that:

1. The individual-average method yielded unreasonable estimated modulus values of the fractured concrete layer at few FWD test locations, which substantially affected the estimated average modulus. Further, the estimated moduli of the rubblized materials and the fractured concrete layers were highly variable. For example, some individual modulus values of the fractured concrete layer at few test sites were higher than the modulus of concrete of 4,000,000 psi and the coefficient of variation was very high. The main reason for this is the high variability in the thicknesses of the two layers. The thickness of each layer may vary from 0 to 9 in. along and across the pavement.

2. The average-average method produced reasonable modulus values of the fractured concrete such that the forwarded calculated deflection basins using these and the average backcalculated layer moduli closely simulate the measured deflection basins. Further, the advantage of this method is that the impact of the variability of the thicknesses of the rubblized material and the fractured concrete layers is minimized. The reason is that, on average, the thickness of each layer is about 4.5 in.

Based on these observations, it was decided to adopt the average-average method. Table 5.13 provides a list of:

1. The test site designation number (a total of 18 FWD test sites were included in this study).

2. The number of FWD tests that were conducted at each test site.

Table 5.13 Backcalculated and estimated pavement layer moduli of 18 rubblized pavement test sites

Test site	No of FWD stations			Backcalculated moduli (ksi)					Estimated moduli (ksi)	
	Total	Converged	Accepted	AC	TCAC	RCS	Base	Roadbed soil	Rubblized material	Fractured concrete
10692-11	40	40	39	317	534	122	25	14	65	256
10692-12	40	40	40	295	573	159	29	17	73	352
10753-11	42	39	34	1,732	1,297	225		17	27	704
10753-12	43	31	20	2,104	1,701	182		19	14	600
11941-21	36	36	27	1,567	1,468	225	44	23	201	360
11941-22	43	42	20	1,247	1,500	182	37	21	144	322
20102-11	40	40	39	710	1,640	61	27	16	44	119
20102-12	40	40	35	517	1,657	46	23	16	31	92
20233-11	52	51	51	433	1,484	50	34	10	15	135
20233-12	26	26	25	150	743	114	29	9	46	287
20273-21	45	41	35	1,891	2,285	117	36	21	24	350
20273-31	40	40	29	470	936	55	17	13	36	109
20273-41	40	39	31	237	608	1,064	50	22	297	2,774
20311-11	40	40	35	637	1,620	414	40	22	191	949
30153-11	43	42	31	2,364	2,165	71	37	20	28	183
30373-51	40	40	35	411	1,192	275	31	16	179	561
30373-52	40	39	38	392	1,407	134	25	15	67	307
30373-61	33	26	17	2,126	2,337	234	38	16	90	592
Minimum				150	534	46	17	9	14	92
Maximum				2,364	2,337	1,064	50	23	297	2,774

TCAC = Temperature corrected asphalt concrete, RCS = Rubblized concrete slab

3. The number of FWD test locations for which the backcalculation of layer moduli routine successfully converged.

4. The backcalculated layer moduli of the AC, rubblized concrete slab and base layers and the roadbed soil.

5. The temperature corrected AC modulus and the design AC modulus (temperature corrected minus two standard deviations).

6. The estimated moduli of the rubblized material and the fractured concrete layers using equations 3 and 4.

The modulus values listed in table 5.13 were used to arrive at the recommended design values. This and other design issues such as the AASHTO layer coefficients are presented in Chapter 6. The applicability of equations 3 and 4 to measured deflection data and discussion of the results are presented in the next section.

6.0 DETAILED EXAMPLE OF BACKCALCULATION OF I-75 SB SECTION 1, TEST SITES 1 AND 2

One of the rubblized pavement projects is located in a rolling terrain in the northern part of the lower peninsula of Michigan along SB I-75 just north of the I-75 and US 31interchange. The original soil consists of Roscommon muck and a deep deposit of poorly drained highly permeable Battlefield sand with gravel. Prior to construction of the original rigid pavement, the muck was excavated and replaced with Battlefield sand, which was compacted to specifications. On site, a seasonal (autumn to spring) high water table exists at a depth of about 0.5 to 1.5 feet from the original ground level. The cross-section of the original concrete pavement consisted of the following layers:

- Nine-in. rubblized JRCP
- Four-in. 22A base
- Four-in. 23A subbase
- Ten-in. class II aggregate subbase

The concrete pavement was rubblized in 1988, and it was capped by an asphalt layer whose thickness varies from 3.5 to 4.8 in.

A test section was selected on the south bound of I-75 about 0.5 miles north of the I-75 and US 31 interchange. Two 100-ft long test sites were marked along the test section such that the two sites were separated by 100-ft. At each test site, FWD tests were conducted and pavement cores were extracted in 2001. The average core thickness for test site 1 was 4.5 in. and for test site 2 was 4.1 in. The measured deflection data were then used to backcalculate the layer moduli using the procedure outlined above. Details of the backcalculation are presented in the next subsections.

6.1 Stiff Layer - Boussinesq Equation

In order to determine whether or not a stiff layer should be incorporated in the backcalculation, the Boussinesq equation (repeated here for convenience) was used to calculate an equivalent modulus.

$$E = \frac{P\left(1-\upsilon^2\right)}{\pi(r)\left(d_r\right)} \tag{5.1}$$

Where E = equivalent modulus
P = applied load = 9000 lbs for the normalized deflection file
υ = Poisson's ratio (assume 0.4)
R = radial distance from the center of the load (in.)
d_r = deflection at distance r from the center of the load (in.)

For each test site, three sets of measured deflection data were selected and for each set, the measured data at each deflection sensor and the Boussinesq equation were used to calculate the equivalent moduli. The results are plotted in figure 5.17. Examination of the figure and comparing it to figure 5.12 indicate that; for test site 1, the calculated equivalent modulus decreases to almost an asymptotic value with increasing distance from the center of the load whereas it decreases and then increases for test site 2.

The two observations imply that a stiff layer should be incorporated in the backcalculation of layer moduli and that the stiff layer for test site 1 is deeper than that for test site 2. The latter finding was confirmed through field investigation. Because of the hilly terrain, test site 1 is located entirely in a 4- to 5-ft deep fill area (after about 4 to 5 ft of muck was removed) while the fill at test site 2 is about 1 ft. That is the original battlefield sand at test site 1 is about 7 ft below the existing pavement surface and at about 3 ft at test site 2. Having determined that a stiff layer should be incorporated into the backcalculation of layer moduli, the next step is to determine the actual depth to stiff layer for both test sites. This was accomplished by comparing the results of the backcalculation obtained by using 3- and 4-layer systems as presented below.

6.2 Depth to Stiff Layer

After scrutinizing the cross-section information of the rubblized pavement on SB I-75, it was assumed that the base and the two subbase layers have similar modulus and therefore they could be combined into one 18-in. thick layer. Hence the backcalculation could be conducted using 4-layer system (AC, rubblized concrete slab, subbase, and roadbed soil) and a stiff layer. Alternatively, the deep gravelly battlefield sand subgrade could also be combined with the base and subbase material and the backcalculation could be conducted using 3-layer system (AC and rubblized concrete slab layers situated directly on roadbed soil) and a stiff layer. The average backcalculated layer moduli of the 4- and 3-layer systems

Table 5.14 Backcalculated layer moduli using 4-layer system with different depths to stiff layer, I-75 SB section 1 test site 1

Depth to stiff layer (in.)	Number of stations converged	Average moduli (psi) and coefficients of variation								Average RMS (%)
		AC	CV (%)	Rubblized	CV (%)	Base	CV (%)	Roadbed	CV (%)	
150	35	1,983,950	46	204,385	103	40,924	70	10,612	8	0.49
200	37	1,948,166	48	223,162	98	30,183	72	13,601	9	0.49
250	37	1,852,974	49	239,186	94	23,018	51	15,702	11	0.49
300	**37**	**1,792,123**	**49**	**249,483**	**91**	**19,699**	**44**	**17,210**	**12**	**0.49**
350	37	1,758,721	49	255,885	90	17,872	42	18,334	13	0.50
400	37	1,744,236	49	259,716	88	16,722	42	19,203	14	0.50
500	38	1,787,859	50	257,718	89	19,590	138	20,359	15	0.52

Table 5.15 Backcalculated layer moduli using 3-layer system with different depths to stiff layer, I-75 SB section 1 test site 1

Depth to stiff layer (in.)	Number of stations converged	Average moduli (psi) and coefficients of variation								Average RMS (%)
		AC	CV (%)	Rubblized	CV (%)	Base	CV (%)	Roadbed	CV (%)	
150	14	1,216,576	24	435,999	46			12,240	6	2.26
200	32	1,407,587	36	298,240	76			14,754	6	1.71
250	38	1,606,831	43	248,394	73			16,143	5	1.28
300	**39**	**1,778,413**	**40**	**218,816**	**72**			**17,042**	**5**	**1.05**
350	37	1,986,909	39	176,534	67			17,750	5	0.96
400	39	2,147,277	40	162,832	67			18,227	5	1.01
500	36	2,295,899	37	136,458	73			18,983	5	1.01

CV (%) = Coefficient of variation = standard deviation divided by average

Table 5.16 Backcalculated layer moduli using 4-layer system with different depths to stiff layer, I-75 SB section 1 test site 2

Depth to stiff layer (in.)	Number of stations converged	Average moduli (psi) and coefficients of variation								Average RMS (%)
		AC	CV (%)	Rubblized	CV (%)	Base	CV (%)	Roadbed	CV (%)	
150	39	1,873,089	55	163,702	58	34,576	35	13,024	14	0.53
200	41	1,799,901	57	186,045	54	26,623	40	16,343	13	0.60
250	**41**	**1,685,368**	**58**	**201,607**	**52**	**22,858**	**43**	**18,630**	**13**	**0.61**
300	42	1,674,405	59	209,546	51	20,776	43	20,290	12	0.63
350	42	1,638,025	60	215,912	50	19,378	44	21,494	12	0.65
400	42	1,620,314	60	220,111	50	18,412	44	22,417	13	0.67
500	42	1,609,033	61	225,294	49	17,173	44	23,733	13	0.70

Table 5.17 Backcalculated layer moduli using 3-layer system with different depths to stiff layer, I-75 SB section 1 test site 2

Depth to stiff layer (in.)	Number of stations converged	Average moduli (psi) and coefficients of variation								Average RMS (%)
		AC	CV (%)	Rubblized	CV (%)	Base	CV (%)	Roadbed	CV (%)	
150	20	912,221	98	722,106	88			15,193	12	3.56
200	29	1,481,824	68	381,263	113			17,529	10	1.93
250	**31**	**1,693,455**	**58**	**274,789**	**116**			**19,357**	**10**	**1.53**
300	31	1,806,179	61	256,115	113			20,160	11	1.36
350	30	1,816,340	63	226,722	118			21,226	11	1.36
400	30	1,806,183	67	223,407	111			21,630	11	1.42
500	27	1,814,783	69	209,135	113			22,418	11	1.59

CV (%) = Coefficient of variation = standard deviation divided by average

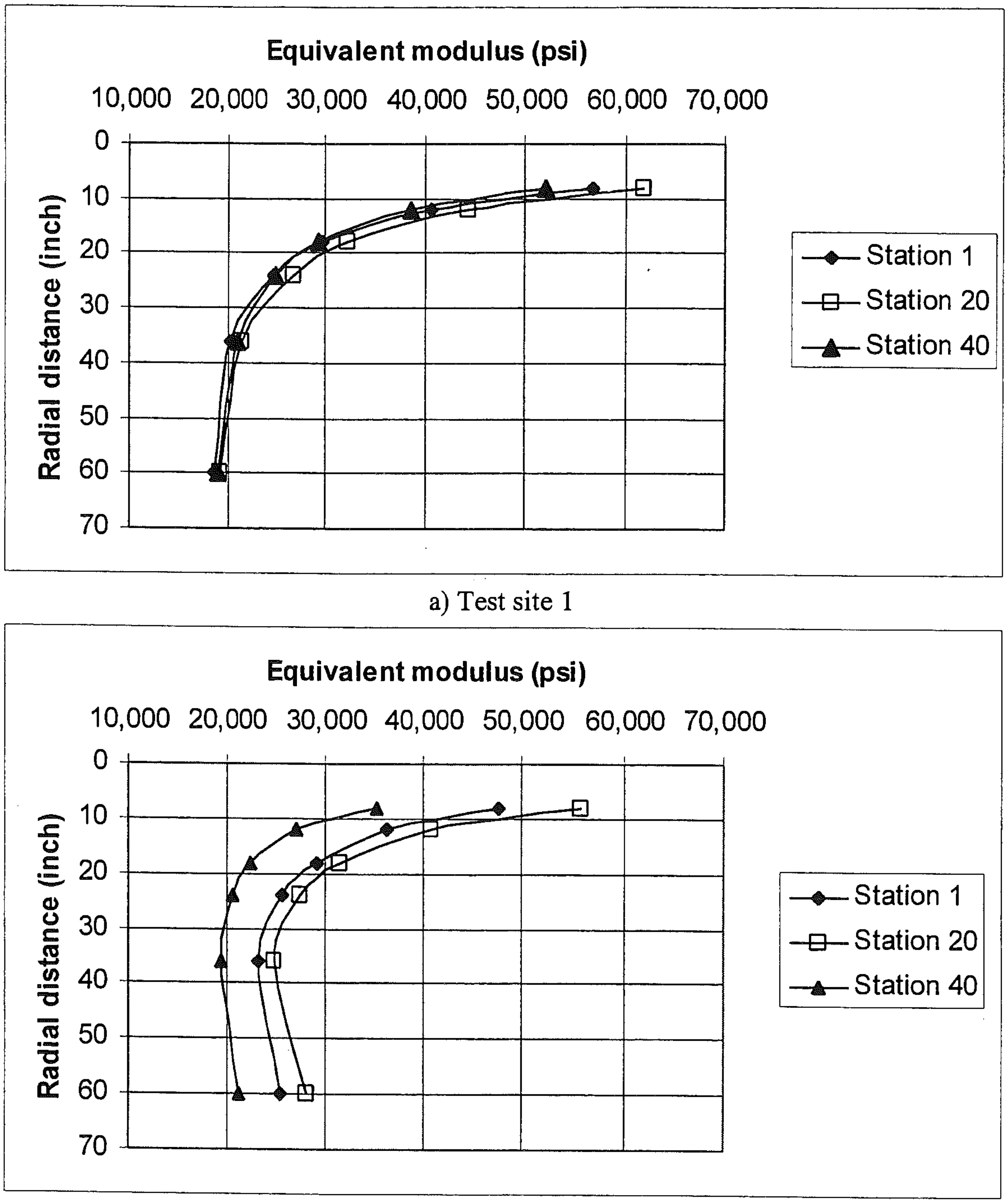

a) Test site 1

b) Test site 2

Figure 5.17 Plots of Boussinesq equivalent modulus of three set of FWD deflections from each test site on I-75 SB section 1 stated above for various depths to stiff layer are listed in tables 5.14 through 5.17. For test site 1, table 5.14 (4-layer system) and table 5.15 (3-layer system) provide lists of:

1. The depths to stiff layer used in the backcalculation.

2. The number of test locations for which the backcalculation was successful (convergence between the measured and calculated deflection basins was achieved).

3. The average backcalculated modulus and the coefficients of variation of:

    - The AC
    - The rubblized concrete slab
    - The base layer (in table 5.14, the base layer is the combination of the one base and two subbase layers stated above).
    - The roadbed soil (in table 5.15, the roadbed soil represents all the material below the rubblized concrete slab).

4. The average root mean square of the errors between the measured and calculated deflection basins.

Tables 5.16 and 5.17 provide similar results for test site 2.

Relative to test site 1 (tables 5.14 and 5.15), the data indicate that the moduli of the various pavement layers and the roadbed soil vary from one FWD test location to another. This is because of the variability in the measured deflection data (see tables 5.4 and 5.5 and figures 5.4 and 5.5), which is caused by variable thicknesses of the AC, rubblized material and fractured concrete layers. Note that among the 18 rubblized projects that were FWD tested in 2001, the measured deflection data along SB I-75 show the highest variation (see table 5.7) and consequently the highest variation in the backcalculated layer moduli (see table 5.18). Finally, the data for site 2 (tables 5.16 and 5.17) show similar results.

Now, let us use the measured deflection data along SB I-75, section 1, test sites 1 and 2 to illustrate the applicability of the procedure, which was presented in the previous subsection, for determining the stiff layer depth. Recall that the backcalculation was accomplished using 3- and 4-layer systems and variable depth to stiff layer. The backcalculated moduli of the AC and roadbed soil for the two test sites are plotted in figure 5.18 (Note that in order to plot the moduli of the two materials on the same graph, the AC modulus was divided by 1,000,000 and the roadbed soil by 10,000 psi). Figure 5.18a shows that the curves representing the backcalculated AC modulus using three and four layer systems intersect around a stiff layer depth of 300 in. Similarly, the curves for the roadbed soil modulus intersect at around 300-in. For test site 2 (figure 5.18b), these intersections are between 240 in. for the AC and 280 in. for the roadbed soil. Although these last two intersections should theoretically be at the same stiff layer depth, the high variation in the measured deflection data makes this not possible. The data, however, suggest that the stiff layer for test site 2 is shallower than 280 in., which is shallower than that for test site 1. This finding is

Table 5.18 Backcalculated moduli and their coefficients of variation of 18 rubblized pavement test sites

Test site	Depth to stiff layer (in.)	Number of stations converged	Modulus (psi)								Average RMS (%)
			AC	CV (%)	Rubblized	CV (%)	Base	CV (%)	Subgrade	CV (%)	
10692-11	150	40	317,448	14	120,329	48	24,826	25	13,785	12	0.54
10692-12	150	40	294,737	20	158,793	32	28,730	21	16,513	15	0.55
10753-11	300	39	1,778,413	40	218,816	72			17,042	5	1.05
10753-12	250	31	1,693,455	58	274,789	116			19,357	10	1.53
11941-21	No stiff layer	36	1,494,031	30	244,821	36	39,767	36	23,438	5	0.43
11941-22	No stiff layer	42	1,457,345	33	205,137	45	39,340	50	17,582	5	0.30
20102-11	500	40	712,346	17	61,512	37	26,261	26	16,248	6	0.45
20102-12	500	40	516,364	14	48,853	35	21,316	33	15,766	3	0.53
20233-11	200	51	437,318	22	50,064	38	34,381	24	10,303	5	0.84
20233-12	200	26	154,165	34	112,020	59	29,107	17	9,198	9	0.81
20273-21	300	41	1,776,844	28	108,717	48	36,515	21	20,765	3	0.68
20273-31	225	41	460,330	18	58,254	34	15,778	24	13,561	5	0.49
20273-41	300	39	230,377	19	1,401,144	76	42,099	52	23,744	35	0.53
20311-11	500	40	619,688	23	671,698	114	35,306	49	22,460	14	0.61
30153-11	500	42	2,182,399	23	90,987	83	31,453	47	20,387	9	0.26
30373-51	400	40	421,812	12	284,801	33	28,806	34	15,878	8	0.63
30373-52	400	39	393,301	25	132,980	46	24,516	33	14,750	10	0.52
30373-61	200	27	2,083,677	27	311,434	52	28,356	62	16,686	11	0.38

CV (%) = Coefficient of variation = standard deviation divided by average

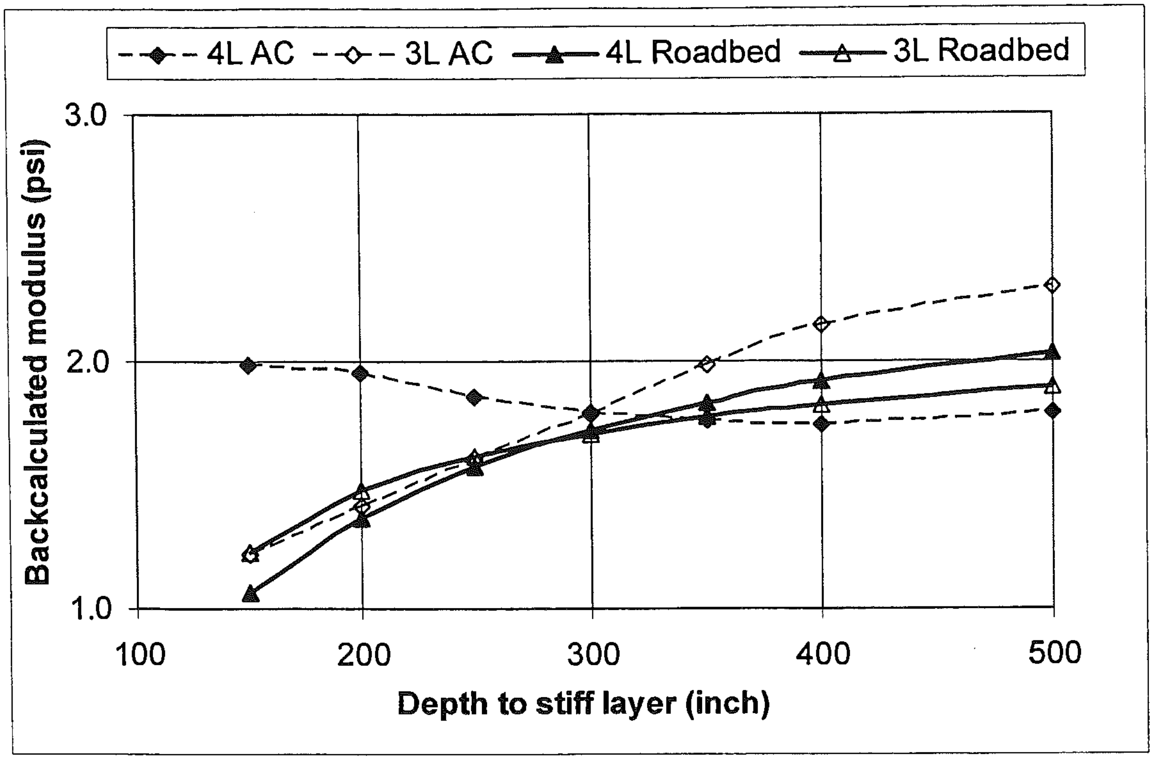

a) Test site 1

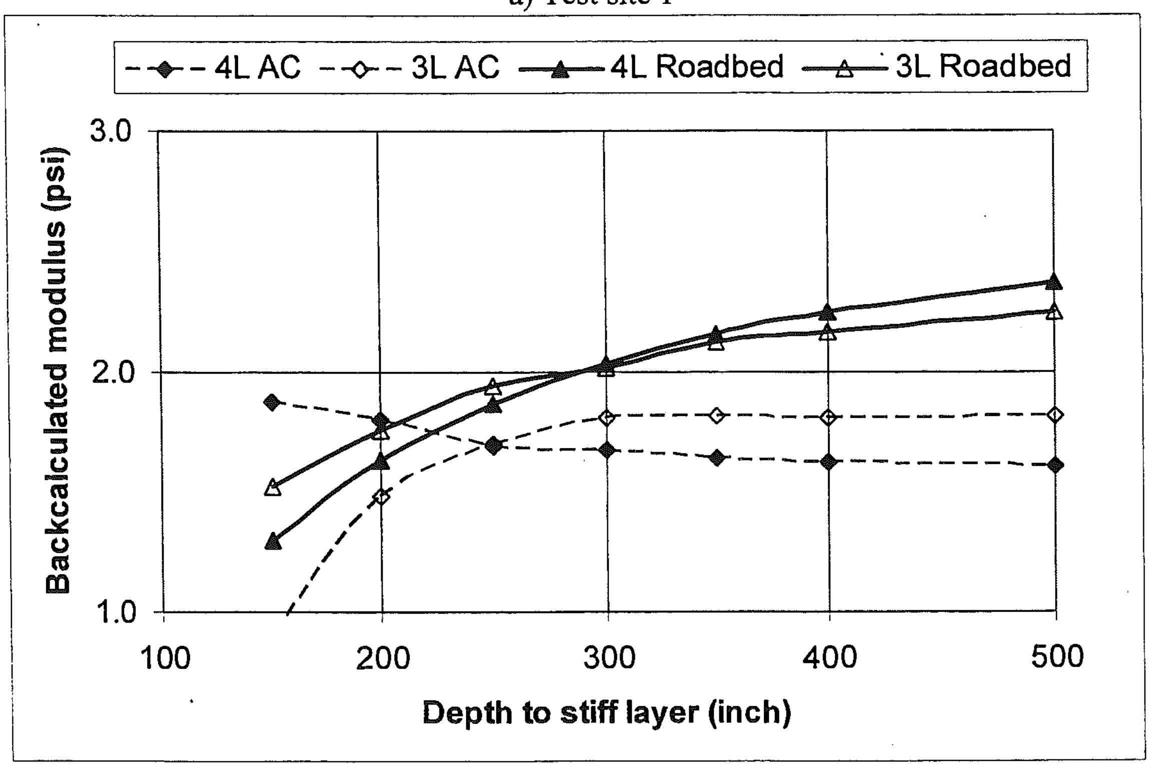

b) Test site 2

Figure 5.18 Intersections of backcalculated AC ($*10^5$) and roadbed soil ($*10^4$) moduli using 3 and 4-layer systems (3L and 4L) also supported by that stated earlier based on Boussinesq equation. One other indicator of the relative depths to stiff layer was found by plotting the backcalculated base and roadbed soil moduli using the 4-layer system against the depth to stiff layer as shown in figure 5.19. The data in the figure indicate that:

- The base and roadbed moduli for test sites 1 and 2 intersect at stiff layer depths of 350 and 300 in., respectively.
- The base modulus is lower than the roadbed modulus at deeper stiff layer depths, which is not probable.
- The stiff layer at test site 2 is shallower than that at test site 1.

Based on the data in figures 5.17, 5.18 and 5.19 and on field observations (the fill thickness at test site 1 is higher than that at test site 2 by about 4 ft) it was decided to use 3-layer system and stiff layer depths of 300 and 250 in. for test sites 1 and 2, respectively for the backcalculation of layer moduli.

Finally, the backcalculated moduli of the rubblized concrete slab were not used in the determination of the stiff layer depths because of the high variability in the thicknesses of the rubblized material and fractured concrete. Such variability significantly affects the accuracy of the backcalculated moduli of the rubblized concrete slab.

6.3 Layer Moduli for SB I-75, Section 1, Test Sites 1 and 2

After the depths to stiff layer was estimated at 250 and 300 in. for test sites 2 and 1, respectively, the deflection data were used to backcalculate the layer moduli using a 3-layer system and the MICHBACK computer program. Results of the MICHBACK include the layer moduli, the root mean square (RMS) of the errors between the measured and calculated pavement deflections and whether or not they converged. After the backcalculation was accomplished, the resulting modulus values of converged FWD test stations were scrutinized. They were rejected when:

1. The RMS was larger than 2 percent.

2. The FWD test was conducted over cracked area.

3. The base modulus satisfies the following equation:

$$MR_{Base} < MR_{RB}/1.1$$

MR_{Base} = backcalculated base modulus; and
MR_{RB} = backcalculated roadbed modulus.

Based on the above criterion, some of the I-75 SB backcalculation results were rejected and the rest of them were accepted and used to calculate the average backcalculated moduli of test sites 1 and 2. Tables 5.19 and 5.20 provide the backcalculated layer moduli for test sites 1 and 2, respectively. The tables also provide the moduli of the rubblized material and the

Table 5.19 Results of the backcalculation and the estimated layer moduli for I-75 SB -section 1 test site 1

FWD station	MDT (^{0}C)	Backcalculated modulus (ksi)					Estimated moduli (ksi)		RMS (%)	Converged	Accepted
		AC	TCAC	RCS	Base	RB	Rubblized material	Fractured concrete			
1	13.1	2040	1472	106	-	16	18	538	1.13	Y	Y
2	13.2	1511	1097	118	-	15	17	611	1.01	Y	Y
4	13.3	1312	958	126	-	17	27	623	1.00	Y	Y
5	13.4	2358	1733	69	-	17	10	357	0.28	Y	Y
6	13.7	1192	889	133	-	17	23	672	0.67	Y	Y
7	13.7	1116	832	134	-	16	20	688	0.33	Y	Y
8	13.7	2411	1797	102	-	16	15	527	0.56	Y	Y
9	14.0	2072	1572	132	-	16	16	686	0.37	Y	Y
10	14.2	1916	1464	103	-	18	14	532	1.08	Y	Y
11	14.4	1986	1540	87	-	17	14	445	1.41	Y	Y
12	14.4	1032	800	168	-	17	31	848	0.24	Y	Y
13	14.6	2533	1985	73	-	18	9	381	1.93	Y	Y
14	14.8	678	537	142	-	17	38	683	1.02	Y	Y
16	15.2	1197	969	215	-	17	42	1080	0.16	Y	Y
18	15.2	1809	1464	204	-	18	31	1045	1.24	Y	Y
19	15.3	1378	1119	265	-	17	56	1317	1.07	Y	Y
20	15.4	1090	892	351	-	18	111	1643	0.55	Y	Y
21	15.4	2826	2313	80	-	18	15	405	1.15	Y	Y
22	15.8	2543	2126	207	-	17	23	1088	1.71	Y	Y
23	15.6	1347	1118	304	-	17	82	1463	0.80	Y	Y
24	15.6	962	799	467	-	17	198	2047	0.58	Y	Y
25	15.4	2352	1931	102	-	18	19	512	1.09	Y	Y
27	15.5	3147	2593	304	-	17	42	1569	0.29	Y	Y
28	15.1	1039	841	561	-	17	308	2259	0.76	Y	Y
29	15.0	2675	2150	104	-	18	17	533	0.50	Y	Y
30	14.8	1552	1239	334	-	17	89	1608	0.71	Y	Y
31	14.6	2966	2341	510	-	15	96	2570	1.19	Y	Y
32	14.6	1255	991	143	-	16	20	737	1.40	Y	Y
35	14.6	941	740	225	-	18	46	1125	0.79	Y	Y
36	14.8	1271	1011	370	-	17	96	1790	0.47	Y	Y
37	14.8	1632	1303	491	-	16	175	2240	1.78	Y	Y
38	14.9	844	677	664	-	16	586	2063	1.10	Y	Y
39	15.1	2235	1808	118	-	18	16	610	0.55	Y	Y
40	15.2	1663	1351	131	-	17	64	551	1.82	Y	Y
3	12.2	2114	1457	91	-	16	-	-	2.32	Y	N
15	16.0	2137	1800	147	-	18	-	-	1.28	Y	N
17	16.0	2719	2289	69	-	18	-	-	2.21	Y	N
34	14.8	2957	2351	132	-	17	-	-	2.65	Y	N
42	14.3	533	412	454	-	18	-	-	1.76	Y	N
26		-	-	-	-	-	-	-	2.32	N	N
33		-	-	-	-	-	-	-	1.74	N	N
41		-	-	-	-	-	-	-	3.85	N	N
Average	14.7	1732	1366	225	-	17	70	1054	0.90		
CV (%)	5	39	40	70	-	5	159	61	53		

MDT = Mid-depth temperature, TCAC = Temperature corrected asphalt concrete, RCS = Rubblized concrete slab, RB = Roadbed, RMS = Root mean square error

Table 5.20 Results of the backcalculation and the estimated layer moduli for I-75 SB -section 1 test site 2

FWD station	MDT (°C)	Backcalculated modulus (ksi)					Estimated moduli (ksi)		RMS (%)	Converged	Accepted
		AC	TCAC	RCS	Base	RB	Rubblized material	Fractured concrete			
2	15.0	1193	957	170	-	17	28	912	0.67	Y	Y
3	14.8	1596	1269	114	-	16	13	627	0.24	Y	Y
4	15.1	3241	2622	123	-	18	7	696	1.55	Y	Y
6	15.2	1743	1412	119	-	18	13	661	0.27	Y	Y
9	15.4	853	702	132	-	21	22	705	1.98	Y	Y
10	15.4	2060	1694	141	-	21	16	779	0.71	Y	Y
12	15.7	2463	2054	136	-	18	33	699	1.20	Y	Y
13	16.2	597	510	150	-	21	24	806	0.62	Y	Y
14	16.2	3050	2606	181	-	21	24	984	0.75	Y	Y
16	16.5	2328	2027	167	-	17	15	931	0.36	Y	Y
22	16.5	2275	1981	208	-	22	38	1102	1.30	Y	Y
30	16.6	2602	2277	133	-	21	13	738	0.31	Y	Y
32	16.5	3088	2688	341	-	17	28	1906	0.41	Y	Y
33	16.4	2134	1849	273	-	17	35	1489	0.84	Y	Y
35	16.3	3220	2777	395	-	18	40	2189	0.83	Y	Y
36	16.3	2325	2005	303	-	19	38	1658	0.50	Y	Y
38	16.1	2659	2271	238	-	18	15	1346	1.17	Y	Y
40	15.9	1210	1023	159	-	21	14	889	0.39	Y	Y
41	16.0	1527	1292	118	-	20	8	664	0.51	Y	Y
42	15.9	1921	1617	50	-	21	3	287	1.28	Y	Y
43	15.9	1419	1195	307	-	20	-	-	0.55	Y	N
7	14.8	1574	1252	71	-	21	-	-	1.41	Y	N
17	15.9	404	341	214	-	22	-	-	1.38	Y	N
5	15.4	563	460	148	-	18	-	-	2.11	Y	N
8	14.8	2333	1855	33	-	21	-	-	2.58	Y	N
19	14.2	168	130	1309	-	18	-	-	3.77	Y	N
21	16.4	431	374	240	-	23	-	-	2.32	Y	N
23	14.2	207	160	1465	-	18	-	-	3.36	Y	N
24	17.5	562	516	385	-	17	-	-	3.19	Y	N
26	18.6	2637	2563	127	-	23	-	-	6.06	Y	N
39	16.9	111	99	571	-	18	-	-	4.82	Y	N
1	-	-	-	-	-	-	-	-	2.98	N	N
11	-	-	-	-	-	-	-	-	2.05	N	N
15	-	-	-	-	-	-	-	-	2.64	N	N
18	-	-	-	-	-	-	-	-	0.80	N	N
20	-	-	-	-	-	-	-	-	2.27	N	N
25	-	-	-	-	-	-	-	-	2.48	N	N
27	-	-	-	-	-	-	-	-	1.23	N	N
28	-	-	-	-	-	-	-	-	2.23	N	N
29	-	-	-	-	-	-	-	-	2.84	N	N
31	-	-	-	-	-	-	-	-	2.48	N	N
34	-	-	-	-	-	-	-	-	1.91	N	N
37	-	-	-	-	-	-	-	-	1.99	N	N
Average	15.9	2104	1782	182	-	19	21	1003	0.79		
CV (%)	3	37	38	47	-	10	54	48	60		

MDT = Mid-depth temperature, TCAC = Temperature corrected asphalt concrete, RCS = Rubblized concrete slab, RB = Roadbed, RMS = Root mean square error

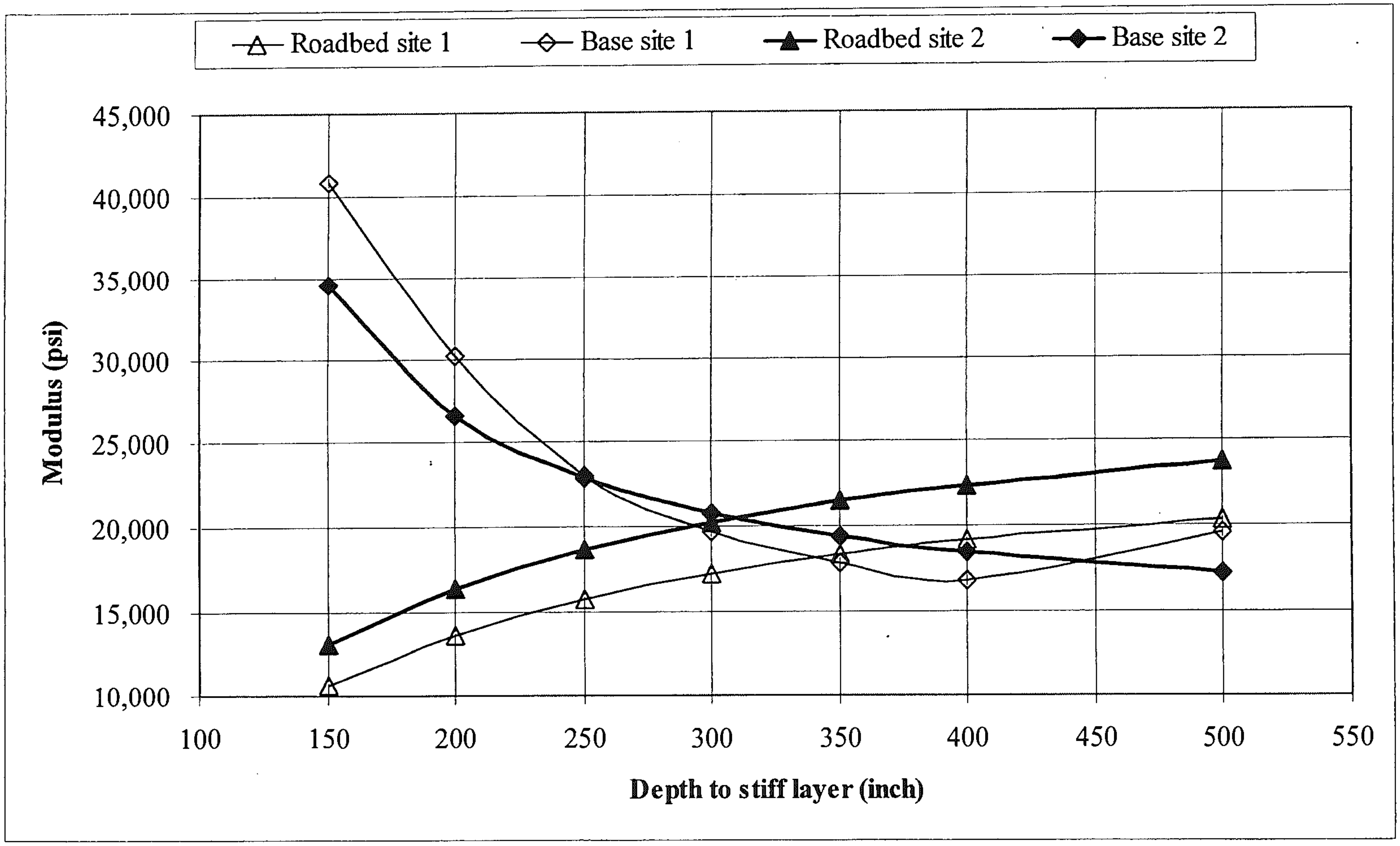

Figure 5.19 Base and roadbed moduli versus depth to stiff layer for I-75 SB, section 1, test sites 1 and 2

fractured concrete layers at each accepted stations that were estimated using equations 3 and 4. As can be seen from the tables, the moduli of the two layers are highly variable. The modulus of the rubblized material varies from 9 to 586 ksi for test site 1 and from 3 to 40 for test site 2. Likewise, the modulus of the fractured concrete layer varies from 357 to 2570 ksi for test site 1 and from 287 to 2189 for test site 2. Once again, the reason for such variation is that the thicknesses of the rubblized material and the fractured concrete layers are not known at any specific location. For this reason, the moduli of the two layers were estimated using equations 3 and 4 and the averages of the AC, roadbed moduli and the average of the measured deflections at the accepted FWD test locations for each test site. The results of the later estimates of the moduli of the two layers are listed in table 5.13 and discussed in section 5 of this chapter.

One last note, for I-75 SB, section 1, test sites 1 and 2, the estimated moduli of the rubblized material and the fractured concrete layers using the individual-average and the average-average methods are listed below. As can be seen, the average-average method yields lower modulus values and more reasonable than the individual-average method.

Test site	Method of calculation	Estimate4d modulus values (ksi)	
		Rubblized material layer	Fractured concrete layer
10753-11	Individual-average	70	1054
	Average-average	27	704
10753-12	Individual-average	21	1003
	Average-average	14	600

Results of the backcalculation of 18 rubblized pavements are summarized in Appendix J along with the deflection.

7.0 SUMMARY

Various nondestructive deflection test and backcalculation of layer moduli issues are discussed in this chapter. These include:

1. The repeatability of the measured deflection data; the MDOT FWD produces repeatable data.

2. The pavement response to load was tested using the FWD. For the pavement projects included in this study, the pavement response to load is more or less linear. Hence, a linear layered-elastic system can be used for the analysis of the pavement sections and for the backcalculation of layer moduli.

3. The measured deflection data along and across a pavement section (within 100-ft test site) are highly variable. Hence, one should expect high variability in the structural capacity of the pavement and in its performance. The variability in the deflection data of rubblized pavement structures is in order of magnitude higher than that for conventional flexible pavements.

4. The sensitivity of the backcalculated layer moduli to several pavement and site variables was discussed. These variables include the accuracy of the layer thicknesses and the depth to stiff layer.

5. A backcalculation procedure was developed during this study and discussed in this chapter. The procedure was successfully applied to real sets of measured deflection data. It is shown that the most difficult problem in the backcalculation of layer moduli is the uncertainty of the thicknesses of the rubblized material and the fractured concrete layers.

6. A statistical model was developed and presented in this chapter for the estimation of the modulus of the rubblized material. The model uses as input, the deflection data and the backcalculated moduli of the AC and roadbed soil.

7. The modulus of the fractured concrete layer can be estimated based on the principles of stress dissipation and on the geometry of the rubblized pavement.

REFERENCES

1. Irwin, L.H., W.S., Yang, and R.N. Stubstad, "Deflection Reading Accuracy and Layer Thickness Accuracy in Backcalculation of Pavement Layer Moduli." The American Society for Testing and Material, STP 1026 1989, Bush/Baladi, editors

2. Harichandran R.S., T. Mahmood and G.Y. Baladi, "Backcalculation of Pavement Layer Moduli, Thicknesses and Stiff Layer Depth Using a Modified Newton Method." The American Society for Testing and Materials, ASTM STP 1198, Philadelphia, PA 1994, Von Quintas, Bush and Baladi, editors

3. Harichandran, R.S., T. Mahmood, A. Raab and G.Y. Baladi "A Modified Newton Algorithm for Backcalculation of Pavement layer properties," Transportation Research Record, 1384, 15-22, 1993

4. Das, Braja M., Principles of Foundation Engineering, 4th edition, 1998

5. AASHTO Guide for Design of Pavement Structures, 1993

6. "Soil Survey of Cheboygan County, Michigan", United States Department of Agriculture, Soil Conservation Service; September 1991.

7. Harichandran, R. S., Ramon, C. M., and Baladi, G. Y., "MICHBACK user's manual.", Department of Civil and Environmental Engineering, Michigan State University, East Lansing, Michigan, 1994

8. Per Ullidtz "Pavement Analysis", Elsevier Science Publishing Company, New York, New York, 1987.

CHAPTER 6
RUBBLIZED PAVEMENT DESIGN PARAMETERS

1.0 PAVEMENT DESIGN PROCEDURES

The design of rubblized concrete pavements can be accomplished by using three different design methods, empirical, mechanistic-empirical or catalogue-based design. Each of the three methods has benefits and drawbacks. Currently, MDOT uses a modified version of the AASHTO 93 empirical design procedure. The inputs to the procedure include the modulus of the various pavement layers and the AASHTO layer coefficients. Hence, one of the objectives of this study is to determine the moduli and coefficients of the rubblized concrete slab.

As noted in chapter 5, the modulus values of the AC, rubblized concrete slab, and base layers and of the roadbed soil were obtained using the MICHBACK computer program and the measured deflection data. Based on the backcalculated modulus of the rubblized concrete slab, on the AC and roadbed modulus values and on the measured deflection data, the modulus values of the rubblized material and the fractured concrete layers were estimated. The estimated and the backcalculated modulus values were reported in table 6.13 (which is, for convenience, repeated herein as table 6.1) and discussed in chapter 5. This chapter addresses the modulus and the layer coefficient values of the rubblized concrete slab, the rubblized material and the fractured concrete layers to be used in mechanistic-based or the AASHTO pavement design procedures.

2.0 RUBBLIZED PAVEMENT DESIGN PARAMETERS

Table 6.1 provides a list of results of the backcalculated and estimated layer moduli of 18 test sites. The list includes:

1. The total number of FWD tests that were conducted at each test site.

2. The number of FWD test locations at which the backcalculation routine achieved convergence between the measured and the calculated deflection data.

3. The number of FWD test stations that were accepted based on the acceptance criteria discussed in chapter 5.

4. For each test site, the average backcalculated modulus values of the AC, rubblized concrete slab, base layers and the roadbed soil. Note that the AC modulus values have been corrected to the standard temperature of 68°F and listed under the title TCAC.

5. The average estimated modulus values of the rubblized material and the fractured concrete.

Table 6.1 Backcalculated and estimated pavement layer moduli of 18 rubblized pavement test sites

Test site	No of FWD stations			Backcalculated moduli (ksi)					Estimated moduli (ksi)	
	Total	Converged	Accepted	AC	TCAC	RCS	Base	Roadbed soil	Rubblized material	Fractured concrete
10692-11	40	40	39	317	534	122	25	14	65	256
10692-12	40	40	40	295	573	159	29	17	73	352
10753-11	42	39	34	1,732	1,297	225		17	27	704
10753-12	43	31	20	2,104	1,701	182		19	14	600
11941-21	36	36	27	1,567	1,468	225	44	23	201	360
11941-22	43	42	20	1,247	1,500	182	37	21	144	322
20102-11	40	40	39	710	1,640	61	27	16	44	119
20102-12	40	40	35	517	1,657	46	23	16	31	92
20233-11	52	51	51	433	1,484	50	34	10	15	135
20233-12	26	26	25	150	743	114	29	9	46	287
20273-21	45	41	35	1,891	2,285	117	36	21	24	350
20273-31	40	40	29	470	936	55	17	13	36	109
20273-41	40	39	31	237	608	1,064	50	22	297	2,774
20311-11	40	40	35	637	1,620	414	40	22	191	949
30153-11	43	42	31	2,364	2,165	71	37	20	28	183
30373-51	40	40	35	411	1,192	275	31	16	179	561
30373-52	40	39	38	392	1,407	134	25	15	67	307
30373-61	33	26	17	2,126	2,337	234	38	16	90	592
Minimum				150	534	46	17	9	14	92
Maximum				2,364	2,337	1,064	50	23	297	2,774
Average						207			87	503

TCAC = Temperature corrected asphalt concrete, RCS = Rubblized concrete slab

6. The maximum and minimum values of the modulus of each material.

7. The overall average (the average of all test sites) modulus values of the rubblized concrete slab, the rubblized material and the fractured concrete. The overall average modulus values of the AC and base layers and of the roadbed soil are not included because various asphalt mixes, base material, and roadbed soil were found at the test sites

Examination of the modulus values of the rubblized concrete slab, and the rubblized material and the fractured concrete layers listed in table 6.1 indicates that the average modulus varies significantly from one test site to another. Indeed, it was shown that the modulus values within one test site also vary significantly. It was discussed in chapter 5 that the main reason of the variations in the modulus within a test site is the high variation in the thicknesses of the rubblized material and the fractured concrete layers. The variation between the test sites is related to the quality (strength) of the concrete before rubblization and to the rubblization process itself. Some projects were rubblized using the resonant frequency breaker whereas others using the multi-hammer breaker. Hence, the issue herein is what modulus value or values should be used in the rubblized pavement design process? These and other design issues are addressed in the next two subsections.

2.1 Design Modulus Values

To satisfactorily answer the question posted above, two step- analyses were undertaken as follows:

1. FWD deflection data obtained from various conventional flexible pavements were used to backcalculate the layer moduli of the pavements. Results of the analysis indicate that the backcalculated modulus values were about twice as high as those used in the pavement design process. Therefore, it was decided to divide the modulus of the rubblized material listed in table 6.1 by a factor of 2. The inherent assumption is that the rubblized material performs like a conventional aggregate base.

2. FWD deflection data obtained from various composite pavements were used to backcalculate the layer moduli of the pavements. Results of the analysis indicate that the backcalculated modulus value of the concrete slab varied from 2,500,000 to 4,500,000 psi. The implication of this is that the backcalculated values are representative of the modulus of the AC slab. Therefore, it was decided to use the backcalculated or estimated modulus values of the rubblized concrete slab and the fractured concrete layer as the design moduli.

Based on the results of the analyses from the two steps, the recommended design modulus values for the rubblized concrete slab, the rubblized material and the fractured concrete layers were calculated and are provided, for each test site, in table 6.2. The table also lists the minimum and maximum modulus values and the overall average moduli of the three materials.

Table 6.2 Recommended design moduli and layer coefficients

Test site	Modulus (ksi)			Layer coefficient					
				AASHTO-based			Mechanistic-based		
	RCS	Rubblized material	Fractured concrete	RCS	Rubblized material	Fractured concrete	RCS	Rubblized material	Fractured concrete
10692-11	122	32.7	256	0.18	0.15	0.23	0.20	0.16	0.25
10692-12	159	36.5	352	0.21	0.16	0.27	0.23	0.17	0.29
10753-11	225	13.7	704	0.26	0.05	0.34	0.26	0.08	0.36
10753-12	182	6.8	600	0.23	-0.02	0.33	0.24	0.02	0.34
11941-21	225	100.6	360	0.26	0.27	0.27	0.26	0.26	0.29
11941-22	182	72.1	322	0.23	0.23	0.26	0.24	0.23	0.28
20102-11	61	22.1	119	0.09	0.10	0.15	0.13	0.12	0.18
20102-12	46	15.6	92	0.06	0.07	0.12	0.10	0.09	0.15
20233-11	50	7.6	135	0.07	-0.01	0.17	0.11	0.03	0.19
20233-12	114	23.2	287	0.17	0.11	0.25	0.19	0.13	0.27
20273-21	117	11.9	350	0.18	0.04	0.27	0.20	0.07	0.29
20273-31	55	18.1	109	0.08	0.08	0.14	0.12	0.11	0.17
20273-41	1,064	148.5	2,774	0.45	0.31	0.49	0.42	0.30	0.49
20311-11	414	95.7	949	0.33	0.26	0.38	0.32	0.26	0.39
30153-11	71	13.8	183	0.11	0.05	0.20	0.15	0.08	0.22
30373-51	275	89.4	561	0.28	0.26	0.32	0.28	0.25	0.33
30373-52	134	33.3	307	0.19	0.15	0.25	0.21	0.16	0.27
30373-61	234	44.9	592	0.26	0.18	0.32	0.27	0.19	0.34
Minimum	46	6.8	92	0.06	-0.02	0.12	0.10	0.02	0.15
Maximum	1,064	148.5	2,774	0.45	0.31	0.49	0.42	0.30	0.49
Average	207	43.7	503	0.20	0.14	0.26	0.22	0.15	0.28

Based on the analyses and the overall average of the moduli of the three materials, it is strongly recommended that the following design modulus values be used in the design of rubblized pavement section:

Material	Design modulus (ksi)
Rubblized concrete slab	207
Rubblized material	43
Fractured concrete	503

2.2 AASHTO Layer Coefficients

Two methods were used to estimate the layer coefficients of the rubblized concrete slab, the rubblized material and the fractured concrete layers. The first method is based on the AASHTO design procedure and the second is based on mechanistic analysis. The two methods are presented and discussed in the next two subsections.

2.2.1 AASHTO-Based Layer Coefficients

In the AASHTO-based layer coefficient method, three procedures were used as follows:

1. The rubblized concrete slab
2. The fractured concrete layer
3. The rubblized material

The three procedures are presented below.

Procedure One - The Rubblized Concrete Slab – In this procedure, the following assumptions were made based on the state of distress of the original concrete pavement prior to rubblization:

1. Since the rubblized concrete slabs consist of two layers; a rubblized material layer and a fractured concrete layer, the rubblized concrete slabs can be treated as a deteriorated concrete slabs in need of AC overlay.

2. The relationship between the modulus of the rubblized concrete slabs and the layer coefficient is analogous to that between cement treated bases and the layer coefficient since both behave like a strong base layer under the AC surface. Hence, the AASHTO proposed relationship between the cement-treated bases and the layer coefficient was used as follows:

$$a_2 = 0.2187*Ln(E_{RCS}) - 2.7547 \qquad (6.1)$$

where: E_{RCS} = the modulus of the fractured concrete slab (ksi); and
Ln = natural logarithm

3. For each mile, the average number of deteriorated joints and transverse cracks in the concrete is 155. This makes the average distance between deteriorated joints and transverse cracks 35 ft. For such a state of distress, the AASHTO design procedure recommends reducing the a_2 value by a factor of 0.65.

4. On average, the concrete pavement has 75 working transverse cracks per mile. That is the average distance between working transverse cracks is about 70 ft. For this scenario, the AASHTO design procedure recommends reducing the a_2 value by a factor of 0.9.

Incorporating the two reduction factors of items 3 and 4 above into equation 6.1 yields the following equation, which relates the design modulus to the AASHTO layer coefficient.

$$a_2 = 0.65*0.9*(0.2187*Ln(E_{RCS})-2.7547) \qquad (6.2)$$

Based on equation 6.2, the layer coefficient of the rubblized concrete slab at each test site was calculated and the results are listed in table 6.2 along with the minimum, maximum and the overall average layer coefficient value.

Procedure Two – The Fractured Concrete Layer – For this material, the first two assumptions (assumptions 1 and 2) of the first procedure were upheld for the same argument. However, assumptions 3 and 4 are not valid for the fractured concrete layer. The layer includes deteriorated joints and transverse cracks as well as micro cracks created by the rubblization process throughout the layer. To account for the micro cracks, the product of the reduction factors (0.65 and 0.9) was further reduced by a factor of 0.85. That is, the reduction factor for the fractured concrete layer is the product of 0.65, 0.9 and 0.85 or 0.5. The final equation relating the modulus of the fractured concrete to its AASHTO layer coefficient is as follows:

$$a_2 = 0.5*(0.2155*Ln(E_{FCL})-0.7266) \qquad (6.2)$$

where: E_{FCL} = the modulus of the fractured concrete layer (ksi); and
Ln = natural logarithm.

The calculated values of the AASHTO layer coefficients of the fractured concrete layer are listed in table 6.2 along with the minimum, maximum and the overall average layer coefficient value.

Procedure Three – The Rubblized Material – The rubblized material layer was assumed to perform like a conventional aggregate base. Therefore the AASHTO recommended relationship between the modulus and the layer coefficient was used as follows:

$$a2 = 0.249*Log(E_{RML})-0.977 \qquad (6.3)$$

where: E_{RML} = the modulus of the rubblized material layer (psi); and
Log = base 10 logarithm.

The calculated values of the AASHTO layer coefficients of the fractured concrete layer are also listed in table 6.2 along with the minimum, maximum and the overall average layer coefficient value.

Based on the assumptions and on the analyses, it is strongly recommended that the following layer coefficients be used in the AASHTO design procedure.

Material	Design modulus (ksi)
Rubblized concrete slab	0.2
Rubblized material	0.14
Fractured concrete	0.26

2.2.2 Mechanistic-Based Layer Coefficients

The layer coefficients of the rubblized concrete slab, the rubblized material and the fractured concrete were also determined using mechanistic-based design (the MICHPAVE computer program was used) coupled with the AASHTO empirical pavement design procedure. Unlike the AASHTO-based layer coefficient, the determination of the mechanistic-based layer coefficients entailed a more in depth procedure as presented below.

1. For each test site, the backcalculated and estimated modulus values of the AC, rubblized slab, aggregate base and roadbed soil were used to determine the design modulus as follows:

    a) For the AC layer, 67 percent of the average backcalculated and temperature adjusted modulus.
    b) For the rubblized concrete slab, the rubblized material and the fractured concrete, the design modulus values listed in table 6.2 were used.
    c) For the aggregate base, 50 percent of the average backcalculated modulus values.
    d) For the roadbed soil, the average value of the backcalculated layer moduli was divided by three as per AASHTO recommendation.

2. The actual layer thicknesses were obtained by coring or from the MDOT project files and used in the analyses.

3. The MICHPAVE computer program was then used to analyze the pavement section and to estimate its fatigue life in terms of 18-kip ESAL.

4. The AASHTO flexible pavement design procedure was then used with the following inputs:

a) The fatigue life obtained from the MICHPAVE program in terms of 18-kip ESAL.
b) The design modulus values of all layers.
c) For all layers except the one whose layer coefficient is being determined, the layer coefficient which was obtained using the design modulus value and the proper AASHTO equation or chart. For the layer in question, a layer coefficient value of 0.25 was assumed.
d) All layer thicknesses except the one whose layer coefficient is being determined.

5. Based on the above input, the AASHTO procedure was used to determine the required thickness (d_{req}) of the layer whose coefficient is being determined.

6. The mechanistic-based layer coefficient was then calculated using the following equation.

$$a_{2Mechanistic} = .25 * \left(\frac{d_{REQ}}{Actual\ thickness} \right) \tag{6.3}$$

The procedure was then repeated for each layer (the rubblized concrete slab, the rubblized material and the fractured concrete).

The mechanistic based layer coefficients of the three materials are also listed in table 6.2. Examination of the AASHTO-based and the mechanistic-based layer coefficients indicate that, on average, the two procedure produce compatible results.

Note that, in all analyses the thickness of each of the rubblized material and the fractured concrete layers was assumed as 4.5-inch (based on a total concrete thickness of 9 in.). The AASHTO-based and the mechanistic-based layer coefficients listed in table 6.2 indicate that the structural number (SN) of the rubblized concrete slab is almost the same as that of the rubblized material and the fractured concrete. That is the pavement designer has the option of using either a 9-inch rubblized concrete slab with a layer coefficient of 0.2 or 4.5 in. rubblized material with a layer coefficient of 0.14 and 4.5 in. of fractured concrete with a layer coefficient of 0.26. This is so because the two methods produce the same structural number as follows:

$$SN = 9*0.2 = 4.5*.14 + 4.5*.26$$

The above observation indicates that the layer coefficients are reasonable and balanced. One word of caution should be exercised however is that, in the above analysis, the AC thickness was fixed at the actual field value obtained by coring. In real life, the pavement design engineer may use the AASHTO design procedure to determine the thickness of the AC. For that case, the required AC thickness will be different if the designer uses one rubblized slab layer than if he/she uses rubblized material and fractured concrete layer. The reason is that the design modulus of the rubblized slab is different than that of the rubblized material. Therefore, the rubblized slab layer will result in a thinner AC thickness.

3.0 SUMMARY

Based on the FWD deflection data and the actual layer thickness, the design modulus value for the rubblized concrete slab, the rubblized material and the fractured concrete were estimated. Two sets of layer coefficients were obtained; one is AASHTO-based and the other is based on mechanistic analysis and design of the pavement structure augmented by the AASHTO empirical pavement design procedure. It is shown that the two sets of layer coefficient values are compatible and almost the same.

CHAPTER 7
MECHANISTIC ANALYSIS OF RUBBLIZED PAVEMENTS

1.0 FIELD OBSERVATIONS

Based on field investigations and observations that were conducted during the rubblization operation and after the completion of construction, the causes of the underperformance of rubblized concrete pavement projects can be related to several attributes as follows:

1. The rubblization procedure
2. The construction of the asphalt mat
3. The asphalt mix

The effects of these attributes on the performance of rubblized concrete pavements are addressed in Chapter 4 and, for convenience, are summarized below. The three attributes may cause the following defects in the rubblized concrete pavements:

1. Joint reflective cracking if the integrity of the joints in the concrete pavement is not completely destroyed.

2. Reflective cracking if the integrity of the concrete in the vicinity of the crack is not destroyed and/or if the temperature steel is not completely debonded or if the rubblized material contains independent large concrete pieces (larger than 6 in.).

3. Localized shear failure if the rubblization procedure caused some large concrete pieces to break loose and rotate or penetrate into the subbase material. Fixing such shear failure requires removal of the AC, base and subbase layers and appropriate compaction of the roadbed soil before AC patches can be placed.

4. Raveling if the asphalt mix was segregated during transportation and/or lay-down operation or if the asphalt content is low (a dry mix). The extent and severity of raveling will depend on the extent and degree of segregation.

5. Top-down cracking due to segregation and/or differential stiffness between the pavement layers. This scenario would happen if the rubblization procedure produces rubblized and fractured concrete sublayers (a soft layer sandwiched between two harder layers), or when the construction procedure causes temperature and/or particle segregations in the AC.

6. Top-down cracking if the rubblization procedure produces uneven surface between the rubblized and fractured concrete sublayers as shown in figures 7.1 and 7.2.

The first two defects are well understood and repeatedly observed in composite pavements. The third one is analogous to bearing capacity failure of the base material. The fourth one (raveling) is observed on all types of AC surfaced pavements and was also studied by various

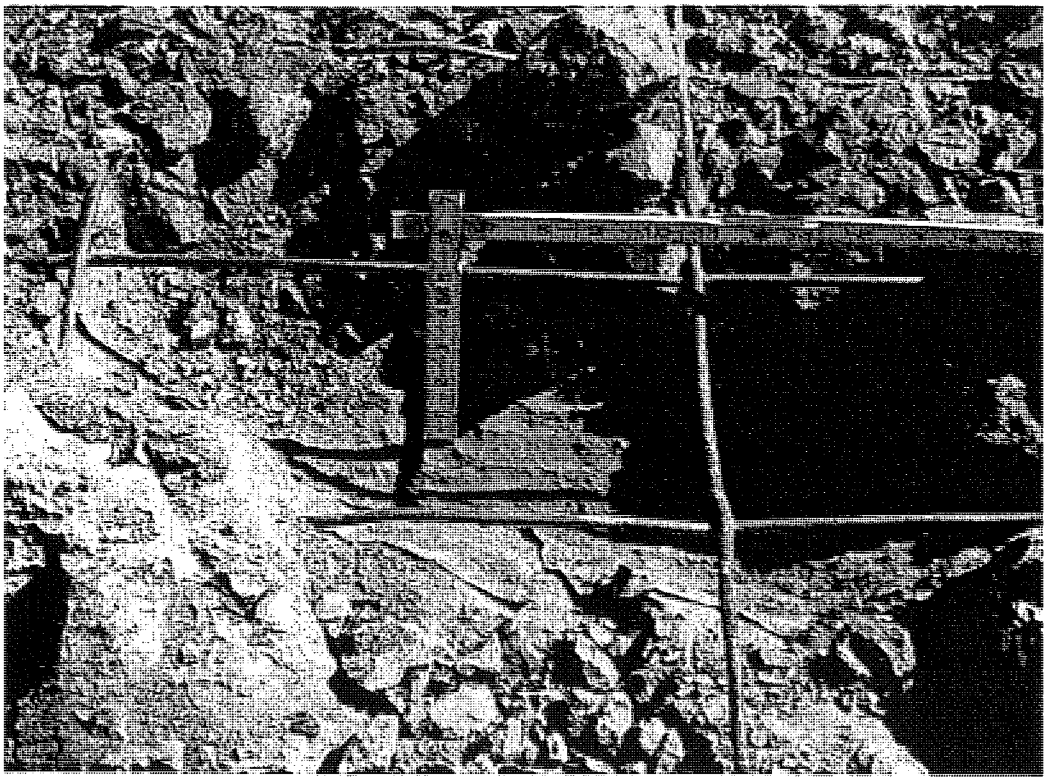

Figure 7.1 Excavated trench in a rubblized concrete slab showing the sand subbase and the fractured concrete

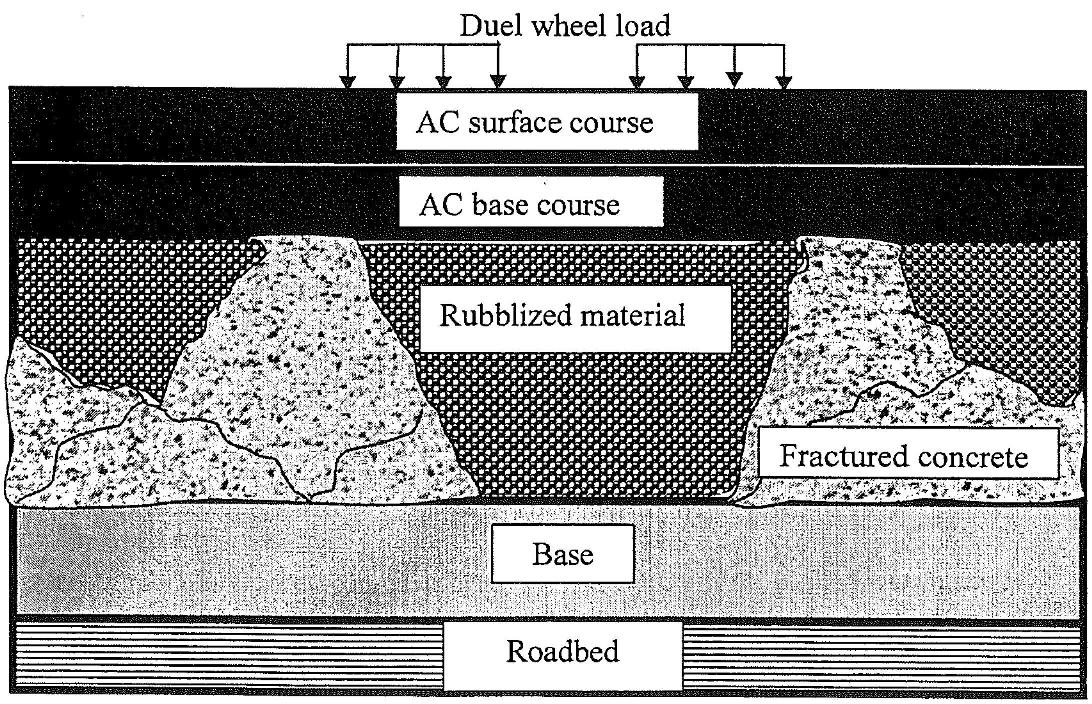

Figure 7.2 Schematic representation of the trench area of figure 7.1 after construction

researchers (see the segregation report submitted to MDOT by the PRCE). Finally, top-down cracking which has recently been reported as a dominant distress in flexible pavements and has been studied by few researchers (see Appendix K). Some stated that TDC are caused by aging of the AC mix, others by environmental conditions, and still others blamed the appearance of TDC on the increasing use of radial tires. Therefore, TDC deserve a special attention and detailed study. In this research study, mechanistic analyses of rubblized pavements were conducted to study the effects of various attributes on the TDC potential. The analyses were based on the following hypothesis:

The main cause of TDC is load-induced surface tensile stresses magnified by asphalt aging, differential stiffness between the pavement layers, segregation and environmental condition.

To verify the hypothesis and to analyze the factors affecting TDC potential, two and three dimensional mechanistic analyses were conducted and the results are presented and discussed in the next sections.

2.0 MECHANISTIC ANALYSIS

As stated above, two and three dimensional mechanistic analyses were conducted to calculate the maximum load-induced surface tensile stress. The analyses were conducted using the following computer programs:

1. CHEVRONX – The CHEVRONX program is a closed form solution of multilayer linear elastic systems. The program is capable of analyzing maximum of 5-layer systems and, for each layer; it requires the input of layer modulus, Poisson's ratio and thickness. In this analysis, the lower layer (the roadbed soil) is assumed to have an infinite extent

2. MICHPAVE – The MICHPAVE is a two-dimensional (2-D) finite element computer program capable of modeling the pavement structure as linear or nonlinear multilayer elastic systems. The linear model was used in this study.

3. ABAQUS – ABAQUS is a finite element computer program capable of modeling the pavement structure as linear or nonlinear multilayer elastic, viscoelastic or plastic systems in two and three dimensions (2-D and 3-D). The linear 3-D elastic system was used in this study.

The objectives of the mechanistic analyses include:

1. Calculate the magnitude and location of the maximum load-induced surface tensile stress and compare the results to field measurements.

2. Study the impact of variations in the thickness and moduli of the AC courses, rubblized materials and fractured concrete layers and variations in the moduli of base and roadbed soil on the maximum load-induced surface tensile stress.

3. Analyze the impact of the geometry of the interface between the rubblized materials and the fractured concrete layers on the load-induced surface tensile stress.

4. Assess the sensitivity of the maximum load-induced surface tensile stress to various rubblization and construction factors.

Based on the objectives and the capabilities of the three computer programs, two basic pavement models were used; they are presented in the next section.

3.0 PAVEMENT MODELS

Two basic pavement models were used in the mechanistic analysis of rubblized concrete pavements. The characteristics of the pavement (thicknesses and moduli) were varied to simulate various pavement cross-section and the effects of the environment and aging on the asphalt mix properties. The two models are detailed below.

1. Figure 7.3 shows two alternatives of the first rubblized pavement model. Both alternatives consist of five layer system as follows:

   Alternative one:

   - A 1.5-in. thick AC surface course.
   - A variable thickness AC base course
   - A 9-in. thick rubblized concrete slab.
   - A variable thickness aggregate base layer.
   - A roadbed soil.

   Alternative two:

   - A variable thickness AC layer.
   - A 4.5-in. thick rubblized material.
   - A 4.5-in. fractured concrete
   - A variable thickness aggregate base layer.
   - A roadbed soil.

   Since the 2-dimensional (2-D) CHEVRONX and MICHPAVE computer programs were used in the analysis of both models, the duel tire was simulated by a 9000-lb single wheel load. In addition, few cases were analyzed using the 2-D option of the ABAQUS computer program. This allowed comparison of the results of the three computer programs. The two alternatives of this pavement model are called the 2-D model.

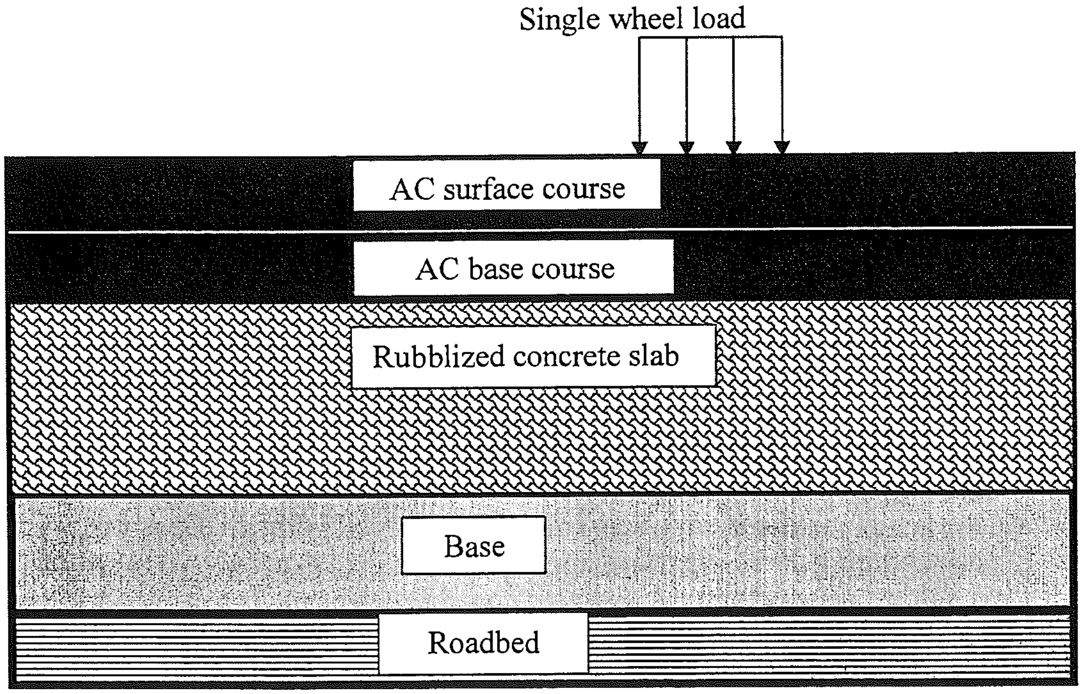

a) Rubblized pavement (2 AC courses and a rubblized concrete slab)

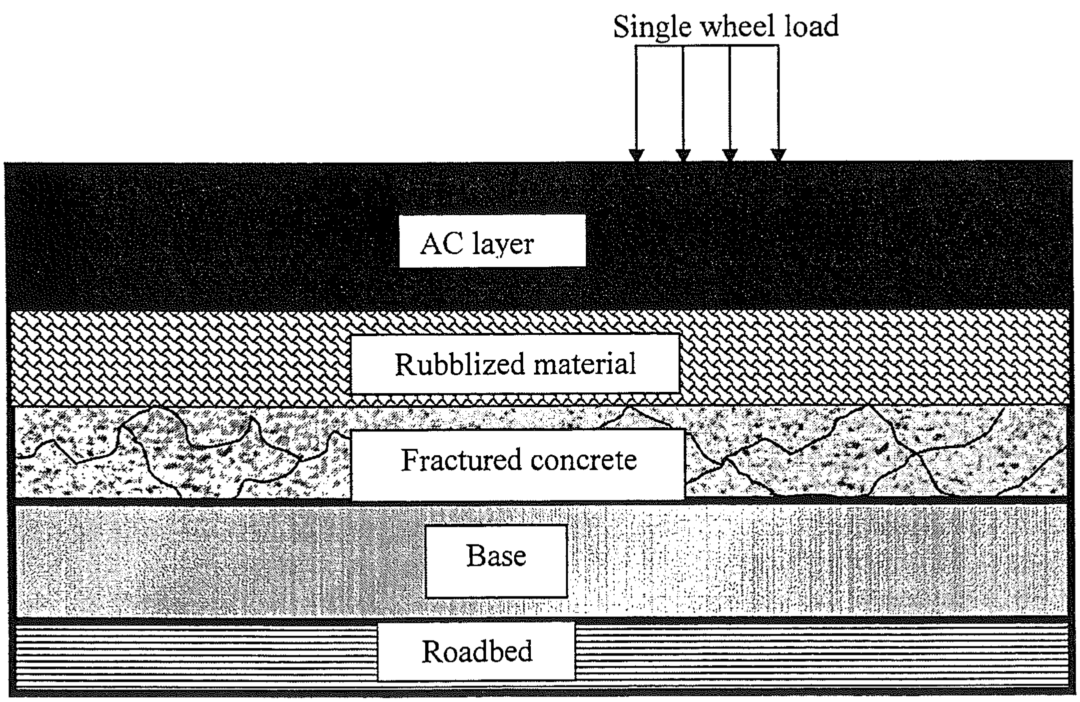

b) Rubblized pavement (an AC, rubblized material and fractured concrete layers)

Figure 7.3 Five layer rubblized pavement models

2. Also two alternatives were used in the second basic rubblized pavement model, uneven with variable geometry and even interface between the rubblized material and the fractured concrete layers as shown in figures 7.2 and 7.4. Both alternatives consist of 6-layer system as follows:

   - Variable AC surface course thickness.
   - Variable AC base course thickness
   - Variable rubblized material thickness.
   - Variable fractured concrete thickness
   - Variable aggregate base layer thickness.
   - A roadbed soil.

   The actual layer thicknesses used in each analysis were the same as the pavement section being analyzed. For example, in the analysis of the rubblized pavement sections along I-75, I-69 and M-37, the actual measured layer thicknesses were used in the analysis. Nevertheless, this 3-D model was used to simulate dual wheel load and the actual rubblized pavement condition observed in the trenches that were excavated during the rubblization operation. This includes the variable thicknesses of the rubblized material and the fractured concrete layers and the various geometry of their interface. The pavement was subjected to a 9000-lb dual wheel load and only the 3-D finite element program, ABAQUS, was used in this analysis. Hence, the model is called the 3-D model.

The main reason for conducting analyses of the two models is to compare the results (the load-induced stresses and strains) obtained from both models. If no significant differences are found, then one can use the first model, which is much simpler, easier to use and less time consuming than the analyses of the second model, which require 3-D type analyses.

Results of the analyses of the two rubblized pavement models and the steps that need to be taken to minimize the TDC potential are presented and discussed in the remaining sections of this chapter.

4.0 MECHANISTIC ANALYSIS USING THE 2-D MODEL

As noted above, due to limitation of the CHEVRONX program, each alternative of the 2-D model consists of 5 layer system as shown in figure 7.3. In the first alternative, the effects of differential stiffness between the AC courses due to aging and/or temperature on the maximum surface tensile stress were analyzed. In the second alternative, the effects of differential stiffness between the rubblized material and the fractured concrete layers on the maximum surface tensile stress were analyzed. In both alternatives, the standard 18-kip single axle load was simulated using a 9000-lb single wheel load having a tire pressure of 100 psi and uniform circular contact area with 5.781-in. radius. In the analysis, the pavement cross-section (layer thicknesses) and the layer properties (modulus) were varied to simulate the actual field condition and the results obtained from the backcalculation.

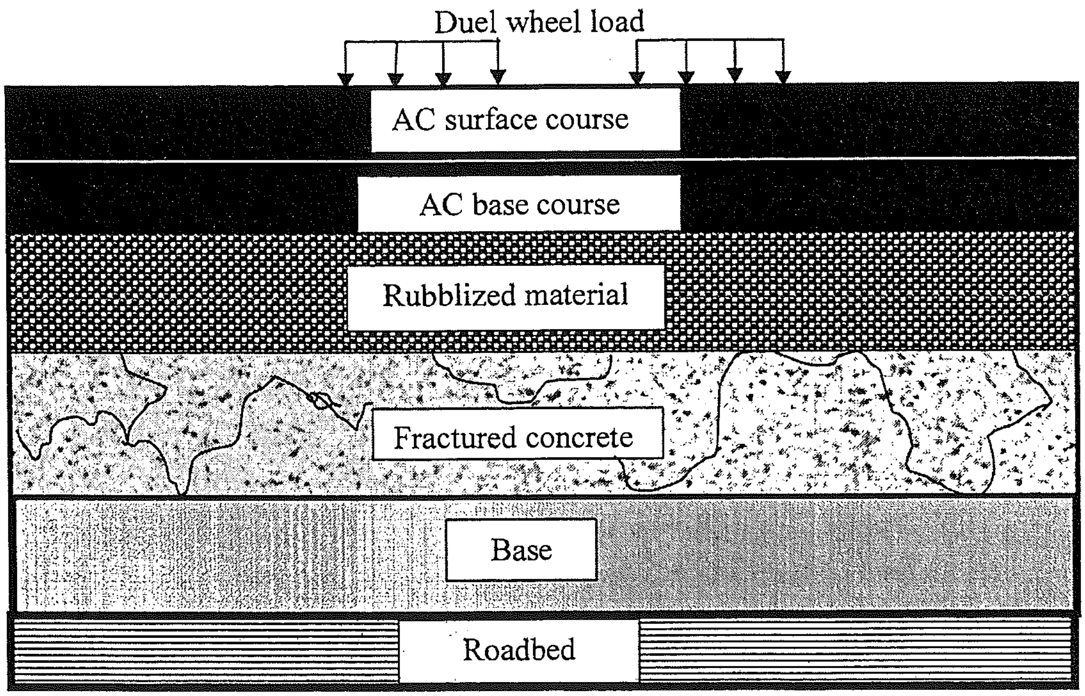

Figure 7.4 Six layer Rubblized pavement model with even interface

Table 7.1 provides a summary of the pavement cross-sections and material properties used in the analysis. As can be seen from the table, the layer thicknesses and engineering properties used in the analysis are:

1. One AC surface course thickness of 1.5 in. and three AC base course thickness of 1.5, 4.5, and 7.5 in. The two courses make the total AC thickness of 3, 6 and 9 in. This represents the spectrum of AC thicknesses used by MDOT. Results of the analysis were used to study the effect of the AC layer thickness on the maximum surface tensile stress.

2. A rubblized concrete thickness or base layer of 9 in.

3. A sand subbase layer thickness of 18 in.

4. The above thicknesses make the total pavement thickness of 30, 33, and 36 in. Such pavement thickness provides frost protection of the roadbed soil as per MDOT specifications.

5. Elastic moduli of the AC surface course of 50, 100, 150, 300, 450, 600, 1200 and 2400 ksi

6. Elastic moduli of the AC base course of 50, 75, 150, 300, 450, 600, 1200, and 2400 ksi.

7. Elastic moduli of the rubblized concrete slab or base layer of 30, 100, 500 and 2000 ksi.

8. An elastic modulus of the sand subbase of 20 ksi.

9. An elastic modulus of the roadbed soil of 5 ksi.

The variation in the AC modulus was thought to reflect different AC mix used by MDOT, to simulate aging (harder AC surface course) and the effect of temperature and differences in temperature (gradients) within the AC layer. The temperature simulation represents the following environmental conditions

1. Constant temperature throughout the AC layer.

2. Cooling cycle (night time and/or abrupt cold wave) where the AC surface course is colder than the AC base course (negative temperature gradient).

3. Heating cycle (day time and/or abrupt heat wave) where the AC surface course is hotter than the AC base course (positive temperature gradient).

The variation in the rubblized concrete slab or base layer modulus was set to serve two functions:

Table 7.1 Layer thicknesses and properties of the pavement models used in mechanistic analyses using the CHEVRONX and the MICHPAVE computer programs

Rubblized pavement cross-section and engineering properties			
Layer	Thickness (in.)	Elastic modulus (ksi)	Poisson's ratio
AC surface course	1.5	50, 100, 150, 300, 450, 600, 1200, 2400	0.3
AC base course	1.5, 4.5, 7.5	50, 75, 150, 300, 450, 600, 1200, 2400	0.3
Total AC thickness	3, 6, 9		0.3
Base/Rubblized concrete slab	9	30, 100, 500, 2000	0.25
Subbase	18	20	0.4
Roadbed soil		5	0.45

1. To simulate the actual condition of the rubblized pavement observed in the trenches. Hence, an elastic modulus of 30 ksi represents a full-depth rubblized concrete slab. Whereas the 2000 ksi modulus represents a full depth fractured concrete resulting from a poor rubblization process. Hence, studying the effects of variation in the base modulus is analogous to studying the effect of the quality of the rubblization process.

2. To simulate the various base layer materials used by MDOT in conventional flexible pavements. For example, the 30 ksi modulus represents a conventional aggregate base, while a 100 ksi modulus represents a stabilized base layer.

Finally, note that the range of the rubblized concrete modulus used in this study was designed to cover the range of moduli of the rubblized concrete slab that was obtained from the backcalculation of layer moduli (see table 5.13 of chapter 5, which is repeated here as table 7.2 for convenience). Further, given the range of layer moduli used in the mechanistic analyses, the results are applicable to both conventional flexible and rubblized pavements.

4.1 Results of Mechanistic Analyses of the 2-D Model

Tables 7.3 through 7.6 and figures 7.5 through 7.9 provide lists and plots of the results of the mechanistic analysis that were obtained from the CHEVRONX and the MICHPAVE computer programs. Examination of figures 7.5 through 7.9 and the data listed in the tables indicates that:

1. For the majority of the cases, both computer programs produce similar results relative to the magnitudes and locations of the maximum surface tensile stresses. Figure 7.5 illustrates a general relationship between the load-induced surface radial stress and the radial distance form the centre of load. As can be seen from the figure, the surface radial stresses can be divided into three zones

   - A high compression zone under the tire
   - A high tension zone around the edge of the tire
   - Low magnitudes compression and/or tension zones further away from the tire

   As it was expected, the magnitudes and locations of the surface radial stresses for each zone vary from one pavement to the other depending on the pavement cross section and the material properties (elastic modulus and Poisson's ratio) of each pavement layer. The magnitudes of the maximum surface tensile stresses for the three pavement sections are listed in tables 7.3, 7.5 and 7.6. For illustrative purposes, the locations of said stress for only one pavement section (total AC thickness of 6 in.) are provided in table 7.4. Note that the locations of the maximum surface tensile stress relative to the center of the loaded area reported in table 7.4 are very close to the field measured distances of the top-down cracks from the center of the wheel paths.

Table 7.2 Backcalculated and estimated pavement layer moduli of 18 rubblized pavements at the indicated test sites

Test site	No of FWD stations			Backcalculated moduli (ksi)					Estimated moduli (ksi)	
	Total	Converged	Accepted	AC	TCAC	RCS	Base	Roadbed soil	Rubblized material	Fractured concrete
10692-11	40	40	39	317	534	122	25	14	65	256
10692-12	40	40	40	295	573	159	29	17	73	352
10753-11	42	39	34	1,732	1,297	225		17	27	704
10753-12	43	31	20	2,104	1,701	182		19	14	600
11941-21	36	36	27	1,567	1,468	225	44	23	201	360
11941-22	43	42	20	1,247	1,500	182	37	21	144	322
20102-11	40	40	39	710	1,640	61	27	16	44	119
20102-12	40	40	35	517	1,657	46	23	16	31	92
20233-11	52	51	51	433	1,484	50	34	10	15	135
20233-12	26	26	25	150	743	114	29	9	46	287
20273-21	45	41	35	1,891	2,285	117	36	21	24	350
20273-31	40	40	29	470	936	55	17	13	36	109
20273-41	40	39	31	237	608	1,064	50	22	297	2,774
20311-11	40	40	35	637	1,620	414	40	22	191	949
30153-11	43	42	31	2,364	2,165	71	37	20	28	183
30373-51	40	40	35	411	1,192	275	31	16	179	561
30373-52	40	39	38	392	1,407	134	25	15	67	307
30373-61	33	26	17	2,126	2,337	234	38	16	90	592
Minimum				150	534	46	17	9	14	92
Maximum				2,364	2,337	1,064	50	23	297	2,774

TCAC = Temperature corrected asphalt concrete, RCS = Rubblized concrete slab

Table 7.3 Magnitudes of the maximum surface tensile stresses for pavements with different AC surface and base moduli

Modulus Ratio	Maximum surface tensile stress (psi)							
	Base Modulus 30 ksi		Base Modulus 100 ksi		Base Modulus 500 ksi		Base Modulus 2000 ksi	
	MICHPAVE	CHEVRONXX	MICHPAVE	CHEVRONXX	MICHPAVE	CHEVRONXX	MICHPAVE	CHEVRONX
0.7	2.3	16.5	8.0	24.5	13.2	30.5	17.2	35.0
1.3	3.1	4.8	6.9	15.9	14.3	26.0	21.2	35.5
2.0	3.7	1.8	8.3	10.1	17.3	24.2	26.4	35.0
4.0	10.7	8.0	16.4	13.4	26.5	23.2	39.4	35.7
6.0	18.8	14.8	24.7	19.6	35.2	30.4	50.7	45.4
8.0	26.3	21.3	32.4	26.9	43.8	36.6	60.4	53.2
16.0	50.2	43.9	57.5	49.3	70.3	58.5	90.2	76.3
32.0	79.7	71.7	87.2	77.1	103.8	86.3	128.2	107.7

Table 7.4 Locations of the maximum surface tensile stresses for pavements with different AC surface and base moduli

Modulus Ratio	Distance from center of load (in.)							
	Base Modulus 30 ksi		Base Modulus 100 ksi		Base Modulus 500 ksi		Base Modulus 2000 ksi	
	MICHPAVE	CHEVRONX	MICHPAVE	CHEVRONX	MICHPAVE	CHEVRONX	MICHPAVE	CHEVRONX
0.7	14.9	5.7	6.1	5.7	6.1	5.7	6.1	5.7
1.3	15.7	5.6	6.6	5.6	6.4	5.7	6.4	5.7
2.0	15.7	15.7	6.9	5.6	6.6	5.7	6.5	5.7
4.0	8.3	7.8	7.4	7.0	6.9	6.9	6.9	6.9
6.0	8.4	7.9	7.6	7.7	7.3	6.9	7.0	6.9
8.0	8.6	8.7	7.8	7.8	7.4	7.0	7.3	7.0
16.0	9.2	8.8	8.3	7.9	7.8	7.8	7.7	7.7
32.0	10.4	10.1	9.0	8.8	8.3	7.9	8.2	7.9

Table 7.5 Magnitudes of the maximum surface tensile stresses of rubblized pavements (base modulus = 100 ksi) with different AC surface moduli and AC thickness

Modulus Ratio	Max. radial tensile stress(psi)					
	3-in. AC layer		6-in. AC layer		9-in. AC layer	
	MICHPAVE	CHEVRONX	MICHPAVE	CHEVRONX	MICHPAVE	CHEVRONX
0.7	3.6	20.3	8.0	24.5	9.3	26.2
1.3	2.9	10.5	6.9	15.9	10.0	19.5
2.0	4.0	2.8	8.3	10.1	12.4	14.5
4.0	6.3	3.0	16.4	13.4	22.2	18.8
6.0	9.7	5.6	24.7	19.6	31.6	26.2
8.0	15.6	11.1	32.4	26.9	40.5	34.3
16.0	35.2	28.8	57.5	49.3	67.8	58.6
32.0	59.4	51.3	87.2	77.1	100.9	89.4

Table 7.6 Magnitudes of the maximum surface tensile stresses for conventional flexible pavements (base modulus = 30 ksi) with different AC surface moduli and AC thickness

Modulus Ratio	Max. radial tensile stress(psi)					
	3-in. AC layer		6-in. AC layer		9-in. AC layer	
	MICHPAVE	CHEVRONX	MICHPAVE	CHEVRONX	MICHPAVE	CHEVRONX
0.7	5.9	15.5	2.3	16.5	4.5	20.5
1.3	10.4	9.4	3.1	4.8	2.9	10.1
2.0	14.8	13.1	3.7	1.8	4.3	3.4
4.0	28.2	25.1	10.7	8.0	12.1	9.0
6.0	40.2	36.4	18.8	14.8	20.1	16.3
8.0	50.7	46.2	26.3	21.3	27.4	22.9
16.0	81.3	74.6	50.2	43.9	51.0	43.6
32.0	116.0	109.4	79.7	71.7	79.3	70.4

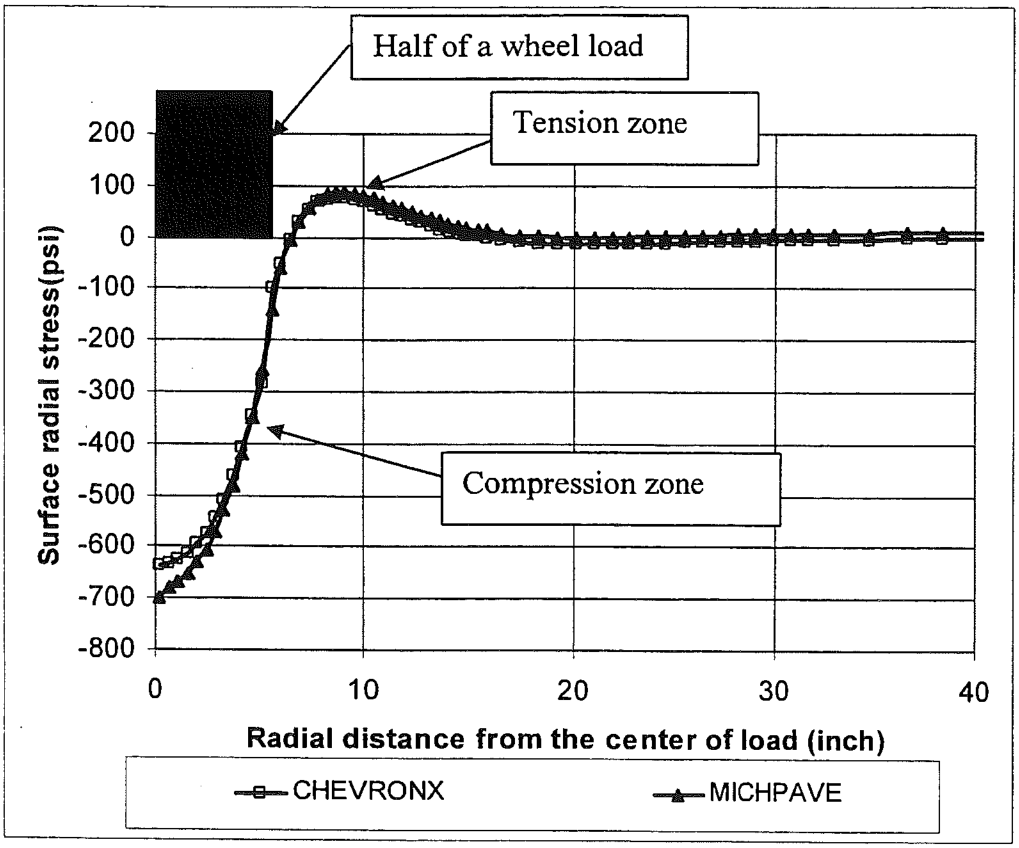

Figure 7.5 Surface radial stresses at various distances from the center of the load

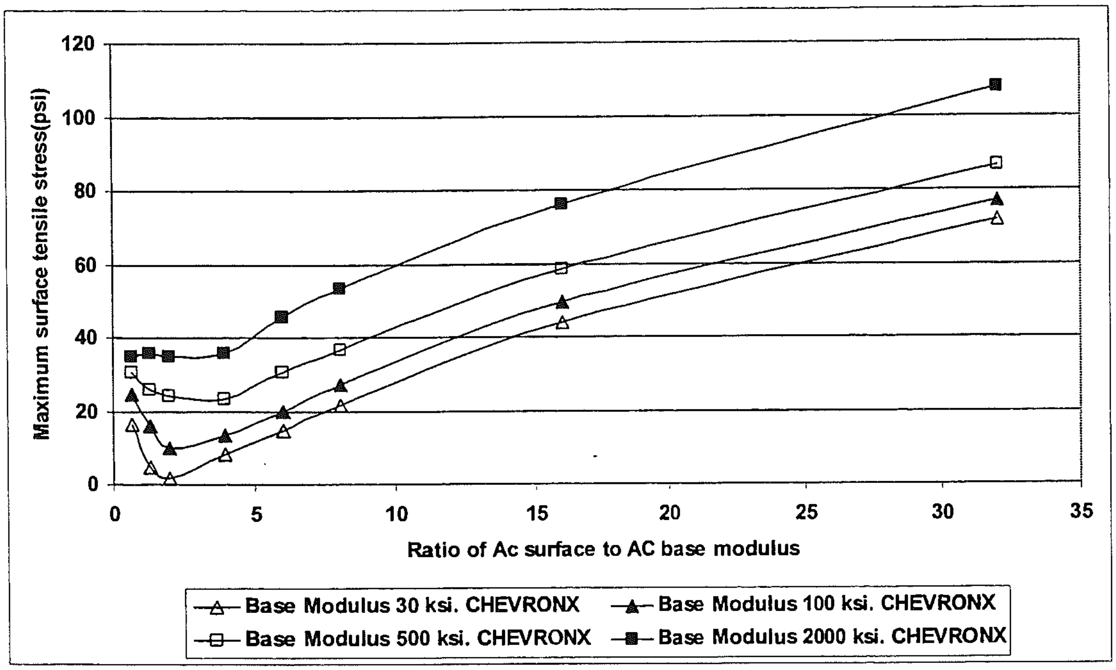

a) Results from CHEVRONX

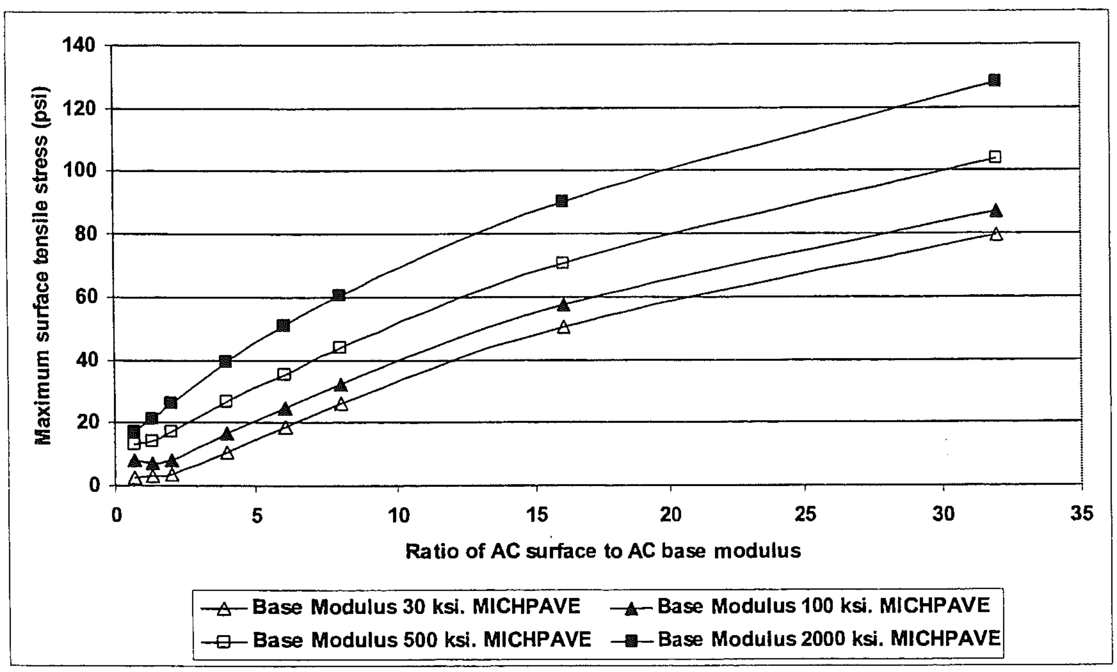

b) Results from MICHPAVE

Figure 7.6 The maximum surface tensile stress for different values of the base modulus as a function of the ratio of the AC surface to the AC base moduli

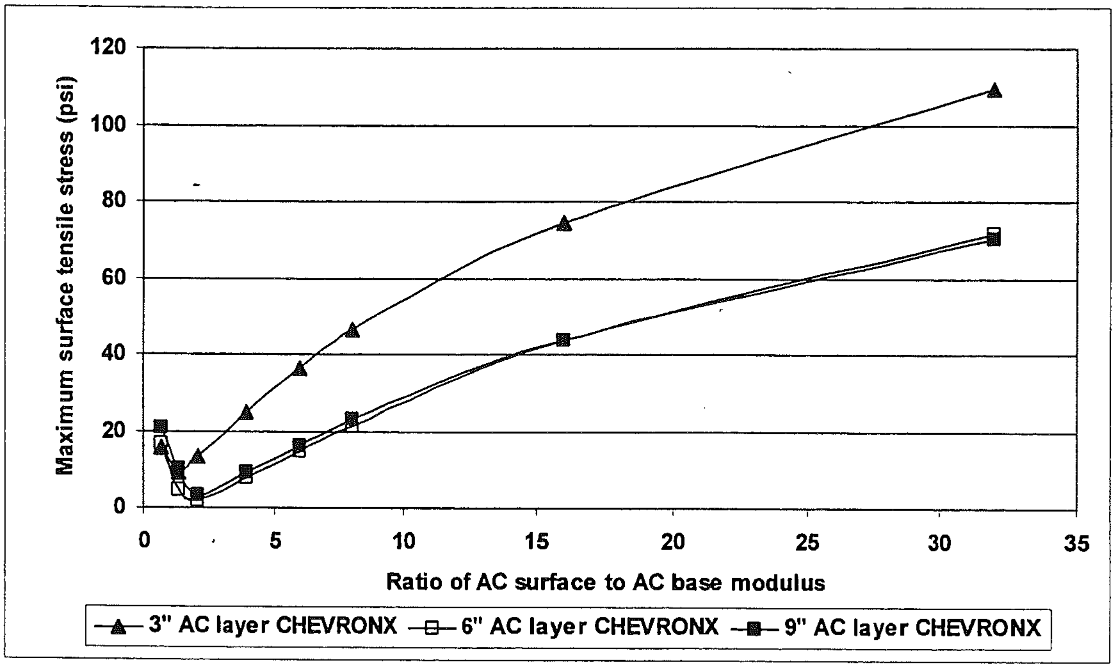

a) Results from CHEVRONX

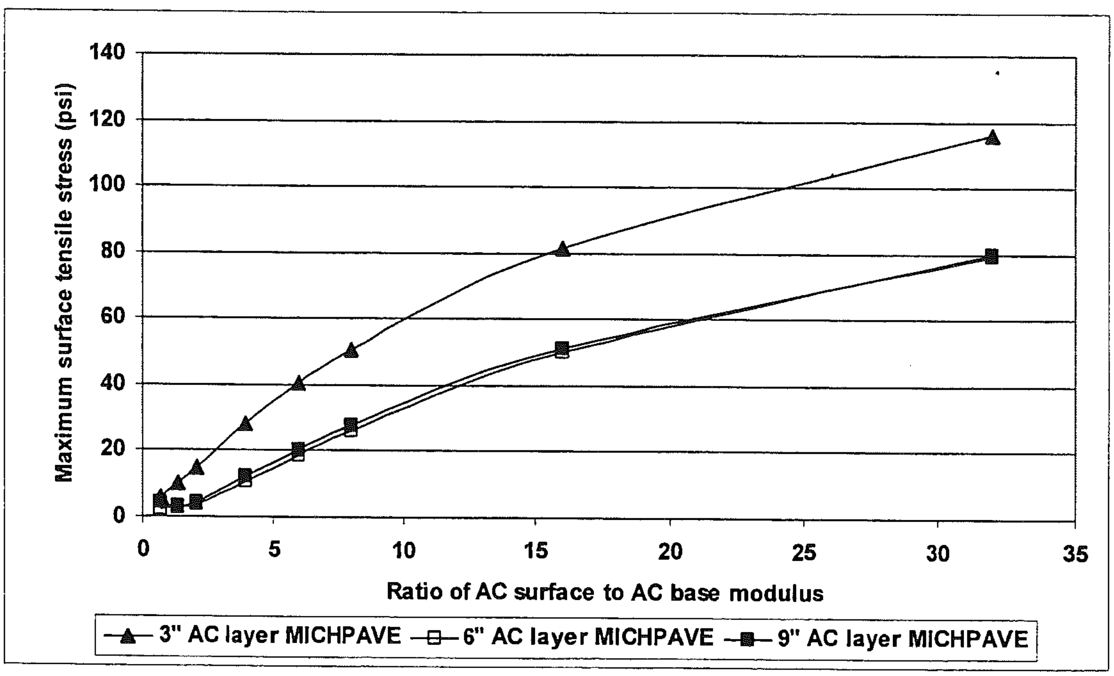

b) Results from MICHPAVE

Figure 7.7 The maximum surface tensile stress in conventional flexible pavements (base modulus = 30 ksi) with different AC layer thickness as a function of the ratio of the AC surface to the AC base moduli

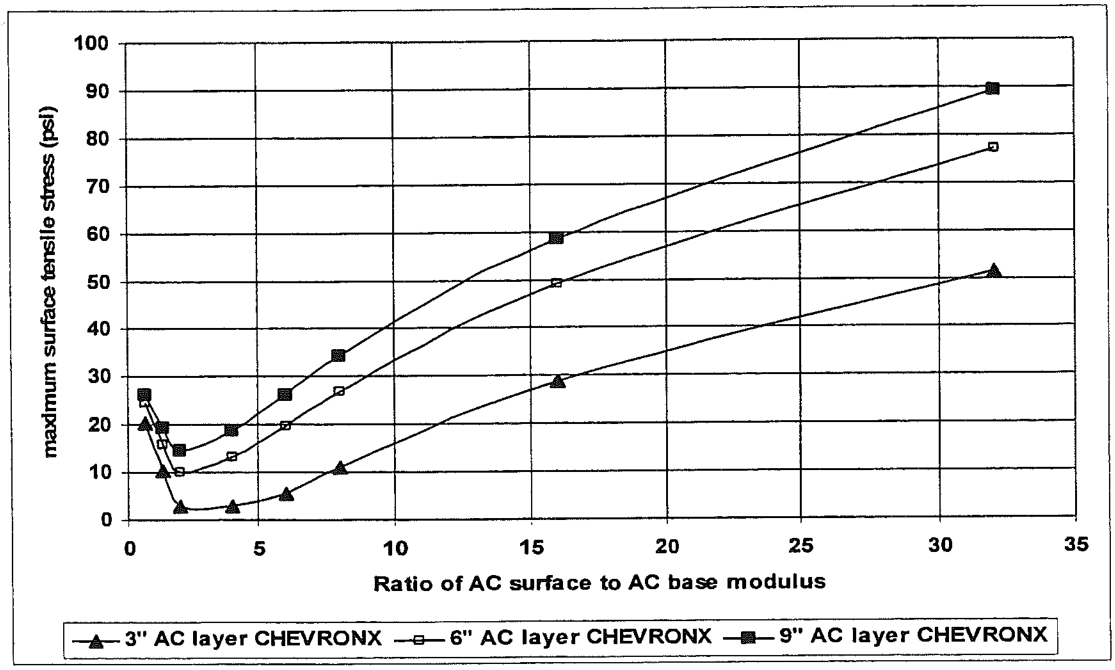

a) Results from CHEVRONX

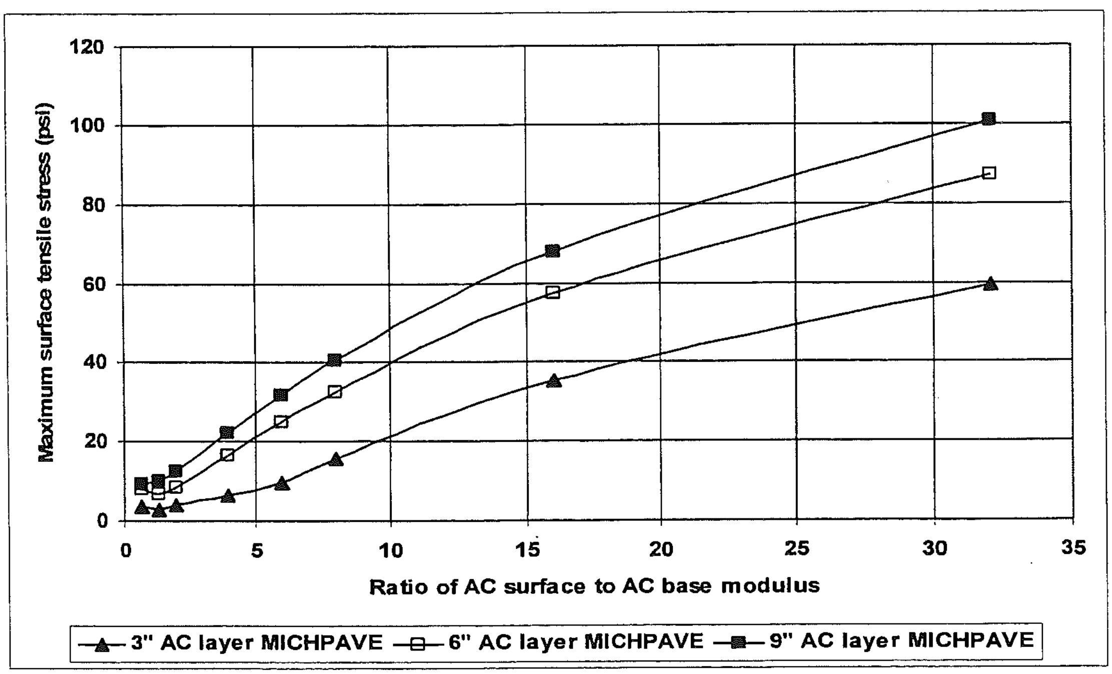

b) Results from MICHPAVE

Figure 7.8 The maximum surface tensile stress on rubblized pavements (base modulus = 100 ksi) with different AC layer thickness as a function of the ratio of the AC surface course to the AC base course moduli

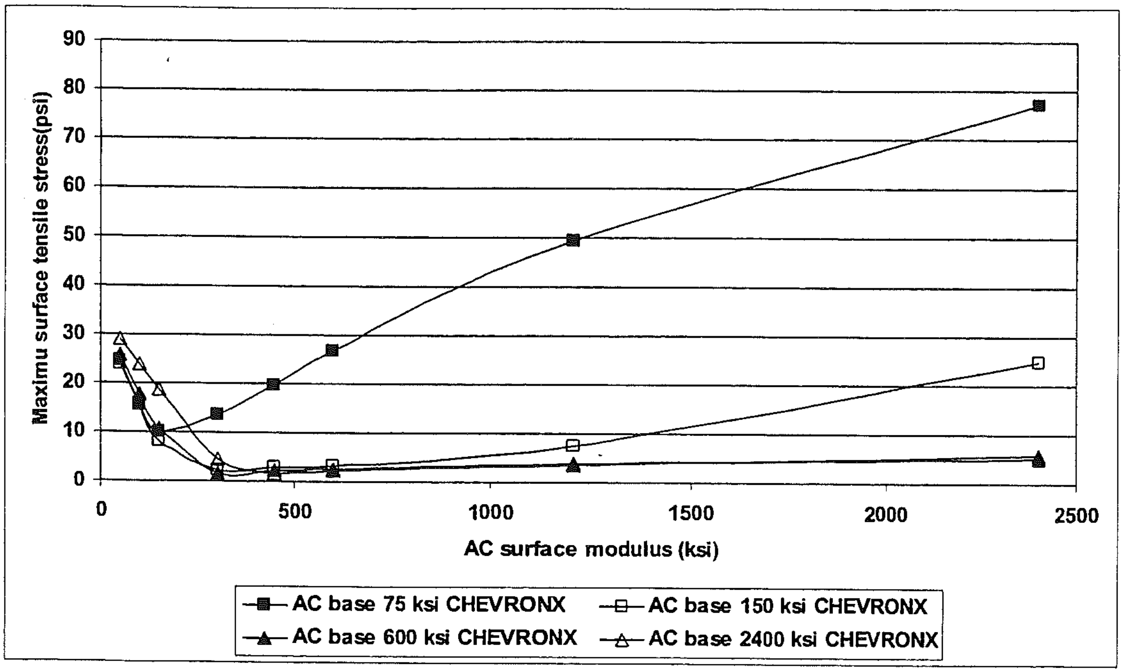

a) Results from CHEVRONX

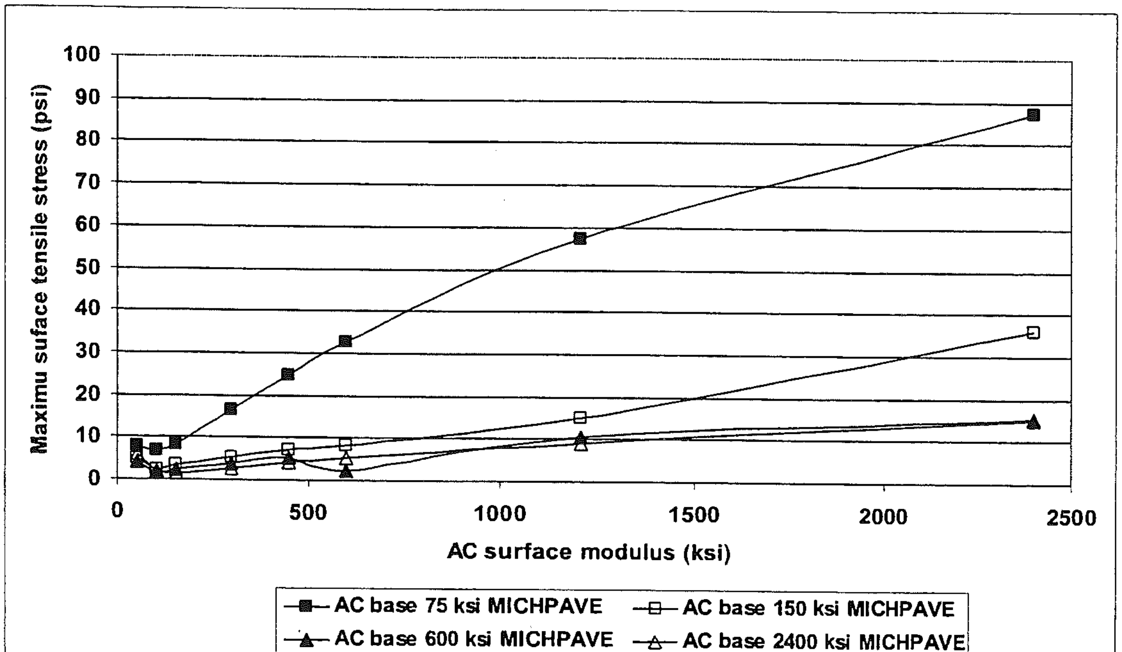

b) Results from MICHPAVE

Figure 7.9 The maximum surface tensile stress on rubblized pavements (base modulus =100 ksi) for different AC base course modulus as a function of the AC surface course modulus

2. Figure 7.6 shows that higher ratios of AC surface to AC base moduli cause higher surface tensile stresses. The high modulus of the AC surface course could be caused by many variables including temperature and age hardening. For example, night time, the temperature of the AC surface course is typically lower than that of the AC base course (a negative temperature gradient); hence, the modulus of the surface course is higher than that of the AC base course. Therefore pavements with higher AC surface modulus due to aging or temperature would have higher TDC potential. This finding supports those reported by Gerritsen et al (1), Wambura et al (2) and Duzauts and Rampal (3), (see Appendix K). The modulus ratio problem could be partially resolved by establishing a balanced asphalt mix design. For example, the asphalt mixes for the AC leveling and base courses could be designed to have higher modulus values than that of the AC mix designed for the surface course. When the pavement is subjected to a negative temperature gradient (lower temperature at the surface of the pavement) the modulus of the AC base course would not be much lower than the modulus of the AC surface course.

3. Two other points can also be deduced by the examination of figure 7.6 as follows:

    b) Higher modulus values of the base layer cause higher surface tensile stress. This is because the combination of a stiff base modulus, a stiff AC surface course modulus and a soft AC base course modulus create what is called a "sandwich model." A soft layer in the middle bordered by two stiff layers. Such a stiff-soft-stiff layer system causes high surface tensile stress.
    c) When the ratio of the AC surface to AC base courses moduli are less than two, the effect of the modulus of the base layer is minimized since the differential stiffness between the AC surface, AC base and the base layer are not high.

4. It can be seen from figures 7.7 and 7.8 that, as was expected, for flexible and rubblized pavements, the thickness of the AC layer has significant effect on the magnitude of the surface tensile stress. In conventional flexible or in full-depth rubblized pavements (figure 7.7) where the base modulus is 30 ksi, increasing AC thickness causes a decrease in the surface tensile stresses. For partial-depth rubblized pavements or for pavements with a stabilized base (figure 7.8) where the modulus of the base layer is 100 ksi, the scenario is reversed and higher AC thickness causes higher surface tensile stress. Note that for all AC layer thicknesses, the thickness of the AC surface course was kept constant at 1.5 in. while the thickness of the AC base course was changed. These findings contradict those reported by Matsuno and Nishizawa (4) and partially support the findings of Uhlmeyer et al (5). However, field observations made during this study indicate that pavements with AC thickness of 4.5 in. or more exhibit TDC, which contradicts the observations of Uhlmeyer et al, that TDC tend to occur in pavements with AC thicknesses of greater than 16 cm (6.3 in.). The crucial point herein is that, in order to minimize the effect of the AC thickness on TDC potential, the ratio of the AC surface to AC base moduli should be less than two. This is the same conclusion as the one stated in the previous paragraph.

5. The data in tables 7.3 through 7.6 and figures 7.5 through 7.9 indicate that all significantly high maximum surface tensile stresses occur between the edge of the tire and 1-ft from the edge of the tire. This finding is supported by field observations of the locations of TDC (see figures 7.19 and 7.20).

4.2 Verification of the Results of the Mechanistic Analysis Using the ABAQUS Program

The CHEVRONX (a close form solution), the MICHPAVE (a 2-D FEM) and the ABAQUS (a 3-D FEM) computer programs were used to analyze a pavement section. The one set of layer thicknesses and the three sets of material properties used in the analyses are listed in table 7.7 under the headings case 1, case 2 and case 3. Results of the analyses are listed in table 7.8. Figure 7.10 depicts three plots of the surface radial stresses obtained from the analysis of case 1 using the three programs. As can be seen from table 7.8 and figure 7.10, the results of the analysis using the ABAQUS program agree very well with the results from the CHEVRONX and the MICHPAVE computer programs. For all three cases, the programs give almost the same magnitudes and locations of the maximum surface tensile stresses. Based on these findings, it was concluded that the results of the 3-D analyses are accurate and comparable to those obtained from the other two programs. Therefore, 3-D analyses of rubblized pavement sections were conducted using the ABAQUS program and the results are discussed in the next section

5.0 MECHANISTIC ANALYSIS USING THE 3-D MODEL AND A DUAL-WHEEL LOAD

The objectives of the 3-D analyses of rubblized pavements using the ABAQUS program are to:

1. Evaluate the effect of the geometry of the interface between the rubblized and the fractured concrete layers on the maximum load-induced surface tensile stresses (TDC potential).

2. Analyze the effect of different differences in temperature within the AC layer on the maximum load-induced surface tensile stress on rubblized pavements with uneven interface between the rubblized and the fractured concrete layers

To accomplish the above objectives, Five3-D finite element models representing rubblized pavement structures were designed and are depicted in figures 7.11 through 7.15. The dimensions of each model were 150 in. in width and length and 100 in. in depth. Due to limitation in the storage capacity of the computer system, the full model was divided along two symmetrical planes into four symmetrical quarters. The dimensions of each quarter were 75 in. in width and length and 100 in. in depth. In all five models, the second tire of the duel wheel is on the right hand side of the figure (the right-hand side mirror image of the figure). In all analyses, the following inputs were used:

Table 7.7 Layer thicknesses and properties of the pavement models used in mechanistic analyses using the CHEVRONX, the MICHPAVE and ABAQUS computer programs

Layers	Thickness (in.)	Elastic modulus (ksi)			Poisson's ratio
		Case 1	Case 2	Case 3	
AC surface	1.5	2,400	1,200	1,200	0.30
AC base	4.5	75	75	150	0.30
Base	9.0	100	100	500	0.25
Subbase	18.0	20	20	20	0.40
Roadbed	67.0	5	5	5	0.45

Table 7.8 Comparison of results of mechanistic analyses using the CHEVRONX, the MICHPAVE and ABAQUS computer programs

	Maximum radial tensile stress	
	Magnitude (psi)	Distance from the center of loaded area (in.)
Case 1		
CHEVRONX	77.0	8.7
ABAQUS	79.6	8.8
MICHPAVE	87.5	9.1
Case 2		
CHEVRONX	49.1	7.8
ABAQUS	52.3	8.0
MICHPAVE	57.8	8.3
Case 3		
CHEVRONX	16.1	6.9
ABAQUS	19.0	7.5
MICHPAVE	29.1	7.4

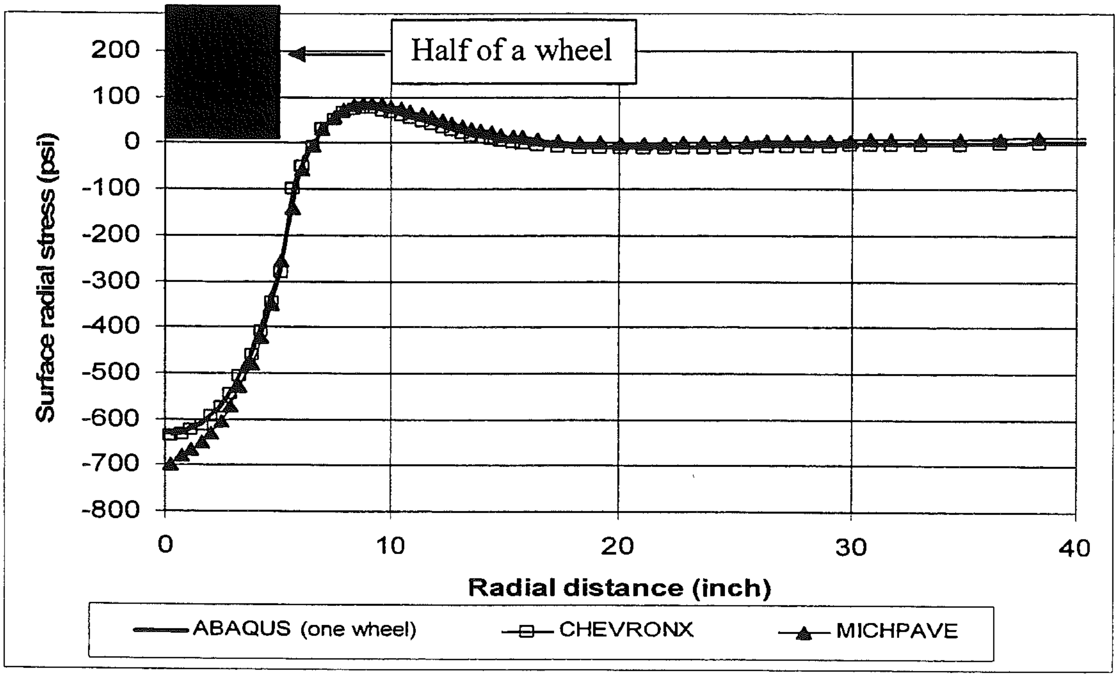

a) Overall view of the three stress zones

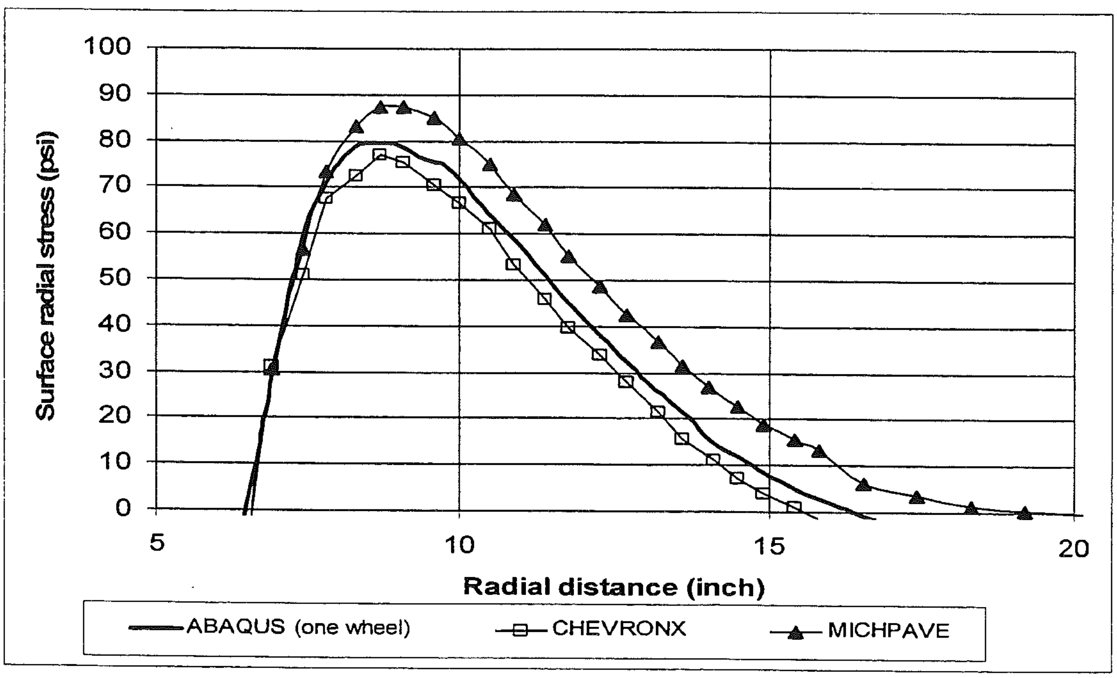

b) Close-up view of the surface tension zone

Figure 7.10 Results of mechanistic analyses of a rubblized pavement subjected to a single-wheel load using CHEVRONX, MICHPAVE and ABAQUS programs

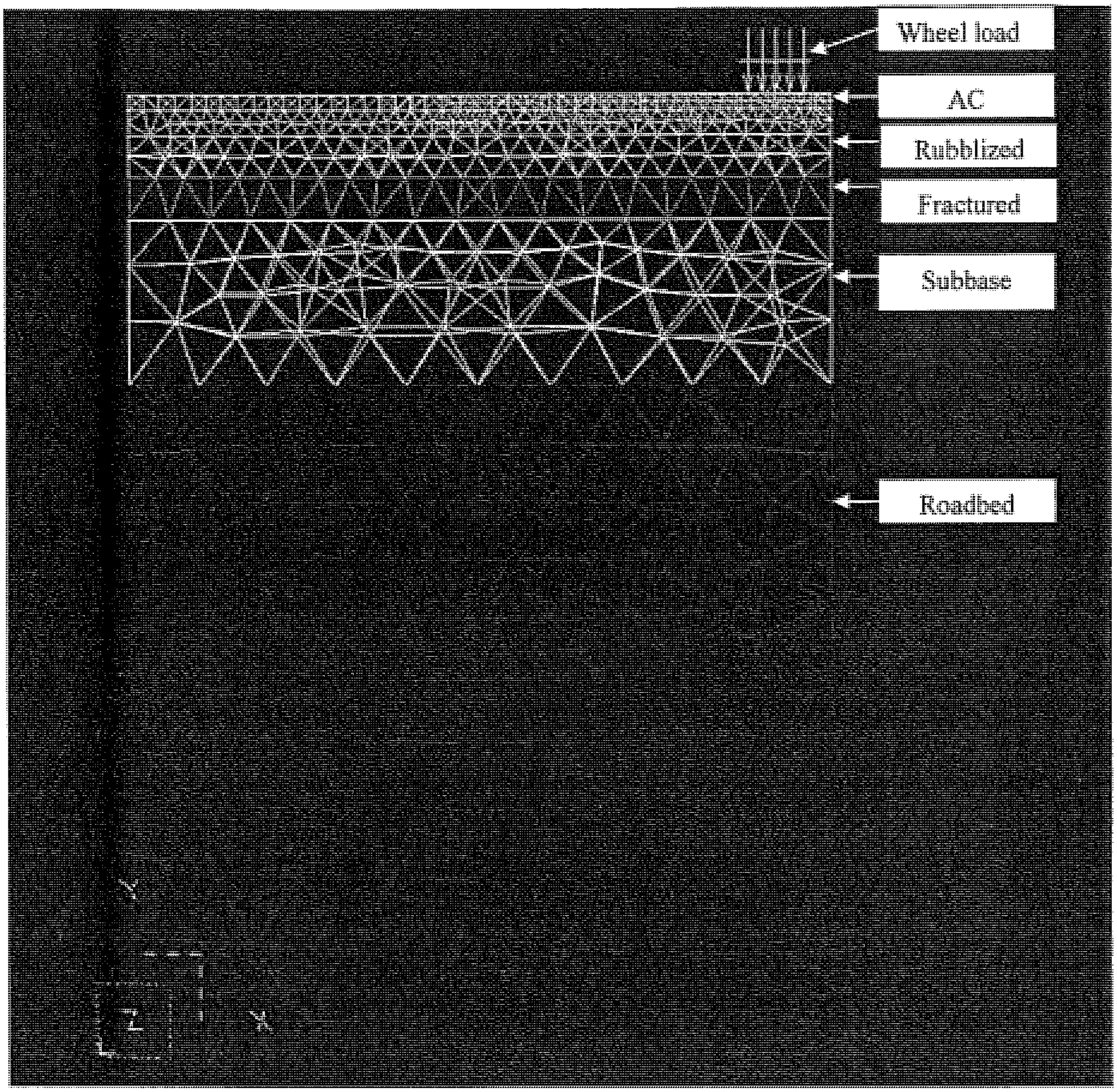

Figure 7.11 The first 3-D model 1 with even interface and equal thickness (4.5 in.) between the rubblized material and the fractured concrete layers

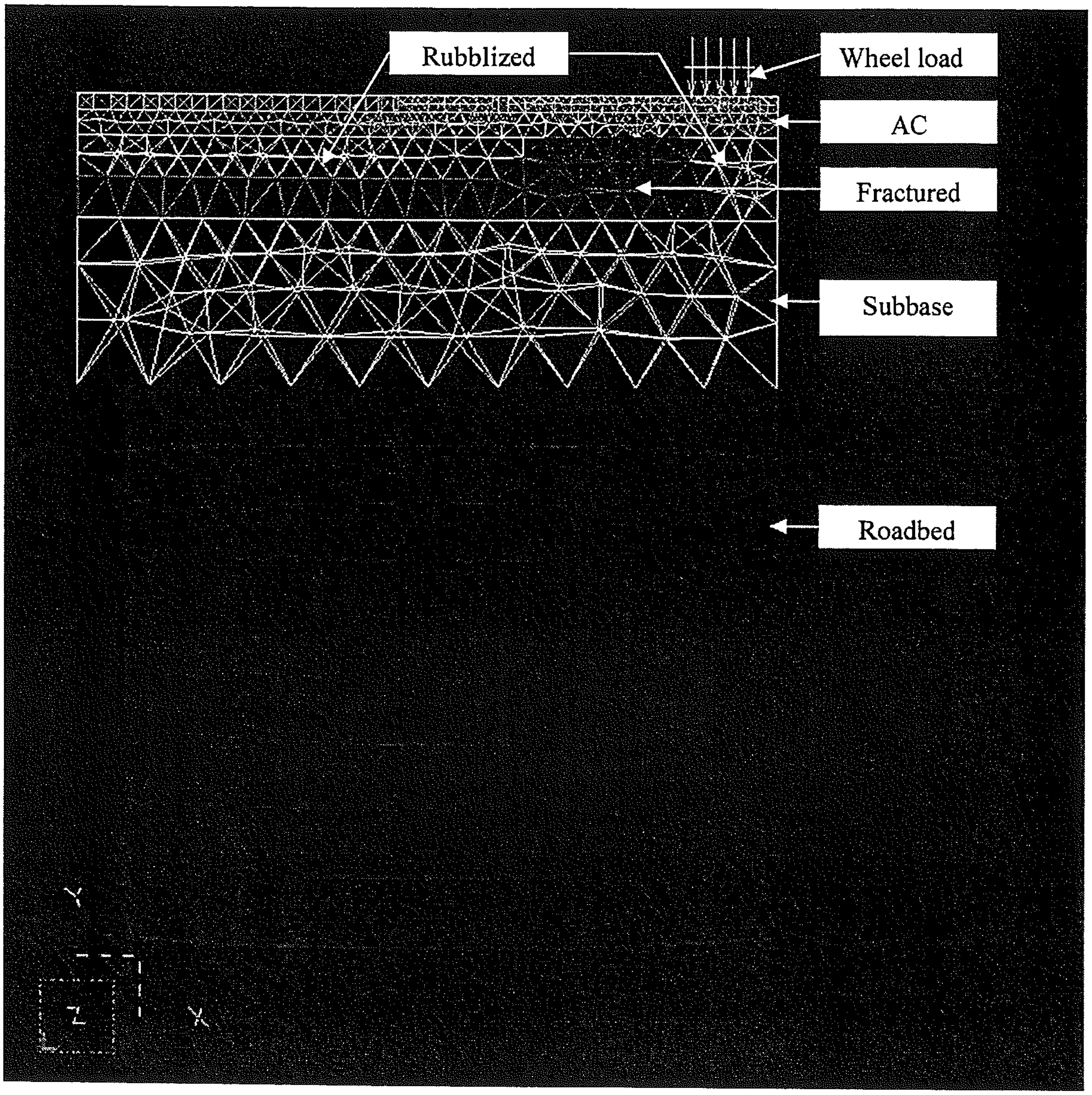

Figure 7.12 The second 3-D model with uneven interface between the rubblized material and the fractured concrete layers and the absence of the fractured concrete layer under the dual-wheel

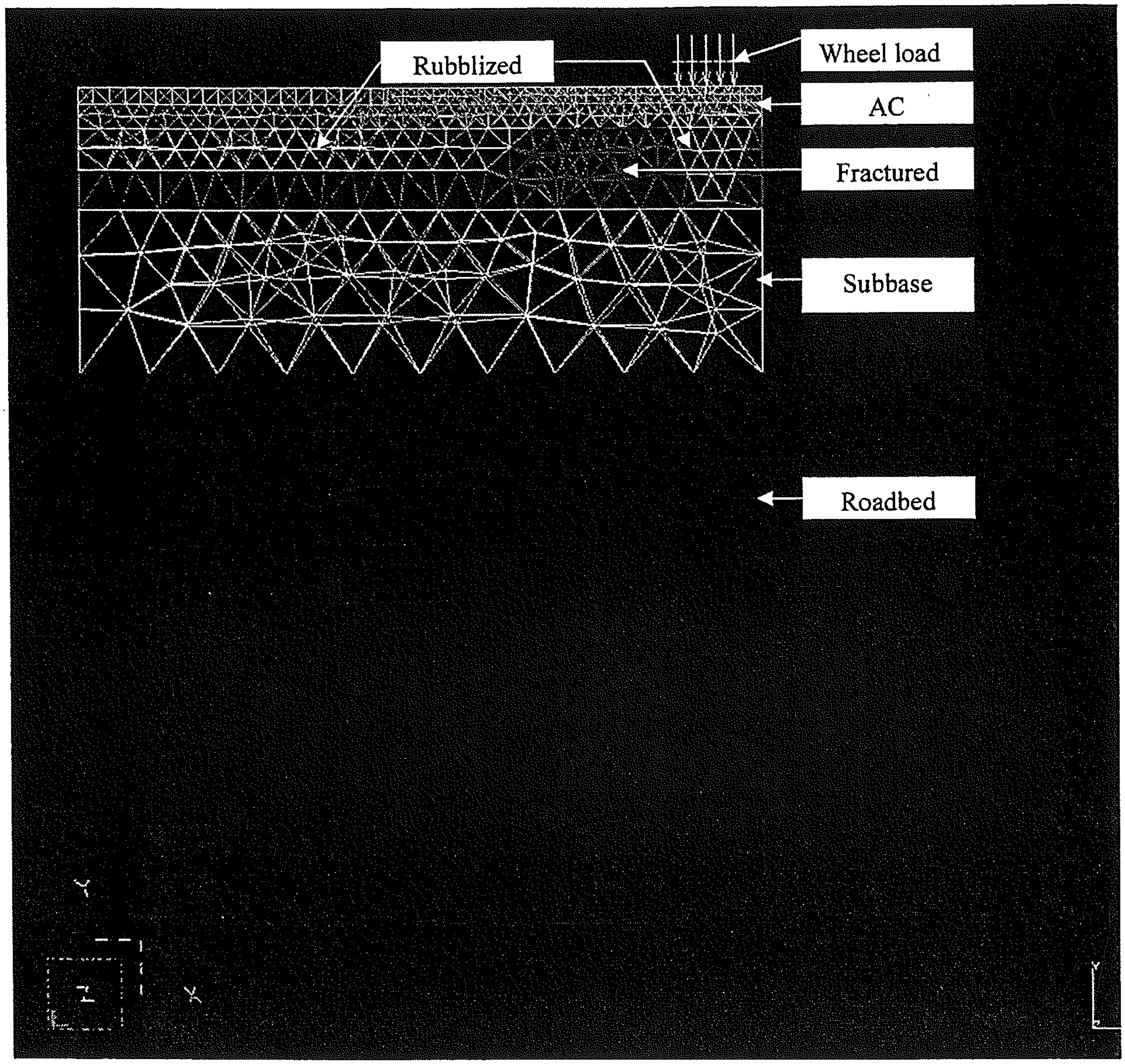

Figure 7.13 The third 3-D model with uneven interface with the presence of fractured concrete under the edges and the center of the dual wheel

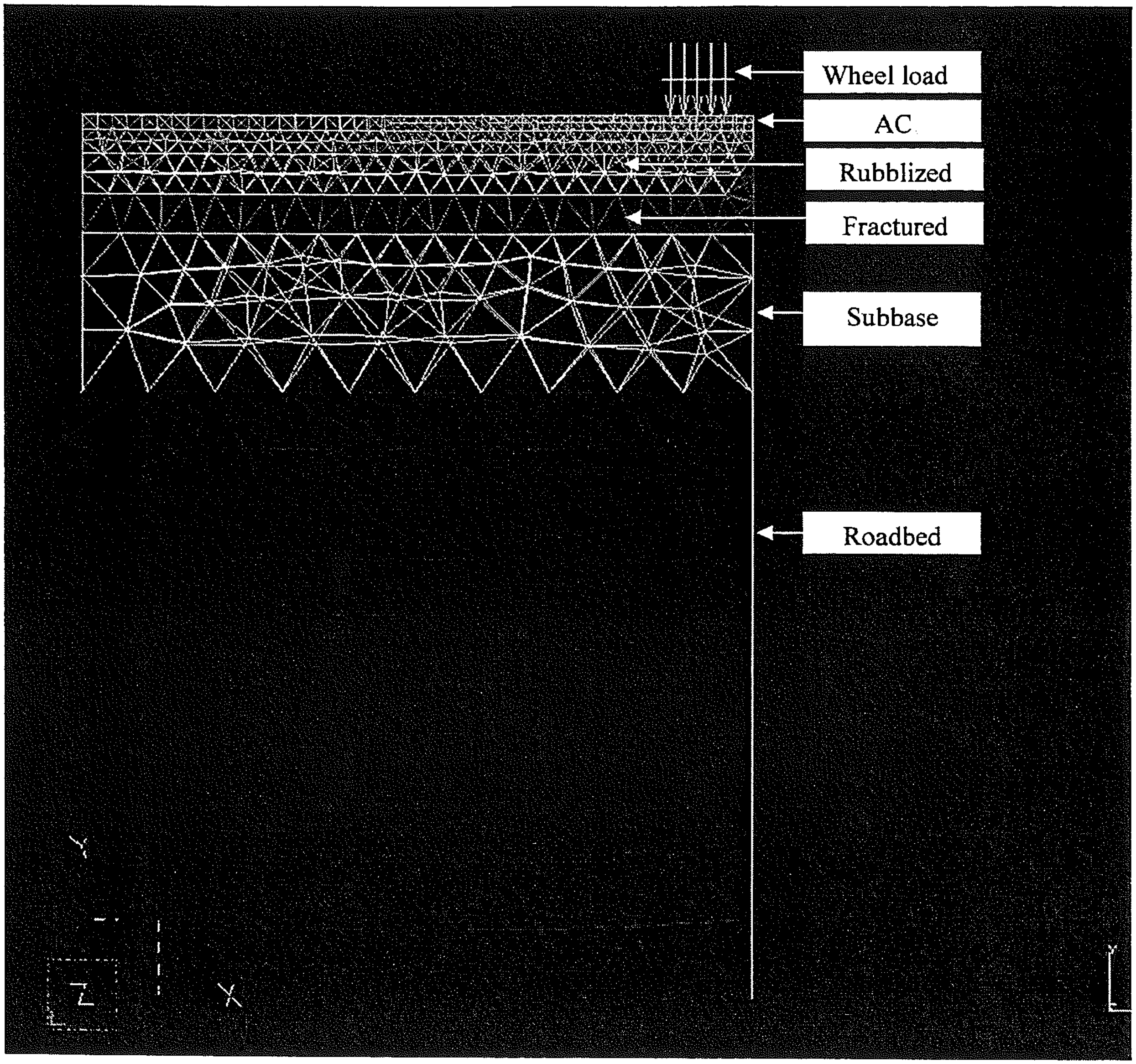

Figure 7.14 The fourth 3-D model with uneven interface with the presence of fractured concrete at the center of the dual-wheel

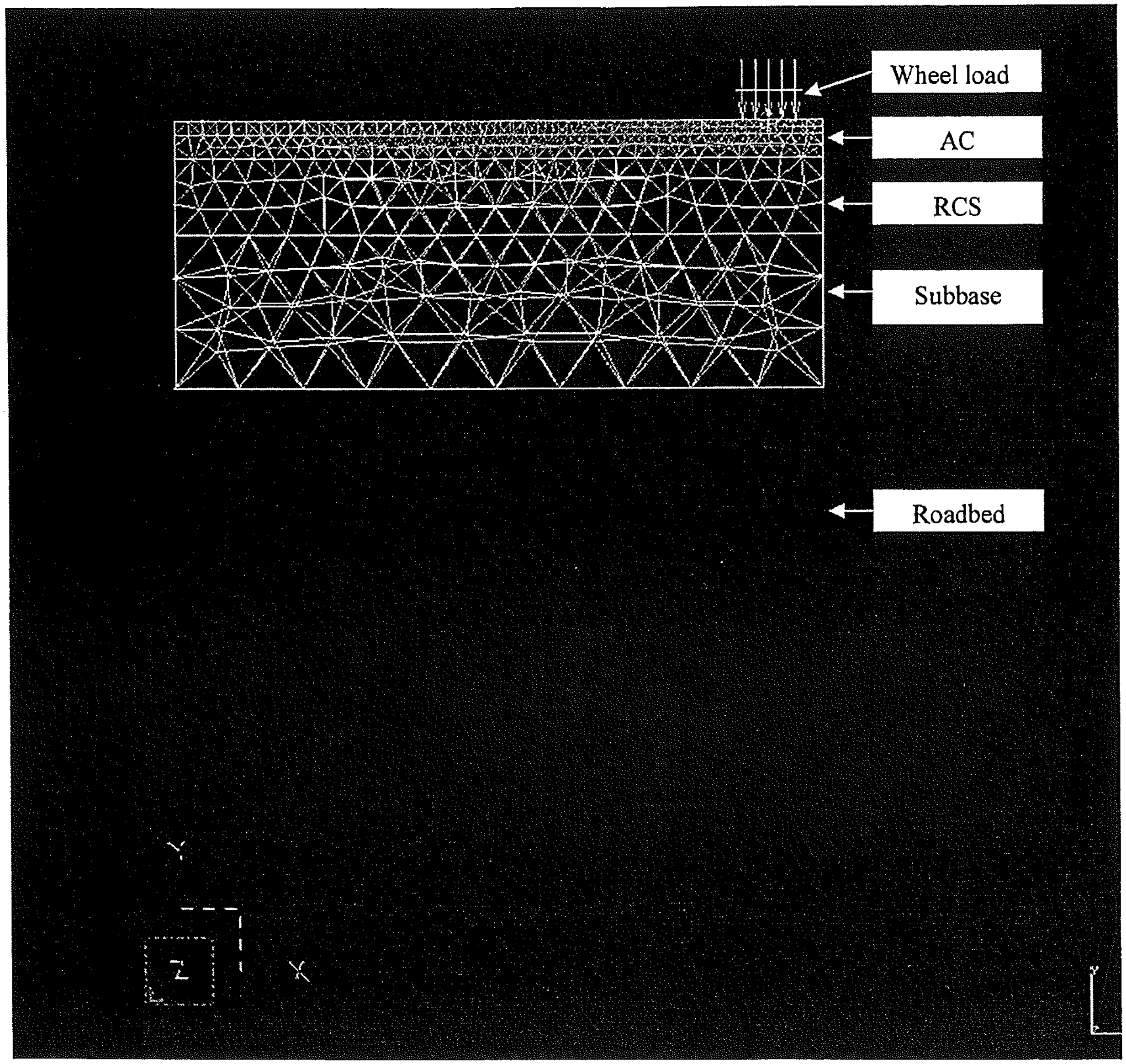

Figure 7.15 The fifth 3-D model with a 9-in. rubblized concrete slab (RCS) representing the rubblized material and fractured concrete layers

A 9000-lb dual wheel load applied to a uniform circular contact area with a radius of 3.785 in. and a tire pressure of 100 psi. The distance between the duel tires was set at 4.43 in.

1. The layer thicknesses and properties of the following four rubblized pavements that were investigated during the Phase II Study:

   - I-69 EB section 1 test site 1, control section 76023 and job number 36020
   - I-75 SB section 1 test site 1, control section 10692 and job number 25559
   - M-15 SB section 1 test site 1, control section 25092 and job number 45534
   - M-37 SB section 6 test site 1, control section 41033 and job number 26691

Each of the five models was used to analyze the effects of certain variable on the maximum surface tensile stress and hence, on TDC potential. Results of the analyses are presented in the next section.

5.1 Results of Mechanistic Analyses Using the 3-D Models

The five 3-D models shown in figures 7.11 through 7.15 were used to conduct detailed mechanistic analyses on the pavement section of I-75, SB, section 1, test site 1. The results of the analyses were divided into two categories as follows:

1. Those results that address the effects of the geometry of the interface between the rubblized material and the fractured concrete layers on the maximum surface tensile stress.

2. Those results that address the effects of differential stiffness in the AC layer (the effects of differences in temperature and/or hardening) on the maximum surface tensile stress.

The two categories are presented below. In addition, after the mechanistic analyses of I-75 SB were completed, the combination of variables (the interface geometry and the differences in temperature) that yielded the highest surface tensile stress were chosen and applied in the mechanistic analysis of the other three pavement sections listed above. Results of the latter analyses are presented in section 5.2.

5.1.1 The Effects of the Geometry of the Interface

Detailed analyses of the effect of different geometry of the interface between the rubblized material and the fractured concrete layers on the maximum load-induced surface tensile stresses were conducted on pavement models representing the rubblized pavement on I-75 SB, section 1 and test site 1. Four different geometries of the interface were used in the analyses as follow:

1. Even interface between the rubblized material and the fractured concrete layers as shown in model 1 of figure 7.11.

2. Uneven interface with the absence of the fractured concrete layer under the dual-wheel as shown in model 2 of figure 7.12.

3. Uneven interface with the presence of fractured concrete at the middle between and at the edge of the dual-wheel as shown in model 3 of figure 7.13.

4. Uneven interface with the presence of fractured concrete at the middle between the dual-wheel as shown in model 4 of figure 7.14.

Further, two 3-D FEM analyses were conducted using the rubblized pavement models with a 9-in. rubblized concrete slab layer as shown in model 5 of figure 7.15. Two modulus values were assigned to the rubblized concrete slab to simulate the following scenarios:

1. A full depth rubblized material layer was simulated through the assignment of a 27,000-psi modulus value to the 9-in. thick rubblized concrete slab.

2. A full depth fractured concrete layer was simulated using a 1,174,000-psi modulus value to the 9-in. thick rubblized concrete slab layer.

In all analyses, negative differences in temperature were assigned to the AC layer such that the AC surface course temperature was 60^0F and the AC base course temperature was 90^0F. The temperature corrected moduli of the AC surface and base courses were calculated using equation 7.1 (6).

$$E_T \quad = E_{20} / 10^{0.0224(T-20)} \qquad (7.1)$$

where

E_T = elastic modulus of the AC course at temperature T ^{0}C
E_{20} = the AC modulus at the standard temperature of 20°C (68°F), which was obtained from the backcalculated and temperature corrected modulus

Results of the 3-D analyses are summarized in table 7.9. Figures 7.16 and 7.17 show the load-induced surface tensile stress as a function of the radial distance from the center of the loaded area (the center of the duel wheel). Examination of the results of the analyses listed in table 7.9 and depicted in figures 7.16 and 7.17 indicates that:

1. Pavement model 2 (uneven interface between the rubblized material and the fractured concrete layers, the duel wheel is setting on a pool of rubblized material and the fractured concrete extends to the bottom of the AC layer at the outer edges of the tires) yielded the highest load induced surface tensile stress. This model simulates the pavement section shown in figure 7.1, depicted in figure 7.2 and the 3-D analysis model is shown in figure 7.12. The maximum load-induced surface tensile stress obtained from model 2 is 86.8 psi. This tensile stress magnitude is much higher than that obtained from

Table 7.9 A summary of the results obtained from 3-D FEM analyses with 6 different conditions of the rubblized concrete slab

Geometry / thickness of the rubblized material	Temperature (^oF)		Modulus (ksi)		Maximum surface radial tensile stress	
	AC surface	AC base	AC surface	AC base	Location (in.)	Magnitude (psi)
Even interface and equal thickness between two layers (model 1)	60	90	1,631	690	17.3	20.0
Uneven interface with the absence of fractured concrete under the dual-wheel (model 2)	60	90	1,631	690	11.5	86.8
Uneven interface with the presence of the fractured concrete at the middle and at the edges of the dual-wheel (model 3)	60	90	1,631	690	0.7	77.3
Uneven interface with the presence of the fractured concrete at the middle of the dual-wheel (model 4)	60	90	1,631	690	24.6	43.6
Full depth rubblized material (model 5)	60	90	1,631	690	24.6	29.3
None rubblized material (full depth fractured concrete), (model 5)	60	90	1,631	690	52.8	1.74

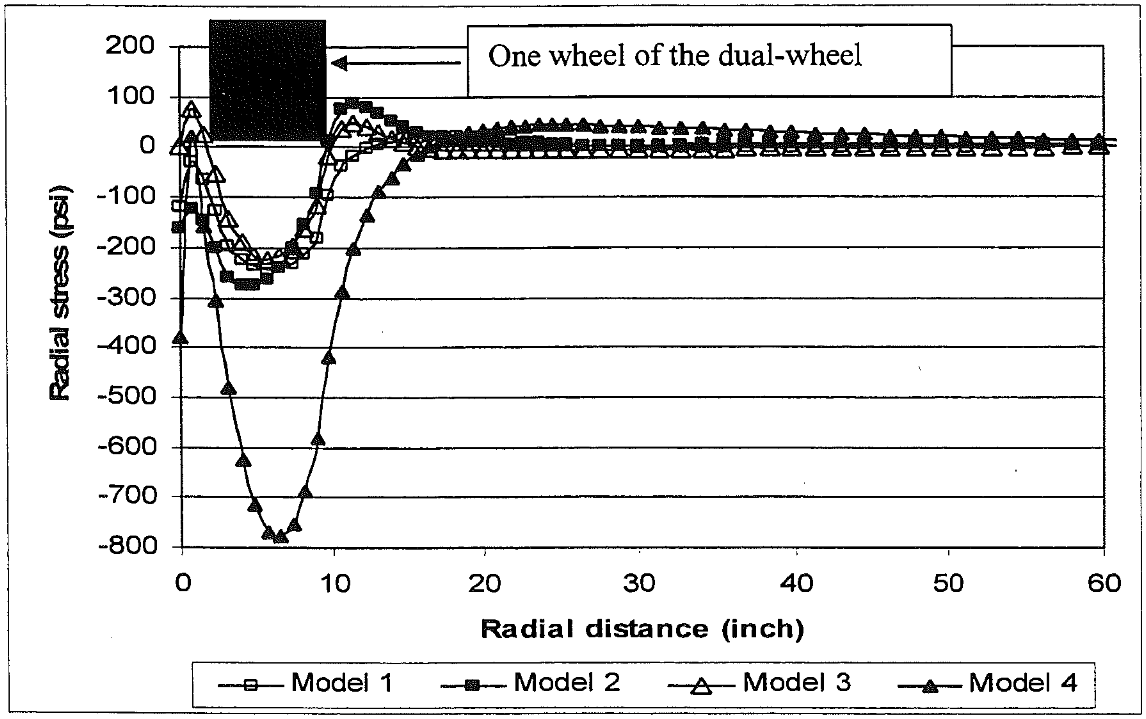

Figure 7.16 Variation in the surface radial stress with the radial distance from the center of the load (analyses of models 1 through 4)

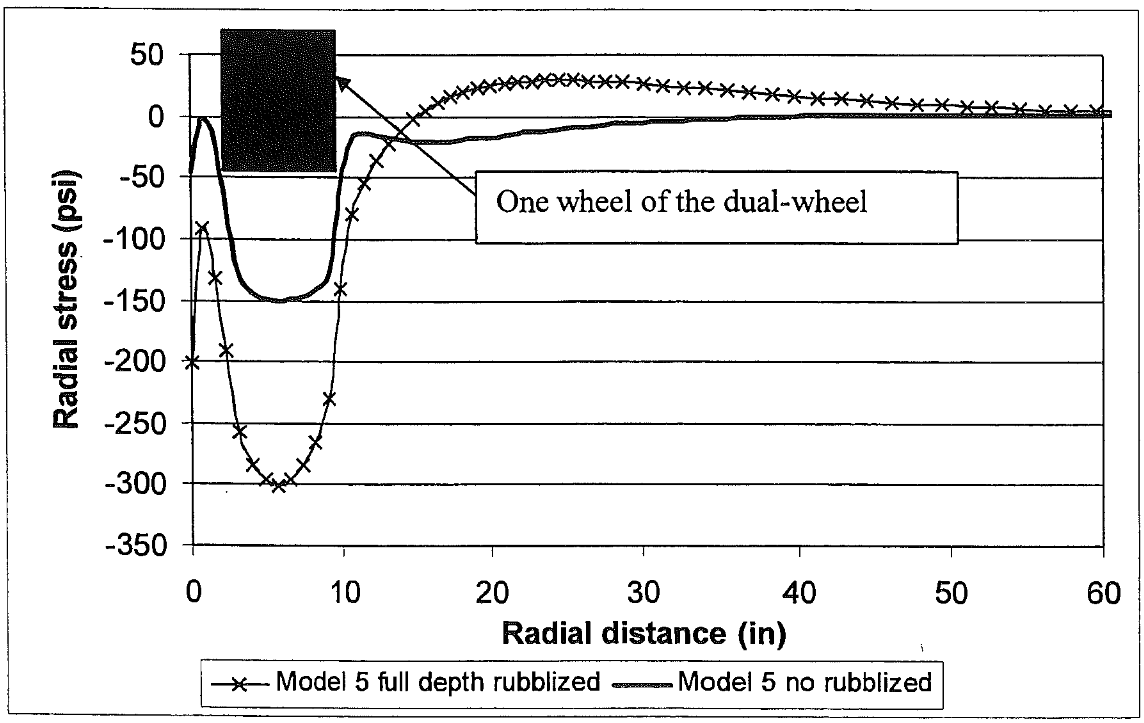

Figure 7.17 Variation in the surface radial stress with the radial distance from the center of the load (analyses of model 5)

model 1, which simulates even interface and equal thickness between the rubblized and the fractured concrete layers. The latter model produced maximum load-induced surface tensile stress of only 20.0 psi.

2. The location of the maximum surface tensile stress in model 2 is 11.7 in. from the center of the load. It is just to the left of the edge of the wheel, which is about 10 in. from the center of the load. For a full depth fractured concrete layer (no rubblized material), the location of the maximum surface tensile stress obtained from the other models, except models 3 and 5, varies from the edge of the wheel to 15 in. away from the edge of the wheel. These locations are similar to those of the maximum surface tensile stress found for the single wheel load case reported in the previous section. The location of the maximum load-induced surface tensile stress for model 3 is at the middle between the two tires (the center of the dual-wheel). This scenario implies that the TDC potential exists in and around the wheel paths. These are the exact locations where TDC were found in real pavements.

3. Although model 5 with full depth fractured concrete or no rubblized material produces low load-induced surface tensile stress, which indicates low TDC potential, it does not mean that this model represents a good rubblized pavement. Since the rubblization operation delivered no rubblized material to the rubblized concrete slab, the integrity of the slab and joint were not destroyed, that is the main objective of the rubblization operation has not been accomplished. As a result, reflective cracks will develop in this pavement within a relatively short period of time.

Based on the above 3-D analyses the geometry of the interface in model 2 has been selected as the critical condition that will create the highest load-induced surface tensile stress. Therefore, model 2 was used to further analyze the effects of differences in temperature within the AC layer on the load-induced surface tensile stress in rubblized pavement. The results of such analyses are presented in the next section.

5.1 The Effects of Differences in Temperature on Load-Induced Surface Tensile Stress

First, recall that the properties of asphalt mixes are temperature dependent. The mix becomes stiff and solid at low temperatures and soft and viscous at higher temperatures. In the field, the temperature in the asphalt layer varies from top to bottom. Hence, temperature gradient exists in the asphalt layer most of the time. As noted earlier, the temperature gradient could be positive where the AC surface course is hotter than the AC base course (day time gradient) or negative (night time gradient) with a reversed temperature scenario. The effects of temperature gradient on the load-induced stresses in rubblized pavements was studied by using different modulus values for the AC surface and AC base courses. For example, for the single wheel load that was analyzed using the CHVERONX and the MICHPAVE computer programs, the effects of the temperature gradients in the AC layers were simulated by differential stiffness (modulus ratio between the AC surface and AC base courses). The results were reported in the previous section. Similarly, in the 3-D analysis, the AC layer was divided into two courses; AC surface and AC base courses. Each course was assigned a temperature and its modulus at that temperature was calculated using the backcalculated modulus value and equation 7.1. Four temperature scenarios were assigned to the AC surface/AC base courses as follows 60°F/80°F, 60°F/70°F, 30°F/60°F and 90°F/120°F and their respective modulus values were calculated. These four temperature scenarios are in addition to the 60°F/90°F scenario that was already analyzed in the previous section. In the analyses of the four temperature scenarios, model 2 shown in figure 7.12 was used. Table 7.10 provides a list of the results of the analyses and figure 7.18 shows the relationship between the differences in temperature and the maximum load-induced surface tensile stress. Examination of the results in table 7.10 and figure 7.18 indicates that, for the same temperature of the AC surface course, the maximum load-induced surface tensile stress increases with increasing negative differences in temperature between the two AC courses. Further, figure 7.18 clearly shows that the maximum load-induced surface tensile stress is linearly related to the differences in temperature between the AC courses. This is because the temperature of the AC surface course for the three data points making-up the straight line in the figure was held constant at 60oF while the AC base course temperature was increased from 70 to 80 and to 90°F. The two data points in the figure that are at a temperature difference of –30°F and are outside the straight line belong to an AC surface course at temperatures of 30 and 90°F. Hence, for the same temperature difference, the maximum load-induced stress is not the same. Stated differently, the effect of differences in the temperature between the AC surface and the AC base courses on the maximum load-induced surface tensile stress is a function of the magnitude of the difference in temperature and the reference temperature of the AC surface course.

The above scenario could also be explained using the data in table 7.10. The data in the table is divided into two groups; a constant AC surface temperature and a variable AC surface temperature. As can be seen from the table, three pavement sections with the same temperature difference of -30°F (30°F/60°F, 60°F/90°F and 90°F/120°F) lead to the same ratio of the AC surface and AC base moduli but not the same maximum load-induced surface tensile stress. Hence, the maximum load-induced surface tensile stress cannot be expressed as a function of the modulus ratio.

5.2 Implementation - Mechanistic Analysis of Four Rubblized Pavements

The results of the mechanistic analyses presented and discussed in the previous sections were based on assumed but reasonable modulus values of the various pavement layers. As stated earlier, the main objective was to discuss the sensitivity of the TDC potential to various input variables. Such variables reflect variations in the rubblization process, construction, material properties and the environment. In this section, results of mechanistic analyses of four rubblized pavement sections are discussed.

Table 7.10 A summary of the results of 3-D FEM analyses with 5 temperature gradients

Geometry of the interface	Temperature profile	Temperature (^{o}F)		Difference in temperature (^{o}F)	Modulus (ksi)		Modulus ratio	Maximum surface radial tensile stress	
		AC surface	AC base		AC surface	AC base		Location (in.)	Magnitude (psi)
Uneven interface with the absence of fractured concrete under the dual-wheel	Constant AC surface course temperature and variable AC base course temperature	60	70	-10	1,631	1,225	1.33	11.5	63.6
		60	80	-20	1,631	919	1.77	11.5	74.9
		60	90	-30	1,631	690	2.36	11.5	86.8
	Variable AC surface and base courses temperature	30	60	-30	3,852	1,631	2.36	12.3	73.6
		60	90	-30	1,631	690	2.36	11.5	86.8
		90	120	-30	690	292	2.36	11.5	80.1

Table 7.11 Layer thickness and layer properties of four rubblized pavements

Pavement	Thickness (in.)				Modulus (ksi)					
	AC surface	AC base and leveling	Total AC	Base	AC surface course at 60F	AC base and leveling at 90F	Rubblized material	Fractured concrete	Base	Roadbed soil
I-69	1.50	6.70	8.2	16	492	301	65	256	25	14
I-75	1.7	2.80	4.5	18	1,631	690	27	704	17	17
M-15	1.50	4.00	5.3	12	2,861	1,130	27	183	37	20
M-37	1.60	4.10	5.7	12	3,129	1,212	90	592	38	16

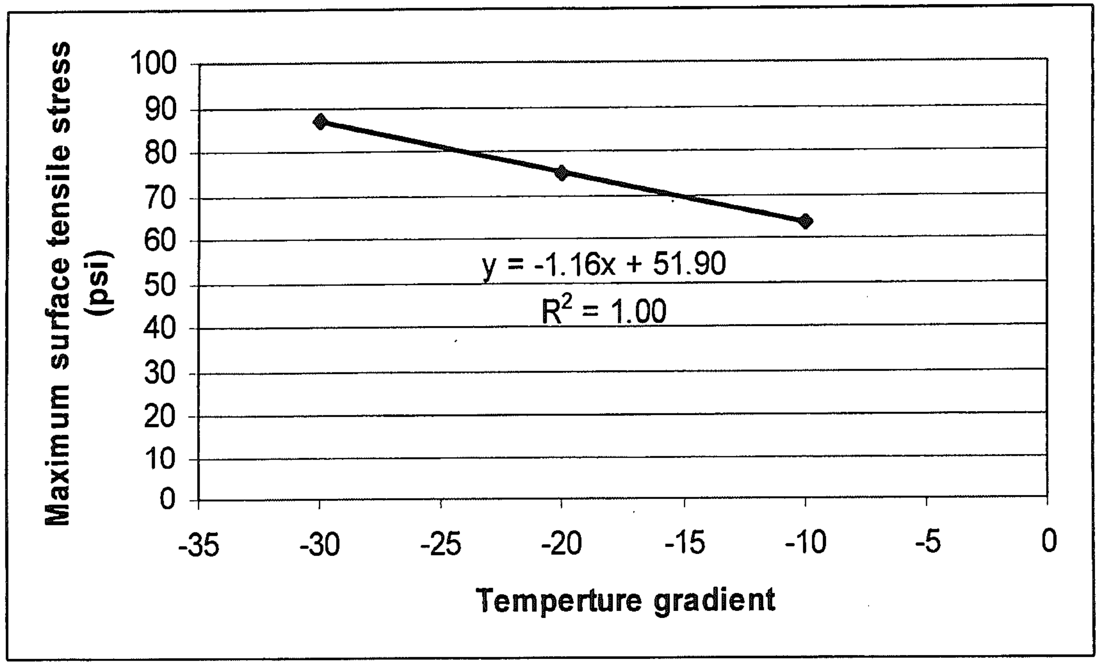

Figure 7.18 Relationship between temperature gradient and the maximum surface tensile stress

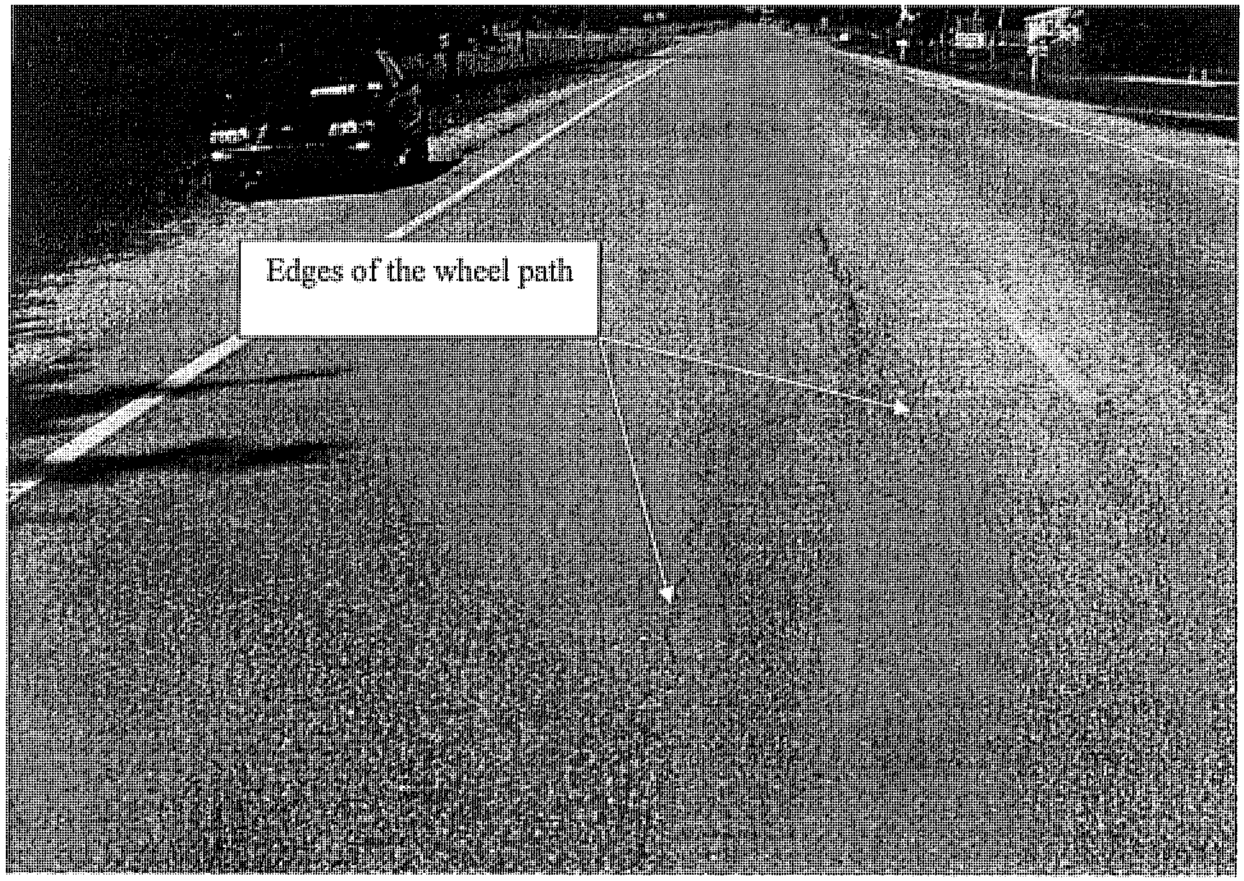

Figure 7.19 Longitudinal top-down cracks at the edges of the wheel path on Saginaw road, CS 36555, JN 35266, August 2001

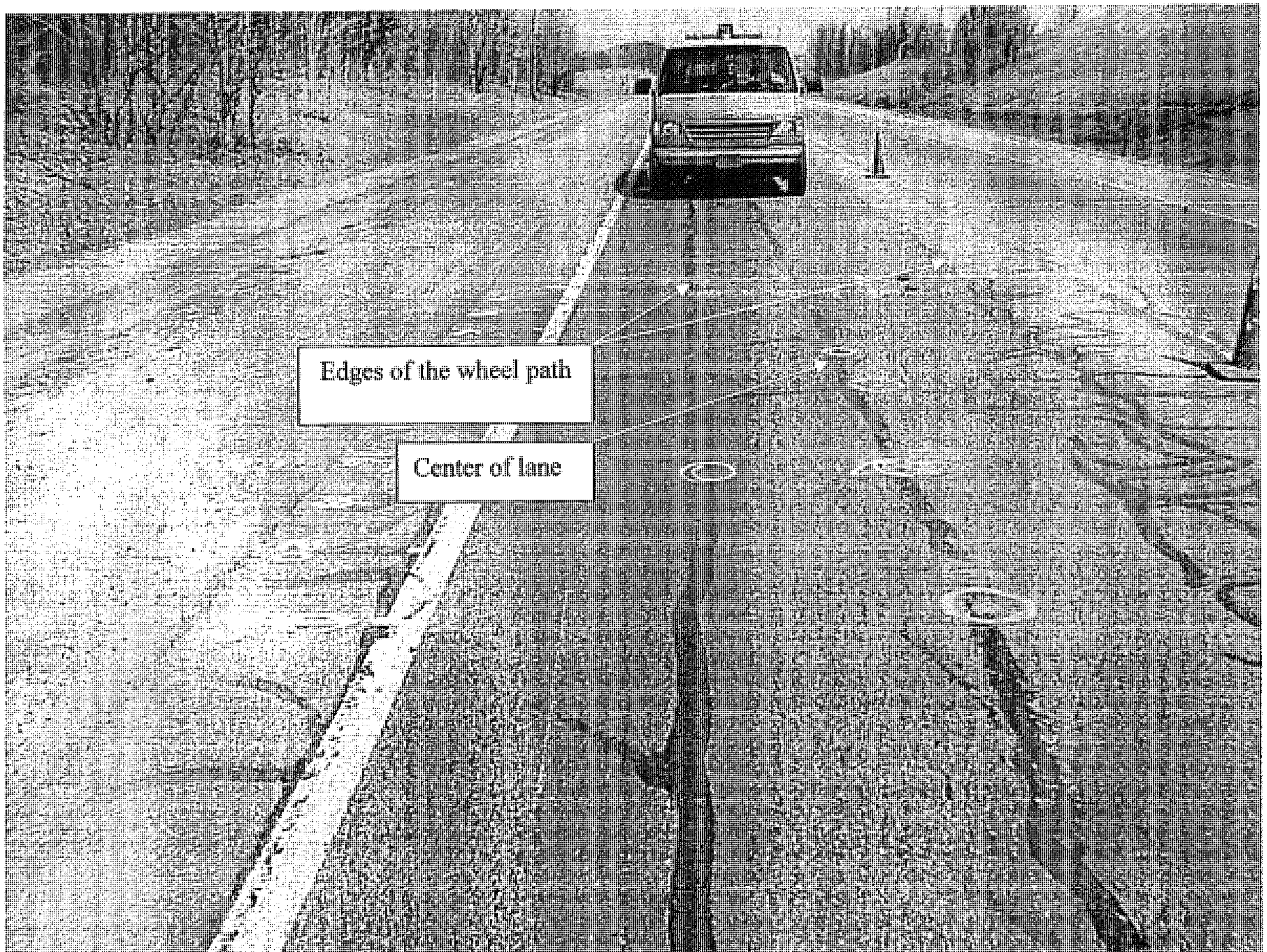

Figure 7.20 Longitudinal top-down cracks at the edges of the wheel paths on M-37 SB, CS 41033, JN 31068, March 2001

In the 3-D analyses of the maximum load–induced surface tensile stress of the four rubblized pavement sections of table 7.11, the geometry of the interface between the rubblized material and the fractured concrete layers of the fifth 3-D model (see figure 7.15) was selected and used. For each pavement section, the moduli of the AC surface and the AC base courses were refigured based on their assigned temperatures of 60°F and 90°F, respectively (a typical night time temperature gradient). The refigured modulus values of the AC courses and the layer thicknesses used in the analyses are listed in table 7.11. Note that the selection of the interface geometry and the temperature difference between the AC surface and the AC base courses was based on:

1. Two and three dimensional analyses of the load-induced surface tensile stress using various interface geometry. The selected interface geometry yielded relatively high tensile stresses.

2. Field observations of rubblized concrete pavements where, prior to placing the AC layer, trenches were excavated in the rubblized material layer to expose the fractured concrete layer (see figures 7.1 and 7.2).

3. Field measurements of night time temperatures of the AC surface and the AC base courses.

In the analyses, the average AC core thickness and the actual thicknesses of the other pavement layers were used. Results of the 3-D mechanistic analyses of the four pavement sections are summarized in table 7.12. The load-induced surface tensile stress on the I-75 section is the highest among the four pavements. This is because the pavement section on I-75 has the lowest rubblized material modulus compared to the other sections. Given the high AC modulus, low rubblized material modulus and high fractured concrete modulus, the effects of the stiff-soft-stiff layers (the sandwich model) on the surface tensile stress is very high. Although the pavement section on M-37 has a rubblized material modulus close to that of the I-75 section, the modulus of the fractured concrete layer is much lower. Hence the effect of the stiff-soft-stiff system is also much lower. Likewise, the AC modulus on the I-69 pavement section is the lowest among the other three sections; this implies lower effects of the sandwich model and, hence, lower surface tensile stress.
Indeed, among the four pavement sections, the I-69 section is the only pavement free of TDC. Based on the distress surveys conducted in 2001 and 2002, the other three sections exhibit TDC that were initiated within medium or high degree segregated areas and have propagated outward. For the I-75 pavement section only, TDC were also found outside the segregated areas. However, the cracks were tighter and exhibited less associated distresses than the ones located within the segregated areas. The implication of this last observation is that TDC in segregated areas were initiated and propagated at much earlier time than those outside the segregated areas.

Note that the thickness and moduli of the pavement layers, especially the rubblized material and the fractured concrete layers, vary from one location to the others. At certain locations the combination of the thicknesses and moduli of the rubblized and fractured concrete layers create more favorable condition for the initiation of

Table 7.12 A summary of the results of 3-D FEM analyses of four rubblized pavements

Pavement	Geometry of the interface	Temperature (^{o}F)		Modulus (ksi)		Maximum surface radial tensile stress	
		AC surface	AC base	AC surface	AC base	Location (in.)	Magnitude (psi)
I-69	Uneven interface with the absence of fractured concrete under the dual-wheel	60	90	492	301	12.1	16
I-75		60	90	1,631	690	11.5	87
M-15		60	90	2757	1089	14.3	25
M-37		60	90	3129	1212	12.3	25

Table 7.13 Applied stress ratio, existence of TDC, degree of segregation and the pavement/surface age for four rubblized pavements

Pavement	Maximum tensile stress (psi)	Indirect tensile strength (psi)	Stress ratio	TDC	Degree of segregation	Pavement/surface age (years)
I-69	16	97	0.16	No	Low	4
I-75	87	146	0.59	Yes	High	13
M-15	25	172	0.14	Yes	Medium	4
M-37	25	143	0.17	Yes	Medium	10

TDC than in other locations. They cause increases in the magnitude of the maximum load-induced surface tensile stress. Hence, the magnitude of the maximum load-induced surface tensile stress listed in table 7.12 may not be the absolute maximum along the pavement section. The results in the table are based on the average values of the layer thicknesses and moduli, which may not be the optimum conditions for the initiation of TDC.

6.0 CAUSES OF TOP-DOWN CRACKS ON THE FOUR PAVEMENT SECTIONS

Results of the 3-D mechanistic analyses of the four pavement sections discussed in the previous section, and the distress data obtained from two distress surveys that were conducted in 2001 and 2002, indicate that the TDC on the three pavement sections along I-75, M-37 and M-15 are caused by the construction and rubblization processes. Construction of the AC caused segregation whereas the rubblization process created differential stiffness between the pavement layers.

The potential for the initiation of TDC depends on the ratio of the applied stress to the available tensile strength of the AC mix (also called the stress ratio). Such ratio can be calculated using the following equation.

$$\text{Stress ratio} = \text{Maximum surface tensile stress} / \text{Tensile strength} \qquad (7.2)$$

Table 7.13 provides the stress ratio and some other information of the four rubblized pavements. As can be seen from the table, only the pavement section along I-69 does not exhibit TDC. Although the pavement age and the stress ratio of the I-69 section are very similar to the M-15 section, the degree of segregation on M-15 section is higher than that on I-69 section. Segregation is a factor that significantly affects the stress ratio and the initiation of TDC. In the area where the pavements experience segregation, the tensile strength of the AC mix will substantially lower than in non-segregated areas. Note that the tensile strengths reported in table 7.13 and in the other tables in this report were obtained from laboratory testing of AC cores that were extracted from non-segregated areas. Hence, the actual stress ratio of the four rubblized pavement sections could be much lower than the values reported in table 7.13.

Finally, it would be of interest to monitor the pavement performance along the I-69 section. Although the pavement did not exhibit any type of distress as of the last distress survey of 2002, the section has been capped by a relatively dry AC mix having high air voids and low tensile strength. It is likely that TDC and other distress (e.g., rut) may initiate on this section within few years.

7.0 SUMMARY

Two- and three- dimensional finite element analyses were conducted on various rubblized pavement sections using various techniques to model the geometry of the interface between the rubblized material and the fractured concrete layers. A single and a dual wheel loads were used in the analyses. The results indicate that:

1. The magnitude and location of the maximum load-induced surface tensile stress are functions of the following variables:

   - Layer thickness and properties
   - Geometry of the interface between the rubblized material and the fractured concrete layers
   - Load configurations

2. The interface geometry between the rubblized material and the fractured concrete layers has a significant impact on TDC potential. For example, analysis of the I-75 section using model 1 (even interface) yielded maximum surface tensile stress of only 20 psi whereas model 2 (uneven interface) produced maximum surface tensile stress of 87 psi.

3. Higher temperature differences between the AC surface and the AC base courses cause increases in the maximum surface tensile stress.

4. For a single wheel loads, the location of the maximum surface tensile stress is in the vicinity of the edge of the tire. For a dual wheel load, the location of the maximum surface tensile stress could be either at the center of the dual or in the vicinity of the tire edges. The exact location is a function of the pavement layer thickness and properties and the geometry of the interface between the rubblized and the fractured concrete layers. These locations agree very well with the locations of the TDC observed during the field investigation.

5. Segregation is a very important construction factor affecting the TDC potential. Segregation causes decrease in the AC tensile strength and increases in the stress ratio. The latter decreases the fatigue life of the mix. In this regard, note that during the 2002 distress survey of rubblized pavements, 42 pavement sections exhibited medium or high degree of segregation out of the 48 pavement sections that exhibited longitudinal TDC. Further, all transverse TDC were located within segregated areas.

REFERENCES

1. Gerritsen, A.H., C. A. P. M. van Gurp, J. P. J. van der Heide, A. A. A. Molenaar and A. C. Pronk. Prediction and Prevention of Surface Cracking in Asphaltic Pavements, Proc. 6th International Conference on the Structural Design of Asphalt Pavements, Ann Arbor, 1987

2. Dauzats, M., and A. Rampal. Mechanism of Surface Cracking in Wearing Courses, Proc. 6th International Conference on the Structural Design of Asphalt Pavements, Ann Arbor, 1987

3. Wambura, J. H. G., J. Maina and H. R. Smith. Kenya Bituminous Materials Study. In Transportation Research Record 1681, TRB, National Research Council, Washington, D.C., 1999, pp. 129-137

4. Matsuno, S., and T. Nishizawa. Mechanism of Longitudinal Surface Cracking in Asphalt Pavement, Proc. 7th International Conference on the Structural Design of Asphalt Pavements, Ann Arbor, 1992

5. Myers, L. A., R. Roque, and B. E. Ruth. Mechanisms of Surface-Initiated Longitudinal Wheel Path Cracks in High-Type Bituminous Pavements. Journal of the Association of Asphalt Paving Technologists, Vol. 67 pp. 401-432, 1998

6. Buch, N., R. S. Harichandran, G. Y. Baladi, D. Park, and H. Kim. Calibration of Michpave's Rut and Fatigue Distress Models and Development of an Overlay procedure in Michback, Research Report RC-1383 , Michigan Department of Transportation, 1999

CHAPTER 8
CONCLUSIONS AND RECOMMENDATIONS

Based on the results of the laboratory and field investigation, analyses of the FWD and the laboratory test data, various conclusions were drawn and recommendations were made. These conclusions and recommendations can be divided into four categories as follows:

1. General

2. Factors influencing the performance of rubblized concrete pavement

    - Project selection
    - The rubblization process
    - The construction procedure
    - The pavement design process
    - The pavement materials
    - Traffic

3. The MDOT special provision for rubblization of concrete pavements

4. Rubblized pavement design parameters

The conclusions and recommendations for each of the above four categories are presented below.

1.0 GENERAL CONCLUSIONS AND RECOMMENDATIONS

During the study, the performance of every MDOT rubblized pavement project in the state of Michigan was studied. In the mean time, in a parallel study, the performance of several conventional asphalt pavement projects was also analyzed. Based on both studies, the following conclusions were made:

1. Rubblization of deteriorated concrete pavements is a viable rehabilitation option that requires more detailed quality control measures than conventional asphalt pavements. That is the performance of rubblized concrete pavements appears to be more sensitive to variation in various pavement parameters than conventional asphalt pavements. Therefore, it is strongly recommended that quality control measures be revisited, tightened and strictly enforced. For example, the MDOT special provision for rubblizing concrete pavements should be modified to include the recommended calibration scheme and should be strictly enforced. Another example is that medium and heavy segregated areas should be milled and repaved.

2. Various distress types that affect the performance of rubblized concrete pavements such as top-down longitudinal and transverse cracking and raveling were also found, but to a slightly lesser extent, on various conventional asphalt pavement projects. In most cases, the TDC were located in segregated areas.

3. Based on several observations of the rubblization operations of the sonic and the multi-head breaker and on the finding in the excavated trenches, it is concluded that the sonic and the multi-head breaker did not deliver the best possible quality of rubblized concrete. In this regard, the sonic breaker delivers, on average, better and more uniform rubblized products than the multi-head breaker. The latter conclusion is based on the following observations:

   a) The resonant frequency breaker delivers much higher percent of debonded steel than the multi-head breaker.
   b) The resonant frequency breaker delivers, on average, higher and more uniform thickness of the rubblized material.
   c) The resonant frequency breaker delivers higher percent of joints where the integrity of the joint is completely destroyed than the multi-head breaker.
   d) The multi-head breaker has higher potential of damaging the newly paved AC layer on the adjacent lane than the resonant frequency breaker.

2.0 FACTORS INFLUENCING THE PERFORMANCE OF RUBBLIZED CONCRETE PAVEMENT

Many factors were found to influence the performance of rubblized concrete pavement projects. Each factor belongs to a certain action that has been taken during the course of project inception to project construction. Therefore, the factors are divided into six groups depending on the type of action (the cause and effects) as presented in the next six subsections.

2.1 Project Selection

For few rubblized pavement projects, some of the factors affecting their performance can be traced back to the project selection process. Such factors could be minimized or eliminated if the following recommendations are implemented:

2.1.1 Candidate Projects

The following deteriorated concrete pavements should not be considered for rubblization options:

2. Concrete pavements that have been cracked and seated in the past.
3. Concrete pavements that are supported on a relatively soft roadbed soil (less than 3000 psi modulus).

4. Concrete pavements with extensive amount of cracking as defined in the MDOT PMS distress manual.

2.1.2 Testing of Candidate Projects

After selecting a candidate project for rubblization, the compressive strength of the existing concrete pavements should be determined. If the concrete pavement consists of two types of concrete (e.g., a widening strip, an added lane and so forth), both concrete types should be tested. The compressive strength data can be used to determine whether or not the pavement should be rubblized using different settings of the rubblizer parameters. For example, if the average compressive strength of the better concrete minus one standard deviation is higher than the average strength of the other concrete plus one standard deviation, then the rubblizer parameters should be calibrated for each type of concrete.

2.2 The Rubblization Process

For each candidate project, the contractor should obtain the compressive strength data of the concrete slab to determine the number of locations at which the operating parameters of the rubblizer should/must be calibrated as per the recommended calibration procedure presented in chapter 4. The operator of the rubblizing equipment should be trained to be cognizant of the impact of the rubblizing process on pavement performance. The following steps could be used as guidelines.

1. Stop the rubblization process and recalibrate the operating parameters if any of the following situations arises:

    a) The steel is not debonded or the concrete pavement is rubblized to shallow depths (less than 4.5 in.).
    b) The integrity of the concrete longitudinal and/or transverse joints is not completely destroyed.
    c) The rubblization is producing numerous large concrete pieces (more than 8 in.).

2. Re-examine the rubblization operation if strips of coarse rubblized material (0.5 to 3 in.) are separated by about 1-in. wide strips consisting of fine materials and/or dust. This indicates an uneven rubblization across the lane.

3. Stop the rubblization operation if the rubblizer causes large concrete pieces especially at the corner of the slab to break free and to rotate and penetrate the base material. This implies that the roadbed soil is soft and that the base layer is being subjected to shear failure, which would be reflected through the finished pavement. It is possible to alleviate the situation by recalibrating the operating parameters of the rubblizer.

4. Stop the rubblization operation and recalibrate if the hammers or the sonic shoe bounce off the pavement surface.

2.3 The AC Construction

Distress survey of all rubblized projects in the State of Michigan indicates that more than sixty percent of the projects have experienced premature distress due mainly to the construction of the asphalt mat. For almost every underperforming project, the premature distress could have been eliminated at no additional cost. Field observations and the premature distress data indicate that, for future projects, premature distress can be eliminated if the following steps are taken:

1. The rubblized concrete is thoroughly inspected for potential defects and variability prior to the placement and compaction of the AC mix.

2. Large but broken concrete pieces are replaced with approved filler aggregate.

3. Areas where asphalt patches were removed are filled with approved filler aggregate and compacted properly.

4. Areas where large concrete pieces were rotated and penetrated the base layer are excavated to the roadbed soil and all the excavated materials are replaced with approved filler aggregate and compacted properly.

5. The asphalt mix is examined to determine whether or not a dry mix is being used; a dry mix would have high potential for raveling and TDC.

6. The paver parameters (speed, the auger rotation rate, the opening of the supply window and the rate at which the AC is being fed to the auger) are calibrated as to eliminate segregation under the gear box and the ends of the auger. Note that, the new AC mixes have high segregation potential and therefore are very easily segregated if any of the above parameter is slightly off the mark. The potential for aggregate segregation could be substantially reduced or eliminated if a windrow step is included in the paving operation.

7. The hopper of the paver is not emptied at any time. This will cause an end of load segregation.

8. The asphalt mat is promptly and evenly compacted as to avoid temperature segregation prior to compaction.

2.4 The Pavement Design Process and Design Parameters

Mechanistic analyses of various rubblized pavement sections indicate that most sections are adequately designed. For few projects such as the one on US 23 by Alpena, the finished pavement sections are thin and lack frost protection of the roadbed soil. Rubblized pavement sections could be designed using either two rubblized concrete layers (one rubblized material and one fractured concrete layers) or one rubblized concrete layer. Regardless of the number of layers used, the layer properties and coefficients stated in chapter 6 are strongly recommended.

2.5 The Pavement Materials

The new superpave mixes being used by the MDOT appear to be very sensitive to the asphalt content and very easy to segregate during the mixing, transportation and paving operations. Slight fluctuation in the ac content may cause a superpave mix to be dry or fat. Further, the high coarse aggregate contents (+ no. 4 sieve) of the mix makes it susceptible to particle segregation due to the slightest variation in the paver operation. The problem could be resolved by using windrow equipment as a part of the paving operation.

2.6 Traffic Control During the Rubblization Operation

Field investigation during the rubblization operation revealed that on some projects, one lane was kept open to traffic while the adjacent lane was being rubblized. When the rubblization of the lane was finished, the rubblized material was capped with AC, the finished pavement on one lane was opened to traffic, and the rubblization of the adjacent lane was commenced. It was observed that while the second lane is being rubblized, the applied pressure due to the hammer impact caused vertical movements in the paved lane (a stone on the pavement lane bounced off the pavement by about 1 in.). Such movement causes cracks or micro cracks in the finished asphalt mat along the paved lane. Over time, such cracks would open up and propagate in various directions. This construction built distress could be eliminated if one of the following steps is taken.

1. If feasible, do not allow any traffic along the project until the rubblization of adjacent lanes is completed. For 2-lanes 2-direction roads, this may imply traffic detour. For 2-lane in one direction roads, this imply diverting the traffic to one of the other two lanes in the opposite direction.

2. If traffic detour or diversion is not possible, rubblize one lane and surface it with 2-in. base course only. Divert the traffic to this lane while the adjacent lane is being rubblized. After the rubblization operation is completely finished, surface the newly rubblized lane using base, leveling and surface courses as needed. Divert the traffic to the finished pavement along one lane and finish paving the other lane.

3.0 THE MDOT SPECIAL PROVISION FOR RUBBLIZATION OF CONCRETE PAVEMENTS

Over time, MDOT has developed a sound and balanced special provision for rubblization of concrete pavements. However, it was observed during construction that, on most projects, the special provisions are totally or partially ignored by the contractors. For example, on certain projects, existing asphalt patches were not completely removed as stated in the provision. It is strongly recommended that the special provisions be strictly enforced.

The following modifications of the special provision are recommended:

1. Include the calibration plan of the rubblizing equipment as stated in chapter 4.
2. Include the items stated in the project selection (section 2.1) of this chapter.
3. Include the traffic control provision of section 2.6.
4. Include a provision for the inspection of the rubblized concrete at joints and mid-slab.

Based on field investigation and distress survey (see table 3.6, which, for convenience, is included herein as table 8.1) of 84 rubblized pavements, the under performance and the causes of the under performance of rubblized concrete pavements are summarized in table 8.2. The data in the table indicate that:

1. Ten projects (12 percent) exhibit no distress as of 2002. All these projects are only 2 to 4 years old.
2. Forty eight projects exhibit longitudinal TDC and twenty eight projects (33 percent) exhibit transverse TDC. All projects that exhibit transverse TDC also exhibited longitudinal distress. All transverse TDC are located in segregated areas and are mainly caused by segregation. On the other hand, 90 percent of all longitudinal TDC are caused by segregation (the cracks were initiated in segregated areas and propagated outward). The other 10 percent of the longitudinal TDC are caused by opening of the paving joints between the two lanes.
3. Twenty six projects (31 percent) exhibit joint reflective cracks and twelve projects (14 percent) are showing the initiation of reflective cracks (rough joints). The main cause of reflective cracks is the failure of the rubblization process to destroy the integrity of the concrete joints.
4. Eleven projects (13 percent) exhibit regular reflective cracks from the underlying concrete pavement. The main cause of these cracks is the failure of the

rubblization operation to rubblize the concrete in the vicinity of the original crack (at discontinuity)

5. Twenty projects (24 percent) exhibit rut. The rut depth varied from about 0.75 to about 0.125 in. with the majority of rut depths below 0.5 in. All rut channels are narrow and therefore the rut problem resides within the AC mix.

6. Finally 19 projects (23 percent) exhibit raveling, which is caused by segregation.

Note that, some pavement projects exhibit more than one type of distress while others exhibit a single distress type.

Alternative to modifying the special provision for rubblizing concrete pavements, the department could develop design, built and warranty provision for rubblized concrete pavements. For this scenario, based on field investigation, the following pavement performance measures are recommended for inclusion in a 5-year warranty period:

1. No longitudinal and/or transverse top-down cracks.
2. No reflective longitudinal or transverse cracks
3. No shear failure
4. No raveling
5. Less than 0.25-in. rut depth

Table 8.1 The number of projects exhibiting the indicated distress observed during the 2002 distress survey

Distress type	No of projects	JTC	TTDC	RTC	LTDC	RLC	ALC	S	R	P	PH	RJ	Rut	B	BC	B-up	D
LTDC/TTDC/S/JTC/R/RTC/RLC/P/PH	1	1	1	1	1	1		1	1	1	1						
LTDC/TTDC/S/JTC/R/P/PH/Rut	1	1	1		1			1	1	1	1		1				
LTDC/TTDC/S/JTC/R/P/Rut/Break up	1	1	1		1			1	1	1			1			1	
LTDC/TTDC/S/JTC/R/P/Bleeding	1	1	1		1			1	1	1				1			
LTDC/TTDC/S/JTC/R/P	1	1	1		1			1	1	1							
LTDC/TTDC/S/JTC/R/RJ	1	1	1		1			1	1			1					
LTDC/TTDC/S/JTC/R/Rut	1	1	1		1			1	1				1				
LTDC/TTDC/S/JTC/RLC/Rut	1	1	1		1	1		1					1				
LTDC/TTDC/S/JTC/Rut/Bleeding	1	1	1		1			1					1	1			
LTDC/TTDC/S/JTC/Rut	2	2	2		2			2					2				
LTDC/TTDC/S/JTC	3	3	3		3			3									
LTDC/TTDC/S/R/P/Rut	1		1		1			1	1	1			1				
LTDC/TTDC/S/R/RLC/P/Block crack	1		1		1	1		1	1	1					1		
LTDC/TTDC/S/R/RLC/Rut	1		1		1	1		1	1				1				
LTDC/TTDC/S/R/Rut	1		1		1			1	1				1				
LTDC/TTDC/S/R	2		2		2			2	2								
LTDC/TTDC/S/RTC	1		1	1	1			1									
LTDC/TTDC/S/RLC	1		1		1	1		1									
LTDC/TTDC/S/Rut	1		1		1			1					1				
LTDC/TTDC/S	3		3		3			3									
LTDC/JTC/S/R/RTC	1	1		1	1			1	1								
LTDC/JTC/S/R/RLC/Rut	1	1			1	1		1	1				1				
LTDC/JTC/S/RTC/RLC/Rut	1	1		1	1	1		1					1				
LTDC/JTC/S/RTC	1	1		1	1			1									
LTDC/JTC/S	2	2			2			2									
LTDC/S/R/RTC/RLC	1			1	1	1		1	1								
LTDC/S/R/RLC/P/PH/RJ	1				1	1		1	1	1	1	1					
LTDC/S/R	1				1			1	1								
LTDC/S/RLC/RJ/Break up	1				1	1		1				1				1	
LTDC/S/RLC/RJ	1				1	1		1				1					
LTDC/S/RLC/P	1				1	1		1		1							
LTDC/S/Rut	1				1			1					1				

Table 8.1 The number of projects exhibiting the indicated distress observed during the 2002 distress survey (continued)

Distress type	No of projects	JTC	TTDC	RTC	LTDC	RLC	ALC	S	R	P	PH	RJ	Rut	B	BC	B-up	D
LTDC/S	4				4			4									
LTDC/RTC/P	1			1	1					1							
LTDC/RLC/RJ	1				1	1						1					
LTDC/Rut	1				1								1				
LTDC	2				2												
TTDC/JTC/S/RLC/RJ	1	1	1			1		1				1					
TTDC/JTC/ALC/Rut	1	1	1				1						1				
JTC/RTC	1	1		1													
JTC/RLC/Rut	1	1				1							1				
JTC/RLC	1	1				1											
JTC	1	1															
S/R/RLC/P/PH	1					1		1	1	1	1						
S/P	1							1		1							
S/PH	1							1			1						
S/RJ	1							1				1					
S/RLC	1					1		1									
S/Depression	1							1									1
S	3							3									
RTC/RLC	2			2		2											
RTC	1			1													
RLC/RJ	1					1						1					
RLC	1					1											
RJ/Rut	2											2	2				
RJ	2											2					
Rut	1												1				
Bleeding	1													1			
No distress	10																
Total	**84**	**26**	**28**	**11**	**48**	**22**	**1**	**53**	**19**	**12**	**5**	**12**	**20**	**3**	**1**	**2**	**1**
Did not survey	2																
Not rubblized	2																

LTDC = Longitudinal top-down cracks, TTDC = Transverse top-down cracks, S = segregation, JTC Joint transverse crack, R = Raveling, RTC = Regular transverse crack, RLC = Regular longitudinal crack, P = Patch, PH = Pothole, RJ = Rough joint, D = Depression, B = Bleeding, ALC = Alligator cracks, BC = Block cracking, and B-up = Break up

Table 8.2 A summary of the attributes to the under performance of rubblized pavements and the associated causes

Attribute of underperformance	Percent of projects showing the underperformance attribute	Causes of the under performance attribute		
		HMA segregation (construction)	Rubblizing procedure	HMA mix (construction)
No distress	12			
Longitudinal TDC	57	90		10
Transverse TDC	33	100		
Joint reflective cracking	31		100	
Reflective cracks	13		100	
Rut	24			100
Rough joint	14		100	
Raveling	23	100		
Potholes	15	83	17	